

VOL. 634 NO. 2 MARCH 26, 1993

THIS ISSUE COMPLETES VOL. 634

JOURNAL OF

CHROMATOGRAPHY

INCLUDING ELECTROPHORESIS AND OTHER SEPARATION METHODS

EDITORS

U.A.Th. Brinkman (Amsterdam)
 R.W. Giese (Boston, MA)
 J.K. Haken (Kensington, N.S.W.)
 K. Macek (Prague)
 L.R. Snyder (Orinda, CA)

EDITORS, SYMPOSIUM VOLUMES,
 E. Heftmann (Orinda, CA), Z. Deyl (Prague)

EDITORIAL BOARD

D.W. Armstrong (Rolla, MO)
 W.A. Aue (Halifax)
 P. Boček (Brno)
 A.A. Boulton (Saskatoon)
 P.W. Carr (Minneapolis, MN)
 N.H.C. Cooke (San Ramon, CA)
 V.A. Davankov (Moscow)
 Z. Deyl (Prague)
 S. Dilli (Kensington, N.S.W.)
 H. Engelhardt (Saarbrücken)
 F. Erni (Basle)
 M.B. Evans (Hatfield)
 J.L. Glajch (N. Billerica, MA)
 G.A. Guiochon (Knoxville, TN)
 P.R. Haddad (Hobart, Tasmania)
 I.M. Hais (Hradec Králové)
 W.S. Hancock (San Francisco, CA)
 S. Hjertén (Uppsala)
 S. Honda (Higashi-Osaka)
 Cs. Horváth (New Haven, CT)
 J.F.K. Huber (Vienna)
 K.-P. Hupe (Waldbronn)
 T.W. Hutchens (Houston, TX)
 J. Janák (Brno)
 P. Jandera (Pardubice)
 B.L. Karger (Boston, MA)
 J.J. Kirkland (Newport, DE)
 E. sz. Kováts (Lausanne)
 A.J.P. Martin (Cambridge)
 L.W. McLaughlin (Chestnut Hill, MA)
 E.D. Morgan (Keele)
 J.D. Pearson (Kalamazoo, MI)
 H. Poppe (Amsterdam)
 F.E. Regnier (West Lafayette, IN)
 P.G. Righetti (Milan)
 P. Schoenmakers (Eindhoven)
 R. Schwarzenbach (Dübendorf)
 R.E. Shoup (West Lafayette, IN)
 R.P. Singhal (Wichita, KS)
 A.M. Sioffi (Marseille)
 D.J. Strydom (Boston, MA)
 N. Tanaka (Kyoto)
 S. Terabe (Hyogo)
 K.K. Unger (Mainz)
 R. Verpoorte (Leiden)
 Gy. Vigh (College Station, TX)
 J.T. Watson (East Lansing, MI)
 B.D. Westerlund (Uppsala)

EDITORS, BIBLIOGRAPHY SECTION

Z. Deyl (Prague), J. Janák (Brno), V. Schwartz (Prague)

ELSEVIER

JOURNAL OF CHROMATOGRAPHY

INCLUDING ELECTROPHORESIS AND OTHER SEPARATION METHODS

Scope. The *Journal of Chromatography* publishes papers on all aspects of **chromatography, electrophoresis** and related methods. Contributions consist mainly of research papers dealing with chromatographic theory, instrumental developments and their applications. The section *Biomedical Applications*, which is under separate editorship, deals with the following aspects: developments in and applications of chromatographic and electrophoretic techniques related to clinical diagnosis or alterations during medical treatment; screening and profiling of body fluids or tissues related to the analysis of active substances and to metabolic disorders; drug level monitoring and pharmacokinetic studies; clinical toxicology; forensic medicine; veterinary medicine; occupational medicine; results from basic medical research with direct consequences in clinical practice. In *Symposium volumes*, which are under separate editorship, proceedings of symposia on chromatography, electrophoresis and related methods are published.

Submission of Papers. The preferred medium of submission is on disk with accompanying manuscript (see *Electronic manuscripts* in the Instructions to Authors, which can be obtained from the publisher, Elsevier Science Publishers B.V., P.O. Box 330, 1000 AH Amsterdam, Netherlands). Manuscripts (in English; *four* copies are required) should be submitted to: Editorial Office of *Journal of Chromatography*, P.O. Box 681, 1000 AR Amsterdam, Netherlands, Telefax (+31-20) 5862 304, or to: The Editor of *Journal of Chromatography, Biomedical Applications*, P.O. Box 681, 1000 AR Amsterdam, Netherlands. Review articles are invited or proposed in writing to the Editors who welcome suggestions for subjects. An outline of the proposed review should first be forwarded to the Editors for preliminary discussion prior to preparation. Submission of an article is understood to imply that the article is original and unpublished and is not being considered for publication elsewhere. For copyright regulations, see below.

Publication. The *Journal of Chromatography* (incl. *Biomedical Applications*) has 40 volumes in 1993. The subscription prices for 1993 are:

J. Chromatogr. (incl. *Cum. Indexes, Vols. 601-650*) + *Biomed. Appl.* (Vols. 612-651):

Dfl. 8520.00 plus Dfl. 1320.00 (p.p.h.) (total ca. US\$ 5622.75)

J. Chromatogr. (incl. *Cum Indexes, Vols. 601-650*) only (Vols. 623-651):

Dfl. 7047.00 plus Dfl. 957.00 (p.p.h.) (total ca. US\$ 4573.75)

Biomed. Appl. only (Vols. 612-622):

Dfl. 2783.00 plus Dfl. 363.00 (p.p.h.) (total ca. US\$ 1797.75).

Subscription Orders. The Dutch guilder price is definitive. The US\$ price is subject to exchange-rate fluctuations and is given as a guide. Subscriptions are accepted on a prepaid basis only, unless different terms have been previously agreed upon. Subscriptions orders can be entered only by calendar year (Jan.-Dec.) and should be sent to Elsevier Science Publishers, Journal Department, P.O. Box 211, 1000 AE Amsterdam, Netherlands, Tel. (+31-20) 5803 642, Telefax (+31-20) 5803 598, or to your usual subscription agent. Postage and handling charges include surface delivery except to the following countries where air delivery via SAL (Surface Air Lift) mail is ensured: Argentina, Australia, Brazil, Canada, China, Hong Kong, India, Israel, Japan*, Malaysia, Mexico, New Zealand, Pakistan, Singapore, South Africa, South Korea, Taiwan, Thailand, USA. *For Japan air delivery (SAL) requires 25% additional charge of the normal postage and handling charge. For all other countries airmail rates are available upon request. Claims for missing issues must be made within six months of our publication (mailing) date, otherwise such claims cannot be honoured free of charge. Back volumes of the *Journal of Chromatography* (Vols. 1-611) are available at Dfl. 230.00 (plus postage). Customers in the USA and Canada wishing information on this and other Elsevier journals, please contact Journal Information Center, Elsevier Science Publishing Co. Inc., 655 Avenue of the Americas, New York, NY 10010, USA, Tel. (+1-212) 633 3750, Telefax (+1-212) 633 3764.

Abstracts/Contents Lists published in Analytical Abstracts, Biochemical Abstracts, Biological Abstracts, Chemical Abstracts, Chemical Titles, Chromatography Abstracts, Current Awareness in Biological Sciences (CABS), Current Contents/Life Sciences, Current Contents/Physical, Chemical & Earth Sciences, Deep-Sea Research/Part B: Oceanographic Literature Review, Excerpta Medica, Index Medicus, Mass Spectrometry Bulletin, PASCAL-CNRS, Referativnyi Zhurnal, Research Alert and Science Citation Index.

US Mailing Notice. *Journal of Chromatography* (ISSN 0021-9673) is published weekly (total 52 issues) by Elsevier Science Publishers (Sara Burgerhartstraat 25, P.O. Box 211, 1000 AE Amsterdam, Netherlands). Annual subscription price in the USA US\$ 4573.75 (subject to change), including air speed delivery. Second class postage paid at Jamaica, NY 11431. **USA**

POSTMASTERS: Send address changes to *Journal of Chromatography*, Publications Expediting, Inc., 200 Meacham Avenue, Elmont, NY 11003. Airfreight and mailing in the USA by Publications Expediting.

See inside back cover for Publication Schedule, Information for Authors and information on Advertisements.

© 1993 ELSEVIER SCIENCE PUBLISHERS B.V. All rights reserved.

0021-9673/93/\$06.00

No part of this publication may be reproduced, stored in a retrieval system or transmitted in any form or by any means, electronic, mechanical, photocopying, recording or otherwise, without the prior written permission of the publisher, Elsevier Science Publishers B.V. Copyright and Permissions Department, P.O. Box 521, 1000 AM Amsterdam, Netherlands.

Upon acceptance of an article by the journal, the author(s) will be asked to transfer copyright of the article to the publisher. The transfer will ensure the widest possible dissemination of information.

Special regulations for readers in the USA. This journal has been registered with the Copyright Clearance Center, Inc. Consent is given for copying of articles for personal or internal use, or for the personal use of specific clients. This consent is given on the condition that the copier pays through the Center the per-copy fee stated in the code on the first page of each article for copying beyond that permitted by Sections 107 or 108 of the US Copyright Law. The appropriate fee should be forwarded with a copy of the first page of the article to the Copyright Clearance Center, Inc., 27 Congress Street, Salem, MA 01970, USA. If no code appears in an article, the author has not given broad consent to copy and permission to copy must be obtained directly from the author. All articles published prior to 1980 may be copied for a per-copy fee of US\$ 2.25, also payable through the Center. This consent does not extend to other kinds of copying, such as for general distribution, resale, advertising and promotion purposes, or for creating new collective works. Special written permission must be obtained from the publisher for such copying.

No responsibility is assumed by the Publisher for any injury and/or damage to persons or property as a matter of products liability, negligence or otherwise, or from any use or operation of any methods, products, instructions or ideas contained in the materials herein. Because of rapid advances in the medical sciences, the Publisher recommends that independent verification of diagnoses and drug dosages should be made.

Although all advertising material is expected to conform to ethical (medical) standards, inclusion in this publication does not constitute a guarantee or endorsement of the quality or value of such product or of the claims made of it by its manufacturer.

This issue is printed on acid-free paper.

CONTENTS

(Abstracts/Contents Lists published in Analytical Abstracts, Biochemical Abstracts, Biological Abstracts, Chemical Abstracts, Chemical Titles, Chromatography Abstracts, Current Awareness in Biological Sciences (CABS), Current Contents/Life Sciences, Current Contents/Physical, Chemical & Earth Sciences, Deep-Sea Research/Part B: Oceanographic Literature Review, Excerpta Medica, Index Medicus, Mass Spectrometry Bulletin, PASCAL-CNRS, Referativnyi Zhurnal, Research Alert and Science Citation Index)

REGULAR PAPERS

Column Liquid Chromatography

- Dispersion in packed-column hydrodynamic chromatography
by G. Stegeman, J.C. Kraak and H. Poppe (Amsterdam, Netherlands) (Received December 16th, 1992). 149
- Cibacron Blue F3G-A-attached monosize poly(vinyl alcohol)-coated polystyrene microspheres for specific albumin adsorption
by A. Tuncel and A. Denizli (Ankara, Turkey), D. Purvis and C.R. Lowe (Cambridge, UK) and E. Pişkin (Ankara, Turkey) (Received November 17th, 1992). 161
- Separation of tetrachloro-*p*-dioxin isomers by high-performance liquid chromatography with electron-acceptor and electron-donor stationary phases
by U. Pyell, P. Garrigues, G. Félix, M.T. Rayez, A. Thienpont and P. Dentraygues (Talence, France) (Received November 18th, 1992) 169
- Extraction chromatography with modified poly(vinyl chloride) and di(2-ethylhexyl)dithiophosphoric acid
by L. Bromberg and G. Levin (Rehovot, Israel) (Received December 16th, 1992). 183
- Examination of the retention behavior of underivatized profen enantiomers on cyclodextrin silica stationary phases
by M.D. Beeson and Gy. Vigh (College Station, TX, USA) (Received December 14th, 1992) 197
- Rapid and complete chiral chromatographic separation of racemic quaternary tropane alkaloids. Complementary use of a cellulose-based chiral stationary phase in reversed-phase and normal-phase modes—a mechanistic study
by Th.R.E. Hampe (Ingelheim, Germany), J. Schlüter (Ingelheim and Münster, Germany), K.H. Brandt (Ingelheim, Germany), J. Nagel (Ridgefield, CT, USA), E. Lamparter (Ingelheim, Germany) and G. Blaschke (Münster, Germany) (Received September 29th, 1992) 205
- Preparative resolution of praziquantel enantiomers by simulated counter-current chromatography
by C.B. Ching, B.G. Lim, E.J.D. Lee and S.C. Ng (Singapore, Singapore) (Received December 14th, 1992) 215
- Sensitive assay system for nitrosamines utilizing high-performance liquid chromatography with peroxyoxalate chemiluminescence detection
by C. Fu, H. Xu and Z. Wang (Baoding, China) (Received November 9th, 1992) 221
- Protein sorting by high-performance liquid chromatography. I. Biomimetic interaction chromatography of recombinant human deoxyribonuclease I on polyionic stationary phases
by J. Cacia, C.P. Quan, M. Vasser, M.B. Sliwkowski and J. Frenz (South San Francisco, CA, USA) (Received December 22nd, 1992) 229
- Semi-automated chromatographic procedure for the isolation of acetylated N-terminal fragments from protein digests
by D.L. Crimmins and R.S. Thoma (St. Louis, MO, USA) (Received November 19th, 1992). 241
- Separation of isomeric compounds by reversed-phase high-performance liquid chromatography using Ag⁺ complexation. Application to *cis-trans* fatty acid methyl esters and retinoic acid photoisomers
by A. Baillet, L. Corbeau, P. Rafidison and D. Ferrier (Chatenay-Malabry, France) (Received December 10th, 1992) 251
- Comparative study of liquid chromatographic methods for the determination of cefadroxil
by C. Hendrix, Y. Zhu, C. Wijssen, E. Roets and J. Hoogmartens (Leuven, Belgium) (Received December 8th, 1992) 257
- Column Liquid Chromatography-Gas Chromatography*
- Combined high-performance aqueous size-exclusion chromatographic and pyrolysis-gas chromatographic-mass spectrometric study of lignosulphonates in pulp mill effluents
by E.R.E. van der Hage, W.M.G.M. van Loon, J.J. Boon, H. Lingeman and U.A.Th. Brinkman (Amsterdam, Netherlands) (Received December 24th, 1992) 263

(Continued overleaf)

Contents (continued)

Comparison of high-performance liquid and gas chromatography in the determination of organic acids in culture media of alkaliphilic bacteria
by S. Paavilainen and T. Korpela (Turku, Finland) (Received December 21st, 1992) 273

Gas Chromatography

Series-coupled capillary columns for the separation of N,(O)-trifluoroacetyl isopropyl derivatives of D,L-aspartic acid and L-hydroxyproline by gas chromatography
by X. Lou, X. Liu and L. Zhou (Dalian, China) (Received December 3rd, 1992) 281

Gas chromatographic determination of sodium monofluoroacetate as the free acid in an aqueous solvent
by B.A. Kimball and E.A. Mishalanie (Denver, CO, USA) (Received December 15th, 1992). 289

Comparison of hydrodistillation and supercritical fluid extraction for the determination of essential oils in aromatic plants
by S.B. Hawthorne (Grand Forks, ND, USA) and M.-L. Riekkola, K. Serenius, Y. Holm, R. Hiltunen and K. Hartonen (Helsinki, Finland) (Received December 10th, 1992) 297

Electrophoresis

Peroxyoxalate chemiluminescence detection in capillary electrophoresis
by N. Wu and C.W. Huie (Binghamton, NY, USA) (Received December 14th, 1992) 309

Automated preseparation derivatization on a capillary electrophoresis instrument
by R.J.H. Houben, H. Gielen and S.J. van der Wal (Geleen, Netherlands) (Received December 3rd, 1992) 317

Determination of salbutamol-related impurities by capillary electrophoresis
by K.D. Altria (Ware, UK) (Received December 28th, 1992) 323

Determination of quaternary alkaloids from Phellodendri Cortex by capillary electrophoresis
by Y.-M. Liu and S.-J. Sheu (Taipei, Taiwan) (Received December 9th, 1992). 329

SHORT COMMUNICATIONS

Gas Chromatography

Golay's paradox: linear *versus* non-linear chromatography
by F.G. Helfferich (University Park, PA, USA) (Received January 11th, 1993) 334

Prediction of the retention of polynuclear aromatic hydrocarbons in programmed-temperature gas chromatography
by T.C. Gerbino, G. Castello and U. Pettinati (Genova, Italy) (Received October 7th, 1992) 338

Chiral recognition of enantiomeric amides on a diamide chiral stationary phase by gas chromatography
by X. Lou, X. Liu and L. Zhou (Dalian, China) (Received January 4th, 1993) 345

Resolution of complex mixtures of flavonoid aglycones by analysis of gas chromatographic-mass spectrometric data
by T.J. Schmidt, I. Merfort and U. Matthiesen (Düsseldorf, Germany) (Received December 24th, 1992) 350

Planar Chromatography

Determination of some narcotic and toxic alkaloidal compounds by overpressured thin-layer chromatography with ethyl acetate as eluent
by J. Pothier, N. Galand and C. Viel (Tours, France) (Received December 24th, 1992). 356

AUTHOR INDEX 360

ERRATA 363

**FOR ADVERTISING
INFORMATION
PLEASE CONTACT OUR
ADVERTISING
REPRESENTATIVES**

USA/CANADA

Weston Media Associates

Mr. Daniel S. Lipner

P.O. Box 1110, GREENS FARMS, CT 06436-1110

Tel: (203) 261-2500, Fax: (203) 261-0101

GREAT BRITAIN

T.G. Scott & Son Ltd.

Tim Blake/Vanessa Bird

Portland House, 21 Narborough Road
COSBY, Leicestershire LE9 5TA

Tel: (0533) 753-333, Fax: (0533) 750-522

JAPAN

ESP - Tokyo Branch

Mr. S. Onoda

20-12 Yushima, 3 chome, Bunkyo-Ku
TOKYO 113

Tel: (03) 3836 0810, Fax: (03) 3839-4344

Telex: 02657617



REST OF WORLD

**ELSEVIER
SCIENCE
PUBLISHERS**

Ms. W. van Cattenburch
Advertising Department

P.O. Box 211, 1000 AE AMSTERDAM,
The Netherlands

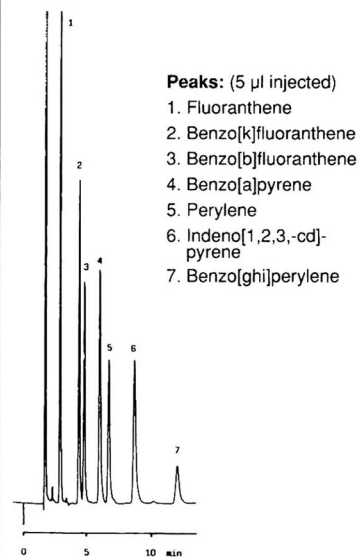
Tel: (20) 515.3220/21/22, Telex: 16479 els vi nl

Fax: (20) 683.3041

The Classic

NUCLEOSIL®
spherically shaped silica
gel for HPLC and GPC

Separation of PAH's



Column: ET 250/8/4 NUCLEOSIL® 5 PAH
Eluent: methanol - tetrahydrofuran (80:20)
Flow rate: 1.5 ml/min
Pressure: 190 bar
Detection: UV, 260 nm

NUCLEOSIL® packings for analytical
and preparative separations

- Spherical silica
- Pore diameters from 50 to 4000 Å
- Outstanding separation performance
and high batch to batch reproducibility
- High pressure stability even for
wide pore packings
- Numerous chemically bonded phases
available

Please ask for further information!

MACHERY-NAGEL



MACHERY-NAGEL GmbH & Co. KG · P.O. Box 10 13 52 · 5160 Düren
Germany · Tel. (0 24 21) 698-0 · Telex 833 893 mana d · Fax (0 24 21) 6 20 54
Switzerland: MACHERY-NAGEL AG · CH-4702 Oensingen · Tel. (062) 76 20 66
France: MACHERY-NAGEL S.à.r.l. · F-67038 Strasbourg Cedex · Tel 88.76.53.34

New Books in the Series

Journal of Chromatography Library

Volume 53

Hyphenated Techniques in Supercritical Fluid Chromatography and Extraction

edited by K. Jinno

This is the first book to focus on the latest developments in hyphenated techniques using supercritical fluids. The advantages of SFC in hyphenation with various detection modes, such as FTIR, MS, MPD and ICP and others are clearly featured throughout the book. Special attention is paid to coupling of SFE with GC or SFC.

1992 x + 334 pages

Price: US \$ 172.00 / Dfl. 275.00

ISBN 0-444-88794-6

Volume 52

Capillary Electrophoresis

Principles, Practice and Applications
by S.F.Y. Li

All aspects of CE, from the principles and technical aspects to the most important applications are covered in this volume. It is intended to meet the growing need for a thorough and balanced treatment of CE. The book will serve as a comprehensive reference work. Both the experienced analyst and the newcomer will find the text useful.

1992 xxvi + 582 pages

Price: US \$ 247.00 / Dfl. 395.00

ISBN 0-444-89433-0

"...anybody wanting to write a book on CE after this would look like a fool. Everything seems to be there, any detection system you have ever dreamed of, any capillary coating, enough electrolyte systems to saturate your wits, and more, and more.

...by far the most thorough book in the field yet to appear."

P.G. Righetti

Volume 51

Chromatography, 5th edition

Fundamentals and Applications of Chromatography and Related Differential Migration Methods

edited by E. Heftmann

Part A: Fundamentals and Techniques

Part A covers the theory and fundamentals of such methods as column and planar chromatography, countercurrent chromatography, field-flow fractionation, and electrophoresis. Affinity chromatography and supercritical-fluid chromatography are covered for the first time.

1992 xxxvi + 552 pages

Price: US \$ 219.00 / Dfl. 350.00

ISBN 0-444-88236-7

Part B: Applications

Part B presents various applications of these methods. New developments in the analysis and separation of inorganic compounds, amino acids, peptides, proteins, lipids, carbohydrates, nucleic acids, their constituents and analogs, porphyrins, phenols, drugs and pesticides are reviewed and summarized. Important topics such as environmental analysis and the determination of synthetic polymers and fossil fuels, are covered for the first time.

1992 xxxii + 630 pages

Price: US \$ 231.50 / Dfl. 370.00

ISBN 0-444-88237-5

Parts A & B

Set price: US \$ 406.50 / Dfl. 650.00

ISBN 0-444-88404-1

Volume 50

Liquid Chromatography in Biomedical Analysis

edited by T. Hanai

This book presents a guide for the analysis of biomedically important compounds using modern liquid chromatographic techniques. After a brief summary of basic liquid chromatographic methods and optimization strategies, the main part of the book focuses on the various classes of biomedically important compounds: amino acids, catecholamines, carbohydrates, fatty acids, nucleotides, porphyrins, prostaglandins and steroid hormones.

1991 xii + 296 pages

Price: US \$ 169.00 / Dfl. 270.00

ISBN 0-444-87451-8

"...will be valuable for anyone involved in liquid chromatography. It is timely and highlights throughout the techniques that are most successful. This is not so much a book to put on the shelf of the specialist for reference purposes, but instead it is a book which is meant to be read by the general reader to obtain perspective and insights into this general area."

Trends in Analytical Chemistry

ORDER INFORMATION

For USA and Canada

ELSEVIER SCIENCE PUBLISHERS

Judy Weislogel

P.O. Box 945

Madison Square Station,
New York, NY 10160-0757

Tel: (212) 989 5800

Fax: (212) 633 3880

In all other countries

ELSEVIER SCIENCE PUBLISHERS

P.O. Box 211

1000 AE Amsterdam

The Netherlands

Tel: (+31-20) 5803 753

Fax: (+31-20) 5803 705

US\$ prices are valid only for the USA & Canada and are subject to exchange rate fluctuations; in all other countries the Dutch guilder price (Dfl.) is definitive. Customers in the European Community should add the appropriate VAT rate applicable in their country to the price(s). Books are sent postfree if prepaid.



ELSEVIER
SCIENCE PUBLISHERS

Dispersion in packed-column hydrodynamic chromatography

Gerrit Stegeman, Johan C. Kraak and Hans Poppe*

Laboratory for Analytical Chemistry, University of Amsterdam, Nieuwe Achtergracht 166, 1018 WV Amsterdam (Netherlands)

(First received October 28th, 1992; revised manuscript received December 16th, 1992)

ABSTRACT

Zone broadening of dissolved polystyrenes in packed-column hydrodynamic chromatography (HDC) was studied for a column filled with 1.5- μm monodisperse non-porous particles. The reduced plate heights were observed to be almost constant with mobile phase velocity for reduced mobile phase velocities in a range 2–>150. In this velocity range, reduced plate heights well below 2 were obtained for polymer samples with molecular masses of 2200, 43 900 and 775 000. A comparison was made between measured plate heights and chromatographic theories of zone spreading. The effects of polymer size, polydispersity and polymer hydrodynamics on the measured plate heights are discussed.

INTRODUCTION

In hydrodynamic chromatography (HDC), macromolecules and particles are separated according to size. The separation mechanism takes advantage of the non-uniform flow profile in an open tube or in the interstitial space in packed columns [1–6]. Because of their size, large molecules are confined more than smaller molecules in the centre of a flow channel. As the streamline velocity is higher in the central part of the channel, large molecules are eluted before smaller molecules.

Research in HDC has so far mainly been aimed at describing the migration behaviour of macromolecules, in both theoretical and experimental studies [2–6], and relatively little attention has been paid to dispersion.

In this paper, we focus on the dispersion of random coil polymers in packed columns. In contrast to common chromatographic practice,

the size of the solutes is no longer infinitely small compared with the inter-particle flow channels. This means that wall exclusion and hydrodynamic particle–wall interactions may come into play.

Brenner and Gaydos [3] showed that a theoretical analysis of the dispersion of finite-sized solutes in open capillary tubes is severely complicated compared with infinitely small solutes. Modifying the Taylor–Aris dispersion theory to account properly for the finite solute to tube radius ratio appeared to be an elaborate process, even for apparently simple solutes such as isolated, neutrally buoyant, rigid spheres. For less symmetrical flow channels or for other than spherical homogeneous particles, realistic modelling becomes extremely involved.

In packed columns, rigorous calculations of the dispersion of finite-sized solutes are impossible because of the complex geometry of the interstitial flow channels. In several studies, therefore, attempts have been made to apply the dispersion models for open capillaries to packed columns. This is done by representing the inter-

* Corresponding author.

stitial flow channels as cylindrical tubes. In the simplest approach, a packed column is seen as a bundle of distinct capillaries without interconnections. This model evidently is an oversimplification as it does not describe the random mixing processes that occur in packed beds. Indeed, the predicted dispersion behaviour was found to be not in very good agreement with experimental observations [7]. Mixing effects are better accounted for when the interstitial channels are depicted as a capillary network, such as proposed by Saffman [8]. Silebi and Viola [9] modified Saffman's analysis by including wall exclusion resulting from the finite solute size. The dispersion behaviour as predicted by this modified model was in fairly good agreement with experimental results, although the effect of solute size on dispersion was not described successfully. A more sophisticated theory of the dispersion of finite-sized solutes in porous media was developed by Brenner and Adler [10,11]. However, from their general theory, it is not yet possible to derive simple relationships between dispersion in packed chromatographic columns and experimentally accessible quantities, because of the complex structure of the local interstitial velocity field.

We follow a different strategy, by starting with accepted chromatographic dispersion theories for zero-sized solutes in packed columns. Such theories have been developed by Giddings [12], Horváth and Lin [13], Huber [14] and Done and Knox [15]. Their models, which have been tested by a wealth of experimental data, are now well established. The most comprehensive analysis of dispersion in the (inter-particle) mobile phase was carried out by Giddings [16,17]. He provided a detailed description of the various contributions to zone spreading and estimated their magnitude. Part of this theory, which is most relevant to our work, will be briefly outlined below.

THEORY

Giddings' general equation for the dispersion in the mobile phase in terms of the plate height H is

$$H = H_L + \sum_i \left(\frac{1}{\frac{1}{H_{D,i}} + \frac{1}{H_{f,i}}} \right) \quad (1)$$

where the H terms are the different plate height contributions which will be treated subsequently. H_L is the plate height contribution from longitudinal molecular diffusion. This term describes the zone spreading along the column axis due to random thermal motion. In packed columns H_L can be written as

$$H_L = 2\gamma D_m / v \quad (2)$$

where γ is an obstructive factor accounting for the obstructions to diffusion along a straight line imposed by the packing particles and is *ca.* 0.6 for randomly packed impervious spheres [16,18], D_m is the diffusion coefficient in the mobile phase and v is the average mobile phase velocity. H_L is predicted by eqn. 2 to be larger for small molecules with large D_m values than for macromolecules with lower D_m values.

The second term (in parentheses) in eqn. 1, called the coupling terms, arises from the non-uniformities of flow velocity in the mobile phase. The summation sign allows for the inclusion of different types of velocity non-uniformities (denoted by i). The exchange of molecules between different velocity domains can occur due to flow and diffusion. Each parameter $H_{D,i}$ describes the plate height corresponding to a non-uniformity i when the flow dispersion would be counteracted by diffusion exclusively. When, in contrast, the exchange between velocity regimes is solely effected by random flow, dispersion resulting from velocity inequalities is represented by a parameter $H_{f,i}$. Coupling of $H_{D,i}$ and $H_{f,i}$, as given in each term of the summation in eqn. 1, amounts to the addition of lateral fluxes due to diffusion and convection in the exchange of molecules between flow paths of unequal velocities.

According to Giddings, the expression for $H_{D,i}$ is

$$H_{D,i} = \omega_i d_p^2 v / D_m \quad (3)$$

where ω_i is a constant for a given velocity inequality i and d_p is the diameter of the packing

particles. $H_{t,i}$ (often called the eddy diffusion term) can be written as

$$H_{t,i} = 2\lambda_i d_p \quad (4)$$

where λ_i is another constant, which depends on the type of velocity inequality.

For columns with non-porous packing particles, four sources of velocity non-uniformities are distinguished: (1) Trans-channel: the velocity in the centre of narrow inter-particle flow channels is higher than near the walls. This is analogous to the convective dispersion in open-tube flow after Taylor–Aris. (2) Short-range inter-channel: in some channels, the velocity is higher than in channels nearby because of differences in shape, openness and obstructions. (3) Long-range inter-channel: in some regions, the velocity is higher than in others because of differences in void geometry. This effect resembles (2) but is of longer range. (4) Trans-column: the velocity is potentially higher near the column wall than at the column centre, owing to looser packing near the wall. Approximate values for the constants ω_i and λ_i as given by Giddings [16] are summarized in Table I.

For a more universal representation of dispersion it is convenient to use dimensionless quantities. In terms of the dimensionless reduced plate height $h = H/d_p$ and reduced velocity $\nu = v d_p / D_m$, the equation for the mobile phase plate height becomes

$$h_{\text{kin}} = \frac{2\gamma}{\nu} + \sum_i \left(\frac{1}{\frac{1}{\omega_i \nu} + \frac{1}{2\lambda_i}} \right) \quad (5)$$

where h_{kin} is used to indicate that only kinetic

TABLE I

APPROXIMATE MAGNITUDES OF THE PARAMETERS ω_i AND λ_i

Type of velocity non-uniformity	ω_i	λ_i
(1) Trans-channel	0.01	0.5
(2) Short-range inter-channel	0.5	0.5
(3) Long-range inter-channel	2	0.1
(4) Trans-column	$0.001\rho^{2a}$	$0.02\rho^{2a}$

^a ρ = Column-to-particle diameter ratio.

contributions to zone broadening are considered. Other, non-kinetic, contributions will be treated in the discussion of the experimental results.

Although it is generally recognized that eqn. 5 has a sound theoretical basis, it does not reproduce experimental data well when the proposed values for λ_i and ω_i are used [19]. This can be ascribed largely to a failure to account correctly for trans-column effects. Giddings predicted an ever-increasing trans-column plate height with increasing column to particle diameter ratio ρ . Since then, it has been found experimentally that ρ does not affect plate heights to the extent of Giddings' predictions. Knox and Parcher [20] found that the trans-column plate height increases with ρ until $\rho \approx 10$ and then attains a constant value. In later work, it was even argued that trans-column effects are likely to become negligible for very large values of ρ [21].

Based on our results for a 4.6 mm I.D. column filled with 1.5- μm particles, Giddings' original theory predicts a trans-column plate height of at least 10^4 for reduced velocities exceeding 1. This is indeed far from our measured values, which were below 2, as will be shown later.

In Fig. 1, the mobile phase plate height contributions according to Giddings are shown for a column with non-porous particles. The

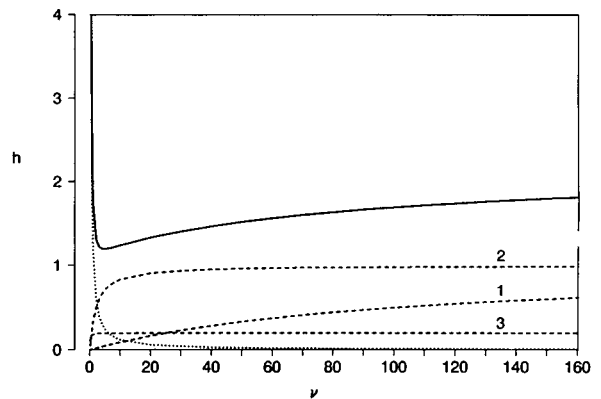


Fig. 1. Mobile phase plate height for unsorbed solutes in an infinite diameter column with non-porous particles. Plate height contributions according to Giddings (eqn. 5). Dotted line, longitudinal molecular diffusion; dashed lines, coupling terms with (1) trans-channel, (2) short-range inter-channel and (3) long-range inter-channel contributions; solid line, sum curve. ω_i and λ_i are taken from Table I; $\gamma = 0.6$.

trans-column effect is not included. As Giddings' trans-column effect results from the influence of the wall on the packing density, Fig. 1 represents the plate height contributions for a so-called "infinite diameter column" (*i.e.*, a column in which the solutes cannot reach the region of disturbed packing near the wall). The reduced velocity range in Fig. 1 corresponds to the range that will be covered by our measurements. It is obvious that at low reduced velocities, the plate height is dominated by the longitudinal molecular diffusion term. After the summed curve has passed through a minimum at $\nu = 5$, h_{kin} is determined mainly by the coupling terms. Note that the relative importance of each of the coupling terms can vary strongly with velocity.

Starting from Giddings' theory, Kennedy and Knox [22] derived a simpler, semi-empirical relationship for h , which in general fits experimental data well. In the Knox equation, the coupling process is approximated by a power term $\alpha\nu^n$ leading to [22]

$$h_{\text{kin}} = \frac{2\gamma}{\nu} + \alpha\nu^n \quad (6)$$

where α is a measure of the quality of the packing; α is usually within the range 0.5–1.5 for a well packed column [23], having a typical value of 1 [17,24]. Values of α below 0.5 have frequently been found for columns with $\rho < 10$ [20,25,26], but not often for $\rho > 10$ [22,27]. The exponent n is usually found to be *ca.* 0.33. When wall effects are eliminated n has been found to be much smaller. For these infinite diameter columns n values as low as 0.20 have been found by Knox and co-workers [20,27] using non-porous glass beads as packing particles. Hence the particular shape of the Knox equation appears to reflect the influence of wall effects.

In Fig. 2, two forms of the Knox equation are shown representing plate height contributions for unadsorbed solutes in (1) an infinite diameter column and (2) a walled column with non-porous particles. The factors α and n were determined by Knox and co-workers from experimental data for non-porous glass beads [22,27]. The most important difference between the infinite diameter column and the walled column is evidently

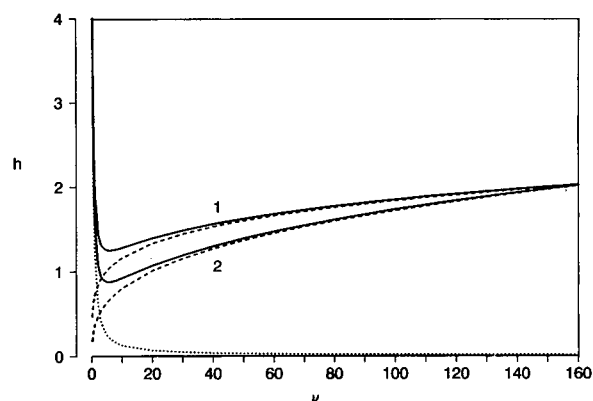


Fig. 2. Two forms of the Knox equation for the mobile phase plate height of unadsorbed solutes in (1) an infinite diameter column and (2) a walled column with non-porous particles (eqn. 6). Dotted line, longitudinal molecular diffusion; dashed lines, contribution from the complex flow pattern, $\alpha\nu^n$, for (1) an infinite diameter column with $\alpha = 0.73$ and $n = 0.20$ [27] and (2) a walled column with $\alpha = 0.37$ and $n = 0.33$ [20,22]; solid line, sum curve. In both instances $\gamma = 0.6$.

the different slope of the summed curves at higher reduced velocities. For the infinite diameter column, h rises more gradually with ν than for the walled column.

Both the Knox semi-empirical equations, which were derived using a curve-fitting procedure, and Giddings' theory, which is more directly related to the transport phenomena in a packed column, will be used in this study of dispersion in packed-column HDC.

EXPERIMENTAL

Materials and chemicals

The HDC column used was a 150×4.6 mm I.D. stainless-steel column (Chrompack, Middelburg, Netherlands), which was laboratory packed with monodisperse non-porous silica spheres. The packing particles were a kind gift from Professor K.K. Unger (Johannes Gutenberg Universität, Mainz, Germany). The size and the size distribution of the particles were determined from electron micrographs. Measurement of the diameter of 50 particles revealed an average particle diameter of $1.50 \mu\text{m}$. The relative standard deviation for the diameter of a single bead was 2.3%. More detailed information about the

higher molecular masses are of great importance for high-resolution separations in HDC. In addition, as H is almost independent of velocity, high-speed separations are possible without loss of resolution. These aspects are treated more extensively elsewhere [28].

Calculating plate heights from the peak width at half-height is only allowed when the peaks are sufficiently symmetrical. The peak shapes for the solutes used were observed to be symmetrical except for a slight tailing effect. Asymmetry factors, measured at one tenth of the peak height, were 1.1 (for toluene) to 1.3 at the lowest eluent velocity. Peak tailing was observed to increase with eluent velocity. At the highest velocity, asymmetry factors up to 1.6 were measured. The peak asymmetry for the polymer peaks was found to depend strongly on polymer concentration. At higher concentrations than those used for Fig. 3, peak asymmetry increased. This effect was more pronounced for higher molecular masses. Also, replacing the 100- μm I.D. tubing between the injector and column by 250- μm I.D. tubing worsened the peak shapes and increased the peak widths, especially for the higher molecular masses. The latter observation indicates that extra-column effects may be partly responsible for observed peak asymmetry.

The experimental results from Fig. 4 are plotted in reduced form in Fig. 5, together with the sum curves from Figs. 1 and 2. As predicted by chromatographic theory, the measured reduced plate heights all fall on a single curve. Comparing the experimental results with the theoretical lines, it is striking that they do not agree well with Knox's empirical line for a walled column. At velocities beyond the minimum in the plate height curve, the measured plate heights appear to depend much less on ν than predicted. The match cannot be improved if we choose a different value for α . Clearly, the exponent n in the Knox equation is too high to fit our results. Both lines for the infinite diameter column, which deviate from one another only slightly, correspond much better to experiment. The exponent $n = 0.20$ in the Knox equation is still too high to match the measured data, but the agreement is much better than for $n = 0.33$. In terms of the slope of the curve at higher

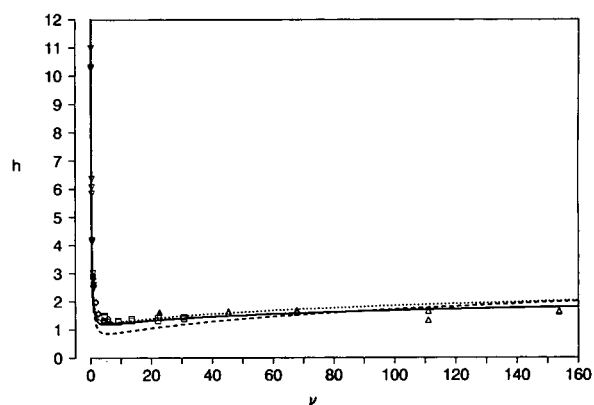


Fig. 5. Reduced plate height versus reduced velocity. Measured data: ∇ = toluene ($D_m = 2.66 \times 10^{-9} \text{ m}^2/\text{s}$ [29]); \diamond = PS 2200 ($D_m = 4.49 \times 10^{-10} \text{ m}^2/\text{s}$ [30]); \square = PS 43 900 ($D_m = 8.31 \times 10^{-11} \text{ m}^2/\text{s}$ [30]); \triangle = PS 775 000 ($D_m = 1.65 \times 10^{-11} \text{ m}^2/\text{s}$ [30]). The theoretical lines are the sum curves from Figs. 1 and 2. Solid line, Giddings, infinite diameter column; dotted line, Knox, infinite diameter column; dashed line, Knox, walled column.

velocities, the theoretical line by Giddings corresponds best to our experimental results.

Fig. 5 seems to indicate that a trans-column effect is absent or at least negligible in our measurements. This can be made more convincing when we look in more detail at the trans-column velocity inequalities.

The effect of the different packing structure near the column wall on axial dispersion was investigated by Knox *et al.* [27]. They concluded that the wall region of disturbed packing extends about 30 particle diameters inwards from the wall, much deeper than suggested in earlier work [20]. The extent to which this wall region affects axial dispersion depends on the fraction of the column cross-sectional area, occupied by the annulus of irregular packing. The effect of the wall region on dispersion thus depends strongly on ρ . For very large values of ρ (>1000), the effect of the wall region is likely to become negligible [21], in contrast to Giddings' prediction of an ever increasing plate height with increasing ρ .

In our column, ρ is as high as 3067, owing to the very small particles used. Assuming a disturbed wall region of 30 particle diameters, this layer still only covers 4% of the cross-sectional area of our column. This fraction is so small that

its effect on the peak shape is probably negligible. Even if wall effects do slightly change the peak shapes, they will not in the first place affect the peak width at half-height (which was used for our plate height calculations), but rather broaden the base of the peaks.

Disturbance of the packing near the wall is not the only source of trans-column velocity variations. Knox *et al.* [27] also measured small velocity variations in the central part of the column. They observed a slight increase in velocity with increasing distance from the column axis. The packing inhomogeneity causing this type of trans-column effect is believed to depend strongly on the packing method and on the uniformity of the packing particles [16,27]. As a major source, it has been put forward that during packing, larger particles tend to settle near the column wall and smaller particles near the centre. The use of very monodisperse packing particles may help to minimize trans-column velocity variations. Our particles being more uniform than those used by Knox and co-workers may be the reason why the slope of our h - v curve is smaller than their curve for infinite diameter columns [20,27].

A negligible trans-column contribution may be the reason why our measured data closely resemble both the theoretical and the empirical lines for an infinite diameter column rather than the empirical line for a walled column. It is, however, too early to conclude that dispersion in HDC is now clarified. Complications, *e.g.*, those arising from the finite solute size, and effects of polydispersity on measured plate heights, have not been considered so far. These aspects are discussed below.

Polydispersity

In the molecular mass distribution of the polymers used is not sufficiently narrow, polydispersity will increase the peak width and lead to higher apparent plate heights. Knox and McLennan [31] studied the effect of polydispersity on the measured plate height in size-exclusion chromatography (SEC). They obtained the following equations for the combined dispersion due to kinetic processes and polydispersity in SEC:

$$h_{\text{app}} = h_{\text{kin}} + h_{\text{poly}} \quad (7)$$

where

$$h_{\text{poly}} = \left(\frac{L}{d_p}\right)(P-1)(1+\beta)\left(\frac{S}{V_R}\right)^2 \quad (8)$$

h_{app} is the apparent (or measured) reduced plate height and h_{kin} and h_{poly} are the kinetic and polydispersity contributions. In the polydispersity term, L is the column length, β is a weak function of $(P-1)$ and has a value of about 1, S is the negative inverse slope of the calibration curve of $-d(V_R)/d(\ln M)$ and V_R is the elution volume of a solute.

It was shown that even in moderately efficient SEC columns, polydispersity is the dominating term in h_{app} unless P is well below 1.01. Whether polydispersity has an equal impact in HDC is easily investigated, as eqns. 7 and 8 are also valid in HDC. For a rough comparison of the effect of polydispersity on h_{app} in SEC and HDC, a comparison of the most relevant parameters h_{kin} and S suffices. In HDC, h_{kin} is usually much smaller than in SEC because of the absence of slow mass transfer between the pore space and the inter-particle channels [32]. In HDC the parameter S , describing the molecular mass selectivity, is not constant with molecular mass, because of the non-linear calibration graph. At the flattest part of the calibration graph the molecular mass selectivity may be as high as in conventional SEC. From this it appears that the impact of polydispersity on plate height in HDC may even be larger than in SEC.

Using eqns. 7 and 8, a more accurate estimate of the effect of polydispersity on the measured plate height can be made. In order to calculate h_{poly} for the polymer fractions used, the values of $(S/V_R)^2$ were determined from the experimental calibration graph which is shown in ref. 28. The values found were 1.39×10^{-5} for PS 2200, 3.78×10^{-4} for PS 43 900 and 6.19×10^{-3} for PS 775 000. Note that the difference in $(S/V_R)^2$ values reflects the distinction in molecular mass selectivity for the polymer samples. Here the column selectivity is clearly highest for PS 775 000 as a result of the curvature of the calibration graph.

Based on the $(S/V_R)^2$ values, the plate height

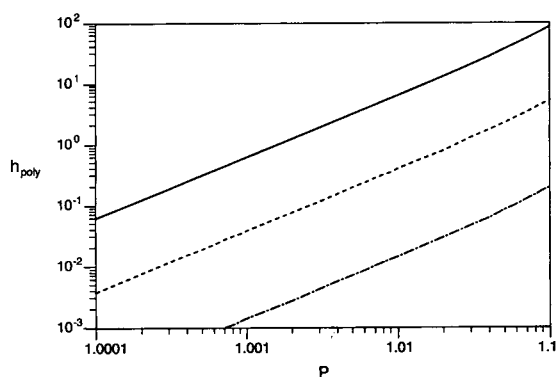


Fig. 6. Contribution from polydispersity to the reduced plate height for (dot-dashed line) PS 2200, (dashed line) PS 43 900 and (solid line) PS 775 000.

contribution from polydispersity, h_{poly} , is calculated as a function of polydispersity in Fig. 6.

For PS 2200, a polydispersity of 1.06 means that $h_{\text{poly}} = 0.1$. This is already relatively large compared with the measured reduced plate heights. For PS 43 900, h_{poly} is 0.4 for the specified polydispersity ceiling value of 1.01. Such a large value of h_{poly} should have increased the measured plate heights significantly compared with those for PS 2200. From Fig. 5 it appears, however, that the measured plate heights for PS 43 900 and PS 2200 are on a smooth curve and are not visibly shifted. Probably the actual polydispersity of the PS 43 900 sample is smaller than the maximum value specified by the manufacturer.

For PS 775 000, the manufacturer's value ($P = 1.01$) yields a calculated h_{poly} value of 6. This value is almost four times higher than the measured (total) reduced plate height. Here it is clear that the stated ceiling value is much higher than the actual polydispersity. The actual polydispersity of PS 775 000 cannot be determined exactly from our measurements as we do not know the precise magnitude of h_{kin} . If h_{app} were entirely determined by polydispersity (*i.e.*, $h_{\text{app}} = h_{\text{poly}} = 1.5$), we calculate a polydispersity of 1.002. Even this low value is actually still too high as it implies that $h_{\text{kin}} = 0$. A more realistic estimate of h_{poly} , on the basis of the plate heights measured for the smaller polymers, indicates that h_{poly} does not exceed 0.3, or in other words $P < 1.0005$.

Large differences between actual polydisper-

sities and ceiling values have been reported before in thermal field flow fractionation [33,34]. The explanation for these differences is that the stated ceiling values are very conservative estimates. Given the error in the individual determinations of the weight- and number-average molecular masses and considering the scatter in these values obtained by various techniques, the specified polydispersities may well be much higher than the actual polydispersities [35].

From the preceding discussion, it appears that the polydispersity of the polymer samples is an important plate height contribution in the high selectivity region of the HDC calibration graph. The separation power of the column used is so high that even for true polydispersities as low as 1.01 the measured plate heights are expected to be dominated by polydispersity. Even though the true polydispersities of the polymer samples used may be much lower than 1.01, the measured plate heights (for PS 43 900 and PS 775 000) are still likely to include a significant polydispersity contribution. In order to be assured that the measured plate heights are equal to h_{kin} , polymer samples with an extremely narrow molecular mass distribution, preferably real monodisperse samples, are required. Unfortunately, such samples are not available in the range of higher molecular masses. Another way to isolate h_{kin} is to measure h_{app} at a fixed eluent velocity on columns of different lengths (see eqns. 7 and 8). Extrapolation of h_{app} to zero column length should give values of h_{kin} . This procedure was not employed by us. As a result, we do not know the absolute magnitude of h_{kin} . The dependence of h_{kin} on ν can nevertheless still be obtained from Fig. 5 as polydispersity shifts the $h_{\text{kin}}-\nu$ curve by a fixed amount (equal to h_{poly}) towards higher apparent plate heights.

Polymer size

When the size of the flow channels is not enormously large compared with the size of the solute molecules, several effects that are not included in dispersion theories for infinitely small molecules may become of importance.

Exclusion regions. Owing to the finite size of the molecules, the centre of mass of a solute molecule is excluded from flow regions in the flow channel, within a distance of one effective

polymer radius from the wall. For flow in narrow channels between parallel plates and for flow in open tubes, the effect of wall exclusion on dispersion (leaving out hydrodynamic wall effects) can readily be expressed in modifications of plate height models for zero-sized solutes [2,36]. DiMarzio and Guttman [2] developed an expression for the convective contribution to axial dispersion for solute particles or radius r_p in open tubes of radius r_c . They found that the finite solute size reduces the convective term by a factor of $[1 - (r_p/r_c)]^6$ compared with the limit for infinitely small molecules. In capillary HDC, where r_p/r_c ratios are usually in the range 0.01–0.3, the reduction of plate heights can be profound.

In packed columns, the effect of wall exclusion on dispersion cannot be described as precisely as for open capillary tubes, so a more approximate approach is required. Exclusion layers are expected to have a predominant influence on the convective dispersion in a single flow channel by reducing the cross-sectional diffusion distance, as illustrated in Fig. 7. In Giddings' theory this implies a reduction of the trans-channel plate height term. As wall exclusion is a short-range effect, it will not in the first place influence the other coupling terms.

There is, however, one effect of longer range we might have to consider, namely the effect of exclusion on the average solute velocity. Wall exclusion causes the average velocity of finite sized solutes to be higher than the average

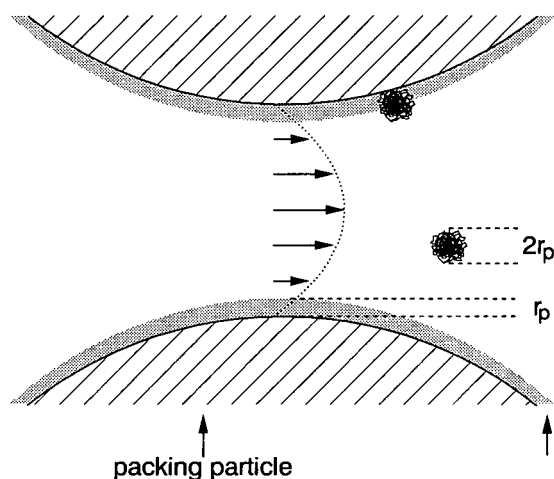


Fig. 7. Wall exclusion in packed columns.

solvent velocity. This exclusion effect is much stronger in narrow than in wider channels. Exclusion may thus partly compensate for the lower average eluent velocity in narrower flow channels and more densely packed column regions. It can therefore reduce the difference in solute velocity between channels of different cross-sectional size. In terms of Giddings' dispersion theory, this would reduce the inter-channel velocity variations for finite-sized solutes. We do not expect that such inter-channel effects are pronounced and rather focus on the trans-channel effect.

We can make a rough estimate of the exclusion effect when we assume that the trans-channel term $h_{D,1}$ in Giddings' model is reduced to the same extent as the convective dispersion in an open tube of comparable cross-sectional size after DiMarzio and Guttman [2]. In order to calculate r_p/r_c we then need to assign an equivalent capillary radius to the flow channels in a packed column. As an equivalent radius we obviously choose the hydraulic radius, because it has been shown to be convenient in modelling size effects on retention behaviour in HDC [1,37]. For the column used, we obtain a hydraulic radius of $0.32 \mu\text{m}$ [28]. Consequently, the r_p/r_c ratios for the polymers used are 0.0034 for PS 2200, 0.020 for PS 43 900 and 0.11 for PS 775 000 [28]. The estimated reduction in ω_1 is then 2%, 11% and 47%, respectively. This reduction seems pronounced but, as it only affects one coupling term, the effect on the overall plate height curve is small. A change in $h_{D,1}$ most severely affects h_{kin} at the higher reduced velocities (see also Fig. 1). At $\nu = 160$ the calculated plate height reduction due to wall exclusion is 0.005 for PS 2200, 0.03 for PS 43 900 and 0.2 for PS 775 000. Under the actual experimental conditions, the shift for PS 2200 and PS 43 900 is even smaller because the reduced velocities for these solutes are smaller.

Hydrodynamic wall effects. When the transport of finite sized particles in small flow channels is considered, hydrodynamic particle–wall interactions should also be accounted for. The role of such interactions in the transport of homogeneous spherical particles in cylindrical tubes has been treated extensively by Brenner and Gaydos [3]. Owing to hydrodynamic wall

effects, the particle diffusivity is not a constant as in unbounded fluids. Rather, axial and transverse diffusivities are functions of the transverse position of the particle, both becoming zero for a sphere in contact with the wall. Consequently, the mean axial molecular diffusion coefficient is diminished below its value in an unbounded fluid. The diffusivity is reduced to a larger extent when the ratio of the particle diameter to the flow channel diameter increases. If we again consider the r_p/r_c values for our packed column, the diffusivity reduction, calculated according to Brenner and Gaydos [3], would be 2%, 7% and 30% for PS 2200, 43 900 and 775 000, respectively. Although these values are strictly valid only for open tubes, they show that a pronounced reduction of diffusivity is also to be expected in our packed column.

Another result of hydrodynamic particle–wall interactions is that the centre of a solute molecule lags the local flow in which it is suspended [1–4]. This hydrodynamic retardation effect (so-called slip flow) also varies with the transverse position of the solute.

When hydrodynamic wall effects are considered together with wall exclusion, the convective dispersion of finite sized particles in an open tube differs from that of zero-sized solutes by a factor of $1 - (1.862r_p/r_c) + 9.68(r_p/r_c)^2$ [3]. From this factor it appears that the finite solute size reduces dispersion compared with infinitely small solutes, provided that the r_p/r_c ratio does not exceed 0.14. If we again depict the interstitial flow channels in a packed column as open tubes, we calculate a reduction in convective dispersion of 0.6%, 3% and 9% for PS 2200, 43 900 and 775 000, respectively. These percentages are substantially lower than those given under *Exclusion regions*, where only wall exclusion was considered. Including hydrodynamic wall effects therefore appears to diminish the overall effect of finite solute size on convective dispersion in an open tube. When the impact of both hydrodynamic wall effects and wall exclusion on h_{kin} is calculated (as under *Exclusion regions*), it appears to be negligibly small for the polymer fractions used. If our calculations are in any way able to give realistic estimates of hydrodynamic wall effects and wall exclusion in packed columns, then the overall effect of finite solute

size on dispersion in packed-column HDC is negligibly small. This is speculative, however, because applying capillary models to describe hydrodynamic wall effects and wall exclusion in packed columns may well prove to be an oversimplification.

Other considerations

In addition to the polydispersity and size effects mentioned above, other factors might also influence the dispersion in packed columns. One important factor might be the distribution of solutes over the accessible radial positions. Until now we assumed this distribution to be uniform, but this need not be so in practice. Owing to, for example, hydrodynamic forces, depletion of macromolecules in the wall regions and enrichment in the centre of a flow channel may occur. Phenomena leading to opposite effects have also been described [28]. A disturbance of the equilibrium concentration profile in a flow channel may either increase or decrease dispersion. A pronounced decrease in dispersion has, for example, been reported in open tubes where particles were focused into an annular ring owing to the “tubular pinch” effect [4,38,39]. Possibly a build-up of a transverse concentration profile occurs also in flow channels in a packed column. However, the effect on h is expected to be smaller than in open tubes, for the following reasons. First, a build-up of a concentration profile in packed columns is counteracted by stream splitting and other randomizing flow phenomena. Second, a concentration profile mainly has a short-range effect, just like wall exclusion. In terms of Giddings’ plate height model, a concentration profile will influence the trans-channel effect, but will not change dispersion resulting from velocity differences existing between neighbouring channels or between certain regions in the column. By changing only one coupling term, the effect of a non-uniform concentration profile on the measured plate height will be relatively small. Accurate estimates are unfortunately obstructed by the complex flow pattern in packed columns.

CONCLUSIONS

In packed-column HDC, the reduced plate

heights for polystyrenes of widely differing molecular masses and toluene appear to lie on one smooth line. Measured reduces plate heights, in a wide range of reduced velocities, are in good accordance with both Giddings' theoretical model and the Knox semi-empirical model for the dispersion of small molecules in packed infinite diameter columns. The measured plate heights indicate that the effect of the disturbed packing near the column wall and other trans-column effects do not influence zone broadening to a large extent. For the higher molecular masses (which are of actual interest in HDC), the main kinetic source of zone spreading is the random flow in a packed column. The polydispersity of the solutes appears to be a severe limitation for obtaining h_{kin} in the high selectivity region of the HDC calibration graph. The effect of size and hydrodynamic particle-wall interactions on dispersion in packed column HDC cannot be determined exactly. According to approximate theoretical calculations and available experimental evidence, they do not affect h to a large extent.

ACKNOWLEDGEMENTS

We very much appreciate the critical comments made on the original manuscript by Dr. R. Tijssen. This work was supported by the Netherlands Foundation for Chemical Research (SON), with financial aid from the Netherlands Organization for Scientific Research (NWO) under grant 700-344-003.

REFERENCES

- 1 A.J. McHugh, *CRC Crit. Rev. Anal. Chem.*, 15 (1984) 63.
- 2 E.A. DiMarzio and C.M. Guttman, *Macromolecules*, 3 (1970) 131 and 681.
- 3 H. Brenner and L.J. Gaydos, *J. Colloid Interface Sci.*, 58 (1977) 312.
- 4 H.J. Ploehn, *Int. J. Multiphase Flow*, 13 (1987) 773.
- 5 R. Tijssen, J. Bos and M.E. van Kreveland, *Anal. Chem.*, 58 (1986) 3036.
- 6 H. Small, *J. Colloid Interface Sci.*, 48 (1974) 147.
- 7 R.F. Stoitsits, G.W. Poehlein and J.W. Vanderhoff, *J. Colloid Interface Sci.*, 64 (1978) 201.
- 8 P.G. Saffman, *J. Fluid Mech.*, 7 (1960) 194.
- 9 C.A. Silebi and J.P. Viola, *Org. Coat. Plast. Chem.*, 42 (1980) 151.
- 10 H. Brenner, *Philos. Trans. R. Soc. London, Ser. A*, 297 (1980) 81.
- 11 H. Brenner and P.M. Adler, *Philos. Trans. R. Soc. London, Ser. A*, 307 (1982) 149.
- 12 J.C. Giddings, *J. Chromatogr.*, 5 (1961) 61.
- 13 C. Horváth and H.J. Lin, *J. Chromatogr.*, 126 (1976) 401.
- 14 J.F.K. Huber, *J. Chromatogr. Sci.*, 7 (1969) 85.
- 15 J.N. Done and J.H. Knox, *J. Chromatogr. Sci.*, 10 (1972) 606.
- 16 J.C. Giddings, *Dynamics of Chromatography. Part 1. Principles and Theory*, Marcel Dekker, New York, 1965.
- 17 J.C. Giddings, *Unified Separation Science*, Wiley-Interscience, New York, 1991.
- 18 J.H. Knox and L. McLaren, *Anal. Chem.*, 36 (1964) 1477.
- 19 J.H. Knox, *Anal. Chem.*, 38 (1966) 253.
- 20 J.H. Knox and J.F. Parcher, *Anal. Chem.*, 41 (1969) 1599.
- 21 J.H. Knox, *J. Chromatogr. Sci.*, 15 (1977) 352.
- 22 G.J. Kennedy and J.H. Knox, *J. Chromatogr. Sci.*, 10 (1972) 549.
- 23 R.W. Stout, J.J. DeStefano and L.R. Snijder, *J. Chromatogr.*, 282 (1983) 263.
- 24 J.N. Done, J.H. Knox and J. Loheac, *Applications of High-Speed Liquid Chromatography*, Wiley-Interscience, London, 1974, Ch. 4.
- 25 R.T. Kennedy and J.W. Jorgenson, *Anal. Chem.*, 61 (1989) 1128.
- 26 K.E. Karlsson and M. Novotny, *Anal. Chem.*, 60 (1988) 1662.
- 27 J.H. Knox, G.R. Laird and P.A. Raven, *J. Chromatogr.*, 122 (1976) 129.
- 28 J.C. Kraak, H. Poppe and R. Tijssen, in preparation.
- 29 R.C. Reid, J.M. Prausnitz and T.K. Sherwood, *The Properties of Gases and Liquids*, McGraw-Hill, New York, 3rd ed., 1977.
- 30 W. Mandema and H. Zeldenrust, *Polymer*, 18 (1977) 835.
- 31 J.H. Knox and F. McLennan, *Chromatographia*, 10 (1977) 75.
- 32 G. Stegeman, J.C. Kraak and H. Poppe, *J. Chromatogr.*, 550 (1991) 721.
- 33 M.E. Schimpf, P.S. Williams and J.C. Giddings, *J. Appl. Polym. Sci.*, 37 (1989) 2059.
- 34 M.E. Schimpf, M.N. Meyers and J.C. Giddings, *J. Appl. Polym. Sci.*, 33 (1987) 117.
- 35 F.P. Warner, personal communication.
- 36 J.C. Giddings, *Sep. Sci. Technol.*, 13 (1978) 241.
- 37 G. Stegeman, R. Oostervink, J.C. Kraak, H. Poppe and K.K. Unger, *J. Chromatogr.*, 506 (1990) 547.
- 38 R.J. Noel, K. Gooding, F.E. Regnier, D.M. Ball, C. Orr and H.E. Mullins, *J. Chromatogr.*, 166 (1978) 373.
- 39 R. Tijssen, in F. Dondi and G. Guiochon (Editors), *Theoretical Advancement in Chromatography and Related Separation Techniques*, Kluwer, Dordrecht, 1992, pp. 397–441.

Cibacron Blue F3G-A-attached monosize poly(vinyl alcohol)-coated polystyrene microspheres for specific albumin adsorption

Ali Tuncel and Adil Denizli

Chemical Engineering Department, Hacettepe University, P.K. 716, Kızılay, 06420 Ankara (Turkey)

Duncan Purvis and Chris R. Lowe

Institute of Biotechnology, Cambridge University, Cambridge (UK)

Erhan Pişkin*

Chemical Engineering Department, Hacettepe University, P.K. 716, Kızılay, 06420 Ankara (Turkey)

(First received August 25th, 1992; revised manuscript received November 17th, 1992)

ABSTRACT

Monosize polystyrene (PS) microbeads (4 μm in diameter) were produced by phase inversion polymerization of styrene in ethanol–methoxyethanol medium. They were coated with poly(vinyl alcohol) (PVAL) by adsorption and chemical cross-linking to decrease the non-specific protein adsorption. Cibacron Blue F3G-A was then attached for specific protein adsorption. The adsorption conditions were optimized to increase the amount of PVAL by changing the initial concentration of PVAL, and using different types of salts at different ionic strengths. Higher amounts of PVAL (up to 19 mg PVAL/g PS) were loaded by increasing the PVAL initial concentration and by using Na_2SO_4 at a higher ionic strength (0.2). Bovine serum albumin (BSA) adsorption and desorption on these PS-based microbeads were also investigated under different conditions. PVAL coating prevented the non-specific BSA adsorption. A higher amount of BSA (up to 60 mg BSA/g dye-attached PS/PVAL) was specifically adsorbed on dye-attached PS microbeads, especially around pH 5 and lower ionic strengths (0.01). About 90% of the adsorbed BSA was desorbed in 1 h by using 0.5 M NaSCN.

INTRODUCTION

The interest in and demand for proteins in biotechnology, biochemistry and medicine have contributed to an increased exploitation of affinity chromatography. Unlike other forms of protein separation, affinity chromatography relies on the phenomenon of biological recognition, which enables biopolymers to recognize specifically, and bind reversibly, their complementary

ligands (*e.g.*, enzymes) and their substrates, hormones and their receptors, antibodies and their antigens [1–3].

Unfortunately, the preparation of sorbents carrying biological ligands is usually very expensive because the ligands themselves often require extensive purification and it is difficult to immobilize them on the carrier matrix with retention of their biological activity. As an alternative to their natural biological counterparts, the reactive triazinyl dyes have been investigated as ligands for protein affinity separation [4–6]. These dyes are able to bind proteins in a remarkably specific

* Corresponding author.

manner. They are inexpensive, readily available, biologically and chemically inert and are easily coupled to support materials. Cibacron Blue F3G-A and many other reactive dyes have been coupled to a variety of supports including agarose, cellulose, polyacrylamide, Sephadex, silica and glass [7–12]. Dye-ligand chromatography has now permitted the purification of a wide range of proteins (*e.g.*, lactate hydrogenase, alcohol dehydrogenase, hexokinase, carboxyl peptidase) [4–12].

Recently we prepared monosize polystyrene (PS) microbeads [13,14], and in this work we attempted to use these microbeads as a carrier matrix for affinity purification of proteins. In order to prevent non-specific interactions between the hydrophobic polystyrene surface and protein molecules, and also to attach the ligand (*i.e.*, Cibacron Blue F3G-A) to the carrier matrix, these microbeads were coated with a hydrophilic layer, namely poly(vinyl alcohol) (PVAL). We selected albumin as a potential model protein. We studied both non-specific albumin adsorption on the polystyrene microbeads and also specific albumin adsorption on the dye-attached PS/PVAL microbeads. This paper describes the methods of preparation of PS/PVAL microbeads and dye attachment, and presents the results of albumin adsorption and desorption studies.

EXPERIMENTAL

Production of monosize PS microbeads

Monosize PS microbeads were produced by phase inversion polymerization of styrene. Details of the polymerization procedure were given elsewhere and are summarized below [15].

Styrene was obtained from Yarpet and was first treated with NaOH solution to remove inhibitor. The solvents, 2-methoxyethanol (BDH) and ethanol (Merck) were used without further purification. The initiator was 2,2'-azobisisobutyronitrile (AIBN) (BDH). The steric stabilizer, polyacrylic acid, was prepared by solution polymerization of acrylic acid (BDH) in 1,4-dioxane (BDH) as described previously [15]. All of the ingredients were dissolved in the solvent mixture. This single phase was polymerized at 75°C for 16 h, and then at 80°C for 8 h.

The stirring rate was 250 rpm. The phase inversion polymerization recipe and conditions to obtain 4- μ m monosize PS microbeads are given in Table I.

The PS microbeads were first cleaned with doubly distilled water by using the serum replacement technique and then treated with an anion- and cation-exchange resin mixture (H⁺ and OH⁻ type, Amberlite) (BDH) to remove the stabilizer and initiator molecules physically attached to the surfaces of the microbeads.

Coating of PS microbeads with PVAL

Monosize PS microbeads were coated with PVAL by a two-step procedure. In the first step, PVAL (average M_r 14 000, 100% hydrolysed) (Aldrich) was deposited on the surface of PS microbeads by a simple adsorption process carried out in an aqueous medium. In order to establish the optimum adsorption conditions, PVAL adsorption experiments were performed in the presence of three different salts, NaCl, CaCl₂ and Na₂SO₄. These adsorption studies were repeated at three different ionic strengths (0.05, 0.1 and 0.2). The initial PVAL concentration was also changed between 10 and 700 mg/l. In a typical adsorption experiment, first a suitable amount of PVAL was dissolved in 100 ml of water and the ionic strength of solution was adjusted by adding salt, then 3 g of dried PS microbeads were added. The solution was stirred for 2 h (*i.e.*, the equilibrium time, determined in preliminary studies) with a magnetic stirrer at 200 rpm at 25°C. At the end of the equilibrium period, microbeads were separated from the solution by centrifugation. The PVAL adsorbed

TABLE I

POLYMERIZATION RECIPE AND CONDITIONS FOR THE PRODUCTION OF MONOSIZE POLYSTYRENE MICROBEADS WITH A DIAMETER OF 4 μ m

AIBN	0.75 g
Styrene	35 ml
Ethanol	100 ml
2-Methoxyethanol	100 ml
Polyacrylic acid	3.5 g
Temperature and time	75°C for 16 h and 80°C for 8 h
Stirring rate	250 rpm

on the PS microbeads was determined by measuring the initial and final concentrations of PVAL within the adsorption medium, according to the KI-I₂ method, spectrophotometrically at 690 nm [16].

In the second step, PVAL molecules adsorbed on the PS microbeads were chemically cross-linked to give a stable PVAL coating on the microbeads. After adsorption of PVAL from a suitable solution, the final acid concentration of the medium was adjusted to 0.1 M by adding HCl. A 10-mg amount of terephthaldehyde (Sigma) was dissolved in 10 ml of water and this solution was added to the previous medium. The batch was first stirred for 48 h at 500 rpm at 25°C. The temperature was then increased to 80°C and cross-linking was completed in 4 h in a sealed reactor with a stirring rate of 400 rpm. The microbeads were filtered and washed several times with distilled water. The PVAL-coated microbeads were stored under distilled water.

Characterization of microbeads

The size and size distribution of PS microbeads were measured by using an optical microscope (Nikon, Alphaphot YS). The PS microbeads were filtered and dried in a vacuum oven and then optical micrographs were taken. The presence of PVAL on the surface of the PS microbeads was confirmed by IR spectrophotometry (Hitachi Model 230 instrument). PS and PS/PVAL microbeads were filtered and washed several times with distilled water and dried in a vacuum oven. The IR spectra of the dried microbeads in a KBr (IR grade, Merck) disc were obtained. The IR spectrum of a KBr disc containing no dried polymeric microbeads was also recorded and no hydroxyl peak which might originate from the moisture of KBr was detected in this spectrum.

Dye attachment to PS/PVAL microbeads

A 300-mg amount of Cibacron Blue F3GA (Polyscience) was dissolved in 10 ml of water. This dye solution was added to the aqueous microbeads latex prepared by dispersing 3.0 g of PS/PVAL microbeads in 90 ml of distilled water, then 4 g of NaOH were added. The medium was heated at 80°C in a sealed reactor for 4 h at a

stirring rate of 400 rpm. The microbeads were filtered and washed with distilled water and methanol several times until all the unbound dye was removed. The microbeads carrying the dye were then redispersed in 30 ml of distilled water.

BSA adsorption and desorption studies

Bovine serum albumin (BSA, lyophilized, Fraction V; Sigma) was selected as a model protein. BSA adsorption on the PS, PS/PVAL and dye-attached PS/PVAL microbeads was studied. Adsorption studies were performed at different pH values. The pH of the adsorption medium was changed between 4 and 8 by using different buffer systems (CH₃COONa–CH₃COOH for pH 4–6, K₂HPO₄–KH₂PO₄ for pH 7 and NH₃–NH₄Cl for pH 8). Adsorption experiments were repeated at two different ionic strengths (0.01 and 0.1, adjusted by using NaCl). The initial BSA concentration was varied between 0.5 and 7.0 mg/ml. In a typical adsorption experiment, BSA was dissolved in 25 ml of buffer solution containing NaCl, 0.2 g of microbeads was added and the adsorption experiments were conducted for 2 h at 25°C at a stirring rate of 100 rpm. At the end of equilibrium period, the microbeads were separated from the solution by centrifugation. The albumin adsorption capacity was determined by measuring the initial and final concentrations of BSA within the adsorption medium spectrophotometrically at 280 nm [17–19].

BSA desorption experiments were performed in a buffer solution containing 0.5 M NaSCN at pH 8.0. The BSA-adsorbed microbeads were placed in the desorption medium and stirred for 1 h at 25°C. The final BSA concentration was determined spectrophotometrically at 280 nm. The desorption ratio was calculated from the amount of BSA adsorbed on the microbeads and the final BSA concentration in the desorption medium.

RESULTS AND DISCUSSION

Characteristics of PS microbeads

As shown in Fig. 1, monosize (R.S.D. <1%) PS microbeads with a diameter of 4 μm were

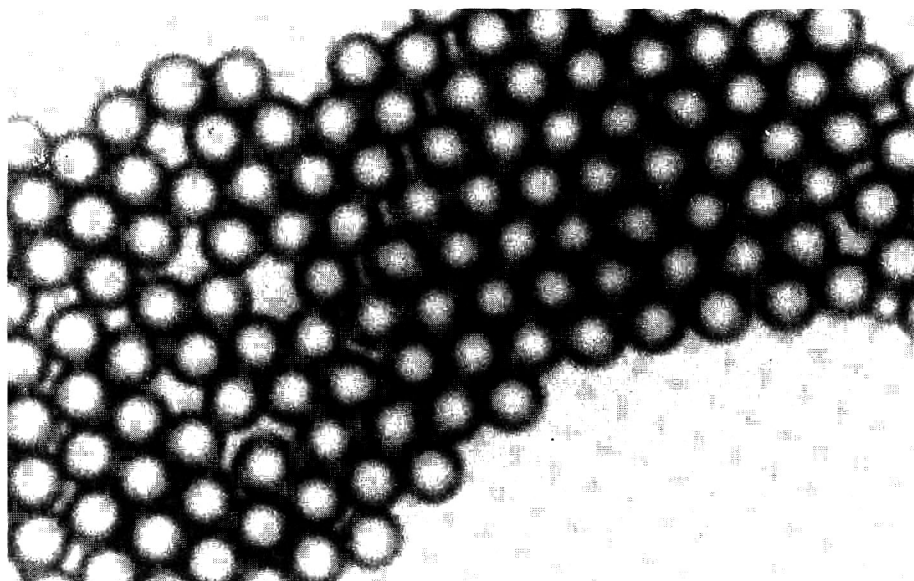


Fig. 1. Optical micrograph of monosize PS microbeads ($4 \mu\text{m}$ in diameter).

obtained at the polymerization conditions given in Table I.

The presence of PVAL on the surface of PS/PVAL microbeads was confirmed by IR spectrophotometry. Fig. 2 shows the IR spectra of both PS and PS/PVAL microbeads. The hydroxyl band observed at 3500 cm^{-1} indicated the presence of PVAL on the PS/PVAL surface.

The blue colour of Cibacron Blue F3G-A-attached PS/PVAL microbeads clearly indicated

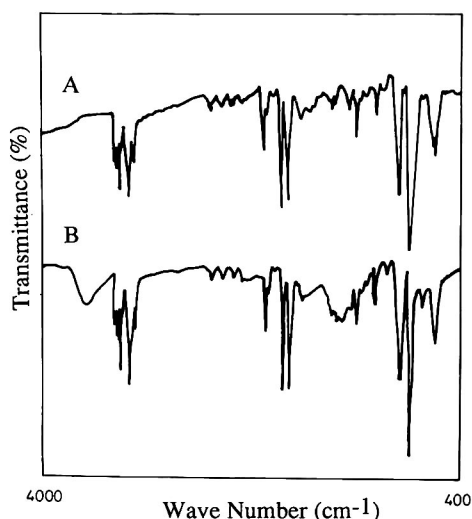


Fig. 2. IR spectra of (A) PS and (B) PS/PVAL microbeads.

the presence of dye on the surfaces of the microbeads.

PVAL adsorption/coating

The PVAL adsorption rate and capacity on PS microbeads were studied in adsorption experiments in which PVAL was adsorbed from aqueous PVAL solutions (consisting of only PVAL and distilled water) with different initial PVAL concentrations. Fig. 3A gives the adsorption rate curves. These curves indicate that the adsorption process was completed within 2 h and this value can be considered to be the equilibrium time for PVAL adsorption. The plateau values of these curves give the adsorption capacities of PS microbeads which change with the initial concentration of PVAL in the adsorption medium. The adsorption isotherm (at 25°C) in Fig. 3B was obtained by using the plateau values of these curves. As can be seen, the amount of PVAL absorbed first increased with increasing initial PVAL concentration, but reached a plateau after an initial PVAL concentration of 500 mg/l . This plateau means that PVAL adsorption on PS microbeads is typically a Langmuir-type monolayer adsorption [14].

In order to increase the amount of PVAL adsorbed on the PS microbeads, three different

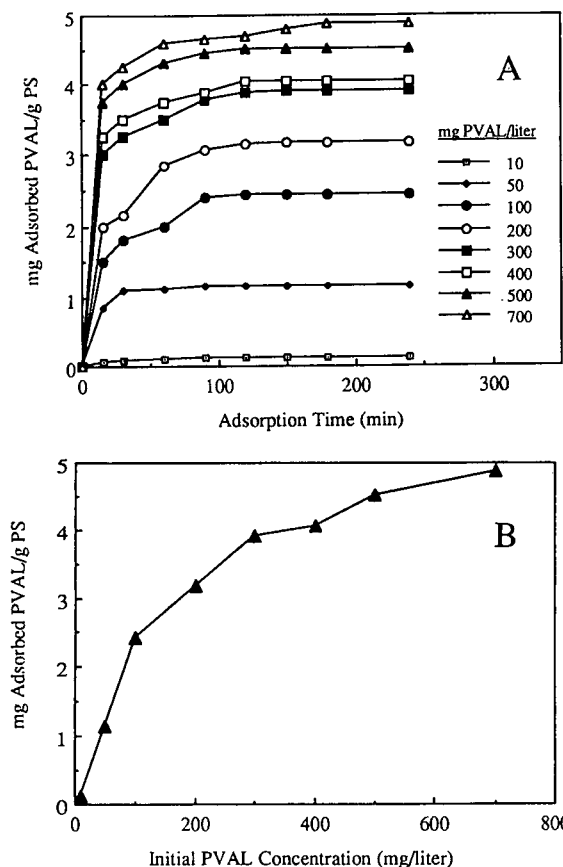


Fig. 3. PVAL adsorption on PS microbeads: (A) PVAL adsorption rate curves; and (B) PVAL adsorption isotherm. Initial PVAL concentration: □ = 10; ◆ = 50; ● = 100; ○ = 200; ■ = 300; ◻ = 400; ▲ = 500; △ = 700 mg/l.

salts, NaCl, CaCl₂ and Na₂SO₄, were added to the adsorption medium. The ionic strength of the medium was also varied between 0.05 and 0.2 by simply changing the concentration of these salts. It should be noted that no aggregation of microbeads was observed within this ionic strength range.

Examples of PVAL adsorption isotherms are given in Fig. 4. The results indicate that the largest amount of PVAL was adsorbed from the medium containing Na₂SO₄. The amount of PVAL adsorbed on the microbeads increased with increasing ionic strength of each salt. The maximum PVAL adsorption capacity obtained in this study was 12.7 mg/m² (or 19.0 mg/g PS) (with an initial PVAL concentration of 700 mg/l, Na₂SO₄ as the salt and the ionic strength 0.2).

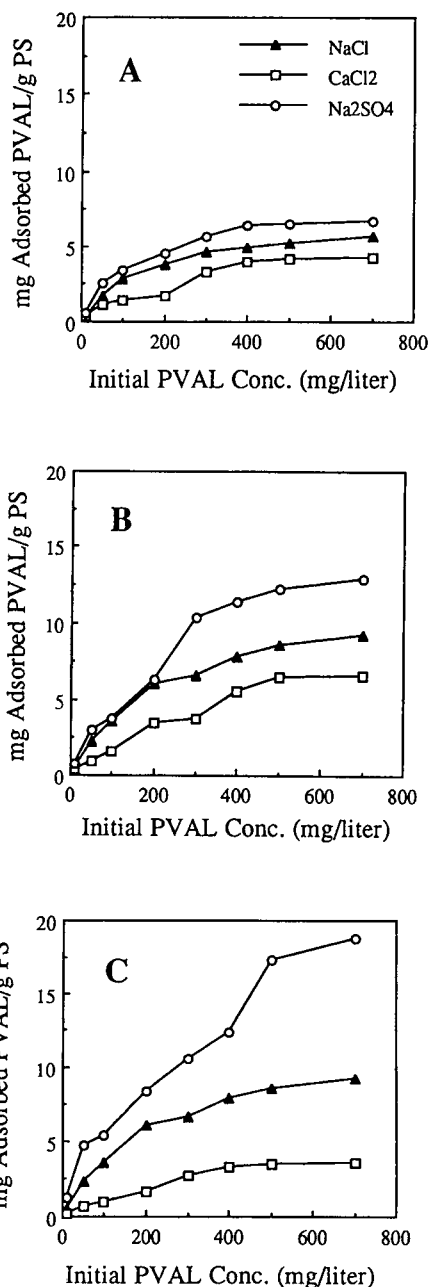


Fig. 4. PVAL adsorption isotherms obtained in the presence of three different salts at three different ionic strengths: (A) 0.05; (B) 0.1; and (C) 0.2. ▲ = NaCl; ◻ = CaCl₂; ○ = Na₂SO₄.

PVAL adsorption on the surface of polystyrene particles produced by conventional emulsion polymerization methods has also been studied previously by several investigators [16,20,21].

The maximum PVAL adsorption capacity obtained with such particles was *ca.* 5–6 mg/m². The difference in the PVAL adsorption may be explained by considering the surface charges of their PS particles and our PS microbeads. Their polymeric particles usually contained strongly acidic groups (*e.g.*, SO₄²⁻) on their surfaces coming from the initiator (*e.g.*, potassium peroxydisulphate) used in their polymerization recipes. However, the PS microbeads produced in the present study exhibit only a small number of weakly acidic groups (carboxylic acid) coming from the steric stabilizer [14,15].

BSA adsorption/desorption studies

Adsorption. Effects of the initial BSA concentration, ionic strength and pH on the adsorption behavior of BSA on the PS, PS/PVAL and Cibacron Blue F3G-A-attached PS/PVAL microbeads were investigated in batch adsorption–equilibrium studies. Typical BSA adsorption data obtained in this group of experiments are given in Fig. 5A and B ionic strengths of 0.01 and 0.1, respectively, adjusted with NaCl. These adsorption isotherms were obtained in experiments in which the pH of the adsorption medium was 5.0 (*i.e.*, the isoelectric point of BSA). As expected, adsorption increased with increasing initial concentration of BSA. There was a pronounced adsorption of BSA on PS microbeads (up to 25 mg/g), possibly because of the hydrophobic interactions between albumin and PS. The PVAL coating significantly decreased the BSA adsorption, as intended. Very high BSA adsorption capacities (up to 60 mg/g) were achieved with Cibacron Blue F3G-A-attached PS/PVAL microbeads. Also, the amount of BSA adsorbed on each microbead decreased with increasing ionic strength at constant initial albumin concentration.

In order to establish the effects of pH on BSA adsorption, adsorption experiments were repeated at different pH values between 4 and 8 at two different ionic strengths (0.01 and 0.1, adjusted with NaCl). In these studies the initial concentration of BSA was 2.0 mg/ml. Fig. 6A and B give typical adsorption data obtained in this group of experiments. As can be seen, in all the cases investigated, the maximum adsorption

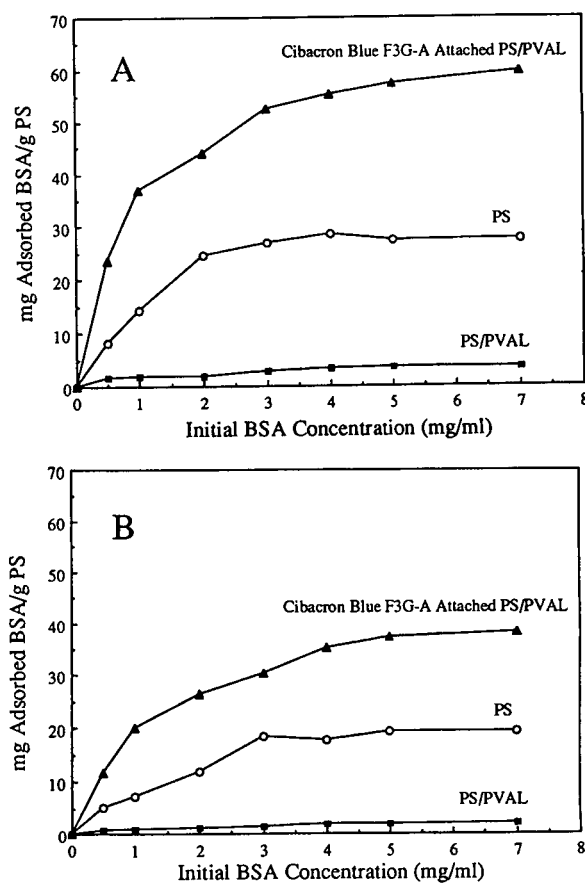


Fig. 5. BSA adsorption on PS-based microbeads at two different ionic strengths: (A) 0.01; (B) 0.1. pH = 5.0; salt used, NaCl.

of BSA was observed around its isoelectric point of 5.0. This is as expected because, as it has been shown that proteins have no net charge at their isoelectric points, the maximum extent of adsorption from aqueous solutions is therefore observed at the isoelectric point [22,23]. Significantly lower adsorption capacities were obtained with all microbeads at acidic and alkaline pH. This is also as expected, because it is known that, below or above the isoelectric points, proteins are charged positively or negatively, respectively. They are more hydrated, which increases their stability and solubility in an aqueous phase (*i.e.*, lower adsorption). It should be noted that there was no adsorption of BSA on PS/PVAL microbeads at pH 7.0 and 8.0 at both ionic strengths of NaCl. This is very important

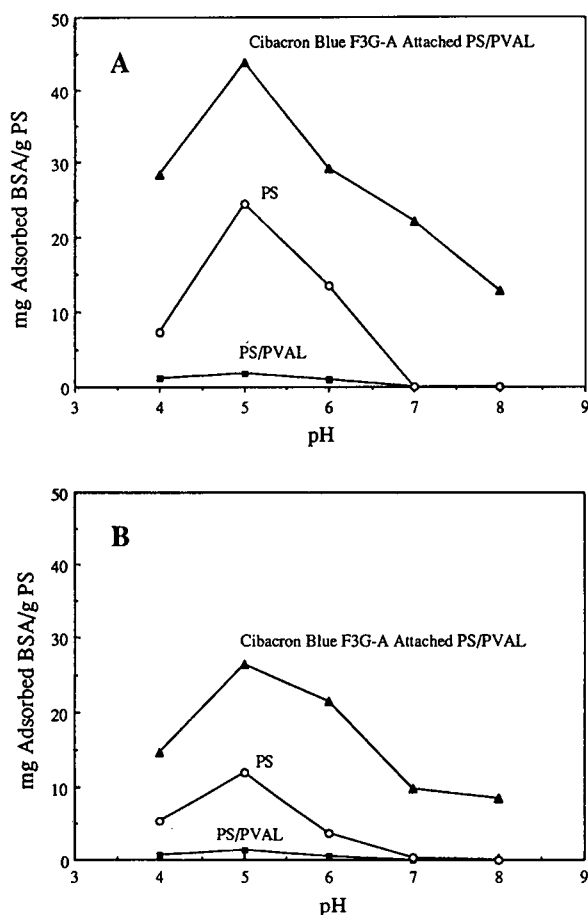


Fig. 6. Effect of pH on BSA adsorption on PS-based microbeads at two different ionic strengths: (A) 0.01; (B) 0.1. Initial BSA concentration, 2.0 mg/ml; salt used, NaCl.

because it means that there will be no non-specific protein adsorption if one works under those conditions.

Desorption. The desorption of the adsorbed BSA from the Cibacron Blue F3G-A-attached PS/PVAL microbeads was also studied in a batch experimental set-up. The dye-attached microbeads loaded with different amounts of BSA were placed within the desorption medium containing 0.5 M NaSCN at pH 8.0 and the amount of BSA released in 1 h was determined. The desorption ratio was then calculated by using the following expression:

$$\text{desorption ratio} = \frac{\text{amount of BSA related to the desorption medium}}{\text{amount of BSA adsorbed on the microbeads}} \cdot 100$$

TABLE II
BSA DESORPTION RATIOS

Desorption medium, 0.5 M NaSCN; pH, 8.0; temperature, 5°C.

Initial BSA concentration (mg/ml)	Desorption ratio (%)	
	I ^a	II ^b
0.5	85	89
1.0	76	85
2.0	84	86
3.0	90	91
4.0	88	85
5.0	85	92

^a Albumin adsorption conditions: ionic strength of NaCl, 0.01; pH, 5.0.

^b Albumin adsorption conditions: ionic strength of NaCl, 0.1; pH, 5.0.

Table II gives typical desorption data obtained in this group of experiments. A significant proportion (up to 92%) of the BSA adsorbed on the microbeads could be recovered with satisfactory desorption ratio values.

REFERENCES

- 1 P.D.G. Dean, W.S. Johnson and F.A. Middle (Editors), *Affinity Chromatography*, IRL Press, Oxford, 1985.
- 2 W.H. Scouten, *Affinity Chromatography*, John Wiley, New York, 1981.
- 3 B.R. Dunlap (Editor), *Immobilized Biochemicals and Affinity Chromatography*, Plenum Press, New York, 1974.
- 4 A. Fiechter (Editor), *Advances in Biochemical Engineering*, Springer, Berlin, 1982.
- 5 Y.D. Clonis, A.A. Atkinson, C.J. Bruton and C.R. Lowe (Editors), *Reactive Dyes in Protein and Enzyme Technology*, Macmillan, Basingstoke, 1987.
- 6 Y.D. Clonis, *CRC Crit. Rev. Biotechnol.*, 7 (1988) 263.
- 7 C.R. Lowe, M. Hans, N. Spibey and W.T. Drabble, *Anal. Biochem.*, 104 (1980) 23.
- 8 S. Angal and P.D.G. Dean, *Biochem. J.*, 167 (1977) 301.
- 9 M.F. Meldolesi, V. Macchia and P. Laccetti, *J. Biol. Chem.*, 251 (1976) 6.
- 10 R.L. Easterday and I.M. Easterday, *Adv. Exp. Med. Biol.*, 42 (1974) 123.
- 11 C.R. Lowe, M. Glad, P.O. Larsson, S. Ohlson, D.A.P. Small, T. Atkinson and K. Mosbach, *J. Chromatogr.*, 299 (1975) 175.
- 12 W.C. Thresher and H.E. Swaisgood, *Biochim. Biophys. Acta*, 749 (1983) 214.

- 13 A. Denizli, *Ph.D. Thesis*, Hacettepe University, Ankara, 1992.
- 14 A. Tuncel, A. Denizli, M. Abdelaziz, H. Ayhan and E. Pişkin, *Clin. Mater.*, 11 (1992) 139.
- 15 E. Pişkin, A. Tuncel, M.T. Ercan and B.E. Caner, *Clin. Mater.*, 8 (1991) 164.
- 16 V.D. Boomgard, T.A. King, F. Tadros, T. Tang and B. Vincent, *J. Colloid Interface Sci.*, 66 (1978) 68.
- 17 H. Shirahama, K. Takeda and T. Suzawa, *J. Colloid Interface Sci.*, 109 (1986) 552.
- 18 M. Okubo, I. Azume and Y. Yamamoto, *Colloid Polym. Sci.*, 268 (1990) 598.
- 19 H. Shirahama and T. Suzawa, *J. Colloid Interface Sci.*, 104 (1985) 416.
- 20 M.J. Garvey, T.F. Tadros and B. Vincent, *J. Colloid Interface Sci.*, 49 (1974) 57.
- 21 M.J. Garvey, T.F. Tadros and B. Vincent, *J. Colloid Interface Sci.*, 55 (1976) 440.
- 22 H. Shirahama, T. Shikawa and T. Suzawa, *Colloid Polym. Sci.*, 267 (1989) 587.
- 23 M. Okubo, K. Ikegami and Y. Yamamoto, *Colloid Polym. Sci.*, 267 (1989) 193.

Separation of tetrachloro-*p*-dioxin isomers by high-performance liquid chromatography with electron-acceptor and electron-donor stationary phases

U. Pyell and P. Garrigues*

URA 348, CNRS, Laboratoire de Photophysique et Photochimie Moléculaire, University of Bordeaux I, 351 Cours de la Libération, F-33405 Talence Cedex (France)

G. Félix

URA 35, CNRS, École Nationale Supérieure de Chimie et de Physique de Bordeaux, F-33405 Talence Cedex (France)

M.T. Rayez

URA 503, CNRS, Laboratoire de Physicochimie Théorique, University of Bordeaux I, F-33405 Talence Cedex (France)

A. Thienpont and P. Dentraygues

URA 35, CNRS, École Nationale Supérieure de Chimie et de Physique de Bordeaux, F-33405 Talence Cedex (France)

(First received July 9th, 1992; revised manuscript received November 18th, 1992)

ABSTRACT

An electron-donor and various electron-acceptor (EA) phases were evaluated for the separation of thirteen tetrachlorodibenzo-*p*-dioxin isomers in both the reversed- and normal-phase modes. It was shown that the selectivity on EA phases can be enhanced to a great extent in the normal-phase mode compared with the selectivity with polar mobile phases. Separation studies showed that the retention mechanism exhibited with non-polar mobile phases is partially masked by solvophobic effects when the same columns are used in the reversed-phase mode.

INTRODUCTION

The synthesis of tetrachlorodibenzo-*p*-dioxin (TCDD) standards often results in a mixture of isomers [1–4]. The isolation of individual isomers is generally accomplished by high-performance liquid chromatography (HPLC). It has been reported that certain pairs (or triads) re-

sisted separation on reversed-phase and silica columns [5].

Therefore, Barnhart and co-workers [5,6] employed an electron-donor phase [1-pyreneethyl-silica gel (PE-SG)] for the separation of TCDD isomers that co-eluted on octadecylsilane (ODS) phases. With the combination of an ODS column and a PE column the separation of 20 of the 22 TCDD isomers was accomplished. The successful separation of polychlorodibenzo-*p*-dioxin (PCDD) isomers which co-eluted on ODS

* Corresponding author.

phases and on PE-SG was reported for an electron-acceptor phase (nitrated phenylethyl silica gel) employed in the reversed-phase mode [7,8]. Swerev and Ballschmiter [9] reported the fractionation of PCDDs on cyanopropyl-, diphenyl- and phenyl-silica gel. According to their results, the selectivity of these columns (used in the reversed-phase mode) is mainly governed by the degree of chlorination, but these phases do not seem to be suitable for the separation of individual isomers.

In this study, we examined systematically the separation of thirteen commercially available TCDD isomers on various electron-acceptor (EA) phases with different electron-acceptor strengths and on an electron-donor (ED) phase, and compared the results with the separation of these isomers on an amino-, a cyano- and a phenyl-silica gel column. We were especially interested in mobile phase effects. Therefore, we studied one EA and the ED phase in both the normal- and reversed-phase modes. The retention of PCDD congeners on EA and ED columns has hitherto only been studied with polar mobile phases [8].

EXPERIMENTAL

Chemicals

All solvents used were of HPLC grade (Rathburn, Walkerburn, UK). Eleven of the isomers were purchased from Cambridge Isotope Labs. (Woburn, MA, USA) as solutions in nonane (50 ± 5 ppm); 1478-, 1236-, 1239-, 1267-, 1378-, 1289- and 2378-TCDD were received as individual isomers. 1237/1238- and 1368/1379-TCDD were received as mixtures of two isomers. The concentrations of the two isomers in the delivered standard mixtures differed considerably. By comparison of the peak height ratios and the retention order on a PONA gas chromatographic capillary column ($5.5 \mu\text{m}$; $50 \text{ m} \times 0.2 \text{ mm}$ I.D.) (Hewlett-Packard, Palo Alto, CA, USA), we succeeded in assigning the peaks of the 1368/1379-TCDD mixture unambiguously (conditions: HP 5970B mass-selective detector with HP 5890A gas chromatograph; injection mode, splitless; temperature programme, 130°C (0.5 min), increased from 130 to 230°C at $30^\circ\text{C}/\text{min}$ and from 230 to 315°C at $1^\circ\text{C}/\text{min}$; carrier

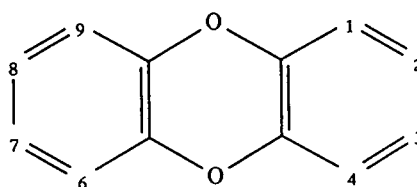


Fig. 1. Numbering of dioxin substituents.

gas, helium). 1237- and 1238-TCDD were assigned according to their shape parameters [10]. 1234- and 1278-TCDD were received as crystals from Cambridge Isotope Laboratories. In Fig. 1 the numbering of dioxin substituents is presented according to IUPAC nomenclature.

Apparatus

An HP 1050 liquid chromatograph (Hewlett-Packard) with a quaternary gradient pump and autoinjector was used in conjunction with an LDC Spectromonitor III spectrophotometric detector. The temperature of the column was controlled by a laboratory-made copper jacket and a water-bath. A PC-based laboratory data system (Hewlett-Packard, Vectra Series) was used to record, store, process and plot the data.

Columns

The following stationary phases were employed: aminopropyl-silica gel (AP-SG); cyanopropyl-silica gel (CP-SG); pentafluorobenzamidopropyl-silica gel (PFB-SG); 3,5-dinitrobenzamidopropyl-silica gel (DNB-SG); tetrachlorophthalamidopropyl-silica gel (TCP-SG/TCP5-SG); 2,4,7-trinitrofluorenone-oxime-O-propyl-silica gel (TNF-SG); phenylpropyl-silica gel (PP-SG); and 1-pyreneethyl-silica gel (PE-SG). Structures are shown in Fig. 2.

The EA phases were prepared in our laboratory according to methods already published: PFB-SG [11], DNB-SG [12], TCP-SG [13] and TNF-SG [14]. The syntheses were performed on a Spherisorb S10W [particle diameter (d_p) = $10 \mu\text{m}$]. In addition, we employed a TCP column ($d_p = 5 \mu\text{m}$), obtained from Société Française Chromato Colonne (Neuilly-Plaisance, France), now available from Silichrom (Pessac, France), prepared according to the method of Félix *et al.* [15,16]. In contrast to the above modified silica

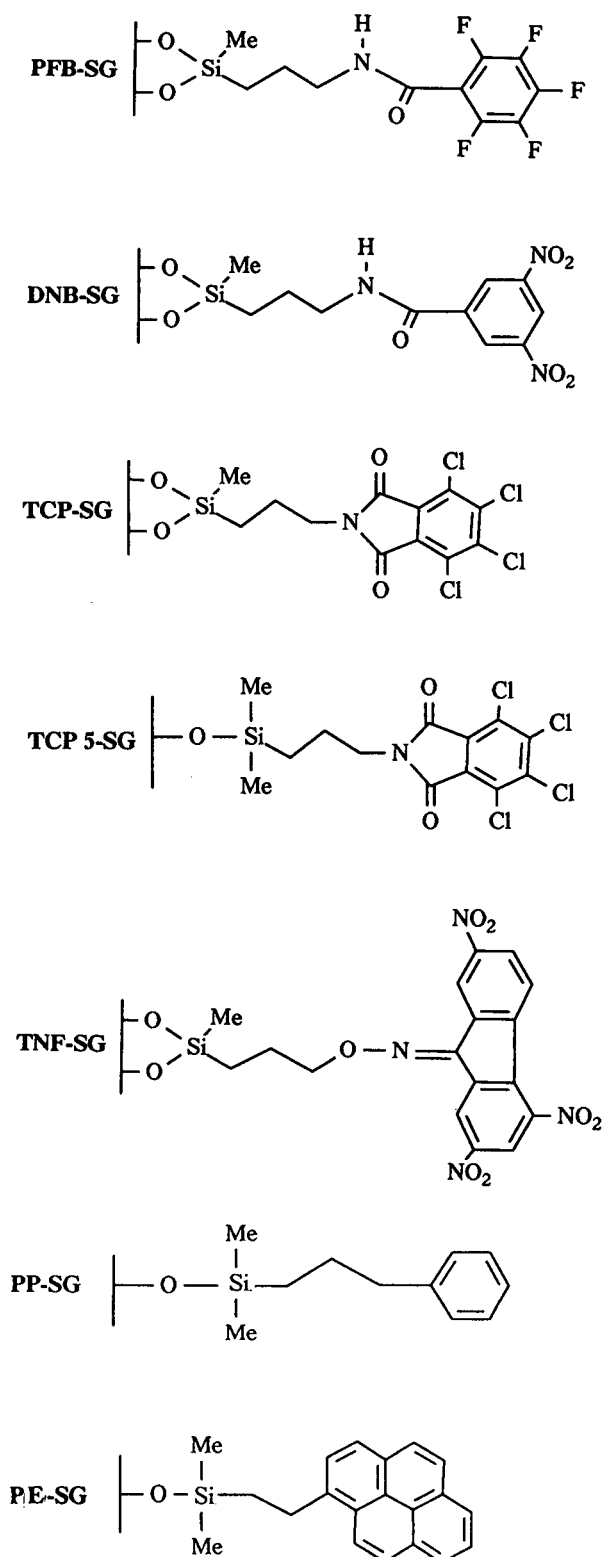


Fig. 2. Structures of the silica gels employed.

gels, the phase of this column was prepared by reaction with a monofunctional silane (*cf.*, Fig. 2). In the following text this phase is abbreviated to TCP5-SG.

The AP-SG column was packed with Spherisorb Amino ($d_p = 5 \mu\text{m}$) by Cluzeau Info Labo (St.-Foy-la-Grande, France). As a CP-SG column we utilized a Chrompack (Middelburg, Netherlands) column packed with Nucleosil-CN ($d_p = 10 \mu\text{m}$). The PP-SG column was prepared in our laboratories according to the method of Thienpont [17] on Spherisorb ($d_p = 5 \mu\text{m}$). The EP-SG column (Cosmosil Pye, $d_p = 5 \mu\text{m}$) was produced by Nacalai Tesque (Kyoto, Japan).

All columns with the exception of the DNB-SG and PP-SG columns (150 mm \times 4.6 mm I.D.) had dimensions of 250 mm \times 4.6 mm I.D.

Chromatographic conditions

All retention data were obtained under isocratic and isothermal (25°C) conditions. The mobile phase was hexane for the EA phases and for AP-SG and CP-SG. TCP-SG was also tested with methanol in the reversed-phase mode. PP-SG and PE-SG were employed in the normal-phase mode (with hexane) and in the reversed-phase mode [methanol–water (80:20, v/v)] and pure methanol, respectively). The flow-rate was 1 ml/min in all instances. The UV detector was operated at 235 nm with a response time of 1 s.

Retention times were measured with solutions of the TCDD isomers in 2-propanol (reversed-phase mode) or hexane (normal-phase mode). The solutions in nonane were diluted with the appropriate solvent. For mixtures the nonane was evaporated before dissolving the standard in 2-propanol in order to avoid peak broadening or distortion due to solvent effects of the standard solution. The injection volume was 10–30 μl , containing 2–30 ng of each isomer.

Calculation of molecular parameters

Quantum chemical calculations (optimization of the three-dimensional structures; computing of ϵ_{LUMO} , ϵ_{HOMO} and dipole moments) were carried out with the semi-empirical method Austin Model 1 (AM1) with the software package AMPAC, run on the IBM 3090 in the

CIRCE at Orsay (France). AM1 is a method that is well adapted to large organic molecules [18]. Details of the optimization procedure are given elsewhere [10].

RESULTS AND DISCUSSION

EA phases in the normal-phase mode

The EA phases chosen for these studies were characterized with a mixture of polynuclear aromatic hydrocarbons (PAHs) by Félix and Bertrand [13]. They classified the PFB-SG as a weak and the DNB-SG as an average EA phase. TCP-SG and TNF-SG were classified as strong EA phases.

The capacity factors of thirteen TCDD isomers on the EA columns obtained in the normal-phase mode are listed in Table I. The analytes are hardly retained on the PFB-SG column, more retained on the DNB-SG column and well separated on the TCP, TCP5 and TNF-SG columns with few co-elutions. Fig. 3 shows a chromatogram of the thirteen TCDD isomers

obtained on the TCP5-SG column. The isomers are well separated with high selectivity. Only two co-elutions were observed: 1238-/1478-TCDD and 1236-/1267-TCDD.

The same results were obtained for the TCP-SG and TNF-SG columns. The selectivity on the TNF phase is not enhanced compared with the TCP phases, but with the same mobile phase the retention times are much longer.

The stationary phases employed were designed for the separation of PAHs by donor–acceptor complex (DAC) LC. If the formation of weak electron donor–acceptor complexes between the solute and the immobilized ligands of the stationary phase is the dominating retention mechanism, the analytes are separated according to the stability of the DACs formed. According to the theory of DACs [19], the stability of this class of complexes depends on the electron affinity of the acceptor and the ionization potential of the donor. These quantities can be approximated via Koopman's theorem by quantum chemically calculated energies of the lowest unoccupied (ϵ_{LUMO}) and highest occupied (ϵ_{HOMO}) molecular

TABLE I

ENERGY OF HOMO (ϵ_{HOMO}), DIPOLE MOMENTS (μ) AND CAPACITY FACTORS (k') OF TCDDs ON ELECTRON-ACCEPTOR PHASES, CYANOPROPYL-SG (CP-SG) AND AMINOPROPYL-SG (AP-SG) WITH HEXANE AS MOBILE PHASE

TCDD isomer	ϵ_{HOMO} (kcal/mol)	μ (D) ^a	μ (D) ^b	k'						
					PFB-SG	DNB-SG	TCP-SG	TCP5-SG	TNF-SG	CP-SG
1368-	-9.063	0.004 ^c	0.023	0.04	0.37	0.64	1.05	2.46	0.18	0.23
1378-	-9.026	0.860	1.323	0.06	0.41	0.77	1.20	2.89	0.22	0.32
1379-	-9.045	0.744	1.221	0.04	0.37	0.76	1.26	3.06	0.22	0.30
2378-	-8.998	0.021 ^c	0.021	— ^d	0.54	0.93	1.37	3.19	0.26	0.41
1237-	-9.000	1.138	1.710	0.09	0.56	1.10	1.69	4.13	0.28	0.43
1238-	-9.001	1.792	2.668	0.09	0.56	1.10	1.87	4.13	0.32	0.61
1478-	-9.073	1.725	2.480	0.10	0.55	1.07	1.87	4.46	0.32	0.42
1278-	-9.004	1.672	2.467	0.13	0.64	1.23	2.12	4.49	0.37	0.70
1236-	-9.012	2.148	3.095	0.10	0.58	1.44	2.42	5.59	0.36	0.60
1267-	-9.019	0.031 ^c	0.023	0.12	0.77	1.51	2.51	5.94	0.40	0.60
1234-	-8.981	2.515	3.727	0.11	0.58	1.57	2.98	6.60	0.35	0.50
1239-	-9.057	2.772	4.121	0.14	0.79	1.81	3.36	7.65	0.49	0.92
1289-	-9.012	2.802	4.220	0.19	0.90	2.53	4.44	8.79	0.69	1.89

^a Calculated by AM1.

^b Calculated by MOPAC (data taken from ref. 26).

^c Not included in correlation analysis.

^d Not measured.

orbitals of the acceptor and the donor, respectively [20].

Under the simplifying assumption that the complex formation is caused by the transfer of an electron from the HOMO of the donor to the LUMO of the acceptor, the corresponding stabilization energy E of structurally related compounds is given by

$$E = \frac{\text{constant}}{\epsilon_{\text{HOMO}} - \epsilon_{\text{LUMO}}} \quad (1)$$

The calculated data for ϵ_{HOMO} are presented in Table I. Compared with ϵ_{HOMO} of strong donors (*e.g.*, PAHs) they are too low for the formation of electron donor–acceptor complexes. We therefore conclude that the retention mechanism of TCDDs on EA phases is not predominantly the formation of DACs.

The immobilized ligands and the TCDDs have

large dipole moments owing to the presence of halogen atoms or nitro groups. This suggests that the predominant forces between the solutes and the stationary phase are dipole–dipole interactions (orientation forces).

Kimata *et al.* [8] studied the retention order of several pairs of PCDD isomers on ODS-SG, PE-SG and an EA phase with methanol as mobile phase. They interpreted the observed retention tendency on the EA phase as the effect of differences in the dipolar character. Isomers with more dipolar character are retained longer than those with less dipolar character. They compared the retention order of isomers produced in the same reaction due to Smiles rearrangement with the magnitudes of the total dipole moment of the solutes.

The use of the total dipole moment as a descriptor in quantitative structure–retention

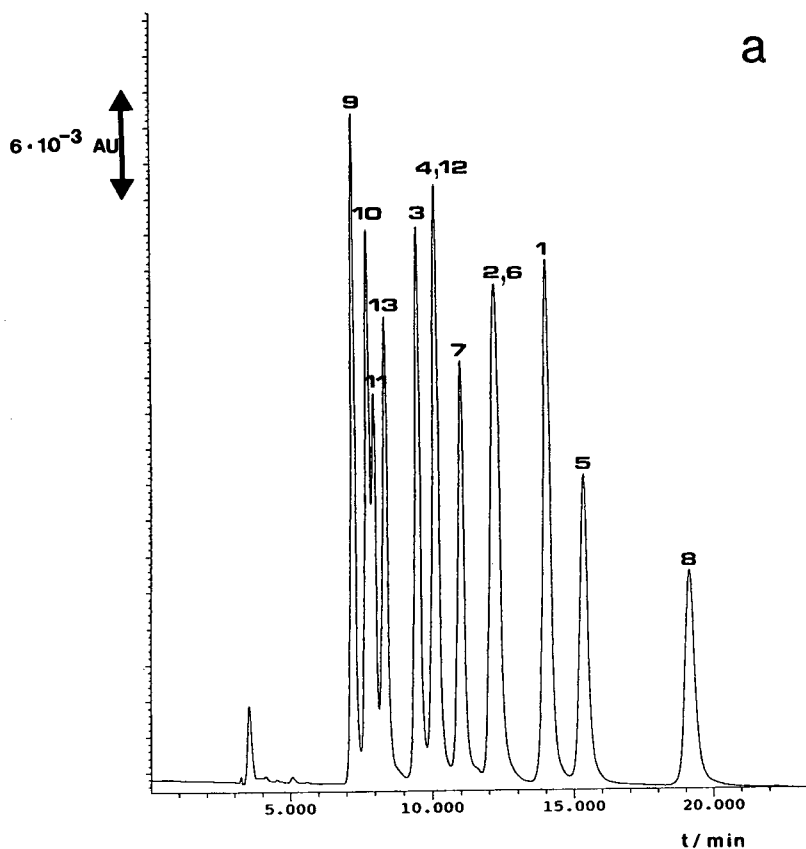


Fig. 3.

(Continued on p. 174)

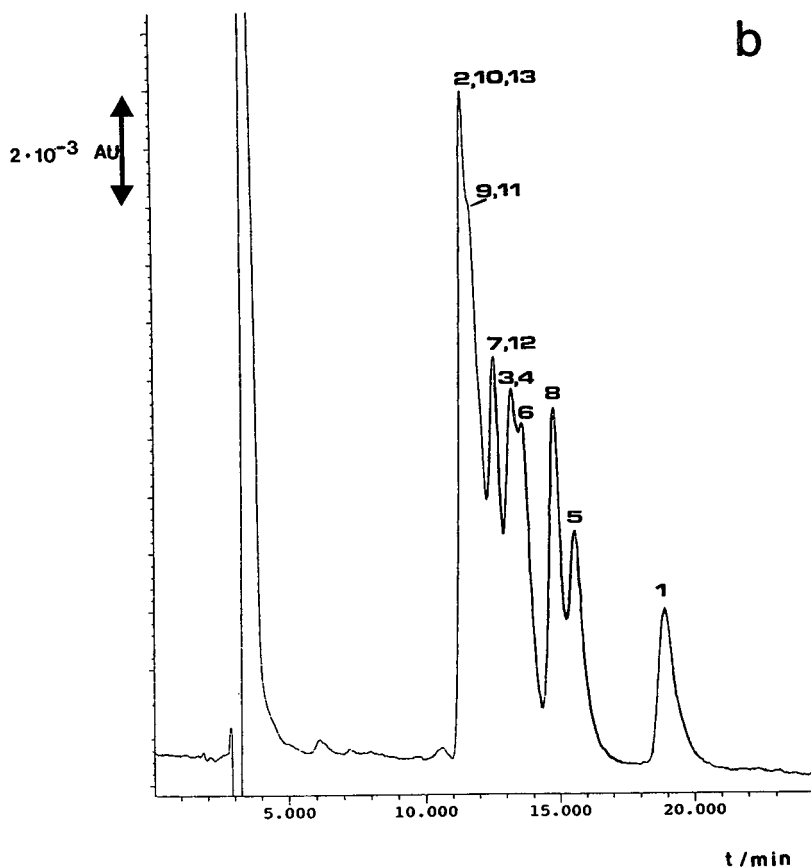


Fig. 3. Chromatograms of TCDD isomers eluted (a) from TCP5-SG with hexane as mobile phase and (b) from TCP5-SG with methanol as mobile phase. Column, 250 mm \times 4.6 mm I.D.; temperature, 25°C; detector wavelength, 235 nm; flow-rate, 1 ml/min. Peaks: 1 = 1234-TCDD; 2 = 1236-TCDD; 3 = 1237-TCDD; 4 = 1238-TCDD; 5 = 1239-TCDD; 6 = 1267-TCDD; 7 = 1278-TCDD; 8 = 1289-TCDD; 9 = 1368-TCDD; 10 = 1378-TCDD; 11 = 1379-TCDD; 12 = 1478-TCDD; 13 = 2378-TCDD.

relationship (QSRR) studies is controversially discussed in the literature [21]. Ong and Hites [22] reported that the square of the total dipole moment is a significant descriptor in a prediction equation for the retention of PCDD congeners on a non-polar column in GC. Kaliszan and co-workers [23–25], however, reported that correlation with retention data is better with a submolecular polarity parameter δ (maximum excess electron charge difference for a pair of atoms in the molecule). They stated [24] that if a solute is in specific contact with a stationary phase, not only will the dipole moment formed by the two atoms closest to the interacting surface count, but also the other more distant dipoles.

In the case of TCDD isomers, δ does not vary

greatly. It is given by the excess electric charge difference between the oxygen and its neighbours. For steric reasons the dipoles formed by the oxygen cancel each other, which does not mean that they are inactive in chromatographic interactions.

The differences between the TCDD isomers are given by the substitution pattern. The total dipole moment of the TCDD molecule is related to the symmetry of the substitution pattern. It is maximum if all the partial dipole moments contribute and do not cancel each other. In Table I the dipole moments, μ , calculated by AM1 are presented. They are compared with the values calculated by Koester and Hites [26], who used the MOPAC program. The deviation of the values calculated by different semi-empirical

methods is systematically about 50% of the value calculated by AM1. Linear correlation of the values obtained by the different methods shows a squared correlation coefficient $r^2 = 0.997$.

Comparing the capacity factors measured with strong EA phases, of TCDD isomers which differ only in the position of one chlorine substituent underlines the tendency already observed by Kimata *et al.* [8]. 1234-, 1236-, 1237- and 1238-TCDD are eluted in the order given by their dipole moments. At the same time it can be seen that the selectivities of TCP-SG, TCP-SG and TNF-SG, which are basically the same, differ for 1237- and 1238-TCDD. The two isomers are only separated on TCP5-SG, although they differ considerably in their dipole moments.

The same tendency can also be observed with isomer pairs that differ only in the position of the two benzene rings with respect to each other (prepared in the same reaction, due to Smiles rearrangement). For the 1267-/1289-TCDD and 1368-/1379-TCDD pairs, those isomers where the partial dipole moments cancel each other are eluted before those with more aligned partial dipole moments.

Under the simple hypothesis that the interaction of the solute and the stationary phase can be described by the interaction of the total dipole moment of the analyte, μ , and the dipole moment of the stationary phase, we would expect the following relationship [22]:

$$\ln k' = a + b\mu^2 \quad (2)$$

Fig. 4 shows the logarithms of capacity factors of TCDD isomers plotted against the square of the dipole moments calculated by AM1. It can be clearly seen that analytes that are symmetrical with respect to the centre of gravity (1267-, 1368- and 2378-TCDD) deviate strongly from the general tendency. Data points for these three isomers are given in brackets in Fig. 4. For symmetry reasons their dipole moments are close to zero. Parts of the molecule, however, exhibit large dipole moments and are therefore able to interact with the stationary phase. If these isomers are excluded from the regression analysis, a high correlation is observed.

In Table II the regression coefficients and regression parameters (a , b) obtained by linear

regression are given. Because of the very short retention times on the PFB-SG column, we did not calculate the regression coefficient for this phase. The need to exclude three isomers from the regression analysis shows that our model is too primitive to describe the retention process fully. Nevertheless, the observed correlation might be helpful in the scope of structure assignment [8].

The correlation is much better with the stronger retaining phases (TCP5-SG and TNF-SG) than with the phases with smaller retention forces. Comparison of the data for k' in Table I shows that there are some isomers that deviate characteristically from the general trend. These isomers are 1234-, 1236- and 1379-TCDD, which elute much earlier from PFB-SG and DNB-SG than expected from the retention order on TNF-SG or TCP-SG, respectively.

Comparison with polar bonded phases

In Table I the capacity factors for TCDDs on AP-SG and on CP-SG are also given. The retention order of the tested TCDDs follows the trend of the EA phases. The isomers 1234-, 1236- and 1379-TCDD show the same characteristic deviation from the retention order as found with PFB-SG and DNB-SG. The selectivity is much better on the very polar AP-SG than on CP-SG.

From this comparison it can be deduced that the retention mechanism on polar bonded phases and on EA phases is basically the same, which supports strongly our assumption that the formation of DACs is not involved in the retention of TCDDs on the studied EA phases. Differences in retention characteristics might be due to differences in polarity and also to differences in the geometric parameters of the immobilized ligands on the silica gel. N-Propyl-2,4,7-trinitrofluorenone is about the same size as the TCDDs, so that interactions can take place between the entire molecules. N-Propyltetrachlorophthalamide is smaller than TNF. The retention times on TCP-SG are shorter than those on TNF-SG, but the retention order was not altered.

DNB and PFB and also the aminopropyl and cyanopropyl groups are much shorter than the sorbed analytes. Interactions between the

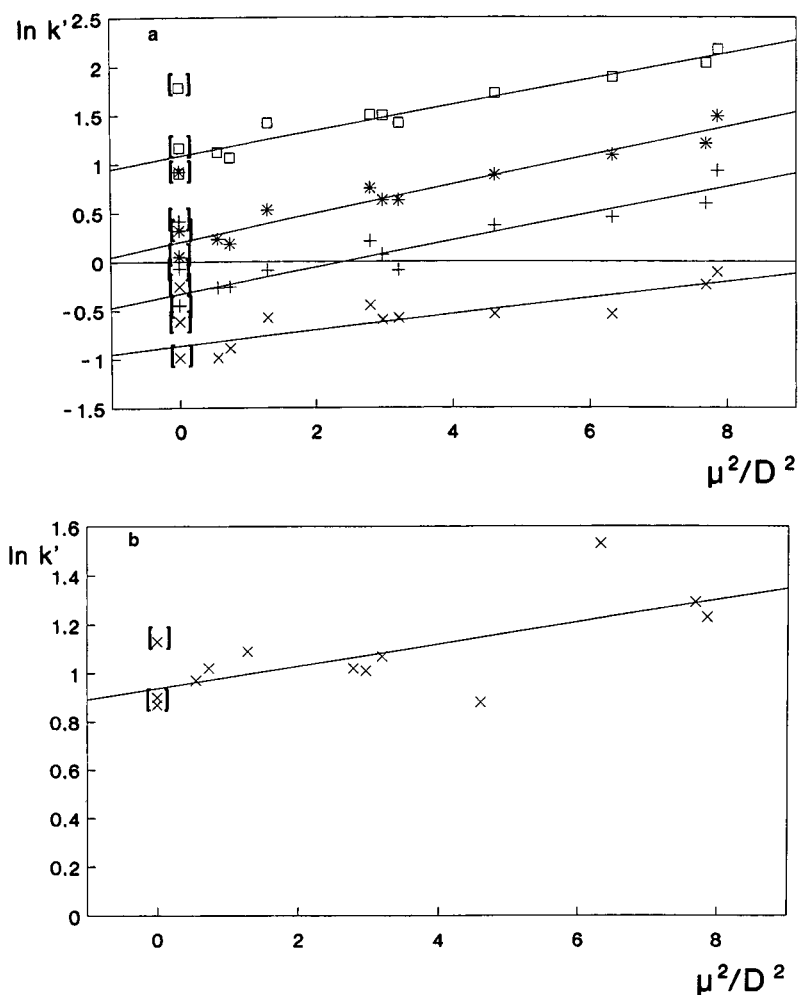


Fig. 4. Logarithms of capacity factor of TCDD isomers, obtained with EA phases, plotted against the square of their dipole moment. Mobile phase: (a) hexane; (b) methanol. Data in brackets were not included in the calculation of the regression line. (a) \times = DNB-SG; $+$ = TCP-SG; $*$ = TCP5-SG; \square = TNF-SG. (b) \times = TCP-SG.

TABLE II
TABULAR FORM OF THE EQUATIONS EVALUATED
BY LINEAR REGRESSION

Silica gel	a	b	R
CP-SG	-1.51	0.11	0.903
AP-SG	-1.18	0.16	0.827
DNB-SG	-0.86	0.083	0.863
TCP-SG	-0.33	0.14	0.952
TCP5-SG	0.20	0.15	0.970
TNF-SG	1.08	0.13	0.974

TABLE III
CAPACITY FACTORS (k') OF TCDDs ON TCP-SG IN
THE REVERSED-PHASE MODE WITH METHANOL
AS MOBILE PHASE

TCDD isomer	k'	TCDD isomer	k'
1368-	2.47	1278-	2.77
1378-	2.77	1236-	2.41
1379-	2.63	1267-	3.09
2378-	2.41	1234-	4.63
1237-	2.96	1239-	3.65
1238-	2.92	1289-	3.42
1478-	2.74		

stationary phase ligand and the solute can only take place with parts of the solute. This “shape effect” might explain the observed alterations in the retention order with respect to the retention order on TNF-SG.

TCP-SG in the reversed-phase mode

The TCP-SG column was also tested in the reversed-phase mode with methanol as the mobile phase. The capacity factors of the thirteen TCDD isomers on the column are presented in Table III. In the reversed-phase mode the retention order of the TCDDs is completely altered with respect to the separation in the normal-phase mode. Fig. 3 shows a chromatogram of the thirteen TCDD isomers obtained with TCP-SG in the reversed-phase mode in comparison with the chromatogram obtained with the same isomers on TCP5-SG with hexane as mobile phase. The alteration in retention order is not simply a reversal. The selectivity is lower compared with the selectivity of the same phase with hexane as the mobile phase. In the normal-phase mode, the selectivity factor α calculated from the first- and the last-eluted peaks is 3.95, whereas α calculated in the same manner after the separation with methanol as mobile phase is only 1.38. All capacity factors are much larger in the reversed-phase mode.

Obviously, in the reversed-phase mode the retention mechanism, which we attribute to dipole–dipole interactions, is partially masked by the separation mechanism of reversed-phase chromatography (separation according to hydrophobicity and geometrical parameters in the analytes).

In Fig. 4b the logarithms of capacity factors are plotted against the squares of the dipole moments of the analytes. The correlation (1267-, 1368- and 2378-TCDD excluded) is much weaker than in the normal-phase mode. The correlation factor is only 0.65.

For the above-discussed cases of very closely related isomers, the retention order still corresponds to the magnitude of the total dipole moment, with the exception of 1236-TCDD, which elutes before 1237- and 1238-TCDD.

Isomers that could not be separated on an ODS, a PE or an EA column (with methanol as

mobile phase) might be separated on an EA column with non-polar mobile phases owing to the higher selectivity of EA phases in the reversed-phase mode.

PE-SG in the normal-phase mode

The capacity factors of thirteen TCDD isomers on the PE-SG column obtained in the normal-phase mode with hexane as the mobile phase are presented in Table IV. The retention order of the analytes is completely different from that on EA phases in the normal-phase mode.

It can be deduced that the retention mechanism on this phase is different from that on the EA phases, which we have suggested to be primarily governed by dipole–dipole interactions. The pyrene immobilized on the column has a very low dipole moment. The dipole moments of PAHs are of the order of $\mu = 0.01$ D [22].

PE-SG was designed as an electron-donor phase for DAC LC. The energies of the lowest unoccupied orbital (ϵ_{LUMO}) of the TCDD isomers, presented in Table IV, are very low and suggest that the TCDDs are strong electron acceptors. For comparison, the values calculated by Koester and Hites [26] using the MNDO method are also given. They correlate excellently with the values calculated by us ($r^2 = 0.999$).

As already described in a previous section, for a retention mechanism involving the formation of DACs, from a theoretical point of view it can be expected that there is a direct but non-linear correlation between $\ln k'$ of the analytes and ϵ_{LUMO} . However, a direct correlation of $\ln k'$ with ϵ_{LUMO} gave unsatisfactory results ($R = -0.05$). In spite of the unobserved correlation of $\ln k'$ with ϵ_{LUMO} , which might be explained by an oversimplified theoretical approach not taking steric effects into account, we attribute the retention mechanism on PE-SG in the normal-phase mode to the formation of DACs. Our assumptions are supported by the following observations. In contrast to PE-SG, we measured no retention of TCDDs on the PP-SG column with hexane as the mobile phase. The phenyl group is a much poorer electron donor than the pyrene group. The retention order of PCDD congeners on PE-SG with non-polar

TABLE IV
ENERGY OF LUMO (ϵ_{LUMO}) AND CAPACITY FACTORS OF TCDDs ON PE-SG AND PP-SG

TCDD isomer	ϵ_{LUMO} (kcal/mol) ^a	ϵ_{LUMO} (kcal/mol) ^b	k'		
			PE-SG ^c	PE-SG ^d	PP-SG ^e
1234-	-0.8505	-1.349	3.19	17.32	6.66
1236-	-0.8280	-1.315	4.18	18.34	5.60
1237-	-0.8744	-1.363	3.90	15.01	4.50
1238-	-0.8731	-1.362	3.63	14.41	4.73
1239-	-0.8205	-1.310	4.22	15.94	4.75
1267-	-0.7925	-1.267	4.04	12.34	4.21
1278-	-0.8524	-1.336	4.01	13.28	4.23
1289-	-0.7892	-1.259	3.78	10.51	4.00
1368-	-0.8350	-1.317	3.42	19.26	6.17
1378-	-0.8743	-1.358	4.02	17.04	4.68
1379-	-0.8408	-1.328	3.63	16.47	5.03
1478-	-0.8116	-1.298	4.78	19.26	5.32
2378-	-0.9095	-1.396	4.74	15.59	3.58

^a Calculated by AM1.

^b Calculated by MOPAC (data taken from ref. 26).

^c Mobile phase: hexane.

^d Mobile phase: methanol.

^e Mobile phase: methanol–water (80:20, v/v).

mobile phases (hexane–dichloromethane) is mainly governed by the degree of chlorination [27]. Studies with EA phases with different immobilized moieties show that an increasing number of electron-withdrawing substituents enhances the ability to form DAC complexes with electron donors [20].

PE-SG in the reversed-phase mode

In Table IV the capacity factors of the thirteen TCDD isomers on the PE-SG column, obtained in the reversed-phase mode (mobile phase methanol), are compared with those obtained in the normal-phase mode. On changing the mobile phase the retention order was completely altered, as can be seen in Figs. 5 and 6. The alteration is not simply a reversal of the retention order.

The separation of TCDD isomers on the PE-SG column with methanol as the mobile phase was extensively studied by Barnhart and co-workers [5]. They compared the selectivity of a PE-SG column with that of an ODS column and reported large differences, which they attributed

to the contribution of charge-transfer interactions.

Alteration of the retention order with respect to the retention order measured in the normal-phase mode suggests that in the reversed-phase mode the retention mechanism of the normal-phase mode, which we attribute to the formation of DACs, is partially superimposed by other retention forces such as the hydrophobicity of the analytes.

The capacity factors measured with methanol as the mobile phase are much larger than those obtained with hexane. The selectivity of PE-SG towards the TCDDs is enhanced in the reversed-phase mode. Fig. 5b presents a chromatogram of the thirteen TCDD isomers separated on a PE-SG column with methanol as the mobile phase. There are only two co-elutions (1239-/2378-TCDD and 1368-/1478-TCDD).

Comparison with Fig. 3 shows that the selectivity of TCP5-SG towards TCDDs in the normal-phase mode is better than the selectivity on PE-SG. Most of the peaks on TCP5-SG are baseline resolved. However, those isomers which

co-elute from TCP5-SG can be easily baseline resolved on PE-SG.

Comparison with PP-SG

The capacity factors of TCDD isomers on PP-SG are given in Table IV in comparison with those on PE-SG. No retention was measured with hexane as the mobile phase.

In the reversed-phase mode the retention order on PP-SG is different from that on PE-SG. PP-SG is not simply a reversed phase. The pair of isomers that cannot be separated with monomeric octadecyl phases (1368-/1379-TCDD) [10] is baseline resolved on PP-SG. Geometric parameters, which greatly influence the separation of TCDDs on polymeric octadecyl (ODS) phases, are obviously of no importance with regard to the retention order. 2378-TCDD, the isomer with the highest length-to-breadth ratio

with respect to the other TCDD isomers [10], is eluted first, which is in contradiction to the theory of shape selectivity on polymeric ODS phases [28].

CONCLUSIONS

The tested DAC phases proved to be very useful for the preparation of pure TCDD standards after synthesis. The selectivities of TNF-SG/TCP-SG and PE-SG are complementary. In addition, these phases can be used in both the reversed- and normal-phase modes, exhibiting different selectivities. The highest selectivities were obtained for TNF-, TCP- and TCP5-SG in the normal-phase mode. The high capacity factors exhibited with PE-SG and methanol as mobile phase might prevent the application of PE-SG with methanol as mobile phase to PCDD

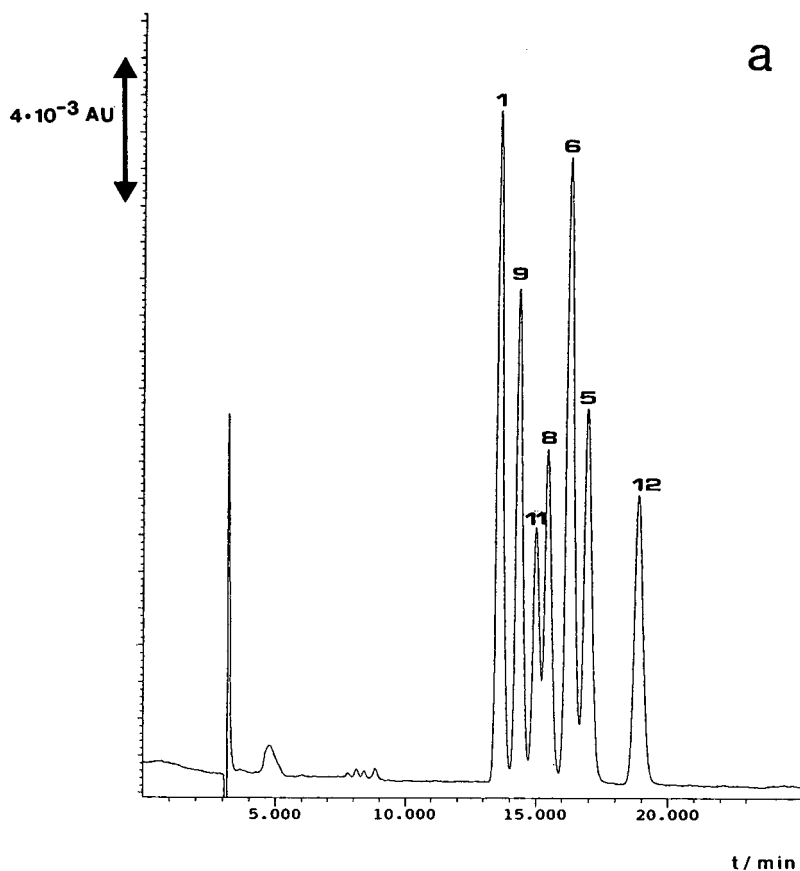


Fig. 5.

(Continued on p. 180)

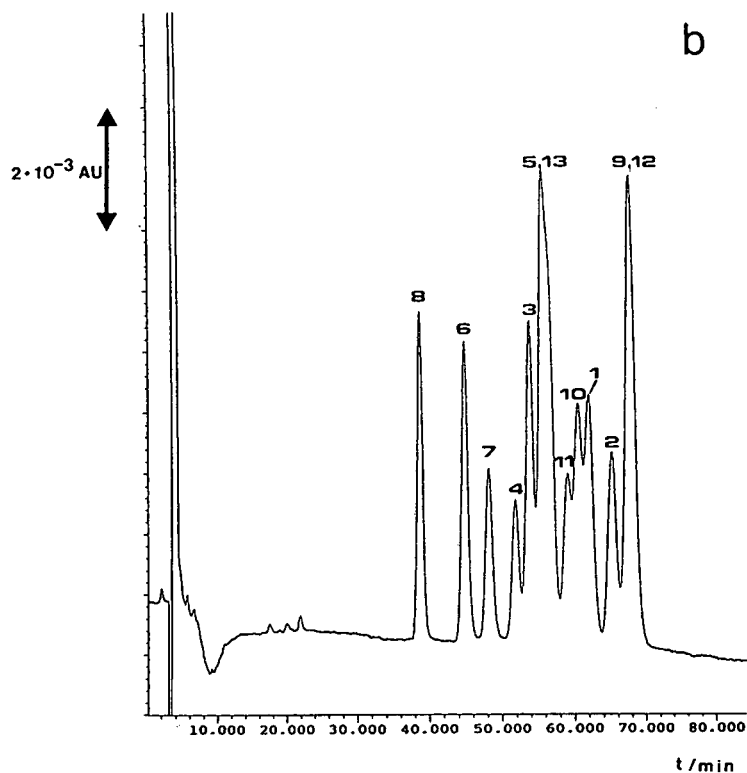


Fig. 5. Chromatograms of TCDD isomers eluted from PE-SG in (a) the normal-phase mode with hexane as mobile phase and (b) the reversed-phase mode with methanol as mobile phase. Column, 250 mm \times 4.6 mm I.D.; temperature, 25°C; detector wavelength, 235 nm; flow-rate, 1 ml/min. Peak identification as in Fig. 3.

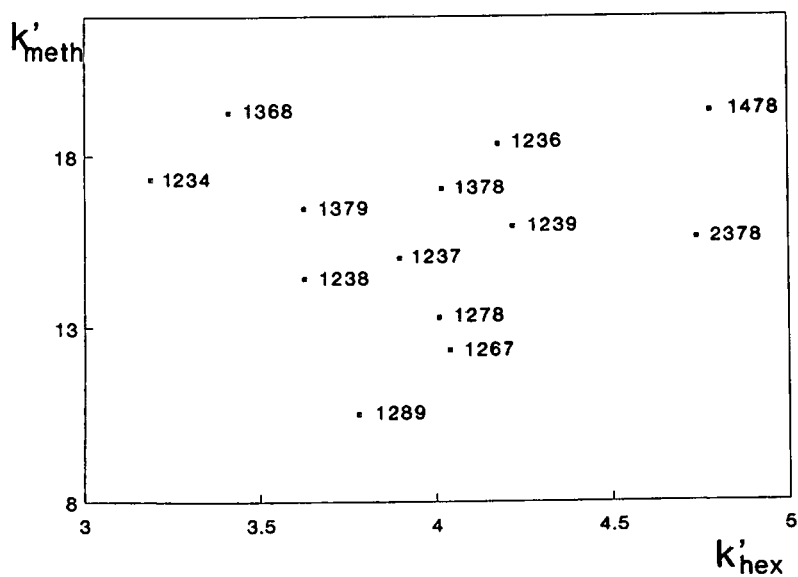


Fig. 6. Plot of capacity factors obtained on PE-SG in the reversed-phase mode (k'_{meth}) against those obtained in the normal-phase mode (k'_{hex}) (experimental parameters as in Fig. 5).

congeners with more than four chlorine substituents.

Application of non-polar mobile phases avoids solubility and possibly baseline shift problems reported by workers who used heart-cutting techniques employing RP-HPLC on various stationary phases for the purification and concentration determination of PCDD and PCDF standard solutions [9].

Another interesting application field of the studied stationary phases is the clean-up of samples prior to PCDD and PCDF analysis. Investigations on this aspect are in progress.

ACKNOWLEDGEMENTS

This work was supported by a grant from the Wissenschaftsausschuss der NATO via Deutscher Akademischer Austauschdienst. We thank Mr. M. Kobayashi (Nacalai Tesque, Kyoto, Japan) who kindly provided us with a Cosmosil Pye column, and Mr. Breda (Atochem, Pierre Bénite, France) for the gift of some standards. The Ministère de la Santé et de l'Action Humaine (France) and Groupe BSN are also acknowledged for financial support of these studies.

REFERENCES

- H.R. Buser and C. Rappe, *Anal. Chem.*, 52 (1980) 2257.
- H.R. Buser and C. Rappe, *Anal. Chem.*, 56 (1984) 442.
- T.J. Nestruck, L.L. Lamparski and R.H. Stehl, *Anal. Chem.*, 51 (1979) 2273.
- T.J. Nestruck, L.L. Lamparski and D.T. Townsend, *Anal. Chem.*, 52 (1979) 1865.
- E.R. Barnhart, D.G. Patterson, Jr., N. Tanaka and M. Araki, *J. Chromatogr.*, 445 (1988) 145.
- E.R. Barnhart, D.L. Ashlay, V.V. Reddy and D.G. Patterson, *J. High Resolut. Chromatogr. Chromatogr. Commun.*, 9 (1986) 528.
- K. Kimata, K. Hosoya, N. Tanaka, T. Araki, E.R. Barnhart, D.G. Patterson and S. Terabe, *J. High Resolut. Chromatogr.*, 13 (1990) 137.
- K. Kimata, K. Hosoya, N. Tanaka, T. Araki and D.G. Patterson, *J. Chromatogr.*, 595 (1992) 77.
- M. Swerev and K. Ballschmiter, *Chemosphere*, 15 (1986) 1123.
- U. Pyell, P. Garrigues and M.T. Rayez, *J. Chromatogr.*, 628 (1992) 3.
- G. Félix and C. Bertrand, *J. High Resolut. Chromatogr. Chromatogr. Commun.*, 7 (1984) 160.
- G. Félix and C. Bertrand, *J. High Resolut. Chromatogr. Chromatogr. Commun.*, 8 (1984) 362.
- G. Félix and C. Bertrand, *Analisis*, 17 (1989) 326.
- H. Hemetsberger, H. Klar and H. Ricker, *Chromatographia*, 13 (1980) 277.
- G. Félix, A. Thienpont and P. Dentraygues, *Pol. Aromat. Comp.*, in press.
- G. Félix, A. Thienpont and P. Dentraygues, *Chromatographia*, submitted for publication.
- A. Thienpont, *Ph.D. Thesis*, University of Bordeaux, Talence, 1991.
- M.J.S. Dewar, E.G. Zoebisch, E.F. Healy and J.J.P. Stewart, *J. Am. Chem. Soc.*, 107 (1985) 3902.
- R. Foster, *Organic Charge Transfer Complexes*, Academic Press, London, 1969.
- L. Nondek and R. Ponec, *J. Chromatogr.*, 294 (1984) 175.
- R. Kaliszan, *Anal. Chem.*, 64 (1992) 619A.
- V.S. Ong and R.A. Hites, *Anal. Chem.*, 63 (1991) 2829.
- K. Ośmiałowski, J. Halkiewicz, A. Radecki and R. Kaliszan, *J. Chromatogr.*, 346 (1985) 53.
- R. Kaliszan, K. Ośmiałowski, S.A. Tomellini, S.H. Hsu, S.D. Fazio and R.A. Hartwick, *J. Chromatogr.*, 352 (1986) 141.
- B.J. Bassler, R. Kaliszan and R.A. Hartwick, *J. Chromatogr.*, 461 (1989) 139.
- C.J. Koester and R.A. Hites, *Chemosphere*, 17 (1988) 2355.
- U. Pyell and P. Garrigues, unpublished results.
- L.C. Sander and S.A. Wise, *CRC Crit. Rev. Anal. Chem.*, 18 (1987) 299.

Extraction chromatography with modified poly(vinyl chloride) and di(2-ethylhexyl)dithiophosphoric acid

Lev Bromberg* and Gideon Levin

Department of Materials and Interfaces, Weizmann Institute of Science, P.O. Box 26, Rehovot 76100 (Israel)

(First received July 23rd, 1992; revised manuscript received December 16th, 1992)

ABSTRACT

A method for the preparation of packed-bed columns made of gelled beads is described. The stable gelled beads composed of dialkyldithiocarbamate- or dialkyldithiophosphate-substituted poly(vinyl chloride) and di(2-ethylhexyl)dithiophosphoric acid were capable of the selective separation of metal ions. The stoichiometries of Ag^+/H^+ and $\text{Cd}^{2+}/\text{H}^+$ extraction were established to be 3:1 and 2:1, respectively. A simple model of Ag^+ extraction kinetics was correlated with the experimental data. The selectivity of metal separations in displacement and elution chromatography was demonstrated.

INTRODUCTION

Extraction chromatography, or reversed-phase chromatography, is a method in which the support, *i.e.*, bed particles in the column, holds the organic phase as the stationary phase, while the aqueous phase is the mobile phase (eluent) [1]. The organic phase contains a specific extractant which is intended to be compatible with the support particles. A number of extractant-support systems have been reported [2]. In pioneering work, Small [3] proposed that a specific extractant should be incorporated in a physically stable gelled phase embedded in the packed beds. Using this idea, beads containing tributyl phosphate as an extractant were prepared from styrene-divinylbenzene copolymers as a support. Recently, we found that di(2-ethylhexyl)dithiophosphoric acid (DTPA) can form stable gelled phases in polymeric systems [4,5]. DTPA, an analogue of di(2-ethylhexyl)orthophosphoric

acid, which is widely used in extraction chromatography [6], possesses a high extraction selectivity and distinguished kinetics.

In general, dialkyldithiophosphoric acids are a well studied class of extraction reagents [7]. DTPA is used commercially in processes for the recovery of zinc and nickel from residues in the hydrometallurgical industry [8]. Cardwell and co-workers demonstrated the possibility of HPLC separations of metal mixed-ligand chelates with dialkyldithiophosphates [9] and, owing to the volatility of some chelates, the possibility of their GC determination [10,11]. Complexes of metals with dialkyldithiophosphates could be determined by TLC [12,13]. A few attempts at extraction chromatography with dialkyldithiophosphates have been reported [14,15]. Bol'shova *et al.* [14] preconcentrated metal solutions using diisopropyldithiophosphate as the stationary phase supported by poly(ethylene tetrafluoride) particles as an inert column carrier. Turanov *et al.* [15] found very high distribution coefficients of trace metal impurities between macroporous resin impregnated with DTPA and aqueous acidic solutions. Their work might have resulted in an effective extractive process if the impreg-

* Corresponding author. Present address: Department of Chemistry, Massachusetts Institute of Technology, Cambridge, MA 02139, USA.

nated resin had been stable. However, owing to emulsification after complexation with metals, DTPA is readily washed out of macropores, hence a reproducible loading–elution process is doubtful.

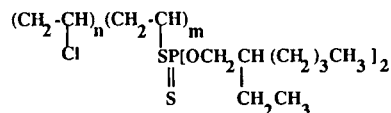
In this work, we combined the excellent extraction properties of DTPA with its ability to form gelled phases to create a new extractant–support system that can be used in packed beds. The extractant is compatible with the modified polymer, leading to gelled phases. In recent papers [5,16], we described the synthesis of modified PVC capable of forming a gel with DTPA. As silver can be extracted preferentially over all other metals [17], we decided to study the recovery of silver from photographic waste waters. The stoichiometry and the kinetics of the extraction process were evaluated.

EXPERIMENTAL

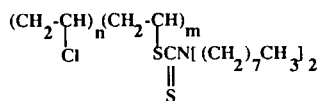
Preparation of column materials

Di(2-ethylhexyl)dithiophosphoric acid (DTPA) was synthesized from 2-ethylhexanol and phosphorus pentasulphide and then purified as described elsewhere [18]. The sodium salt of dioctyldithiocarbamate (DODTC) was prepared by reacting dioctylamine with carbon disulphide in the presence of NaOH [5]. Sodium salts of DTPA or DODTC were used to modify poly(vinyl chloride) (PVC, 43 grade; Frutarom, Israel) by nucleophilic substitution of chlorine. The experimental details of the reaction have been given elsewhere [5,16].

The formulae of the modified polymers (MP) obtained are as follows:



MP based on di(2-ethylhexyl)dithiophosphate-substituted PVC



MP based on dioctyldithiocarbamate-substituted PVC

Preparation of beads

Beads based on dioctyldithiocarbamate-substituted PVC

System 1. A mixture of modified polymer (MP) (S 4.9%, Cl 42.5%), PVC and DTPA in the mass ratio 1.0:2.3:3.4 was stirred in dioxane at 40°C until a clear solution was obtained. The concentration of dioxane in the solution was 83% (w/w). The viscous polymeric solution was then extruded into drops by means of a syringe and a needle into a stirred bath filled with the coagulation solution. To obtain beads of different sizes, needles of various inner diameter were used. The coagulation solution was 4% (v/v) of surfactant (polyethylene glycol, $M_w = 4000$) in deionized water. An abrupt coagulation led to round-shaped bead formation. The coagulation solution was filtered off and the beads were dried under vacuum. The composition of the dried beads was S 7.7%, Cl 29.5%.

System 1a. The above mixture was dissolved in dioxane containing 5% (v/v) of dichloroethane. The concentration of the dioxane–dichloroethane mixture in the solution was 85% (w/w). The content of the beads obtained after coagulation was: S 7.2%, Cl 28.2%.

System 2. A mixture of MP (S 6.1%, Cl 36.6%), PVC and DTPA in the mass ratio 1.0:4.7:5.7 was stirred in dioxane as described above. The concentration of dioxane in the mixture was 81% (w/w). The composition of the resulting beads was S 8.3%, Cl 26.9%.

System 3. The composition of MP used was as described for system 2, PVC and DTPA were taken in the mass ratio 1.0:10.2:9.0. The resulting beads contained S 6.4%, Cl 32.9%.

Beads based on di(2-ethylhexyl)dithiophosphate-substituted PVC

System 4. A mixture of MP (S 4.10%, Cl 42.1%), PVC and DTPA in the mass ratio 1.0:0.9:1.1 was stirred in dioxane as described above. The beads contained S 7.0%, Cl 32.9%.

System 4a. The mixture as described in system 4 was dissolved in dioxane containing 5% (v/v) of dichloroethane. The resulting beads prepared as in system 1a contained S 6.1%, Cl 31.6%.

Blank material without any polymer modi-

fication was prepared by mixing 0.22 g of PVC and 0.22 g of DTPA in 5 g of dioxane at 40°C. Beads (S = 8.6%, Cl = 33.65%) were prepared as described above.

Preparation of columns

A series of ion-exchange columns were prepared. Each column consisted of a polyethylene tube (I.D. 4.5 mm) closed at the end by a three-way stopcock connected to a syringe. A weighed amount (0.2–0.3 g) of beads was transferred in small increments into a column and pressed gently with a flat-ended rod to remove voids and to pack it uniformly. The bed height was set at 33–35 mm. The dried beads were preliminarily treated with 0.1 M H₂SO₄ and then rinsed with distilled water.

Procedure

In chromatographic experiments, an aqueous solution of the corresponding metal acetate or nitrate was passed through the resin bed (in some experiments until the breakthrough point). The percolation of the solution was then discontinued and the bed was rinsed with three bed volumes of distilled water. The solutions were eluted from the columns at room temperature at a flow-rate of 7–15 ml/min (if not stated otherwise).

Waste solutions from a photographic process were obtained from photofinisher using Kodak developers and contained 1.4 mM silver, 1.3 M Na₂S₂O₃, 0.12 M Na₂SO₃ and 10 mM NaBr. The solutions were carefully filtered before use.

Metal ion concentrations in the effluent were monitored with a Perkin-Elmer Model 5100 PC atomic absorption spectrometer, pH values were measured on a Corning Model 240 pH meter. Scanning electron microscopy (SEM) was performed on a Philips Model 505 scanning electron microscope using a MicroScan Tracor energy-dispersive spectroscopy attachment.

Partition measurements were made in the following manner: weighed amounts of the beads were vigorously stirred with definite volumes (10–12 ml) of metal solutions of known concentrations in tightly closed flasks in which the pH

and metal concentrations (collecting samples of 0.1 ml each) were periodically measured. In some experiments the kinetics of sorption were interrupted by separating the beads from the solution. The beads were filtered off, kept for 1 day in air-dry conditions and then replaced in the same solution.

The extent of sorption of metal ions into the resin was calculated from the difference in metal concentrations in solution before and after sorption by the resin. The sorption was also measured by stripping the sorbed metal from the resin and determining the metal concentration in the stripped solution. The metal uptake (U) was obtained using the equation $U = 1 - (C_t/C_\infty)$, where C_t and C_∞ are the concentrations of metal in the solution at a given time t and at equilibrium, respectively.

RESULTS AND DISCUSSION

Method of preparation

Preliminary experiments were performed in order to establish the stability of the gel with the specific extractant (DTPA). Mixtures of the modified polymer and DTPA were dissolved in tetrahydrofuran (THF), resulting in clear solutions. The solutions were then dried by keeping them in a closed box containing silica gel. After drying, the resulting mixtures were checked to see if homogeneous gel was formed. Polymeric materials such as PVC, poly(vinyl acetate), diethyldithiocarbamate-substituted PVC, dibenzylidithiocarbamate-substituted PVC and their mixtures were investigated. These materials do not form gelled phases with DTPA. The gel formation was observed only when dioctyldithiocarbamate or diisooctyldithiophosphate was used to substitute chlorine in PVC. The reason for this may lie in the fact that the nucleophiles used are compatible with the extractant and chemically closely resemble one another.

Many techniques were attempted in order to obtain round, non-agglomerated beads stable in packed-column chromatography. The optimum requirements were found to be as follows: the modified polymer and DTPA should form a homogeneous solution in a specific solvent; the

solution formed from MP and DTPA should be heavier than water so that a drop will sink immediately after it enters the coagulation bath; the solvent in which MP and DTPA are dissolved should be completely removed from the beads during their coagulation in the aqueous solution; the surface of the beads formed should be non-“sticky”; and the beads formed should contain a large amount of DTPA in order to achieve a high capacity.

In order to meet the above requirements, we attempted to use solvents giving homogeneous solutions with MP and DTPA, such as THF, dimethyl sulphoxide (DMSO), dioxane and their mixtures. Attempts to precipitate the beads from THF solution resulted in an irregular-shaped polymer precipitate floating on the water (as THF is lighter than water). On the other hand, DMSO appeared to be a poor solvent for the polymeric mixture. Dioxane was found to be an appropriate solvent. To prevent bead agglomeration, we replaced some of the MP with PVC. By doing so we lowered the MP concentration leaving the DTPA concentration constant. The resulting technique for bead preparation (see Experimental) was found to be optimum. This

approach differs substantially from conventional methods for the preparation of impregnated resins in which the beads are swollen in a solution of modifier, then washed (or dried) and micellized in water [19,20].

Structure of the beads

Beads consisting of several polymeric systems were studied using SEM. Fig. 1 shows a typical photomicrograph of internal and external parts of the cross-cut bead composed of system 4 (see Experimental). It can be seen that the bead of about 1 mm diameter was round with a developed external surface. The internal part had a well defined wall and a very friable central part. However, a cross-cut resulted in marked smoothing of the flexible wall. The use of a very thin needle allowed the bead to be opened without damaging the wall (Fig. 2). This illustrates the fine internal structure of the bead. Microscopic examinations suggest that the beads are actually hollow spheres or spheroid membranes.

The origin of the spheroids can be explained as follows. Viscous DTPA-containing solution being extruded through the needle shows very

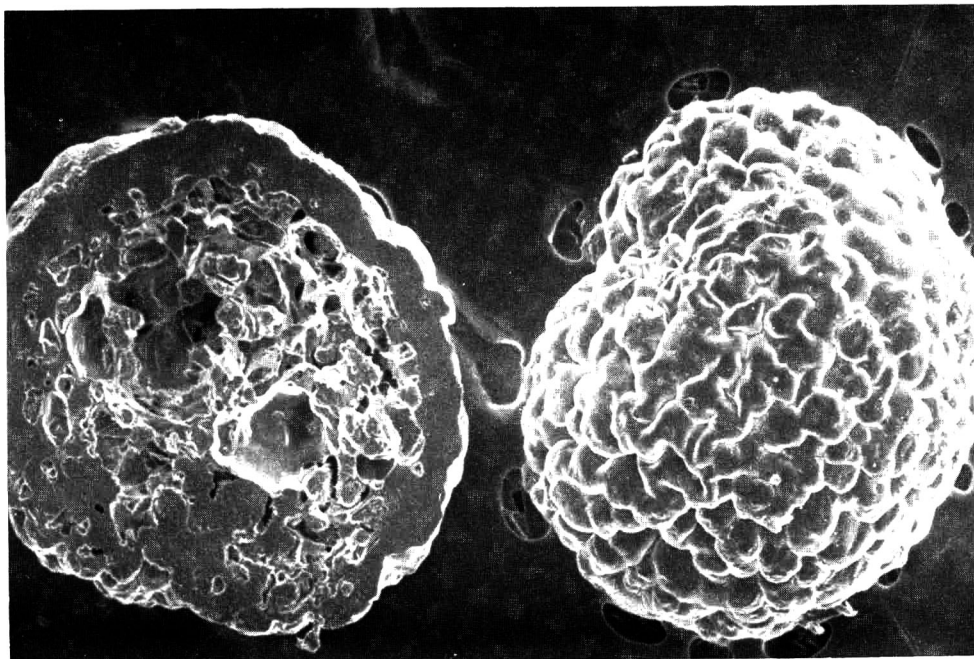


Fig. 1. External (right) and internal (left) parts of a cross-cut bead composed of system 4; magnification $\times 70$.

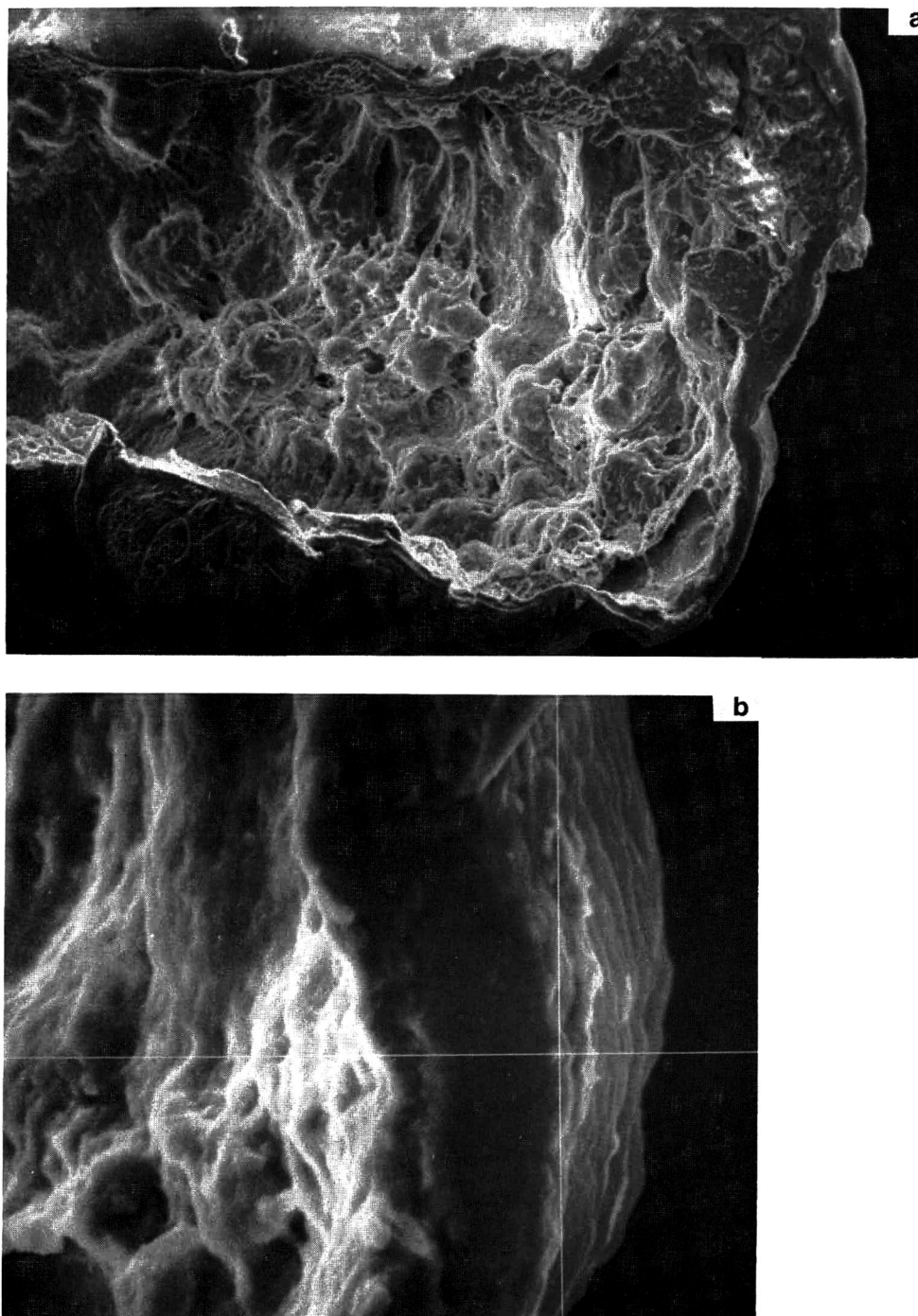


Fig. 2. Internal structure of the bead (system 4). (a) Magnification $\times 120$; (b) magnification $\times 1100$.

high adhesion to the walls of the needle. A hollow “tube” is formed, which on dropping into the water coagulates and produces spheres. The

thickness of the wall is 10–20 μm . The external surface contains small specks of the extractant (Fig. 3). SEM using energy-dispersive X-ray

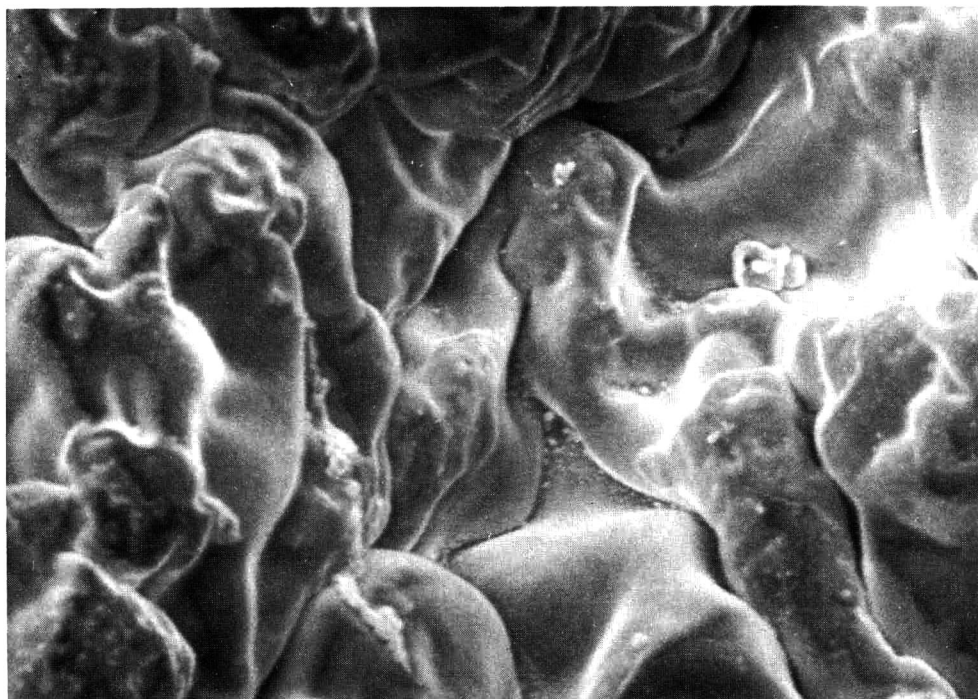


Fig. 3. External surface of a bead (system 1); magnification $\times 250$.

analysis showed that the surface of the wall is enriched by sulphur and phosphorus and thus contains a high concentration of DTPA (Fig. 4). Addition of water-insoluble dichloroethane to the dioxane solution before the coagulation results in a more friable structure of the beads, which was also shown to contain pores (Fig. 5).

Fig. 6 shows spot analyses of silver bound to the beads kept for 48 h in 1 M AgNO_3 solution. It can be seen that the external surface of the beads (a) contains much more silver than the

internal surface (b). Hence the extraction of the metal ions results in a thin layer of the metal ion bound to the extractant in the external wall of the beads. This layer is probably thinner than even the wall itself (*i.e.*, $< 10\text{--}20\ \mu\text{m}$). Hence it can be predicted that the overall velocity of the extraction process should be only surface reaction limited.

Stoichiometry of extraction

Consideration of the stoichiometry of the extraction yields the retention mechanism of the chromatographic process. Based on analogy with liquid–liquid extraction, the reaction between a metal ion M^{n+} and DTPA adsorbed on gelled MP and PVC can be written as



with an equilibrium constant

$$K = \{[(\text{MSR}_n)_{\text{a.gel}}][\text{H}_{\text{aq}}^+]^{na}/[\text{M}^{n+}]_{\text{aq}}^a[\text{HSR}]_{\text{gel}}^{na}\}_{\text{eq}} \\ = D[\text{H}^+]_{\text{aq}}^{na}/[\text{HSR}]_{\text{gel}}^{na} \quad (2)$$

where D is the effective distribution coefficient

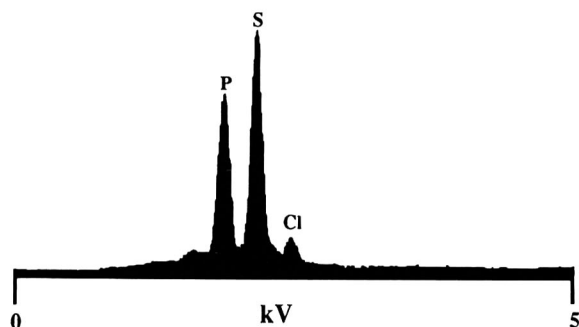


Fig. 4. Spot analysis on an external surface of a bead (system 4).

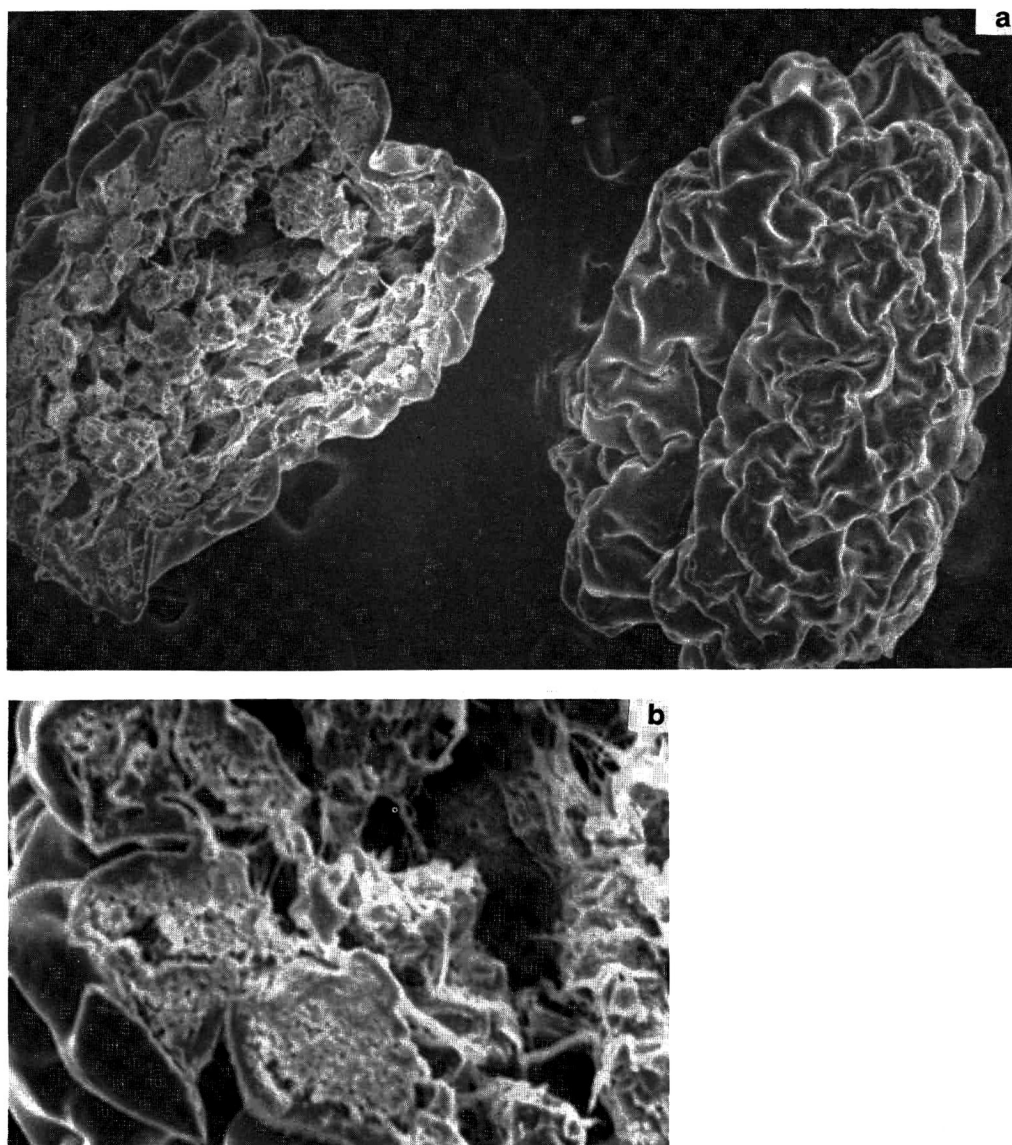


Fig. 5. (a) External (right) and internal (left) parts of a cross-cut bead composed of system 4a; magnification $\times 95$; (b) internal surface of a bead composed of system 1a; magnification $\times 185$.

of the metal between the beads and the aqueous phase and a is the degree of association of DTPA.

When a stripping agent (ligand) is used in aqueous solution, the K value should be modified as follows:

$$K_1 = K / \left(1 + \sum_{i=1}^n \beta_i c_i^i \right)$$

where β_i is the stability constant of the metal–

ligand complex and c_i is the concentration of the ligand.

The mechanisms of liquid extraction (reaction 1) in which DTPA participates have been investigated by a number of workers (for a review, see ref. 7). We shall limit ourselves by the extraction of silver and cadmium.

Assuming that DTPA is trimerized while contacted with silver [21], we obtain from eqns. 1 and 2 the following expression:

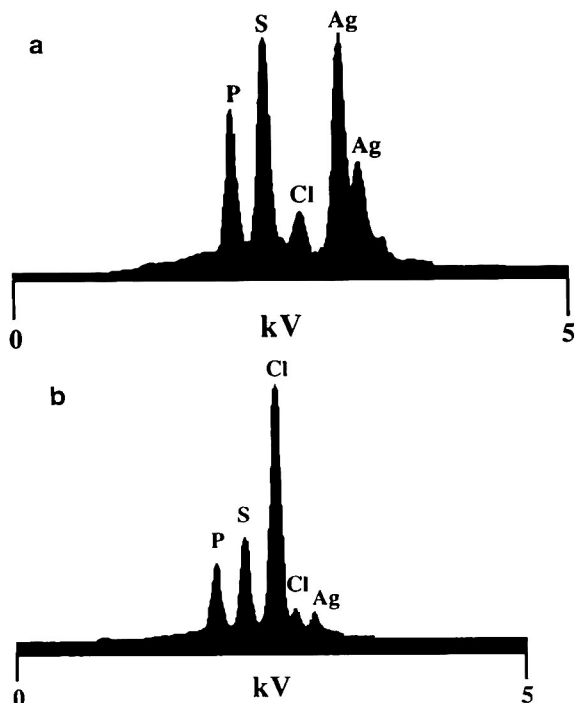


Fig. 6. Cross-section analysis of the beads (system 4) saturated by Ag. (a) Analysis of the external surface of the bead; (b) analysis of the internal surface of the bead.

$$K = D(1 + D)^2 [H^+]_{aq}^3 / ([Ag^+]_{aq}^{in})^2 [HSR]_{gcl}^3 \quad (3)$$

where $[Ag^+]_{aq}^{in}$ is the initial silver concentration in the aqueous phase set in the experiment.

It can be seen from the definition of D that

$$[Ag^+]_{gcl} / [Ag^+]_{aq}^{in} = D / (D + 1) \quad (4)$$

Therefore, for a given concentration of DTPA in the beads, using eqns. 3 and 4 one can obtain the following equation:

$$\log D + 2 \log(D + 1) = -3 \log[H^+]_{aq} + \text{constant} \quad (5)$$

Fig. 7 shows a plot of the left-hand side of eqn. 5 versus $\log(\text{sulphuric acid concentration})$. D was obtained by dividing the silver concentration per gram of beads by the silver concentration per gram of aqueous solution of H_2SO_4 containing 0.4 M thiourea. Yukhin *et al.* [21] used solvent extraction experiments to show that thiourea is an excellent stripping agent for silver. In order to measure D accurately, we lowered its value by adding thiourea to the solution. The

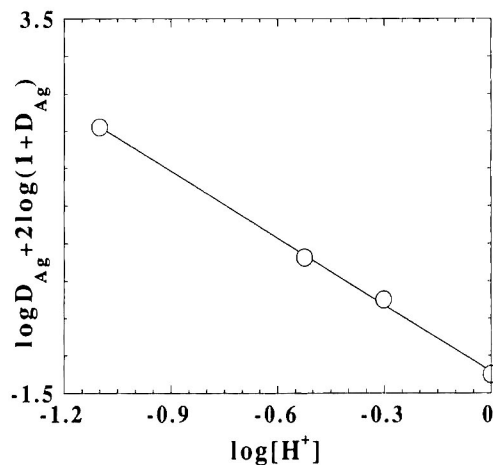


Fig. 7. Relationship between the distribution coefficient (D_{Ag}) for silver and H_2SO_4 concentration. Beads (system 3; loading 15.0 g l^{-1} ; temperature 22°C) were equilibrated with $AgNO_3$ (initial concentration 1.0 mM) solutions of H_2SO_4 containing 0.4 mM thiourea.

slope of the straight line in Fig. 7 of 2.95 fits fairly well the assumptions made in eqn. 3. These data strongly correlated with membrane transport experiments in which silver diffused through gelled phases containing DTPA and PVC [4]. The dependence of the distribution coefficient on the DTPA concentration in the membrane indicated trimerization of DTPA taking place in the gelled membrane phase [4].

It can be seen from Fig. 8 that silver can be

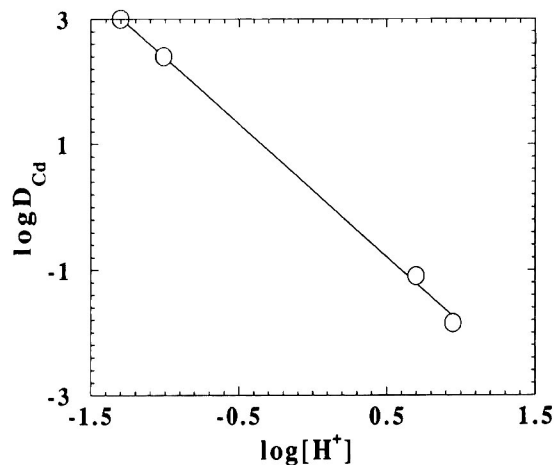


Fig. 8. Relationship between the distribution coefficient (D_{Cd}) for cadmium and HCl concentration. Beads (system 2; loading 14.0 g l^{-1} ; temperature 20°C) were equilibrated with $Cd(NO_3)_2$ (initial concentration 0.1 mM) solutions of HCl.

effectively stripped from the beads by acidic solutions saturated with thiourea.

As cadmium–dialkyldithiophosphate complexes have been reported to be non-associated in dilute solutions of hydrocarbons [22], we consider the expression

$$K = D[H^+]_{\text{aq}}^2/[HSR]_{\text{gel}}^2 \quad (6)$$

to be relevant in the extraction of Cd^{2+} . Fig. 8 shows a logarithmic plot of D versus the concentration of hydrochloric acid in the stripping solution. The slope is close to 2 and fits eqn. 6. A 9 M HCl concentration almost completely strips cadmium from the beads.

Kinetics of extraction

Eqn. 1 can be expressed as follows:



where $K = k_1/k_2$ is the equilibrium constant. K is extremely high ($2 \cdot 10^{41}$ [21]). Considering that interruption of the extraction process had no influence on the kinetic curves (see Experimental), we assume the process to be reaction controlled [23]. This assumption is in accordance with the SEM data showing the presence of DTPA as a thin layer on the wall of the beads (see Fig. 6).

In this case the overall reaction rate according to eqn. 7 is described by

$$\partial q/\partial t = k_1[q_{\text{Ag,aq}}^3 q_{\text{HSR}}^3 - (1/K)qq_{\text{H,aq}}^3] \quad (8)$$

where q is the effective DTPA-complexed silver concentration in the beads, q_{HSR} is the effective concentration of DTPA in the beads, $q_{\text{H,aq}}$ is the proton concentration in the aqueous solution appearing as a result of the reaction (eqn. 7) and $q_{\text{Ag,aq}}$ is the silver concentration in the aqueous solution.

The dissociation of the silver–DTPA complex is negligible, so a reasonable approximation is

$$\begin{aligned} q_{\text{H,aq}} &= q_{\text{HSR}} = q_{\text{SH}} - q; \\ q_{\text{Ag,aq}} &= q_{\infty} \text{ at } 0 \leq r \leq r_0 \end{aligned} \quad (9)$$

where q_{SH} is the effective concentration of the reactive SH groups in the beads, q_{∞} is the concentration of silver in the bead phase at

equilibrium with the silver in the bulk solution and r_0 is the average external radius of the beads.

Initial and boundary conditions are given as follows:

$$q_{\text{H}} = q_{\text{SH}}; \quad q = 0; \quad t = 0 \quad (10)$$

$$r = r_0 \quad (11)$$

where q_{H} is the proton concentration in the beads.

The fractional attainment of equilibrium is given by

$$U = q/q_{\text{SH}} \quad (12)$$

Substituting eqns. 9 in eqn. 8, we have

$$\partial q/\partial t = k_1(q_{\text{SH}} - q)^3(Kq_{\infty}^3 - q)/K \quad (13)$$

Solving eqn. 13 with the use of eqns. 9–12, we obtain

$$\begin{aligned} &[1/2(1 - U)^2] - [1/(KB - 1)(1 - U)] \\ &+ [1/(KB - 1)^2] \ln[(KB - U)/K(1 - U)] \\ &= k_1 q_{\text{SH}}^3 r_0^2 (KB - 1) \tau / KD_c \\ &= k_1 q_{\text{SH}}^2 (Kq_{\infty}^3 - q_{\text{SH}}) t / K \end{aligned} \quad (14)$$

where $B = q_{\infty}^3/q_{\text{SH}}$, $t = D_e \tau / r_0^2$ and D_e is the effective diffusion coefficient of silver in the beads. Assuming $K \rightarrow \infty$, eqn. 14 becomes

$$1/(1 - U)^2 = 2k_1 q_{\text{SH}}^2 q_{\infty}^3 t \quad (15)$$

Experimental and theoretical uptake data are shown in Fig. 9. Note that the U values obtained for small ($r_0 = 0.05$ mm) and large ($r_0 = 0.5$ mm) beads are almost identical. This is additional evidence for the assumption that the kinetics are reaction limiting. Had it been a diffusion-limiting process, we should have obtained a strong dependence of U on r_0 [23]. The theoretical uptake dependence calculated using eqn. 15 is shown as a solid line. In calculations the following values were used: $q_{\infty} = 12.3$ mol m^{-3} , $q_{\text{SH}} = 700$ mol m^{-3} and $k_1 = 4.2 \cdot 10^{-11}$ m^{15} mol $^{-5}$ s $^{-1}$. The q_{∞} and q_{SH} values were found experimentally and k_1 was calculated. It can be seen (Fig. 9) that the experimental and theoretical uptake data agree fairly well.

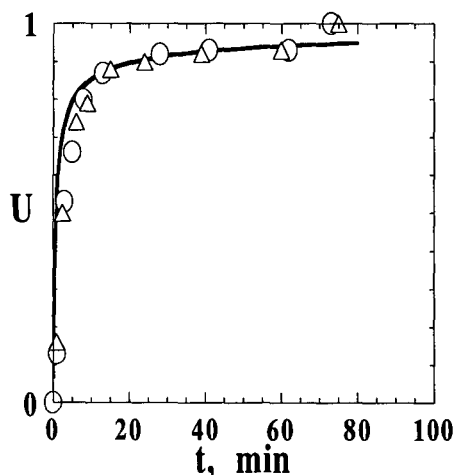


Fig. 9. Rate of uptake of silver under vigorous agitation. Initial concentration of AgNO_3 in water, 0.74 mM; initial pH, 7.2; bead loading, 14.3 g l^{-1} ; temperature, 18°C . \circ = Data obtained with the beads made of system 3, average diameter 1.0 mm; \triangle = data obtained with the beads made of system 4a, average diameter 0.1 mm; solid line = theoretical dependence.

Ion separations

Frontal separations give information about the equilibrium separation factor α :

$$\alpha = (1 - N)n / (1 - n)N \quad (16)$$

where N and n are the mole fractions of a certain ion relative to the sum of the ions to be separated in the resin and in solution, respectively.

Value of α can be characteristic of the selectivity of the extraction by the beads. Figs. 10–12 show typical output curves obtained in the frontal separation of metal ion mixtures. The equilibrium degree of retention was obtained using the difference between the amounts of a certain ion entering and leaving the column:

$$N = \left[\sum_i^j (V_i - V_v) C_{in} - \sum_i^j V_i C_i \right] / Q \quad (17)$$

where V_i is the volume of i th sample, V_v is the void volume of the column estimated in the separate experiments to be 10–15% of the column volume, C_{in} is the concentration of the initial solution, C_i is the concentration in the i th sample, j is the number of the sample after the removal of which the initial solution emerges

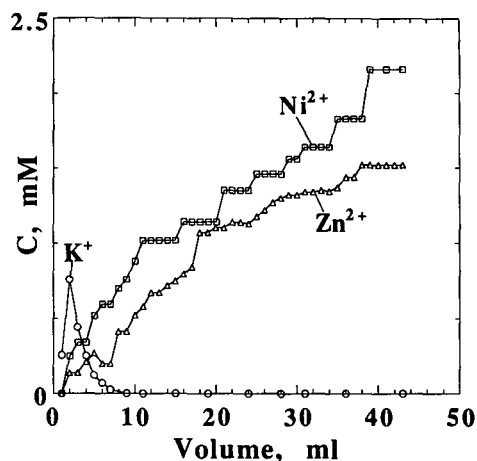


Fig. 10. Output curves obtained by displacement of K^+ by Ni^{2+} and Zn^{2+} ion mixture. Column (beads of system 4, $r_0 = 0.05\text{--}0.1 \text{ mm}$) was saturated with KNO_3 , then $\text{Ni}(\text{CH}_3\text{COO})_2$ and $\text{Zn}(\text{CH}_3\text{COO})_2$ solution was run. For initial composition of the eluent, see Table I.

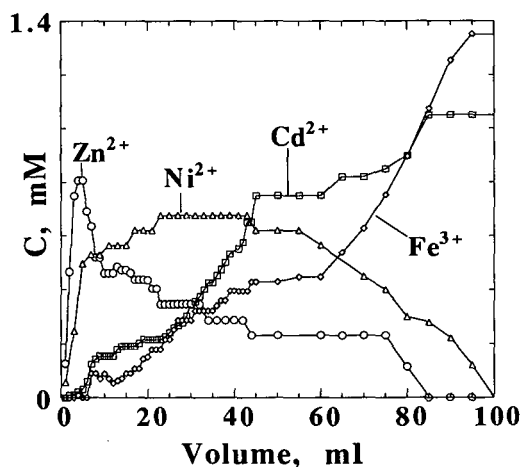


Fig. 11. Output curves obtained by displacement of Ni^{2+} and Zn^{2+} ion mixture in the column by $\text{Cd}(\text{CH}_3\text{COO})_2$ - and $\text{Fe}(\text{NO}_3)_3$ -containing eluent. See Fig. 10 and Table I.

from the column and Q is the amount of all ions extracted by the resin on equilibration.

The main results of the experiments shown in Figs. 10–12 are given in Table I. It can be seen that the separation factor α is in excellent agreement with the extraction sequence of metals by DTPA [7], viz., $\text{Ag} \geq \text{Hg} > \text{Pb} > \text{Fe(III)} > \text{Cd} > \text{Ni} > \text{Zn} \geq \text{K}$. At equilibrium silver replaces all other metals in the column.

In the experiments with the blank material

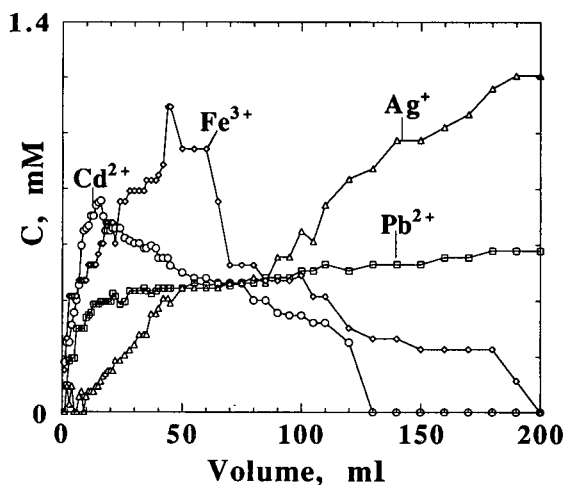


Fig. 12. Output curves obtained by displacement of Cd^{2+} and Fe^{3+} ion mixture in the column by $\text{Pb}(\text{CH}_3\text{COO})_2$ - and AgNO_3 -containing eluent. See Fig. 11 and Table I.

composed of unmodified PVC and DTPA, the beads were dispersed into separated fibrils and almost entirely lost their ion-exchange capacity after the first extraction–stripping cycle. In contrast, the cation-exchange columns containing modified polymer gelled with DTPA and PVC demonstrated an ability to work satisfactorily during 20 or more extraction–stripping cycles without losing their ion selectivity. The ion-exchange capacity of the beads decreased by 20–30% during the first 5–10 cycles and then reached equilibrium. The composition of the beads after 25 cycles was S = 3–5%, Cl = 42.3–47.5%.

Figs. 13–15 illustrate the performance of the columns in elution chromatography. Fig. 13

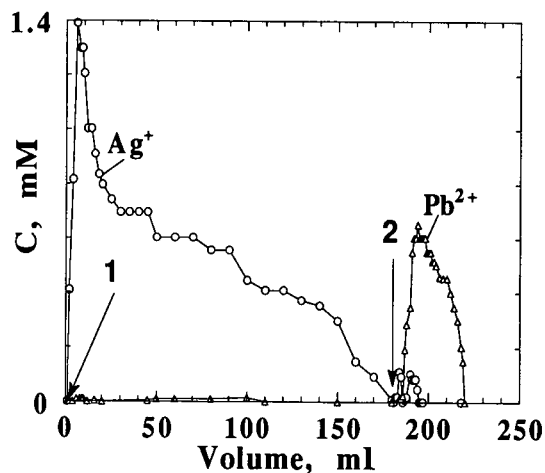


Fig. 13. Elution of Ag^+ and Pb^{2+} from the column (see Fig. 12) by 1 M H_2SO_4 saturated with thiourea (after arrow 1) and by 0.13 M sodium ethylenediaminetetraacetate (after arrow 2).

represents the elution of Ag^+ and Pb^{2+} from the column equilibrated in the experiment shown in Fig. 12.

Figs. 14 and 15 demonstrate the performance of the columns in the separation of micro-amounts of the metal ions. Mixtures of the corresponding cations which form strong neutral or anionic complexes were stripped off preferentially by passing through the beads eluent solutions containing the appropriate complexing anion. One cation after another could be stripped off by changing the eluent. Thus, Ag^+ and Hg^{2+} were separated from many other metal ions by stripping with acidic solutions saturated with thiourea. The stripping sequences and conditions were found to be in accordance with

TABLE I

SEPARATION OF METAL IONS BY FRONTAL CHROMATOGRAPHY

System	Metal ion	C_{in} (mM)	n_i	N_i	Q (μmol)	α
$\text{Zn}(\text{CH}_3\text{COO})_2, \text{Ni}(\text{CH}_3\text{COO})_2$ [KNO_3]	Zn^{2+}	1.52	0.41	0.29	46.1	1.70
	Ni^{2+}	2.16	0.59	0.54		1.23
$\text{Fe}(\text{NO}_3)_3, \text{Cd}(\text{CH}_3\text{COO})_2$ [$\text{Zn}(\text{CH}_3\text{COO})_2, \text{Ni}(\text{CH}_3\text{COO})_2$]	Cd^{2+}	1.05	0.44	0.31	82.1	1.75
	Fe^{3+}	1.35	0.56	0.54		1.08
$\text{AgNO}_3, \text{Pb}(\text{CH}_3\text{COO})_2$ [$\text{Fe}(\text{NO}_3)_3, \text{Cd}(\text{CH}_3\text{COO})_2$]	Pb^{2+}	0.58	0.32	0.09	68.7	4.76
	Ag^+	1.21	0.68	0.69		0.95

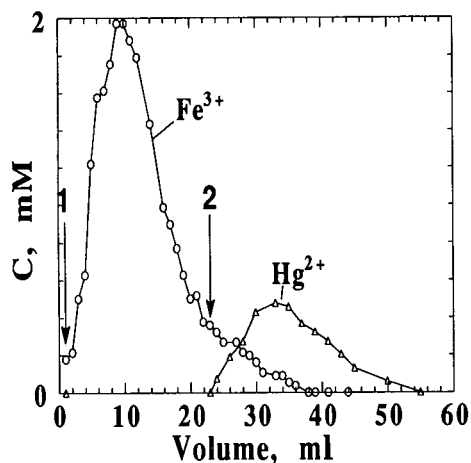


Fig. 14. Elution of Fe^{3+} and Hg^{2+} from the column (beads of system 3) by 1 M oxalate (after arrow 1) and by 1 M H_2SO_4 saturated with thiourea (after arrow 2).

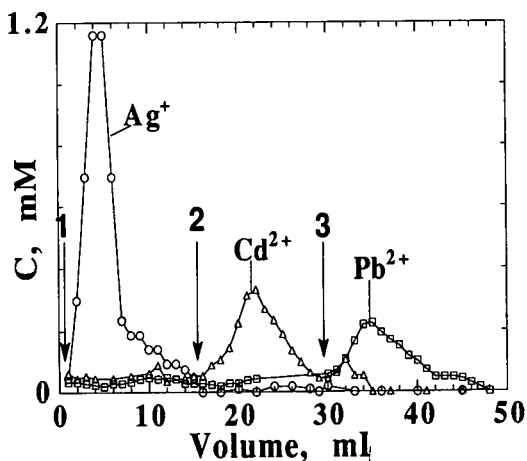


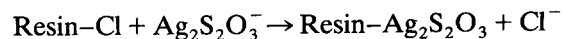
Fig. 15. Elution of Ag^+ , Cd^{2+} and Pb^{2+} from the column (beads of system 1) by 1 M H_2SO_4 saturated with thiourea (after arrow 1), 9 M HCl (after arrow 2) and 0.13 M sodium ethylenediaminetetraacetate (after arrow 3). The column was rinsed with 5–10 ml of distilled water before the eluent had to be changed. Rinsing is not shown.

the extractability of the corresponding complexes used in the stripping phases [4,16]. We hope that extraction chromatography based on the materials developed can be used for analytical purposes in the future. Obviously, DTPA with its extremely wide range of extraction constants for a variety of metal cations (from 10^{41} for mercury to 10^{-6} for Mn^{2+} [24]) can be advantageously used compared with di(2-ethylhexyl)orthophosphoric acid, which possesses a much narrower

range of extractability. The disadvantages of DTPA are its unpleasant odour and its tendency to oxidize on contact with nitric or sulphuric acid [18]. These problems, however, can be overcome by the use of DTPA or even its oxidized products [25] stabilized by a gelled polymeric network.

Recovery of silver from wash waters

Methods such as metal replacement, precipitation, ion exchange or extraction are used [26] to recover silver from dilute (1–50 μM) fixing baths after electrolytic purification. Conventionally, to recover silver from thiosulphate- and halide-containing solutions from photofinishers, a strongly basic anion-exchange resin is used. In this resin, chloride is the mobile ion and it exchanges with the silver thiosulphate to release a chloride ion while capturing the silver complex:



However, special efforts should be made to recover silver from the resin, which is usually burned to remove the metal, greatly increasing the expense of the process.

In order to extract silver from photographic waste waters, an extractant should possess an extremely high complexation ability. DTPA was

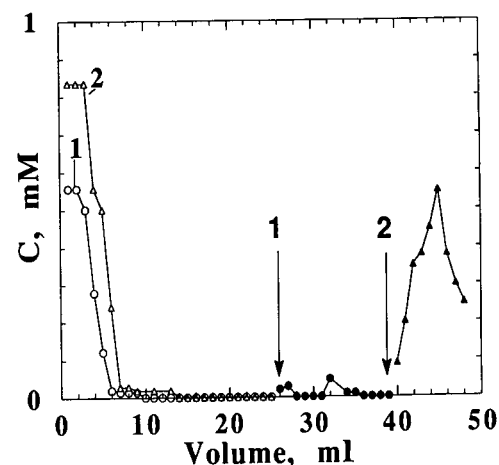


Fig. 16. Recovery of silver from aqueous solutions. Curve 1 represents the removal of silver by the beads of system 4 from AgNO_3 solution in distilled water and curve 2 the removal of silver from Kodak wastewater. Silver was eluted from the column by 1.3 M $\text{Na}_2\text{S}_2\text{O}_3$ solution (after arrow 1) and 1 M H_2SO_4 saturated with thiourea (after arrow 2).

found to be an excellent extractant for silver and may be embedded in a supported liquid membrane [17]. However, the membrane process has the drawback that it requires too long a time to recover silver at levels below 1–2 μM because the driving force of the process, the membrane concentration gradient, then becomes very low, thus lowering the flow-rate through the membrane. The stability of the membrane may then become the main problem [4]. In contrast to the above method, extraction chromatography can be favourably applied, providing the possibility of recovering silver in a few cycles.

Fig. 16 demonstrates the performance of the column in the extraction and elution of silver, which was effectively removed from both AgNO_3 solution in deionized water (curve 1) and from Kodak waste silver solution containing sodium thiosulphate (curve 2). Then, 1.3 M $\text{Na}_2\text{S}_2\text{O}_3$ solution was run through the column (after the first arrow). Virtually no silver was stripped off. In contrast, silver was effectively removed from the column by 1 M H_2SO_4 containing 0.75 M thiourea (after the second arrow).

The possibility of substantial purification of silver solutions is illustrated by Fig. 17. Curve 1 corresponds to the experiment shown in Fig. 16 (curve 1). Curve 2 in Fig. 17 represents the thorough analysis of curve 1 after the silver had

reached the ppb ($\leq 1 \mu\text{M}$) level. After the first run (curves 1 and 2), the fractions containing micromolar concentrations were combined and then the solution was run again. The results of the second elution (curve 3) are compared with those for the first run (curve 2). It can be seen that silver was removed from about 0.6 mM to about 0.2–0.8 μM in the first run and was further removed to a level of 0.1–0.5 μM in the second run. Obviously, complete purification depends mainly on the quality of the column packing, which we believe can be improved by tightening the packing of the beads and by using smaller beads.

CONCLUSIONS

Extraction chromatography based on modified poly(vinyl chloride) and di(2-ethylhexyl)-dithiophosphoric acid as a gelled phase was developed. The optimum method for the preparation of gelled beads for packed columns was elucidated. SEM investigations demonstrated that the beads obtained are spheroid membranes. The stoichiometry of Ag^+ and Cd^{2+} extraction was established. The kinetics of silver extraction by the beads were shown to be reaction controlled. Model considerations yielded the kinetic constant of the extraction reaction. Selective ion separations in frontal analysis and elution chromatography were achieved. The possibility of the use of the developed chromatographic material for the substantial purification of photographic waste waters was demonstrated.

ACKNOWLEDGEMENTS

The authors are grateful to Dr. Lev Margulis for his help with electron microscopy and Ms. Rina Barzilai for assistance with analytical measurements. A Sir Charles Clore Fellowship to L.B. is gratefully acknowledged.

REFERENCES

- 1 E. Cerrai and G. Ghersini, *Adv. Chromatogr.*, 9 (1970) 3.
- 2 T. Braun and G. Ghersini (Editors), *Extraction Chromatography*, Akadémiai Kiadó, Budapest, 1975.

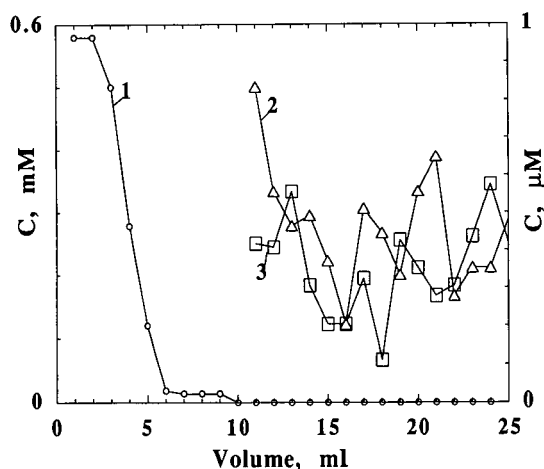


Fig. 17. Recovery of silver from aqueous solution. Curve 1 corresponds to curve 1 in Fig. 16. The rate of elution is 0.2 ml min^{-1} . Curve 2 represents the silver concentration in the first run below the micromolar level; curve 3 is the second run compared with the first run. For explanation, see text.

- 3 H. Small, *J. Inorg. Nucl. Chem.*, 18 (1961) 232.
- 4 L. Bromberg, G. Levin and O. Kedem, *J. Membr. Sci.*, 71 (1992) 41.
- 5 G. Levin and L. Bromberg, *J. Appl. Polym. Sci.*, in press.
- 6 I. Fidelis and S. Siekierski, *J. Chromatogr.*, 17 (1965) 542.
- 7 I.P. Alimarin, T.V. Rodionova and V.M. Ivanov, *Russ. Chem. Rev.*, 58 (1989) 863.
- 8 J. Draxler, W. Furst and R. Marr, *J. Membr. Sci.*, 38 (1988) 281.
- 9 T.J. Cardwell and D. Caridi, *J. Chromatogr.*, 288 (1984) 357.
- 10 T.J. Cardwell, P.J. Marriott and P.S. McDonough, *J. Chromatogr.*, 193 (1980) 53.
- 11 P.J. Marriott and T.J. Cardwell, *J. Chromatogr.*, 234 (1982) 157.
- 12 A.R. Timerbaev, V.V. Salov and O.M. Petrukhin, *Zh. Anal. Khim.*, 40 (1985) 237.
- 13 V.V. Salov, O.M. Petrukhin, Yu.A. Zolotov, V.P. Shevchenko and N.F. Myasoedov, *Zh. Anal. Khim.*, 41 (1986) 256.
- 14 T.A. Bol'shova, E.N. Shapovalova, G.A. Okuneva, T.V. Rodionova and E.M. Fedorova, *Zh. Anal. Khim.*, 44 (1989) 284.
- 15 A.N. Turanov, N.K. Evseeva and T.N. Kremenskaya, *Radiokhimiya*, 28 (1986) 64.
- 16 L. Bromberg and G. Levin, *J. Appl. Polym. Sci.*, in press.
- 17 L. Bromberg, I. Lewin and A. Warshawsky, *J. Membr. Sci.*, 70 (1992) 31.
- 18 L. Bromberg, I. Lewin, H. Gottlieb and A. Warshawsky, *Inorg. Chim. Acta*, 197 (1992) 95.
- 19 A. Warshawsky, in J.A. Marinsky and Y. Marcus (Editors), *Ion Exchange and Solvent Extraction*, Vol. 8, Marcel Dekker, New York, 1981, Ch. 3, p. 229.
- 20 D.N. Muraviev, *Chem. Scr.*, 29 (1989) 9.
- 21 Yu.M. Yukhin, N.E. Kozlova, L.A. Novoseltseva and I.S. Levin, *Izv. Sib. Otd. Akad. Nauk SSSR, Ser. Khim.*, 7 (1974) 64.
- 22 O.I. Poddubnaya, A.I. Zubenko, L.N. Yakubenko and A.T. Pilipenko, *Dokl. Akad. Nauk SSSR, Ser. Khim.*, 304 (1989) 364.
- 23 F. Helfferich, *Ion Exchange*, McGraw-Hill, New York, 1962.
- 24 O.M. Petrukhin and N.A. Borshch, *Koord. Khim.*, 81 (1982) 22.
- 25 L. Bromberg, I. Lewin and A. Warshawsky, *Hydrometallurgy*, in press.
- 26 D.J. Degenkolb and F.J. Scobey, *J. Soc. Motion Pictures and Television Engineers*, 86 (1977) 65.

Examination of the retention behavior of underivatized profen enantiomers on cyclodextrin silica stationary phases

Michelle D. Beeson and Gyula Vigh*

Department of Chemistry, Texas A&M University, College Station, TX 77843-3255 (USA)

(First received December 2nd, 1992; revised manuscript received December 14th, 1992)

ABSTRACT

The separation of the enantiomers of five widely used profen-type non-steroidal anti-inflammatory agents: fenoprofen, flurbiprofen, ibuprofen, ketoprofen and naproxen was studied using four commercially available cyclodextrin silica stationary phases operated in the reversed-phase mode. The retention behavior of all profens was similar on all the cyclodextrin silica stationary phases studied, but the chiral selectivities differed significantly. Complete separation was achieved for the enantiomers of ibuprofen, flurbiprofen and naproxen.

INTRODUCTION

The 2-aryl propionic acids, or profens, belong to the family of non-steroidal anti-inflammatory drugs (NSAIDs). Once it became known that the different profen enantiomers have different pharmacokinetic properties, interest in their chromatographic separation has increased [1–20]. Some of the profen enantiomers were separated in both the derivatized form [2–9], and in the underivatized form [10–20]. According to the derivatization approach, the carboxyl group of the enantiomers was converted into an ester group [2,3,9], an anilide group [4,5,8], or an amide group [1,2,5–7,9] resulting in improved separation [1–3,5,7–9], and/or improved detection limits [4]. In some of the schemes, the profens were derivatized with an enantiomerically pure reagent leading to the formation of diastereomers [4,6], which then were separated

either on a chiral (*R*)-*N*-(3,5-dinitrobenzoyl)-phenylglycine-based silica column [4] or on an achiral octadecyl silica column [6]. In other schemes, a non-chiral reagent was used to derivatize the profen enantiomers followed by their separation on one of the cellulose-based stationary phases, Chiralcel OC [1] or Chiralcel OJ [3], or on the (*R*)-*N*-(3,5-dinitrobenzoyl)phenylglycine-based silica column [1,2,5,7,9], the (*R*)-*N*-(2-naphthyl)alanine-based silica column [8], or on the chiral stationary phase derived from (*S*)-*N*-(1-naphthyl)leucine [10]. Enantiomers of some of the underivatized profens have also been separated using this stationary phase [10,11], as well as the α_1 -acid glycoprotein stationary phase [12,13], the human serum albumin stationary phase [14], the Cyclobond-I β -cyclodextrin silica phase [18], the Cyclobond-I-SN naphthylethylcarbamoylated cyclodextrin silica phase [15], and an acetylquinidine-silica column used in conjunction with quinidine as a mobile phase additive [16]. In our laboratory, we have been interested in the direct preparative-scale separation of the enantiomers of some of

* Corresponding author.

the profens, primarily using cyclodextrin silica stationary phases [17–20].

Cyclodextrins are toroidally shaped molecules containing 6, 7, or 8 glucose units (α -, β - or γ -cyclodextrins). Cyclodextrins have a hydrophobic cavity and two hydrophilic lips with secondary hydroxyl groups on the larger lip and primary hydroxyl groups on the smaller lip [21,22]. Cyclodextrins can include molecules into their cavities and form host-guest complexes [23]. The stability of the complex depends on the snugness of the fit between the molecule and the cavity and the strength of the polar intermolecular interactions between the host and the guest [24]. The secondary hydroxyl groups can be derivatized to extend the depth of the cavity and/or change the nature of the polar interaction sites.

The commercially available cyclodextrin silica HPLC phases contain cyclodextrin moieties which are chemically bonded to the silica support via the 3-glycidoxysilane [25] spacer. Hydroxypropylated cyclodextrin silicas of the desired chirality are produced by first reacting the cyclodextrin with the appropriate propylene oxide, followed by binding of the modified cyclodextrin to the glycidoxysilylated silica [26,27]. Naphthylethylcarbamoylated cyclodextrin silica stationary phases are produced by further reacting the cyclodextrin silica, *in situ*, with (*S*)-(+)- or (*R*)-(–)-1-(1-naphthyl)ethyl isocyanate [28].

EXPERIMENTAL

A custom-built liquid chromatograph consisting of an LC 2010 pump (Varian, Walnut Creek, CA, USA), a pneumatically activated Type 7000 injection valve (Rheodyne, Cotati, CA, USA), an LC 2050 variable-wavelength UV detector (Varian) set at 254 nm, and a Series RI-3 differential refractive index detector (Varian), was used for the experiments. The detector signals were recorded and analyzed by a Maxima Workstation (Millipore–Waters, Milford, MA, USA). Stainless-steel columns, 250 mm \times 4.6 mm I.D. (BST, Budapest, Hungary), were custom packed with 5- μ m cyclodextrin silicas (ASTEC, Whippany, NJ, USA) using a Model

53127-2 air amplifier pump (Haskel, Burbank, CA, USA). All columns were jacketed and thermostatted at 30°C by a Type UF3 circulating water bath (Science/Electronics, Dayton, OH, USA). All separations were completed at an eluent flow-rate of 1 ml/min.

The stationary phases used in this work are the native β - and γ -cyclodextrin silicas, as well as the (*S*)- and racemic-2-hydroxypropyl- β -cyclodextrin silicas (average degree of substitution: 7.9 hydroxypropyl units per cyclodextrin) [27], and the (*S*)-naphthylethyl carbamoylated β -cyclodextrin [4] silica (average degree of substitution: 6.3 naphthylethyl units per cyclodextrin) [28]. These materials are all commercially available from ASTEC under the trade names of Cyclobond I, Cyclobond II, Cyclobond I-SP,

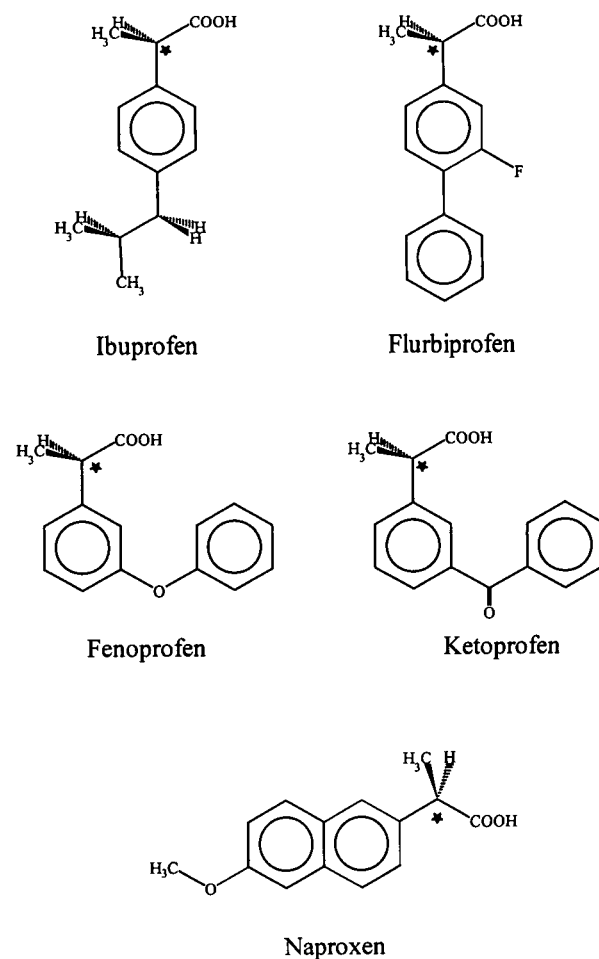


Fig. 1. Structures of the profens used in this study.

Cyclobond I-RSP, and Cyclobond I-SN, respectively.

The eluents were prepared as described before [29] from HPLC-grade acetonitrile (EM Science, Gibbstown, NJ, USA), water produced by a Milli-Q unit (Millipore, Bedford, MA, USA), and sodium citrate and citric acid, both from Aldrich (Milwaukee, WI, USA). The eluent pH values reported here are apparent pH values measured in the hydroorganic eluent using a glass electrode (Corning, Medfield, MA, USA) calibrated with standard aqueous buffers (Fisher Scientific, Fair Lawn, NJ, USA) as recommended in refs. 30 and 31. Racemic ibuprofen and racemic naproxen were gifts from ASTEC. Ketoprofen, flurbiprofen, and (*S*)-naproxen were obtained from Sigma (St. Louis, MO, USA). (*S*)-Ibuprofen was obtained from Aldrich. Fenoprofen calcium was a gift from Eli Lilly (Indianapolis, IN, USA). (The solute structures are shown in Fig. 1.) The solutes were dissolved in the eluents immediately prior to use. The injected amounts were kept at minimum to approximate infinite dilution conditions and were adjusted to yield a signal-to-noise ratio of about 10 to 50.

RESULTS

β -Cyclodextrin silica (Cyclobond I) column

Because in a chiral separation it is the more retained enantiomer that experiences all the possible binding interactions to the fullest, the capacity factors of the more retained enantiomers (k'_2) are used in this paper to discuss the retention behavior of the five profens. The k'_2 obtained on the native β -cyclodextrin silica stationary phase (Cyclobond I) are plotted in Figs. 2 and 3 as a function of the acetonitrile concentration of the eluent at two different pH values: at pH 4, which is below, and at pH 6, which is above the pK_a values of all the profens studied here. On native cyclodextrin silicas operated in the reversed-phase mode, solute retention is attributed to the concerted action of the hydrophobic interactions between the hydrophobic parts of the solute and the hydrophobic interior of the cyclodextrin cavity (inclusion phenomenon), and the hydrogen bonding inter-

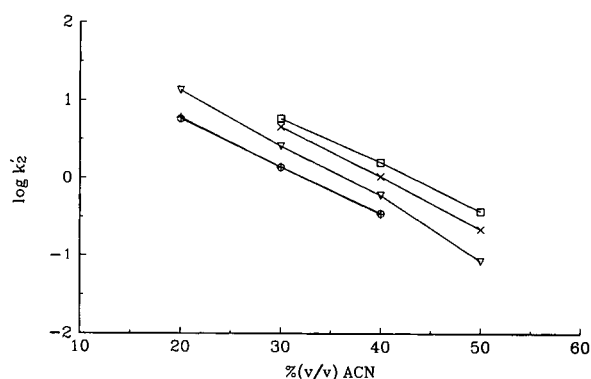


Fig. 2. Capacity factors of the more retained enantiomers of profens as a function of the % (v/v) acetonitrile (ACN) concentration in the pH 4.0, 5 mM citrate buffer eluents on the Cyclobond I β -cyclodextrin silica column. Flow-rate: 1 ml/min, temperature: 30°C, UV detection at 254 nm. Symbols: □ = ibuprofen; × = flurbiprofen; ▽ = fenoprofen; + = naproxen, ○ = ketoprofen.

actions between the polar functional groups of the solute and the hydroxyl groups of the cyclodextrin [22]. As can be seen in Figs. 2 and 3, the logarithm of the capacity factors of the profens decreases almost linearly as the concentration of acetonitrile in the eluent is increased, just as in a regular reversed-phase system consisting of an octadecyl silica stationary phase and a buffered hydroorganic eluent [32]. However, as long as there is more than 30% (v/v) acetonitrile in the eluent, the dissociated profen anions (predominant in the pH 6 eluents) are more

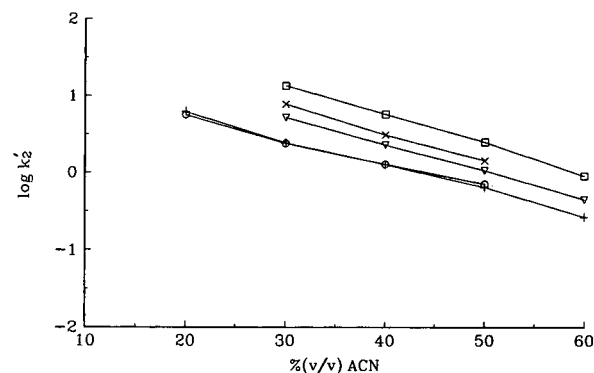


Fig. 3. Capacity factors of the more retained enantiomers of profens as a function of the % (v/v) acetonitrile concentration in the pH 6.0, 5 mM citrate buffer eluents on the Cyclobond I β -cyclodextrin silica column. Other conditions and symbols as in Fig. 2.

strongly retained than the non-dissociated, free acid profens (predominant in the pH 4.0 eluents). This behavior is exactly opposite of what one can observe in a regular reversed-phase system [32]: it indicates that in the presence of an organic solvent the sum of the hydrophobic and the hydrogen bonding interactions between the anions and the cyclodextrin are stronger than those between the free acids and the cyclodextrins. As the acetonitrile concentration is decreased, the strength of the bonding interactions between the anions and the cyclodextrin increases only slightly, while the strength of the bonding interactions between the free acids and the cyclodextrins increases strongly. Eventually, in pure aqueous eluents, the free acids are bonded more strongly than the respective anions. This observation agrees qualitatively with our recent finding in capillary electrophoresis, that in a pure aqueous buffer the value of the formation constant of the cyclodextrin–profen acid complex is larger than that of the cyclodextrin–profen anion complex [33].

With regard to chiral selectivity, an interesting trend can be observed in Fig. 4. As long as the concentration of acetonitrile is higher than 20% (v/v), chiral separation is observed only in the high-pH eluent, and only for ibuprofen. As the acetonitrile concentration is decreased, the chiral selectivity coefficient for ibuprofen increases towards a limiting α value of about 1.06. In eluents with acetonitrile concentrations higher

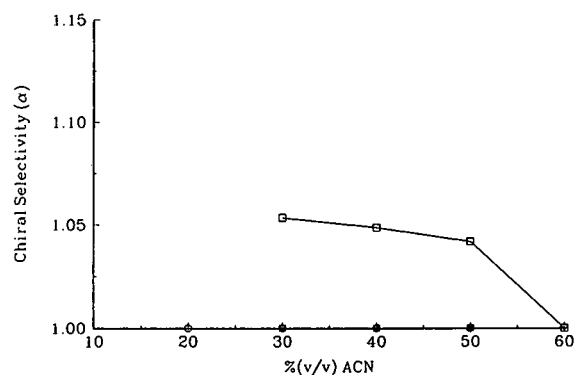


Fig. 4. Chiral selectivity as a function of the % (v/v) acetonitrile concentration in the pH 6.0, 5 mM citrate buffer eluents for profens on the Cyclobond I β -cyclodextrin silica column. Other conditions and symbols as in Fig. 2.

than 50% (v/v), chiral discrimination is lost, even in high-pH eluents. Though it would be interesting to compare the chiral recognition mechanisms operative in HPLC and capillary electrophoresis (where a limiting α value of about 1.04 has been observed for ibuprofen in low-pH buffers at a temperature of 37°C [33]), the HPLC α values for ibuprofen could not be determined in purely aqueous eluents, either at high pH or at low pH, because the k'_2 values were excessively high (well over 100).

Because good chiral separation was observed for the ionic form of ibuprofen, the buffer strength of the eluent was varied to see if solute retention and chiral selectivity could be controlled by this parameter, and/or chiral separation could be achieved for the other profens. While increased buffer strength greatly decreased the capacity factors of the profens both in high- and low-pH eluents, due to the increased competition of the buffer species for the available cyclodextrin binding sites [34], it did not lead to chiral recognition for any of the other profens.

The effect of column temperature on the chiral selectivity was also examined. For ibuprofen, a regular Van 't Hoff plot was obtained, similar to the ones reported earlier [19], and the chiral selectivity improved from $\alpha = 1.054$ at 30°C to $\alpha = 1.075$ at 2°C. However, chiral separation could not be achieved for the other profens, even at 2°C.

Naphthylethylcarbamoylated β -cyclodextrin silica (Cyclobond I-SN) column

On the naphthylethylcarbamoylated β -cyclodextrin silica column, the logarithms of the capacity factors decrease linearly with the increasing acetonitrile concentration: the rate of decrease is once again faster at pH 4 (Fig. 5) than at pH 6 (Fig. 6). When the acetonitrile concentration in the eluent is less than 20% (v/v), retention in the low pH eluents (non-dissociated profens) becomes stronger than in the high pH eluents (anionic profens). In the high-pH eluents, the k'_2 values on the native and on the naphthylethylcarbamoylated β -cyclodextrin silica columns are identical within experimental error. However, in low-pH eluents,

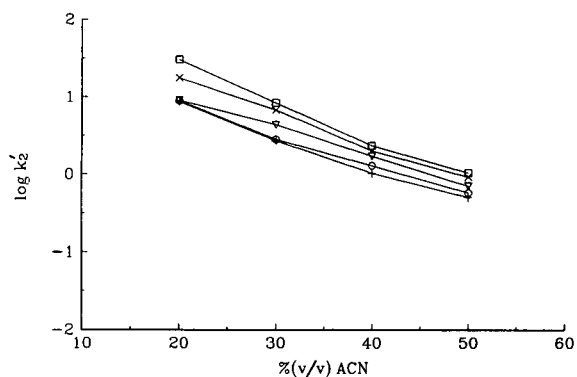


Fig. 5. Capacity factors of the more retained enantiomers of profens as a function of the % (v/v) acetonitrile concentration in the pH 4.0, 5 mM citrate buffer eluents on the Cyclobond I-SN naphthylethylcarbamoylated β -cyclodextrin silica column. Other conditions and symbols as in Fig. 2.

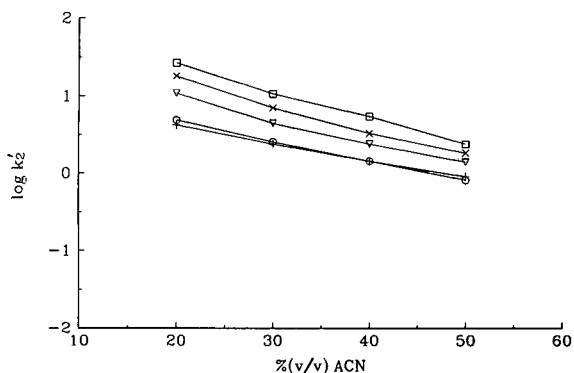


Fig. 6. Capacity factors of the more retained enantiomers of profens as a function of the % (v/v) acetonitrile concentration in the pH 6.0, 5 mM citrate buffer eluents on the Cyclobond I-SN naphthylethylcarbamoylated β -cyclodextrin silica column. Other conditions and symbols as in Fig. 2.

the k'_2 values are about 10–15% higher on the naphthylethylcarbamoylated β -cyclodextrin silica column than on the native β -cyclodextrin silica column.

As shown in Figs. 7 and 8, chiral selectivity on the naphthylethylcarbamoylated β -cyclodextrin silica (Cyclobond I-SN) column is better than on the native β -cyclodextrin silica column. In the pH 6.0 eluents, the highest selectivity factor value found for ibuprofen is $\alpha = 1.126$, much higher than the 1.054 value on the native cyclodextrin silica (Cyclobond I) column. Additionally, chiral separation is observed for flurbiprofen as well: the highest selectivity value is

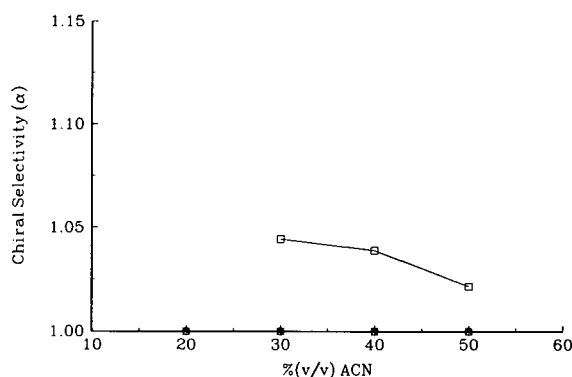


Fig. 7. Chiral selectivity as a function of the % (v/v) acetonitrile concentration in the pH 4.0, 5 mM citrate buffer eluents for profens on the Cyclobond I-SN naphthylethylcarbamoylated β -cyclodextrin silica column. Other conditions and symbols as in Fig. 2.

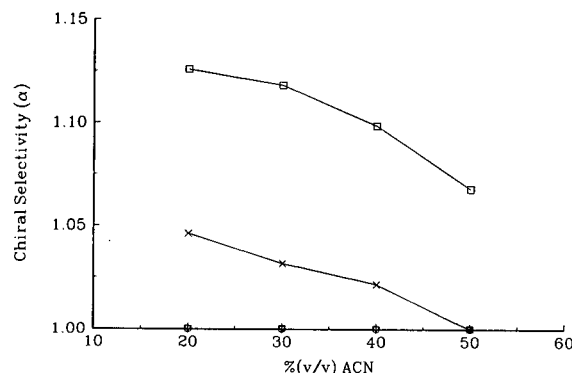


Fig. 8. Chiral selectivity as a function of the % (v/v) acetonitrile concentration in the pH 6.0, 5 mM citrate buffer eluents for profens on the Cyclobond I-SN naphthylethylcarbamoylated β -cyclodextrin silica column. Other conditions and symbols as in Fig. 2.

$\alpha = 1.046$ (Fig. 8). At pH 4.0, chiral separation is observed only for ibuprofen (Fig. 7), and the chiral selectivity is worse ($\alpha = 1.044$) than at pH 6.0. When the acetonitrile concentration becomes higher than 50% (v/v), the chiral separation is lost, both at high pH and low pH, for both ibuprofen and flurbiprofen, following the trend that was observed on the Cyclobond I column (Figs. 7 and 8).

Hydroxypropylated β -cyclodextrin silica (Cyclobond I-SP) columns

The retention and the selectivity values observed on the (*S*)-hydroxypropylated β -cyclo-

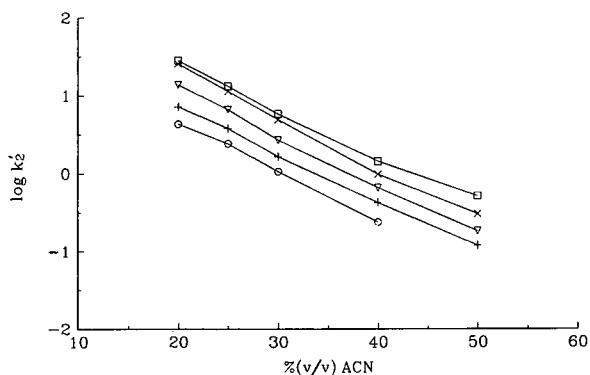


Fig. 9. Capacity factors of the more retained enantiomers of profens as a function of the % (v/v) acetonitrile concentration in the pH 4.0, 5 mM citrate buffer eluents on the Cyclobond I-SP (*S*)-hydroxypropylated β -cyclodextrin silica column. Other conditions and symbols as in Fig. 2.

dextrin silica stationary phase (Figs. 9–11) follow the trends observed with the native and the naphthylethylcarbamoylated β -cyclodextrin silicas: the k'_2 values are lower in the acetonitrile-rich eluents at pH 4 than at pH 6.5, the k'_2 values are higher in the purely aqueous eluents at pH 4 than at pH 6.5, the slopes of the k'_2 vs. % ACN curves are steeper at pH 4 than at pH 6.5. In the pH 4 eluents, solute retention on the native β -cyclodextrin and the (*S*)-hydroxypropylated cyclodextrin silica is also identical within experimental error. However, when it comes to chiral selectivity, an important difference is observed. Enantiomeric separation is achieved

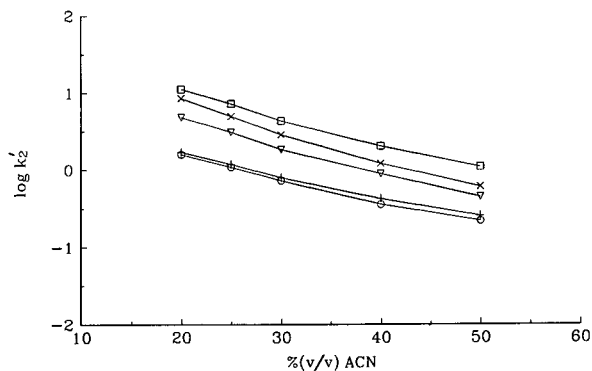


Fig. 10. Capacity factors of the more retained enantiomers of profens as a function of the % (v/v) acetonitrile concentration in the pH 6.5, 5 mM citrate buffer eluents on the Cyclobond I-SP (*S*)-hydroxypropylated β -cyclodextrin silica column. Other conditions and symbols as in Fig. 2.

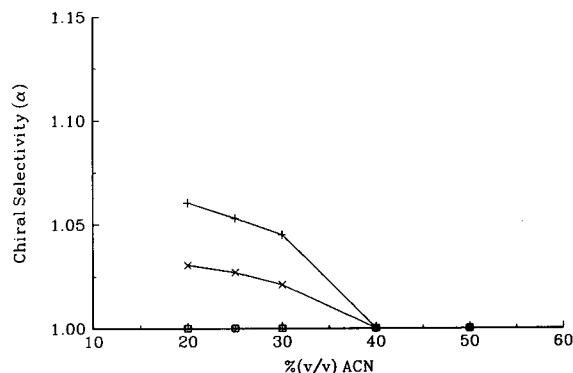


Fig. 11. Chiral selectivity as a function of the % (v/v) acetonitrile concentration in the pH 4.0, 5 mM citrate buffer eluents for profens on the Cyclobond I-SP (*S*)-hydroxypropylated β -cyclodextrin silica column. Other conditions and symbols as in Fig. 2.

solely at pH 4.0, and only for flurbiprofen and naproxen.

The racemic hydroxypropylated β -cyclodextrin stationary phase (Cyclobond I-RSP column) was also evaluated. Using the same eluents, similar chiral selectivity was observed for the naproxen and the flurbiprofen on both the (*S*)-hydroxypropylated (Cyclobond I-SP) and the racemic hydroxypropylated β -cyclodextrin silicas (Cyclobond I-RSP). Retention was slightly lower, though, on the racemic hydroxypropylated β -cyclodextrin. No separation was achieved for the other profens either at low pH or at high pH. Thus, for the separation of the profen enantiomers, the use of the more expensive (*S*)-hydroxypropylated cyclodextrin column offers no advantage.

γ -Cyclodextrin silica (Cyclobond II) columns

Again, the same type of retention behavior was observed; as the concentration of acetonitrile increases, the logarithms of the k'_2 values decrease faster at pH 4.0 than at pH 6.0. However, regardless of the acetonitrile concentration, the retention times of the profens are very similar to each other, with the exception of flurbiprofen which is more retained. This indicates a lack of differentiation by the γ -cyclodextrin phase for the profens (Figs. 12 and 13). No separation of the enantiomers of any of the profens was observed using γ -cyclodextrin silica.

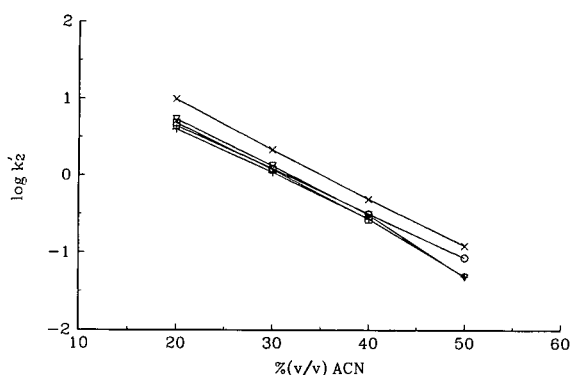


Fig. 12. Capacity factors of the more retained enantiomers of profens as a function of the % (v/v) acetonitrile concentration in the pH 4.0, 5 mM citrate buffer eluents on the Cyclobond II γ -cyclodextrin silica column. Other conditions and symbols as in Fig. 2.

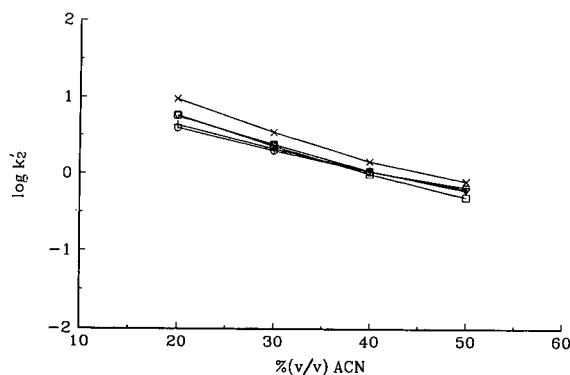


Fig. 13. Capacity factors of the more retained enantiomers of profens as a function of the % (v/v) acetonitrile concentration in the pH 6.0, 5 mM citrate buffer eluents on the Cyclobond II γ -cyclodextrin silica column. Other conditions and symbols as in Fig. 2.

CONCLUSIONS

All the cyclodextrin silica columns investigated display similar retention behavior. Chiral separation was observed on the Cyclobond-I β -cyclodextrin silica column for ibuprofen at high pH, on the Cyclobond I-SN naphthylethylcarbamoylated β -cyclodextrin silica column for ibuprofen and flurbiprofen at high pH, and for ibuprofen at low pH, and on the Cyclobond I-SP and Cyclobond I-RSP hydroxypropylated β -cyclodextrin silica columns for flurbiprofen and naproxen at low pH. The Cyclobond-II γ -cyclodextrin silica column could not

differentiate either between the various profens, or their enantiomers.

ACKNOWLEDGEMENTS

Partial financial support for this project was provided by the National Science Foundation (CH-8919151) and the Dow Chemical Company. The authors are indebted to ASTEC for providing us with the stationary phases used in this study. Ely Lilly and Company is acknowledged for their donation of the fenoprofen calcium sample.

REFERENCES

- 1 D. McDaniel and B. Snider, *J. Chromatogr.*, 404 (1987) 123.
- 2 I. Wainer and T. Doyle, *J. Chromatogr.*, 284 (1984) 117.
- 3 H. Aboul-Enein and S. Bákr, *J. Liq. Chromatogr.*, 15 (1992) 1983.
- 4 W. Pirkle and P. Murray, *J. Liq. Chromatogr.*, 13 (1990) 2123.
- 5 W. Pirkle and J. McCune, *J. Chromatogr.*, 471 (1989) 271.
- 6 S. Pedrazzini, W. Zanaboni-Muciaccia, C. Sacchi and A. Forgione, *J. Chromatogr.*, 415 (1987) 214.
- 7 D. Nicoll-Griffith, *J. Chromatogr.*, 402 (1987) 179.
- 8 J. Kern, *J. Chromatogr.*, 543 (1991) 355.
- 9 W. Pirkle and C. Welch, *J. Liq. Chromatogr.*, 14 (1991) 3387.
- 10 W. Pirkle, C. Welch and B. Lamm, *J. Org. Chem.*, 57 (1992) 3854.
- 11 W. Pirkle and C. Welch, *J. Liq. Chromatogr.*, 15 (1992) 1947.
- 12 J. Andersen and S. Hansen, *J. Chromatogr.*, 577 (1992) 362.
- 13 J. Hermansson and M. Eriksson, *J. Liq. Chromatogr.*, 9 (1986) 621.
- 14 T. Noctor, G. Felix and I. Wainer, *Chromatographia*, 31 (1991) 55.
- 15 D. Armstrong, C. Chang and S. Lee, *J. Chromatogr.*, 539 (1991) 83.
- 16 C. Patterson and C. Gioeli, *J. Chromatogr.*, 435 (1988) 225.
- 17 Gy. Farkas, G. Quintero and Gy. Vigh, *J. Chromatogr.*, 506 (1990) 481.
- 18 Gy. Vigh, Gy. Farkas and G. Quintero, in J. Nikelly and Cs. Horváth (Editors), *Analytical Biotechnology (ACS Symposium Series, No. 434)*, American Chemical Society, Washington, DC, 1990, p. 181.
- 19 Gy. Farkas, L. Irgens, G. Quintero, M.D. Beeson, A. Al-Saeed and Gy. Vigh, *J. Chromatogr.*, submitted for publication.

- 20 P. Camacho, L. Irgens, C. Piggee, M. Miner, A. Al-Saeed and Gy. Vigh, in M. Perrut (Editor), *Proceedings of the Prep '92 Symposium, Nancy, April 6–8, 1992*, Société Française de Chimie, 1992, p. 383.
- 21 M. Bender and M. Komiyama, *Cyclodextrin Chemistry*, Springer, Berlin, 1978.
- 22 J. Szejtli, *Cyclodextrins and Their Inclusion Complexes*, Akadémiai Kiado, Budapest, 1982.
- 23 L. Spino and D. Armstrong, in W. Hinze and D. Armstrong (Editors), *Ordered Media in Chemical Separations (ACS Symposium Series, No. 342)*, American Chemical Society, Washington, DC, 1987, p. 235.
- 24 Y. Yamamoto and Y. Inoue, *J. Carbohydr. Chem.*, 8 (1989) 29.
- 25 D. Armstrong, *US Pat.*, 4 539 999 (1985).
- 26 D. Armstrong, L. Weiyong, C. Chang and J. Pitha, *Anal. Chem.*, 62 (1990) 914.
- 27 A. Stalcup, S. Chang, D. Armstrong and J. Pitha, *J. Chromatogr.*, 513 (1990) 181.
- 28 D. Armstrong, A. Stalcup, M. Hilton, J. Duncan, J. Faulkner, Jr. and S. Chang, *Anal. Chem.*, 62 (1990) 1610.
- 29 Gy. Vigh, G. Quintero and Gy. Farkas, *J. Chromatogr.*, 484 (1989) 237.
- 30 R.G. Bates, *Determination of pH—Theory and Practice*. Wiley-Interscience, New York, 1973.
- 31 A. Leitold and Gy. Vigh, *J. Chromatogr.*, 257 (1983) 384.
- 32 B.L. Karger, J.N. LePage and N. Tanaka in Cs. Horváth (Editor), *High Performance Liquid Chromatography—Advances and Perspectives*, Vol. 1, Academic Press, New York, 1980, pp. 113–204.
- 33 Y. Rawjee, D. Staerk and Gy. Vigh, *J. Chromatogr.*, in press.
- 34 G. Quintero, *Thesis*, Texas A&M University, College Station, TX, 1990, p. 59.

Rapid and complete chiral chromatographic separation of racemic quaternary tropane alkaloids

Complementary use of a cellulose-based chiral stationary phase in reversed-phase and normal-phase modes —a mechanistic study

Th.R.E. Hampe

Department of Pharmaceutical Research, Boehringer Ingelheim KG, W-6507 Ingelheim (Germany)

J. Schlüter

Department of Pharmaceutical Development, Boehringer Ingelheim KG, W-6507 Ingelheim (Germany) and Institute of Pharmaceutical Chemistry, University of Münster, W-4400 Münster (Germany)

K.H. Brandt

Department of Pharmaceutical Research, Boehringer Ingelheim KG, W-6507 Ingelheim (Germany)

J. Nagel

Boehringer Ingelheim Pharmaceuticals, 175 Briar Ridge Road, Ridgefield, CT 06877 (USA)

E. Lamparter

Department of Pharmaceutical Development, Boehringer Ingelheim KG, W-6507 Ingelheim (Germany)

G. Blaschke

Institute of Pharmaceutical Chemistry, University of Münster, W-4400 Münster (Germany)

(First received April 3rd, 1992; revised manuscript received September 29th, 1992)

ABSTRACT

Complete chromatographic separations of a wide range of different tropane alkaloid stereoisomers on a commercially available cellulose-based chiral stationary phase (CSP) are described. The separations were achieved by using cellulose tris(3,5-dimethylphenyl)carbamate as CSP with both an aqueous and an organic mobile phase with different ionic modifiers. The effects of totally different modifiers in both mobile phases on the chromatographic resolution are described.

Correspondence to: Th.R.E. Hampe, Department of Pharmaceutical Research, Boehringer Ingelheim KG, W-6507, Ingelheim, Germany.

INTRODUCTION

Tropane alkaloids are anticholinergic drugs. Well known are the esters of tropic acid with scopine (scopolamine) and tropine (atropine). The racemate atropine (3-tropoyloxytropine) is a mixture of the (*S*)- and (*R*)-hyoscyamine enantiomers, whereas the mixture of (*R*)- and (*S*)-scopolamine enantiomers is called atrosine (3-tropoyloxy-6 β ,7 β -epoxytropine). The chromatographic enantioseparation of the tertiary compounds atropine and atrosine have been described previously [1,2]. By quaternization of these tropane alkaloids the central effects of these drugs are avoided. These compounds are in use as neurotropic spasmolytics in modern therapy. Until now no methods existed (except for the imprecise measurement of optical rotation) for the determination of the enantiomeric purity of these compounds [3]. We describe here conditions for the determination of the optical purity of these drugs by chromatographic methods.

STEREOCHEMISTRY

Anticholinergics of the tropane alkaloids are esters of the N-alkylated nortropine (1) and norscopine (2) and racemic tropic acid (3). The quaternary N,N-dialkylated noratropine (4) and N,N-dialkylated noratrosine (5) molecules have one chiral centre in the 2'-position and two pseudoasymmetric centres in the C-3 and N-8 positions (see Fig. 1).

The direct chromatographic separation of the racemates refers to the chiral centre in the 2'-position in all instances. Therefore, tropine is characterized as 1(*R*),3(*r*),5(*S*),8(*r*)-azabicyclo[3.2.1]octan-3-ol. For quaternary N,N-dialkylated nortropine the pseudoasymmetric nitrogen in the 8-position is described as "r" for $R_1 > R_2$ and "s" for $R_1 < R_2$.

The introduction of the epoxy group into the piperidine system leads to atrosine with a completely converted configuration of the saturated cyclic system. Therefore, the absolute configuration of scopine is described as 1(*S*),3(*s*),5(*R*),6(*R*),7(*S*),8(*s*)-aza-6,7-epoxybicyclo[3.2.1]-octan-3-ol.

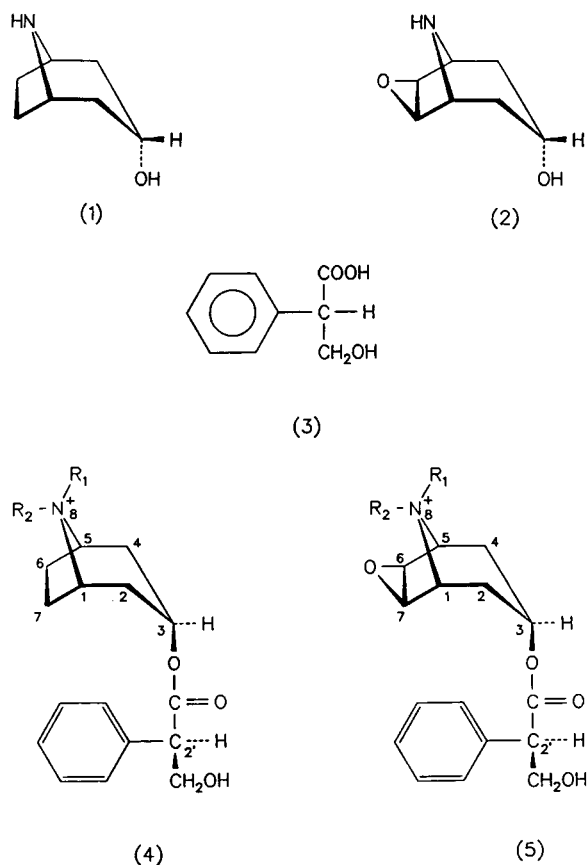


Fig. 1. Structures of nortropine (1), norscopine (2), tropic acid (3), quaternary N,N-dialkylated noratropine (4) and quaternary N,N-dialkylated noratrosine (5).

Similarly to N,N-dialkylnortropine, the quaternary N,N-dialkylnorscopine with different alkyl chains fixes the pseudoasymmetric centre in the 8-position, characterized as "s" for $R_1 > R_2$ and "r" for $R_1 < R_2$ [4–7].

EXPERIMENTAL

The quaternary tropane alkaloids tested were obtained from Boehringer Ingelheim (Ingelheim, Germany). The solvents used for chromatography were of HPLC grade and were used as received. The different ionic modifiers were of analytical-reagent grade.

Chromatography

Separation of the enantiomers was achieved by a column based on the chiral stationary phase

(CSP) tris(3,5-dimethylphenyl)carbamate cellulose [8], commercially available as Chiralcel OD (Daicel). All mobile phases were premixed and degassed by ultrasonic treatment for 3 min. The enantiomeric separations were performed using two totally different mobile phases, one organic and the other aqueous.

The organic mobile phase always consisted of *n*-hexane–ethanol–methanol (600:150:250) with different modifiers when not specified otherwise. The modifier was dissolved in the alcoholic part of the mobile phase and diluted with *n*-hexane.

For the aqueous mobile phase [9], different modifiers were dissolved in water and mixed with methanol or acetonitrile.

All chromatographic studies were performed with a flow-rate of 0.5 ml/min. Detection was carried out at a wavelength of 230 nm unless stated otherwise. The volume injected was 10 μ l at a concentration of 1 mg/ml.

RESULTS AND DISCUSSION

Stereochemistry of the tested racemates

The investigated racemates are quaternary N,N-dialkylated derivatives of noratropine and noratropine. Different chain lengths of the axial bonded R_1 and the equatorial R_2 substituent lead to (*r*)- and (*s*)-configurations.

When the equatorial bonded substituent (R_2) is larger than the axial bonded substituent (R_1), the quaternary nitrogen of atropine has the (*s*)-configuration, and when R_1 is larger than R_2 the molecule has the (*r*)-configuration. Analogous substitution in N-alkylated atropine converts the configuration of the saturated ring system completely, including the quaternary nitrogen. In contrast to all other racemates, the racemates **4b** and **4p** have (*s*)-configuration in the 3-position (pseudotropine = β -tropine).

The compounds can be divided structurally as follows.

(1) Compounds **4a** to **4g** are of (*s*)-configuration (except **4b**) with increasing R_2 (equatorial) alkyl chain length and a methyl group in R_1 (axial);

(2) Compounds **4a**, **4h** to **4l** are of (*r*)-configuration with a methyl group in R_2 (equatorial) and increasing alkyl chain length in R_1 (axial);

(3) Compounds **4a**, **4m** and **4n**: the substances have in each instance the same alkyl substituents in equatorial (R_2) and axial (R_1) positions increasing in size from **4a** to **4n**;

(4) Compounds **4o** to **4q** are three of the four possible stereoisomers of the racemic tropic ester of N-isopropylmethyl-3- β -tropine;

(5) Compounds **4b** and **4p** are 3 β -derivatives of **4a** and **4o** (so-called pseudotropines);

(6) Compounds **5a** to **5f** are of (*s*)-configuration with a methyl group in R_2 (equatorial) and increasing alkyl chain length in R_1 (axial);

(7) Compounds **5d** and **5q** are the (*r*)- and (*s*)-configuration racemic tropic esters of N-butylmethyl-3 α -tropine;

(8) Compounds **5a** and **5h**: the nitrogen of **5a** is substituted with two methyl groups whereas the nitrogen of **5h** is substituted with two ethyl groups.

TABLE I

QUATERNARY N,N-DIALKYL DERIVATIVES OF NORATROPINE (4) AND NORATROSCINE (5)

Compound	R_1 (axial)	R_2 (equatorial)	Configuration
4a	CH ₃	CH ₃	–
4b	CH ₃	CH ₃	– (β -tropine)
4c	CH ₃	C ₂ H ₅	<i>s</i>
4d	CH ₃	C ₄ H ₉	<i>s</i>
4e	CH ₃	C ₅ H ₁₁	<i>s</i>
4f	CH ₃	C ₆ H ₁₃	<i>s</i>
4g	CH ₃	C ₇ H ₁₅	<i>s</i>
4h	C ₂ H ₅	CH ₃	<i>r</i>
4i	C ₃ H ₇	CH ₃	<i>r</i>
4k	C ₄ H ₉	CH ₃	<i>r</i>
4l	C ₅ H ₁₁	CH ₃	<i>r</i>
4m	C ₂ H ₅	C ₂ H ₅	–
4n	C ₄ H ₉	C ₄ H ₉	–
4o	iso-C ₃ H ₇	CH ₃	<i>r</i>
4p	iso-C ₃ H ₇	CH ₃	<i>r</i> (β -tropine)
4q	CH ₃	iso-C ₃ H ₇	<i>s</i>
5a	CH ₃	CH ₃	–
5b	C ₂ H ₅	CH ₃	<i>s</i>
5c	C ₃ H ₇	CH ₃	<i>s</i>
5d	C ₄ H ₉	CH ₃	<i>s</i>
5e	C ₅ H ₁₁	CH ₃	<i>s</i>
5f	C ₆ H ₁₃	CH ₃	<i>s</i>
5g	CH ₃	C ₄ H ₉	<i>r</i>
5h	C ₂ H ₅	C ₂ H ₅	–

Chromatographic results

The two different mobile phases were able to resolve all the investigated quaternary tropane alkaloids (see Table I). In all instances complete baseline separations with separation factors of up to 7.0 were achieved.

The chromatographic data presented in Tables II and III show similar results. In both systems racemic quaternary tropane alkaloids with larger axial alkyl groups were resolved with significantly higher separation factors than the respective N-epimers in the 8-position.

With mobile phase system A (Table II) the α -values are constant for larger equatorially bonded groups whereas more voluminous axially bonded groups show increasing separation factors leading to a maximum with the propyl-substituted molecule. Longer alkyl chains result in poorer separations. These effects are shown in

TABLE II

MOBILE PHASE A: CAPACITY AND SEPARATION FACTORS OF QUATERNARY TROPANE ALKALOIDS USING *n*-HEXANE-ETHANOL-METHANOL (60:15:25) CONTAINING 2 mM OF TETRAPROPYLAMMONIUMBROMIDE

Compound	t_1	t_2	k'_1	k'_2	α
4a	8.67	13.02	0.84	1.77	2.11
4b	8.30	8.76	0.77	0.86	1.12
4c	8.14	10.69	0.73	1.27	1.74
4d	7.20	8.91	0.53	0.90	1.70
4e	6.84	8.09	0.46	0.72	1.57
4f	7.07	8.78	0.50	0.87	1.74
4g	7.05	8.76	0.50	0.86	1.72
4h	8.53	23.48	0.81	4.00	4.94
4i	7.86	26.88	0.67	4.72	7.04
4k	7.26	15.96	0.54	2.40	4.44
4l	7.21	10.89	0.53	1.32	2.49
4m	8.10	17.54	0.72	2.73	3.79
4n	6.39	11.38	0.36	1.42	3.94
4o	9.34	36.84	0.99	6.84	6.91
4p	8.25	9.74	0.76	1.07	1.41
4q	7.67	9.57	0.63	1.04	1.65
5a	9.29	14.69	0.98	2.13	2.17
5b	9.83	33.99	1.09	6.23	5.72
5c	8.81	27.99	0.87	4.96	5.70
5d	8.27	19.95	0.76	3.24	4.26
5e	7.83	15.15	0.67	2.22	3.31
5f	8.64	14.90	0.84	2.17	2.58
5g	8.25	10.92	0.76	1.32	1.74
5h	9.70	26.78	1.06	4.70	4.43

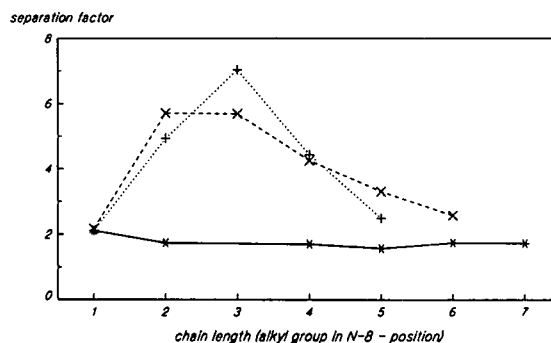


Fig. 2. Separation factor versus chain length (mobile phase A). Solid line = quaternary N-alkyl-N-methylnoratropine (s); dashed line = N-alkyl-N-methylnoratropine (r); dotted line = quaternary N-alkyl-N-methylnoratropine (s).

Fig. 2. The same tendency is shown by the (s)- and (r)-configuration quaternary N-alkyl-N-methylatropine derivatives.

With system B (see Table III) the separation factors do not depend on the chain length of the

TABLE III

MOBILE PHASE B: CAPACITY AND SEPARATION FACTORS OF QUATERNARY TROPANE ALKALOIDS USING 0.05 M SODIUM PERCHLORATE (pH 2)-ACETONITRILE (75:25) AS MOBILE PHASE

Compound	t_1	t_2	k'_1	k'_2	α
4a	9.41	10.27	0.74	0.90	1.21
4b	9.75	—	0.81	—	1.00
4c	11.53	15.17	1.14	1.81	1.59
4d	24.51	43.91	3.54	7.13	2.02
4e	37.14	45.67	5.88	7.46	1.27
4f	92.64	120.63	16.16	21.34	1.32
4g	198.99	265.67	35.85	48.20	1.34
4h	11.43	12.55	1.12	1.32	1.19
4i	15.67	25.84	1.90	3.79	1.99
4k	24.66	29.79	3.57	4.52	1.27
4l	36.81	45.23	5.82	7.38	1.27
4m	14.18	18.94	1.63	2.51	1.54
4n	64.60	143.00	10.96	25.48	2.32
4o	16.92	34.49	2.13	5.39	2.53
4p	15.43	—	1.86	—	1.00
4q	15.50	17.41	1.87	2.22	1.19
5a	8.90	10.07	0.65	0.86	1.33
5b	9.35	12.88	0.73	1.39	1.89
5c	14.25	20.54	1.64	2.80	1.71
5d	22.85	34.89	3.23	5.46	1.69
5e	39.89	64.83	6.39	11.01	1.72
5f	77.97	140.12	13.44	24.95	1.86
5g	22.31	28.08	3.13	4.20	1.34
5i	14.25	18.42	1.64	2.41	1.47

analytes. There is a linear dependence of $\log k'_1$ on chain length for both atropine and atrosine derivatives (Fig. 3). This is opposite of the chromatographic results with system A, where the capacity factors of the (*s*)-enantiomers decreased with increasing chain length of the alkyl chain in the 8-position (except for **4a**).

In both systems A and B the quaternary tropane alkaloids with both R_1 and R_2 alkyl groups of increasing size (**4a**, **4m**, **4n**; **5a**, **5i**) are separated with higher separation factors. Esters of α -tropanol were obviously resolved better than the respective esters of β -tropanol (**4b**, **4p**). The separation of these compounds is similar to that of compounds with larger equatorial alkyl chains [(*s*)-configuration for N-alkyl-N-methylnoratropine derivatives and (*r*)-configuration for N-alkyl-N-methylnoratrosine derivatives]. With mobile phase system B no separations of esters of β -tropanol were observed.

Figs. 4 and 5 show examples of the complete direct enantioseparation of selected racemates.

Influence of different modifiers

The above-mentioned correlations between retention behaviour and stereochemistry are also valid for the subsequently investigated modifiers.

Alkylsulphonic acids. In addition to the already described effects, the following dependences of the separation on the alkyl chain of the alkylsulphonic acids can be observed (methanesulphonic acid = MSA; butanesulphonic acid = BSA; heptanesulphonic acid = HSA; camphorsulphonic acid = CSA). With system A (Table

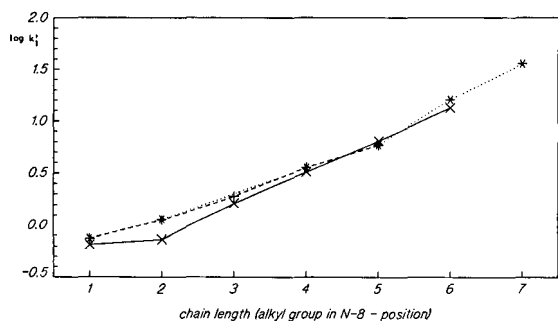


Fig. 3. Log (capacity factor, k'_1) versus chain length (mobile phase B). Dotted line = quaternary N-alkyl-N-methylnoratropine (*s*); dashed line = quaternary N-alkyl-N-methylnoratropine (*r*); solid line = N-alkyl-N-methylnoratrosine (*s*).

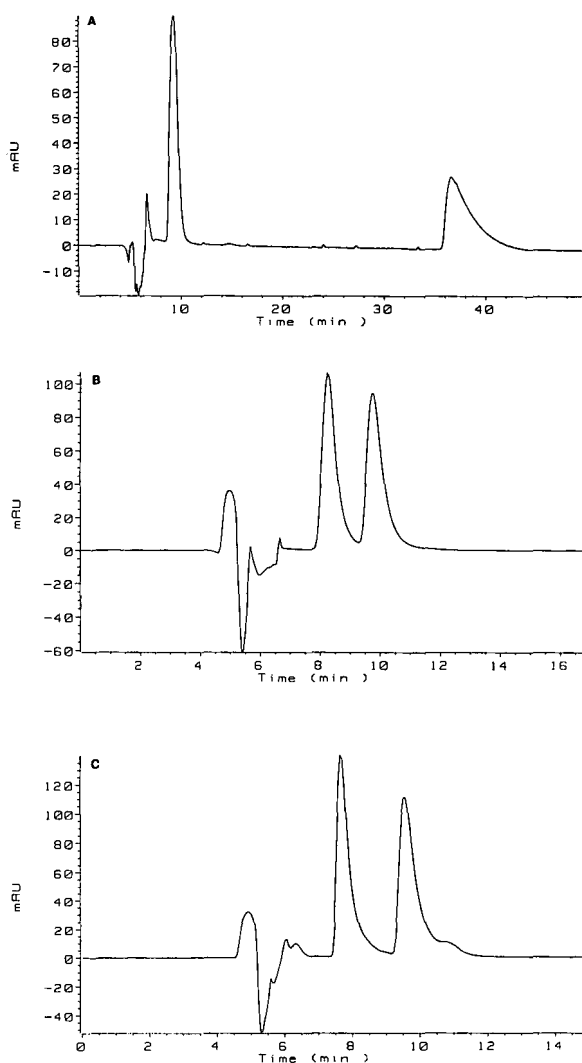


Fig. 4. Separation of (A) **4o**, (B) the respective β -tropine form **4p** and (C) the N-epimer **4q** with mobile phase system A (for eluent, see Table II).

IV) the capacity factors decrease with increasing size of the alkyl groups of the sulphonic acids, whereas no significant effect towards enantioselectivity is observed. In contrast, a minimum of retention with BSA as modifier in mobile phase system B (Table V) is found. The highest α -values (except for the N,N-dimethyl derivatives **4a** and **5a**) are observed with HSA as modifier.

Halogen-containing modifiers. The influence of halogen-containing modifiers was tested. The following dependences of the separation on the

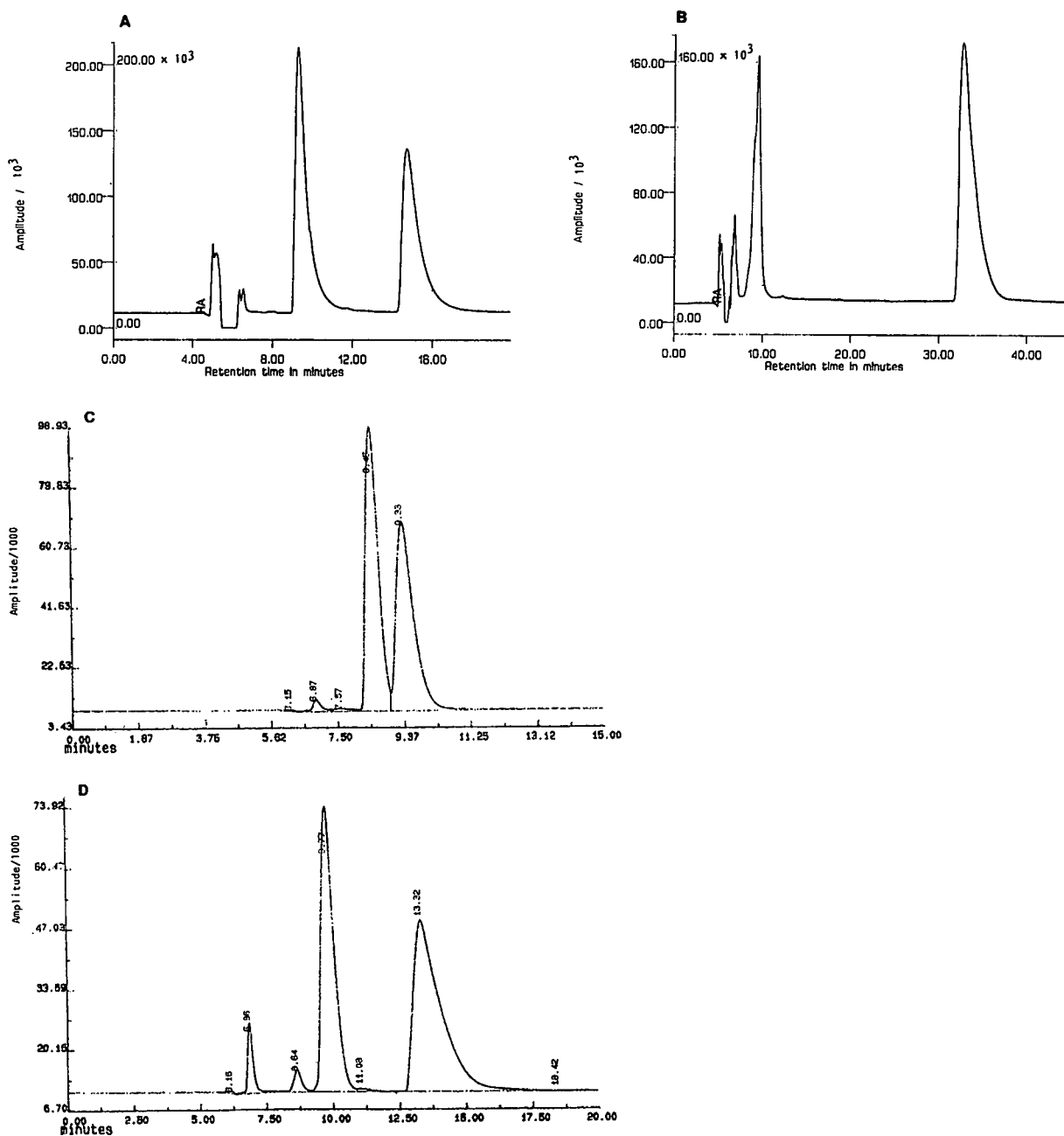


Fig. 5. Separation of the racemates **5a** and **5b** with both mobile phase systems (for eluents, see Tables II and III). (A) Racemate **5a** in mobile phase A; (B) racemate **5b** in mobile phase A; (C) racemate **5a** in mobile phase B; (D) racemate **5b** in mobile phase B.

alkyl chain length of the halides as anionic modifiers were observed. With mobile phase system A (Table VI), the capacity factors increase with increasing atomic number of the halide. The

retention behaviour of the quaternary tropane alkaloids is independent of the cation of the modifier. Sodium bromide and tetrapropylammonium bromide as modifiers result in compar-

TABLE IV

CAPACITY AND SEPARATION FACTORS OF SELECTED QUATERNARY COMPOUNDS USING DIFFERENT ALKYL SULPHONIC ACIDS (2 mM) AS MODIFIERS IN MOBILE PHASE A

Compound	MSA			BSA			HSA		
	k'_1	k'_2	α	k'_1	k'_2	α	k'_1	k'_2	α
4e	0.45	0.51	1.13	0.34	0.49	1.44	0.32	0.42	1.31
4c	0.72	1.11	1.54	0.51	0.91	1.78	0.49	0.83	1.69
4h	0.79	3.17	4.01	0.64	2.87	4.48	0.51	2.72	5.33
4l	0.49	1.02	2.08	0.47	0.87	1.85	0.45	0.79	1.76
5b	0.94	4.79	5.10	0.74	4.28	5.78	0.68	4.17	6.13
5e	0.51	1.51	2.96	0.49	1.36	2.78	0.45	1.28	2.84

TABLE V

CAPACITY AND SEPARATION FACTORS OF SELECTED QUATERNARY COMPOUNDS USING DIFFERENT ALKYL SULFONIC ACIDS (0.05 mM) AS MODIFIERS IN MOBILE PHASE B

Compound	MSA			BSA			HSA			CSA		
	k'_1	k'_2	α									
4a	0.22	0.56	2.50	–	–	–	0.65	0.72	1.12	0.30	0.67	2.35
4h	0.81	–	1.00	0.34	–	1.00	0.91	1.02	1.12	2.91	2.63	1.20
4c	0.81	1.15	1.41	0.33	0.44	1.35	0.94	1.37	1.46	0.41	0.56	1.36
4e	7.92	8.57	1.08	2.42	4.11	1.70	7.89	14.34	1.82	2.94	4.85	1.65
4l	1.00	1.15	1.15	1.32	1.58	1.20	4.18	5.26	1.26	1.59	1.93	1.21
5a	0.37	0.48	1.30	0.21	0.24	1.14	0.57	0.70	1.22	0.22	0.28	1.25
5b	0.59	0.93	1.56	0.27	0.41	1.53	0.78	1.32	1.68	0.33	0.52	1.56
5e	4.00	7.33	1.83	1.46	2.39	1.64	5.01	8.18	1.63	1.74	2.85	1.64

TABLE VI

CAPACITY AND SEPARATION FACTORS OF SELECTED QUATERNARY COMPOUNDS USING DIFFERENT HALOGEN-CONTAINING SALTS (2 mM) AS MODIFIERS IN THE MOBILE PHASE A

Compound	NaF			TMeACl			TPrABr			KI			NaBr		
	k'_1	k'_2	α												
4c	0.45	1.06	2.36	0.64	1.11	1.73	0.79	1.38	1.75	1.06	1.77	1.67	0.74	1.30	1.76
4e	0.28	0.45	1.61	0.40	0.51	1.28	0.47	0.77	1.64	0.60	0.98	1.63	0.47	0.74	1.57
4h	0.70	1.30	1.86	0.70	3.60	5.14	0.87	4.53	5.21	1.15	4.89	4.25	0.81	4.26	5.26
4l	0.47	0.70	1.49	0.45	1.17	2.60	0.57	1.43	2.51	0.72	1.91	2.65	0.53	1.38	2.60
5b	0.40	0.64	1.60	0.87	5.55	6.38	1.09	6.23	5.72	1.43	7.66	5.36	1.02	6.70	6.57
5e	0.43	0.74	1.72	0.45	1.89	4.20	0.64	2.21	3.45	0.89	2.53	2.84	0.62	2.17	3.50

able capacity and separation factors. It can be concluded that the chromatographic behaviour is strictly independent of the different cations, but is clearly determined by the anion. The use of fluoride leads to lower α -values for the analytes with larger axial substituents, whereas no significant differences were observed with the other halides.

With mobile phase system B (Table VII) no significant difference between the different halides and the perchlorate anion was observed.

Influence of modifier concentration. All tropane alkaloids displayed similar behaviour in each of the mobile phase systems (see Tables VIII and IX).

Discussion of the separation mechanism

For the counter ion bromide the capacity factor k'_1 increases with increasing concentration of the counter ion up to a point where ion-pair formation reaches a maximum and then remains constant. Knox and Laird [10] suggested that a combination of adsorption (partition) and cluster formation may be the dominant factor for retention. At lower concentrations, partitioning of the ion pair into the stationary phase may be the major factor controlling the retention. As proof of this theory, the chromatographic data without the use of an ionic modifier can be considered: no separation occurs with mobile phase systems B and distorted peak shapes were observed; with

mobile phase A also very poor peak shape were obtained, thus giving only very slight separations.

When cluster formation occurred at higher concentrations, the solubility of the ion pair increased in the mobile phase, resulting in a decrease in retention [11]. The curves show a concentration maximum of about 2 mmol for mobile phase A (Fig. 6) and about 10 mmol for mobile phase B (Fig. 7). These are the optimum concentrations of bromide for maximum retention for the tested racemates. The optimum concentrations are dependent on the strength of the ion pair formed, the extent of adsorption on the stationary phase and the extent of the formation of clusters of the counter ion bromide.

The chromatographic data show a dependence of capacity factors on the concentration of the ionic modifier and so participation of an ion-pair mechanism can be concluded.

The ion-pair mechanism for the relationship between retention times and modifier concentration is not useful for explaining the enantiomeric separation. A possible interpretation may be the inclusion of ion pairs in cellulose cavities, similarly to the mechanism discussed for a CSP in the normal-phase mode (hexane–propanol). Hence an interplay between an ion-pair mechanism and inclusion leads to the direct enantiomeric separations of the quaternary tropane alkaloids achieved here.

TABLE VII

DEPENDENCE OF CAPACITY AND SEPARATION FACTORS OF QUATERNARY COMPOUNDS ON HALIDE AND PERCHLORATE ANIONS IN MOBILE PHASE B (0.05 M; pH 2)

Compound	NaBr			NaCl			NaF			NaClO ₄		
	k'_1	k'_2	α	k'_1	k'_2	α	k'_1	k'_2	α	k'_1	k'_2	α
4a			1.31			1.44			2.26			1.21
4c	0.24	0.32	1.31	0.26	0.34	1.32	0.27	0.36	1.33	1.14	1.81	1.59
4h	0.25	–	1.00	0.86	–	Shoulder	0.96	–	Shoulder	1.12	1.32	1.19
4e	1.76	2.86	1.62	1.88	3.01	1.60	1.89	3.09	1.63	5.88	7.46	1.27
4l	0.98	1.17	1.19	1.06	1.23	1.16	1.09	1.29	1.18	5.82	7.38	1.27
5a	0.17	–	Shoulder	0.44	–	Shoulder	0.51	0.61	Shoulder	0.65	0.86	1.33
5b	0.20	0.30	1.48	0.22	0.33	1.48	0.24	0.34	1.42	0.73	1.39	1.89
5e	1.02	1.61	1.59	1.04	1.67	1.61	1.13	1.73	1.54	6.39	11.01	1.72

TABLE VIII
DEPENDENCE OF CAPACITY AND SEPARATION FACTORS OF SELECTED QUATERNARY COMPOUNDS ON TETRAPROPYLAMMONIUM BROMIDE CONCENTRATION IN SYSTEM A

Compound	0 mM			0.02 mM			0.56 mM			2 mM			18 mM			34 mM			50 mM		
	k'_1	k'_2	α	k'_1	k'_2	α	k'_1	k'_2	α	k'_1	k'_2	α	k'_1	k'_2	α	k'_1	k'_2	α	k'_1	k'_2	α
4c	0.47	0.87	1.85	0.40	0.70	1.75	0.74	1.30	1.76	0.79	1.38	1.75	0.64	1.17	1.83	0.53	1.02	1.92	0.64	1.00	1.56
4e	0.31	0.48	1.55	0.13	0.40	3.08	0.45	0.79	1.76	0.47	0.77	1.64	0.38	0.66	1.74	0.36	0.57	1.58	0.34	0.60	1.77
4h	0.59	1.78	3.02	0.43	2.00	4.65	0.83	4.00	4.82	0.87	4.53	5.21	0.70	3.89	5.56	0.62	3.43	5.53	0.68	2.89	4.25
4l	0.39	0.83	2.13	0.36	0.72	2.00	0.47	1.34	2.85	0.57	1.43	2.51	0.45	1.23	2.73	0.38	1.11	2.92	0.38	1.00	2.63
5b	0.70	2.74	3.91	0.45	3.19	2.74	0.79	5.94	7.52	1.09	6.23	5.72	0.89	6.00	6.74	0.79	5.34	6.76	0.79	4.34	5.49
5e	0.46	1.24	2.70	0.45	1.26	2.80	0.45	1.98	4.40	0.64	2.21	3.45	0.47	1.98	4.21	0.40	1.74	4.35	0.60	1.49	2.48

TABLE IX
DEPENDENCE OF CAPACITY AND SEPARATION FACTORS OF SELECTED QUATERNARY COMPOUNDS ON THE CONCENTRATION OF SODIUM BROMIDE IN SYSTEM B

Compound	0.001 M			0.002 M			0.005 M			0.01 M			0.05 M		
	k'_1	k'_2	α	k'_1	k'_2	α	k'_1	k'_2	α	k'_1	k'_2	α	k'_1	k'_2	α
4a	0.20	-	1.00	0.12	0.24	1.98	0.12	0.23	1.91	0.11	-	1.00	0.19	0.25	1.31
4c	0.27	0.39	1.41	0.31	0.43	1.39	0.28	0.39	1.39	0.32	0.45	1.39	0.24	0.32	1.31
4h	0.28	-	1.00	0.31	-	1.00	0.30	-	1.00	0.33	-	1.00	0.25	-	1.00
4e	2.13	3.83	1.80	2.17	4.06	1.87	2.16	3.86	1.79	3.60	5.88	1.63	1.76	2.86	1.62
4l	1.14	1.42	1.24	1.26	1.54	1.23	1.16	1.42	1.22	1.31	1.61	1.23	0.98	1.17	1.19
5a	0.19	-	Shoulder	0.22	-	Shoulder	0.21	-	Shoulder	0.23	0.27	1.17	0.17	-	Shoulder
5b	0.23	0.36	1.55	0.27	0.42	1.56	0.25	0.37	1.48	0.27	0.42	1.55	0.20	0.30	1.48
5e	1.34	1.91	1.42	0.72	1.16	1.61	0.51	0.85	1.44	0.77	1.29	1.45	1.02	1.61	1.59

The peak shape in the absence of modifier is distorted and the results cannot be evaluated.

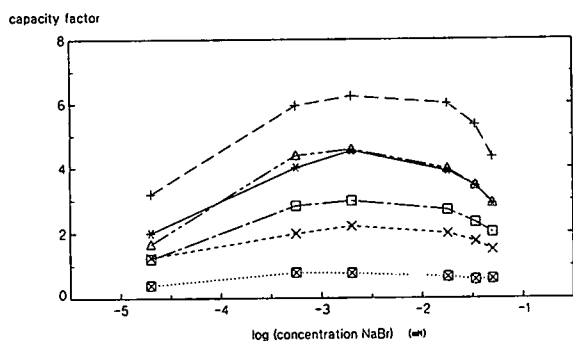


Fig. 6. Dependence of capacity factor (k'_2) on log (modifier concentration) with a maximum at a concentration at 2 mM (mobile phase A). Δ = 4c; \square = 4e; * = 4h; \square = 4l; + = 5b; \times = 5e.

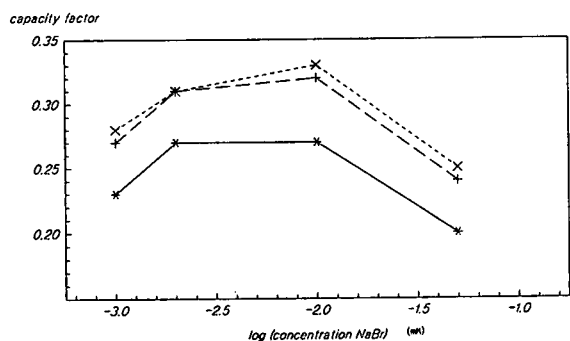


Fig. 7. Dependence of capacity factor (k'_1) on the log (modifier concentration) with a maximum at a concentration at 10 mM (mobile phase B). + = 4c; \times = 4h; * = 5b.

CONCLUSIONS

Because of the relationship between the retention behaviour of the racemates and the the ionic modifiers used, the involvement of an ion-pair mechanism in chiral recognition can be concluded. For the resolution of the tertiary derivatives of atropine and atroscine inclusion in the

chiral cavities of the cellulose carbamate is sufficient whereas for quaternary derivatives the formation of ion pairs is a basic requirement. Systematic investigations on the separation mechanism permit the separation of quaternary tropane alkaloids to be predicted.

In addition to the known synthetic methods for the preparation of quaternary tropane alkaloids, there is now an alternative possibility of obtaining enantiomerically pure drugs by methods of preparative liquid chromatography.

ACKNOWLEDGEMENTS

We express our sincere thanks to Dr. Banholzer and Dr. Pook whose active support concerning the complicated stereochemistry of the quaternary tropane alkaloids has been of utmost value.

REFERENCES

- 1 Y. Okamoto, M. Kawashima and K. Hatada, *J. Chromatogr.*, 363 (1986) 173.
- 2 G. Schill, I. Wainer and S. Barkan, *J. Liq. Chromatogr.*, 9 (1986) 641.
- 3 *Nachr. Chem. Tech.*, 14 (1966) 167.
- 4 IUPAC, *J. Org. Chem.*, 35 (1970) 2849.
- 5 K.-H. Pook, W. Schulz and R. Banholzer, *Justus Liebigs Ann. Chem.*, (1975) 1499.
- 6 W. Schulz, R. Banholzer and K.-H. Pook, *Arzneim.-Forsch.*, 26 (1976) 960.
- 7 A. Heusner, *Arzneim.-Forsch.*, 3 (1956) 105.
- 8 Y. Okamoto, S. Honda, I. Okamoto, H. Yuki, S. Murata, R. Noyori and H. Takaya.
- 9 K. Ikeda, T. Hamasaki, H. Kohno, T. Ogawa, T. Matsumoto and J. Sakai, *Chem. Lett.*, (1989) 1089.
- 10 J.H. Knox and G.R. Laird, *J. Chromatogr.*, 122 (1976) 17.
- 11 R. Gloor and E.L. Johnson, *J. Chromatogr. Sci.*, 15 (1977) 413.
- 12 *J. Am. Chem. Soc.*, 103 (1981) 6971.

Preparative resolution of praziquantel enantiomers by simulated counter-current chromatography

C.B. Ching and B.G. Lim*

Department of Chemical Engineering, National University of Singapore, 10 Kent Ridge Crescent, Singapore 0511 (Singapore)

E.J.D. Lee

Department of Pharmacology, National University of Singapore, 10 Kent Ridge Crescent, Singapore 0511 (Singapore)

S.C. Ng

Department of Chemistry, National University of Singapore, 10 Kent Ridge Crescent, Singapore 0511 (Singapore)

(First received September 22nd, 1992; revised manuscript received December 14th, 1992)

ABSTRACT

The continuous chromatographic separation of a racemic anthelmintic drug, praziquantel, was carried out using a simulated counter-current system. The system consists of four identical columns (445 mm × 12.5 mm I.D.) connected in series through solenoid valves. The chiral stationary phase used is microcrystalline cellulose triacetate and the eluent is methanol. Feed at 50 mg/ml was continuously introduced into the system at 0.3 ml/min and 429 mg/h of (+)-praziquantel and 404 mg/h of (–)-praziquantel were obtained from the extract and raffinate streams, respectively. The optical purity of the products was more than 90%. This method provides an extremely useful technique for preparative-scale enantioseparation. Compared with conventional batch preparative-scale processes, this system offers a higher solute to adsorbent mass ratio.

INTRODUCTION

In recent years, there has been an increasing trend towards restricting the use of chiral drugs as racemates. This has created a demand for preparative-scale techniques for the separation of the enantiomers for pharmaceutical applications. Classical methods of optical resolution, based on recrystallization of diastereomeric salts, are not suitable for industrial scale-up and automation [1]. A more promising technique which has attracted attention recently is the resolution of enantiomers by liquid chromatography, using chiral stationary phases. Several semi-prepara-

tive- or preparative-scale batch chromatographic processes based on this direct resolution principle have been developed for the separation of enantiomeric drugs. Although the process is relatively simple and offers operating flexibility, it suffers from the following disadvantages: the whole sorbent bed is not effectively utilized and large amounts of expensive adsorbents are required; a large amount of diluent is consumed, resulting in undesired dilution of the products; and the operation is discontinuous, which makes it difficult to integrate it with other continuous processes.

In this paper, a continuous chromatographic separation of an anthelmintic racemic drug, praziquantel, based on a simulated counter-current system is reported. Praziquantel (Fig. 1)

* Corresponding author.

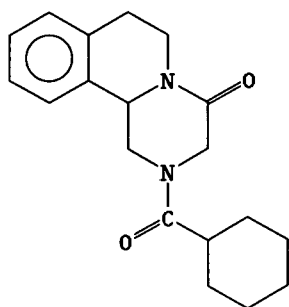


Fig. 1. Structure of praziquantel ($C_{19}H_{24}N_2O_2$).

was recommended as the drug of choice in the treatment of the parasitic disease schistosomiasis in 1977 [2]. Preliminary studies have shown that the primary therapeutic effect of praziquantel resides in its *levo*-isomer. *levo*-Praziquantel has the advantage of high efficacy and low toxicity compared with *rac*-praziquantel [3]. To the best of our knowledge, no preparative-scale chromatographic resolution of praziquantel enantiomers has been reported. In one of the methods reported, the enantiomers were obtained via resolution of an intermediate during the synthesis of praziquantel [4]. However, no details of this method have been elaborated.

A simulated counter-current system retains the main advantage of an equivalent counter-current

system where the average driving force is maximized, thus increasing the efficiency with which the adsorbent is utilized. Circulation of the solid adsorbent can be simulated using a multiple column fixed-bed system with an appropriate sequence of column switching, in which effective counter-current operation is achieved by moving sequentially the feed, eluent and draw-off points through the bed in the direction of fluid flow. In this way the adsorbent is seen to be in effect moving counter-current to the fluid flow direction. With sufficiently small elemental beds switched with appropriate frequency such a system indeed becomes a perfect analogue of a counter-current flow system. More detailed information on this separation technique and its design principle can be found in a review by Ruthven and Ching [5].

EXPERIMENTAL

Chemicals

The adsorbent used was microcrystalline cellulose triacetate (MCTA) (Merck, Darmstadt, Germany) with a particle size of 25–40 μm . Prior to packing, the adsorbent was allowed to swell in boiling ethanol [6]. It was packed into the column using the slurry method via a res-

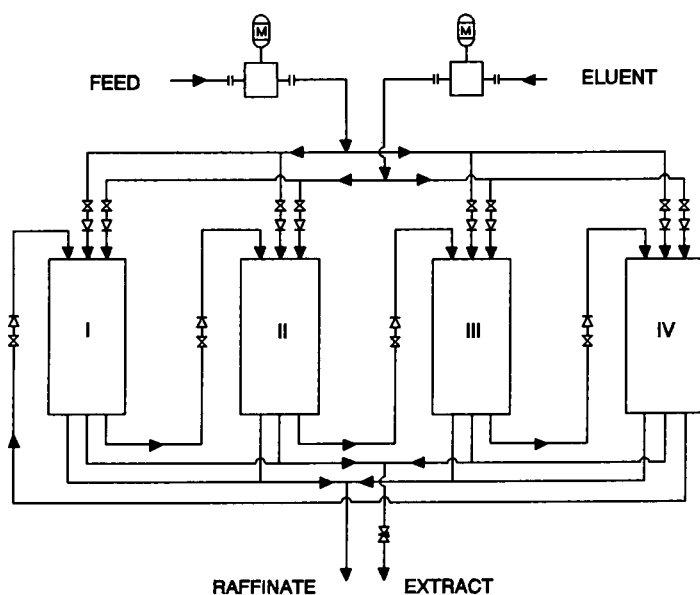


Fig. 2. Schematic diagram of the continuous simulated counter-current system.

ervoir and at a constant flow-rate of 6 ml/min using an HPLC pump (Model 2510, Varian, Palo Alto, CA, USA). The diluent was HPLC-grade methanol (Fisher Scientific, Pittsburgh, PA, USA). The feed was prepared by dissolving *rac*-praziquantel (Sigma, St. Louis, MO, USA) in methanol (50 mg/ml).

Instrumentation

A schematic diagram of the simulated counter-current system which consists of four chromatographic columns is shown in Fig. 2. The columns are made of stainless steel and have dimensions of 445 mm × 12.5 mm I.D. The columns are connected in series through solenoid valves that allow the introduction of feed and withdrawal of products in addition to providing the transfer of the streams. Counter-current contact between the solid and the fluid phases was simulated by switching the feed and eluent inlets and product withdrawal points, *i.e.*, by opening and closing specific groups of valves, at fixed time intervals in the direction of liquid flow. Operation of the solenoid valves was governed by a programmable logic controller. The schematic flow diagram of the four stages in a cycle of the system is shown in Fig. 3.

The flow-rates of the feed and eluent were controlled by two solvent metering pumps (Varian Model 2510). Flow meters were installed at

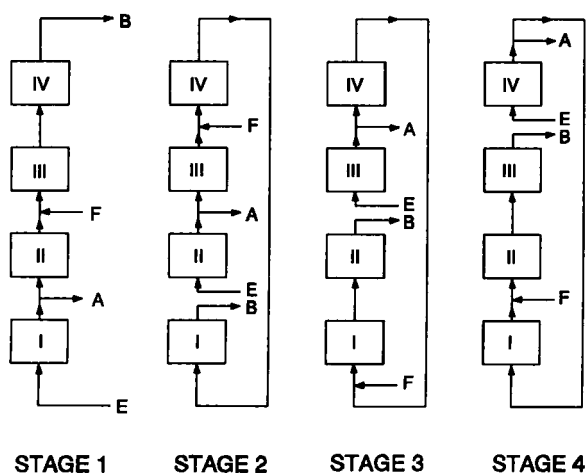


Fig. 3. Schematic flow diagram of the four stages in a cycle of the system. E = Eluent; F = feed; A = extract; B = raffinate.

the outlet of extract and raffinate streams to monitor the extract and raffinate flow-rates. A needle valve was also installed at the outlet of extract stream to control the flow-rate further.

The concentrations of the extract and raffinate streams for each stage were analysed using a standard analytical liquid chromatographic system. An analytical Chiralcel OD column [cellulose tris(3,5-dimethylphenylcarbamate) polymer absorbed on 10- μ m macroporous silica, 250 mm × 4.6 mm I.D.] (Daicel Chemical Industries, Tokyo, Japan) was used. The mobile phase was a mixture of HPLC-grade hexane and 2-propanol (80:20) (Fisher Scientific). The solvent-delivery system was a high-pressure liquid chromatographic pump (Model LC-9A, Shimadzu, Tokyo, Japan) and sample injection was performed using a syringe loading valve (Model 7125, Rheodyne, Cotati, CA, USA) fitted with a 10- μ l sample loop. The eluting enantiomers were monitored with a Varian Model 2070 spectrofluorimeter with excitation and emission wavelengths set at 270 and 300 nm, respectively.

Measurement of the optical rotation of the separated enantiomers showed the more adsorbed component (extract) to be (+)-praziquantel and the less adsorbed component (raffinate) (-)-praziquantel. The eluting sequence of the enantiomers on the analytical Chiralcel OD column was the same as that on MCTA.

RESULTS AND DISCUSSION

The chromatogram for the separation of *rac*-praziquantel (2.5 mg) on a 445 mm × 12.5 mm I.D. column packed with 22 g of MCTA is shown in Fig. 4. The capacity factors were found to be 0.43 and 1.47. Based on these values, the following operating conditions were selected for the subsequent work: eluent flow-rate = 4.10 ml/min; feed flow-rate = 0.30 ml/min; extract flow-rate = 2.60 ml/min; raffinate flow-rate = 1.80 ml/min; and switch time = 45.0 min.

Approximately three complete cycles (9 h) were required for the system to approach the final quasi-steady state. Operation was continued for six complete cycles (18 h). The steady-state concentrations, the recoveries and the optical purities of the extract and raffinate streams were

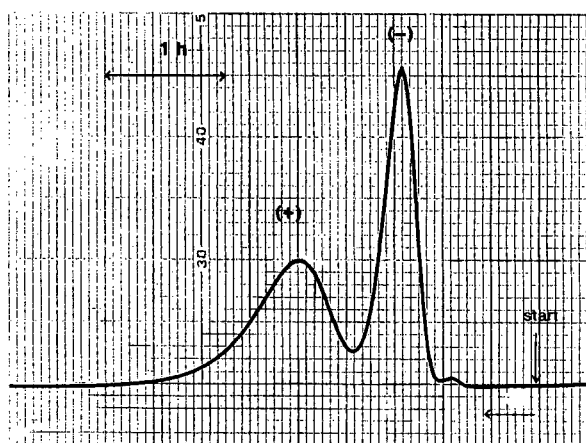


Fig. 4. Separation of *rac*-praziquantel (2.5 mg) on a 445 mm \times 12.5 mm I.D. column packed with 22 g of MCTA. Eluent flow-rate, 1.00 ml/min.

as follows: for the extract, (+)-praziquantel 2.710 mg/ml, (-)-praziquantel 0.298 mg/ml, (+)-praziquantel recovery 423 mg/h and optical purity 90.09%; and for the raffinate, (+)-praziquantel 0.252 mg/ml, (-)-praziquantel 3.736 mg/ml, (-)-praziquantel recovery 404 mg/h and optical purity 93.68%. The chromatograms of the feed, extract and raffinate streams are shown in Fig. 5.

In this preliminary study, an optical purity

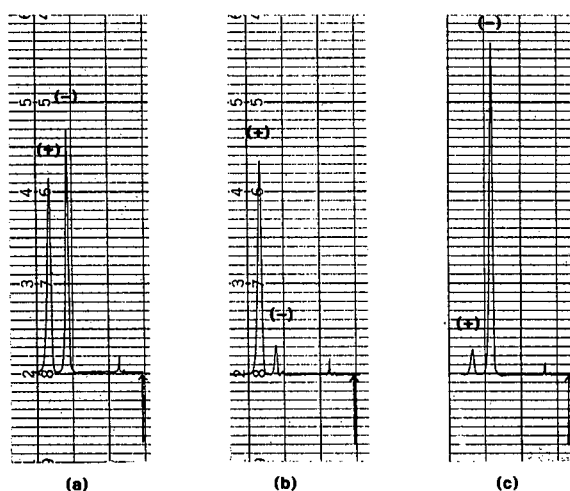


Fig. 5. Chromatograms of (a) feed (tenfold dilution), (b) extract stream and (c) raffinate stream at quasi-steady state on an analytical Chiralcel OD column.

close to 100% has not yet been achieved. However, from the computer simulation result, it is expected that pure enantiomers can be obtained by adding a few more columns (preferably 2–4 columns) to the system. This is currently being investigated.

One of the advantages of the continuous simulated counter-current system is its ability to utilize the whole sorbent bed effectively and to achieve a higher mass ratio of solute to sorbent. In our system, *ca.* 22 g of adsorbent were used for each column. If eight columns were to be used (to achieve 100% purity) for this separation, only 176 g of adsorbent would be required. If the present run conditions were used, 900 mg of *rac*-praziquantel would be separated per hour under steady-state conditions.

As the separation of praziquantel enantiomers by preparative-scale batch chromatography has not been reported, two of the runs reported on oxapadol and methylcyclohexylethylbarbituric acid [7] using the same adsorbent were analysed to compare the performance of the continuous system used in this study. The result reported for oxapadol showed that 2.1 g of racemic compound were separated into enantiomers in 48 h by the use of a 700 mm \times 38 mm I.D. column packed with 380 g of MCTA. The eluent flow-rate was 90 ml/h. For the separation of *rac*-methylcyclohexylethylbarbituric acid, 205 mg were reported to be separated on 210 g of MCTA (column 85 mm \times 25 mm I.D.) in 22 h at an eluent flow-rate of 50 ml/h. If the present result is compared with that reported on oxapadol and methylcyclohexylethylbarbituric acid, on an hourly basis, the grams of solute per gram of adsorbent that our system can handle are much higher than for a batch system. The grams of solute separated per hour are also much higher compared with a batch system. Even if the difference in eluent flow-rate is considered, the difference between these two systems is still significant. Differences in capacity factors and separation factors for the three compounds might have introduced some difficulties, however, in obtaining an accurate comparison between the batch and continuous systems. Nevertheless, a comparison of the general performance could still be made.

CONCLUSIONS

As the cost of most chiral stationary phases is generally very high, the use of a continuous simulated counter-current chromatographic system will provide a better utilization of the whole sorbent bed and a reduction in the cost of the expensive adsorbent. With the other advantages associated with a continuous process, the use of the present system for the resolution of optical isomers for pharmaceutical application is expected to provide an efficient and cost-effective separation method.

REFERENCES

- 1 S. Allenmark, *Chromatographic Enantioseparation, Methods and Applications*, Ellis Horwood, Chichester, 2nd ed., 1991, p. 230.
- 2 R.D. Pearson and R.L. Guerrant, *Ann. Intern. Med.*, 99 (1983) 195.
- 3 M.H. Wu, C.C. Wei, Z.Y. Xu, H.C. Yuan, W.N. Lian, Q.J. Yang, M. Chen, Q.W. Jiang, C.Z. Wang, S.J. Zhang, Z.D. Liu, R.M. Wei, S.J. Yuan, L.S. Hu and Z.S. Wu, *Am. J. Trop. Med. Hyg.*, 45 (1991) 345.
- 4 Y.H. Liu, Y.D. Chen, G.H. Li, J. Liu, S.Z. Lu, M.X. Qian, Q.N. Wang, R.Q. Wang and X.G. Wang, *Chin. Med. J.*, 99 (1986) 935.
- 5 D.M. Ruthven and C.B. Ching, *Chem. Eng. Sci.*, 44 (1989) 1011.
- 6 A. Mannschreck, H. Koller and R. Wernicke, *Kontakte*, 1 (1985) 40.
- 7 G. Blaschke, *J. Liq. Chromatogr.*, 9 (1986) 341.

Sensitive assay system for nitrosamines utilizing high-performance liquid chromatography with peroxyoxalate chemiluminescence detection

Chengguang Fu*, Hongda Xu and Zhi Wang

Research Centre of Physical and Chemical Analysis, Hebei University, Baoding 071002 (China)

(First received August 19th, 1992; revised manuscript received November 9th, 1992)

ABSTRACT

A high-performance liquid chromatographic system in combination with postcolumn chemiluminescence detection for the determination of nitrosamines was developed. The stability of the chemiluminogenic reagent solution was investigated using a conventional high-performance liquid chromatograph with a UV-Vis spectrophotometric detector, and the optimum conditions for chemiluminescence intensity were also established with a single reagent pump postcolumn detector. The sample was first denitrosated with hydrobromic acid-acetic acid to produce the corresponding secondary amines, which were then subjected to reaction with dansyl chloride to form dansyl derivatives. The reaction mixtures were separated on a Perkin-Elmer HS3 C₁₈ reversed-phase column with acetonitrile-water (63.5:36.5, v/v) as mobile phase, with 3.0 mmol/l of imidazole added as a catalyst for chemiluminescence and with the pH adjusted to 6.2 with oxalic acid to give a better separation, followed by detection with a postcolumn chemiluminescence detector using bis(2-nitrophenyl) oxalate and hydrogen peroxide as chemiluminogenic reagents. The sensitivity of this method was more than 120 times greater than that of fluorescence detection and four orders of magnitude greater than that of UV-Vis spectrophotometric detection. The detection limits with this procedure at a signal-to-noise ratio of 4 were between 0.31 and 1.20 pg and the relative standard deviations were between 2.8% and 6.7% for six nitrosamines. The linearity of the calibration graphs and the correlation coefficients were good.

INTRODUCTION

N-Nitrosamines are now known to be widely distributed in the human environment and can also be formed in the human body. Owing to their potential carcinogenic properties, great interest has been focused on the development of methods for the determination of nitrosamines at trace levels. High-performance liquid chromatography (HPLC) is a useful method for the trace determination of the nitroso compounds, and several methods for the detection and determination of these compounds have been reported [1–7]. The thermal energy analyser is a

highly selective detector for gas chromatography [3], and its use in combination with HPLC has been described [4], but the results showed that it cannot be operated with a reversed-phase mobile phase or inorganic buffer solutions, and the sensitivity was *ca.* 100 times lower than those obtained with other methods. On the other hand, we have previously developed methods for the determination of nitrosamines by HPLC with precolumn fluorescence derivatization [5–7] and obtained good results. In subsequent work, a fluorescence detection method for the determination of nitrosamines [6], based on denitrosation with hydrobromic acid-acetic acid to produce secondary amines, followed by reaction with dansyl chloride to form dansyl derivatives, was studied further. However, peroxyoxalate chemiluminescence has been shown to provide a

* Corresponding author.

highly sensitive detection method [8–10], and the sensitivity for secondary amines was much higher than that of fluorescence detection by using dansyl chloride [11]. In this paper, we present some improved results obtained by HPLC combined with a sensitive postcolumn bis(2-nitrophenyl) oxalate–hydrogen peroxide chemiluminescence detection method for the determination of six nitrosamines.

EXPERIMENTAL

Reagents

Nitrosodimethylamine (NDMA), nitrosopyrrolidine (NPy), nitrosodiethylamine (NDEA), nitrosopiperidine (NPip), nitrosodipropylamine (NDPA) and nitrosodibutylamine (NDBA) were prepared and purified by conventional procedures [12] and were identified by mass spectrometry. Bis(2-nitrophenyl) oxalate (2-NPO) was synthesized [13], further purified by washing with chloroform and recrystallization from ethyl acetate and identified by mass spectrometry. Hydrogen peroxide (30%), acetone, acetonitrile, dichloromethane, hydrobromic acid, acetic anhydride, ethyl acetate, imidazole, oxalic acid, sodium hydrogencarbonate and hydrochloric acid (all of analytical-reagent grade) were obtained from Beijing Chemical Works (Beijing, China), and were used as received. Dansyl chloride (puriss. grade) were obtained from Fluka. Redistilled water was used throughout.

Nitrosamine stock solution. Each nitrosamine was dissolved in dichloromethane and made up to a concentration of $1 \cdot 10^{-4}$ mol/l with the same solvent.

Dansyl chloride solution. A $1 \cdot 10^{-5}$ mol/l dansyl chloride solution was prepared by dissolving dansyl chloride in acetone.

2-NPO stock solution. This solution was prepared by dissolving 2-NPO in ethyl acetate to give a concentration of 10 mmol/l.

Hydrogen peroxide stock solution. This solution contained 300 mmol/l of hydrogen peroxide in ethyl acetate.

Hydrobromic acid–acetic anhydride solution. A 1:4 (v/v) solution was prepared by dissolving

1 ml of hydrobromic acid in 4 ml of acetic anhydride.

Sodium hydrogencarbonate solution. A solution of 0.25 mol/l NaHCO_3 was prepared in redistilled water.

Hydrochloric acid. Solutions of 0.01 and 0.1 mol/l in redistilled water were prepared.

Instrumentation and chromatographic conditions

A schematic diagram of the system is shown in Fig. 1. It consisted of a Model 114M eluent-delivery pump (Beckman), a Model E-120-S-2 reagent-delivery pump for the chemiluminogenic reagent solution (Eldex), a C_{18} ($3 \mu\text{m}$) analytical column ($83 \text{ mm} \times 4.6 \text{ mm I.D.}$) (Perkin-Elmer), a Model 7125 injection valve with $20\text{-}\mu\text{l}$ loops (Rheodyne), a mixing device and chemiluminescence detector made in our laboratory, a detector consisting of a $40\text{-}\mu\text{l}$ quartz worm pipe micro flow cell, a photomultiplier tube (GDB-52QD), a high-voltage supply, a weak signal amplifier and a recorder were used.

The mobile phase was acetonitrile–water (63.5:36.5, v/v) with a catalyst (imidazole) added (3.0 mmol/l) and the pH was adjusted to 6.2 with oxalic acid; the flow-rate was 0.5 ml/min. The postcolumn chemiluminogenic reagent solution contained 3.0 mmol/l of 2-NPO and

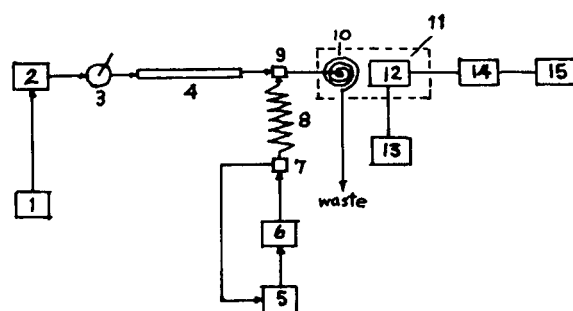


Fig. 1. Schematic diagram of the liquid chromatographic system with postcolumn chemiluminescence detection for the determination of nitrosamines. 1 = Mobile phase container; 2 = LC pump; 3 = injection valve; 4 = HPLC column; 5 = chemiluminogenic reagent solution container; 6 = postcolumn reaction pump; 7 = by-pass device (by-pass ratio = 1:10); 8 = coil ($1.5 \text{ m} \times 0.1 \text{ mm I.D.}$); 9 = mixer; 10 = flow cell ($40 \mu\text{l}$); 11 = dark box; 12 = photomultiplier tube (GDB-52QD); 13 = high-voltage supply; 14 = weak signal amplifier; 15 = recorder.

10.0 mmol/l of hydrogen peroxide in acetone–ethyl acetate binary solvents and the flow-rate was 100 μ l/min.

Preparation of dansyl derivatives of nitrosamines

A portion of a mixed standard solution of nitrosamines containing 100 pmol of each of the species was placed in a graduated test-tube fitted with a stopper and evaporated to dryness in a stream of nitrogen. To the residue was added 20 μ l of hydrobromic acid–acetic anhydride solution for denitrosation and the mixture was allowed to stand in the dark for 10 min at 70°C, then evaporated to dryness in a stream of nitrogen. To the residue 100 μ l of 0.25 mol/l NaHCO₃ solution and 100 μ l of dansyl chloride solution were added, the mixture was allowed to stand for 30 min at 40°C and then diluted with mobile phase to 1.0 ml. For HPLC assay, a blank experiment was required.

Recovery test

A synthetic standard mixture containing 100 pmol of each nitrosamine was added to 100 ml of redistilled water and the pH was adjusted to 7.0. The solution was passed through a mini activated carbon (100–120 mesh) column (20 mm \times 1.2 mm I.D.) [4] by a sweep pump at a flow-rate of 0.5 ml/min. After elution with acetone, the eluate (0.5 ml) was collected in a graduated test-tube fitted with a stopper, evaporated to dryness in a stream of nitrogen, and then subjected to the proposed method as described above.

RESULTS AND DISCUSSION

Stability of chemiluminogenic reagent solution

In order to investigate the stability of 2-NPO in the presence of hydrogen peroxide, the residual 2-NPO was determined using reversed-phase liquid chromatography with UV–Vis spectrophotometric detection. The 2-NPO was separated using a Shimpack ODS (5 μ m) column (150 mm \times 6 mm I.D.) with acetonitrile–water (86:14, v/v) as mobile phase at a flow-rate of 1.0 ml/min with detection at 298 nm. The percent-

tage of residual 2-NPO was calculated from the peak heights at the same retention time on traces obtained for chemiluminogenic reagent solutions stored for different periods of time.

The effects of organic solvents on the stability of 2-NPO in the presence of hydrogen peroxide were examined and the results are shown in Fig. 2.

2-NPO decomposed to a significant extent in anhydrous solvents such as absolute methanol and acetonitrile, but it was much more stable in ethyl acetate, acetone and ethyl acetate–acetone. Hence the latter solvents were suitable for use in reversed-phase liquid chromatographic chemiluminescence detection. Moreover, ethyl acetate was suitable for the preparation of the 2-NPO and hydrogen peroxide stock solutions because the 2-NPO was more stable than in other solvents, and to improve the mutual solubility of the reversed-phase mobile phase and the chemiluminogenic reagent solution acetone was used as the diluent of the stock solution. When the concentrations of 2-NPO and hydrogen peroxide in the chemiluminogenic reagent solution were 3.0 and 10.0 mmol/l, respectively, the proportions of ethyl acetate and acetone in the mixture were 33:67 (v/v). However, the results showed that the stability of 2-NPO in the presence of hydrogen peroxide was hardly affected by variations in the proportions of the binary

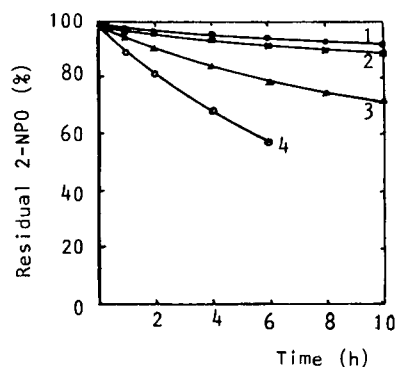


Fig. 2. Effects of organic solvents on the stability of 2-NPO in the presence of hydrogen peroxide. The concentrations of 2-NPO and hydrogen peroxide were 3.0 and 20.0 mmol/l, respectively. Solvents: 1 = ethyl acetate; 2 = acetone; 3 = acetonitrile; 4 = methanol.

solvent components. The stability of 2-NPO in the mixed solvents lay between those of ethyl acetate and acetone, as shown in Fig. 2.

The effect of the concentration of hydrogen peroxide on the stability of 2-NPO was studied and the results are shown in Fig. 3.

The decomposition of 2-NPO was accelerated with increase in the concentration of hydrogen peroxide in the chemiluminogenic reagent solution. On the other hand, the hydrolysis of 2-NPO also increased rapidly with increase in the concentration of water, which might result in a gradual decrease in the chemiluminescence intensity because the hydrogen peroxide is commercially available as a 30% aqueous solution and hence an increase in hydrogen peroxide concentration is accompanied by an increase in water concentration. For this reason the concentration of hydrogen peroxide was usually kept below 20.0 mmol/l, and the chemiluminogenic reagent solution was prepared with a stock solution just before use to prevent the decomposition of 2-NPO.

Optimization of chemiluminescence conditions

In order to examine the maximum chemiluminescence intensity of dansyl derivatives of nitrosamines under the optimum conditions, the effects of variations in the concentrations of of

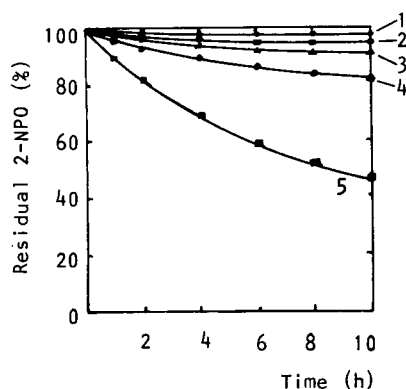


Fig. 3. Effect of the concentration of hydrogen peroxide on the stability of 2-NPO in ethyl acetate–acetone binary solvents. The concentration of 2-NPO was fixed at 3.0 mmol/l. Hydrogen peroxide concentrations: 1 = 5.0; 2 = 10.0; 3 = 20.0; 4 = 50.0; 5 = 100.0 mmol/l.

hydrogen peroxide and 2-NPO and the flow-rate of the chemiluminogenic reagent solution on the relative chemiluminescence intensity, *i.e.*, relative peak heights in the chromatogram, for a test sample were examined. As the test sample 500 fmol of dansylnitropyrrrolidine was selected.

The effects of the concentration of 2-NPO on the relative chemiluminescence intensity are shown in Fig. 4. The relative chemiluminescence intensity increased with increasing concentration of 2-NPO, and reached a nearly constant value at *ca.* 3.0 mmol/l.

Fig. 5 shows the effects of the concentration of hydrogen peroxide on the relative chemiluminescence intensity of the test sample. The relative chemiluminescence intensity increased with increasing concentration of hydrogen peroxide, and reached a nearly constant value at a concentration of 10.0 mmol/l. Therefore, the concentration of 2-NPO was fixed at 3.0 mmol/l and that of hydrogen peroxide at 10.0 mmol/l.

These conditions were adopted for chemiluminescence detection at a fixed flow-rate. Fig. 6 shows the common effects of the concentration of 2-NPO and the flow-rate of the chemiluminogenic reagent solution on the relative chemiluminescence intensity of the test sample. When the flow-rate was increased from 40 to 150 μ l/

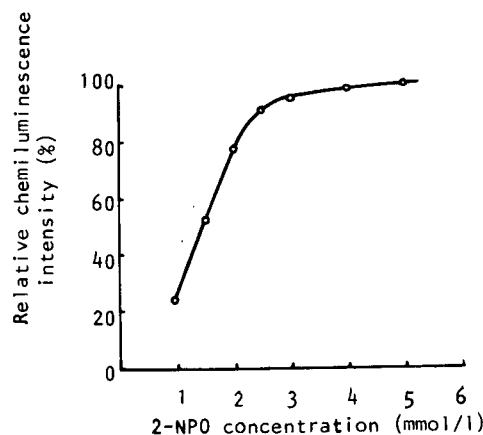


Fig. 4. Effect of the concentration of 2-NPO in the chemiluminogenic reagent solution on the relative chemiluminescence intensity. The concentration of hydrogen peroxide was fixed at 20.0 mmol/l and the flow-rate at 100 μ l/min.

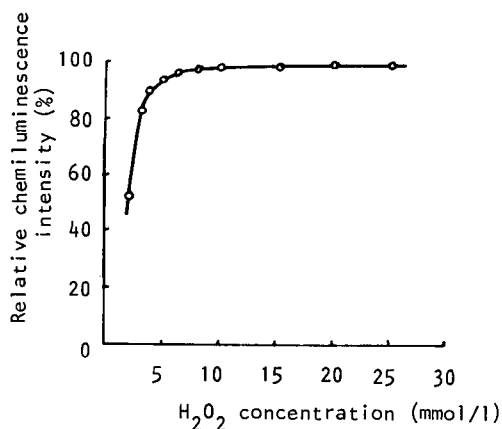


Fig. 5. Effect of the concentration of hydrogen peroxide in the chemiluminogenic reagent solution on the relative chemiluminescence intensity. The concentration of 2-NPO was fixed at 3.0 mmol/l and the flow-rate at 100 μ l/min.

min, the relative chemiluminescence intensity increased to a maximum and then decreased gradually at a fixed concentration of 2-NPO. When the concentration of 2-NPO was increased, the maximum of the relative chemi-

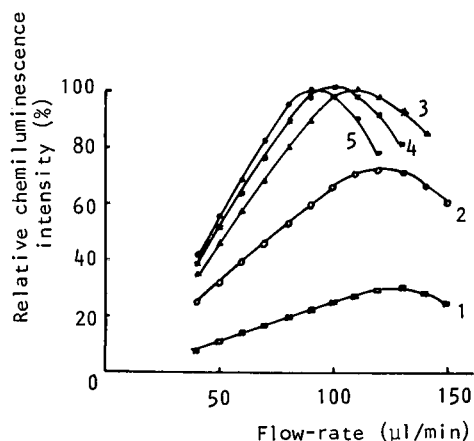


Fig. 6. Simultaneous effects of the concentration of 2-NPO and the flow-rate of the chemiluminogenic reagent solution on the relative chemiluminescence intensity. The concentration of hydrogen peroxide was fixed at 10.0 mmol/l. Concentrations of 2-NPO: 1 = 1.0; 2 = 2.0; 3 = 3.0; 4 = 4.0; 5 = 5.0 mmol/l.

luminescence intensity shifted toward the direction of lower flow-rates.

On the basis of these results, the optimum chemiluminescence conditions were established

TABLE I
RESULTS OF CALIBRATION, DETECTION LIMITS AND PRECISION

Parameter	NDMA	NPY	NDEA	NPip	NDPA	NDBA
Linear range (pmol)	0.02–20	0.02–20	0.02–20	0.02–20	0.02–20	0.02–20
Detection limits:						
fmol	6.9	6.5	8.6	8.0	7.4	9.4
g	$3.1 \cdot 10^{-13}$	$4.6 \cdot 10^{-13}$	$6.3 \cdot 10^{-13}$	$6.8 \cdot 10^{-13}$	$7.5 \cdot 10^{-13}$	$1.2 \cdot 10^{-12}$
Intercept	0.6	0.4	0.6	0.7	0.6	0
Slope	21.43	22.8	17.16	17	20.16	14.64
Correlation coefficient	0.9993	0.9991	0.9994	0.9998	0.9992	0.999
R.S.D. (%) ($n = 7$) ^a	4.3	3.4	2.8	5.5	4.0	6.7

^a 0.2 pmol of each nitrosamine.

TABLE II
RECOVERIES FROM A WATER SAMPLE

Parameter	NDMA	Npy	NDEA	NPip	NDPA	NDBA
Amount added (pmol)	100.0	100.0	100.0	100.0	100.0	100.0
Amount recovered (pmol)	73.4	103.3	100.3	97.0	100.8	93.9
Recovery (%)	73.4	103.3	100.3	97.0	100.8	93.9

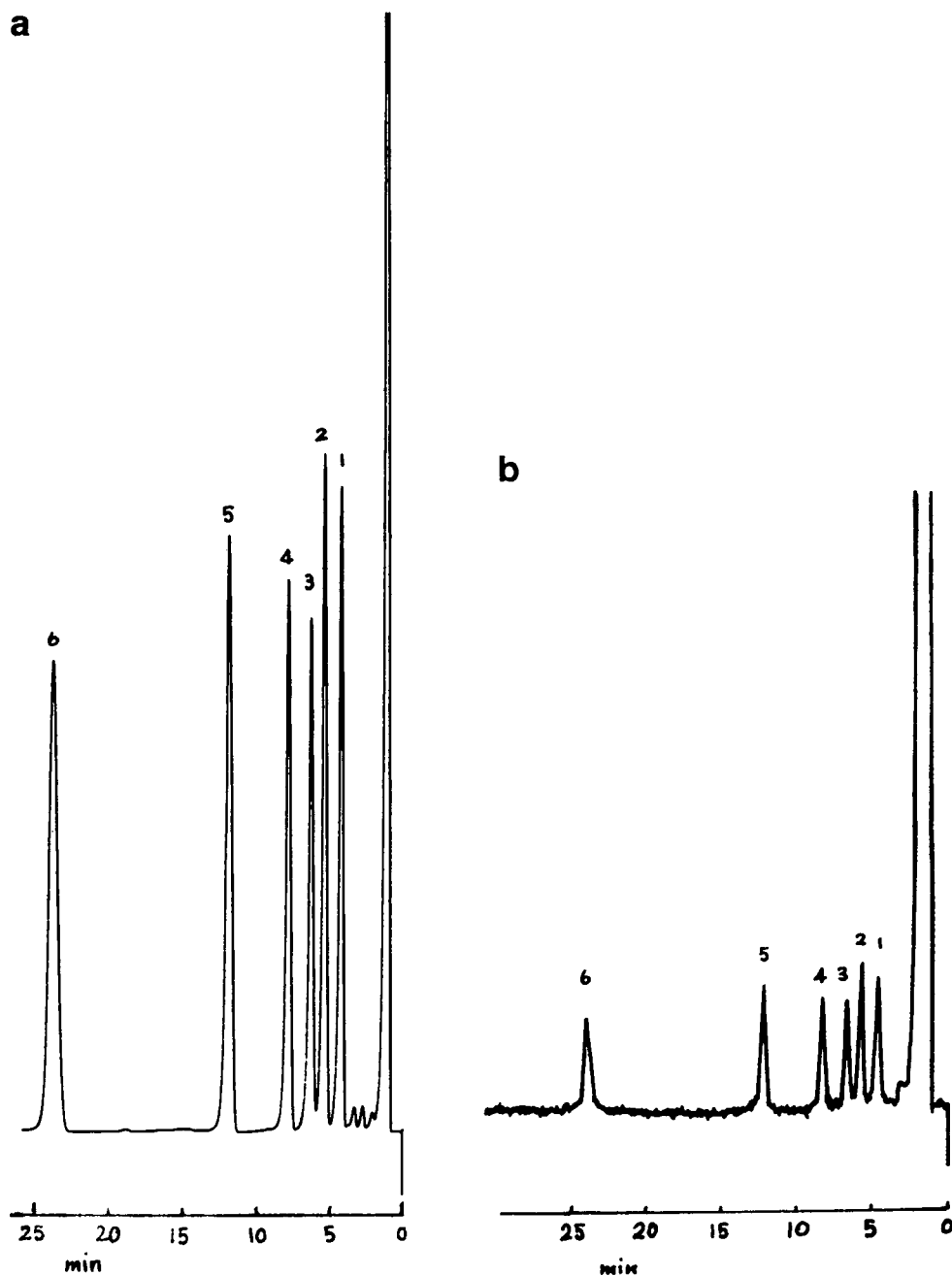


Fig. 7. Separation of standard mixtures of six nitrosamines containing (a) 500 and (b) 20 fmol/l on a Perkin-Elmer HS3 C₁₈ column. Mobile phase, acetonitrile–water (63.5:36.5, v/v) containing 3.0 mmol/l of imidazole and the pH adjusted to 6.2 with oxalic acid; flow-rate, 0.5 ml/min; detection, postcolumn chemiluminescence with 2-NPO–hydrogen peroxide system; concentrations of 2-NPO and hydrogen peroxide in the chemiluminogenic reagent solution, 3.0 and 10.0 mmol/l, respectively, in ethyl acetate–acetone (33:67, v/v), at a flow-rate of 100 μ l/min. Peaks: 1 = dansylnitrosodimethylamine; 2 = dansylnitrosopyrrolidine; 3 = dansylnitrosodiethylamine; 4 = dansylnitrosopiperidine; 5 = dansylnitrosodipropylamine; 6 = dansylnitrosodibutylamine.

as follows: concentration of chemiluminogenic reagent solution, 3.0 mmol/l for 2-NPO and 10.0 mmol/l for hydrogen peroxide, in ethyl acetate–acetone (33:67, v/v), delivered at a flow-rate of 100 μ l/min.

Fig. 7 shows two chromatograms obtained for mixtures of dansylated nitrosamines, containing (a) 500 and (b) 20 fmol of each.

Calibration, detection limits and precision

The relationship between the peak height and the amounts of six dansylnitrosamines was evaluated over the range 0.02–20 pmol. In order to verify the linearity of the chemiluminescence intensity under the optimum conditions at the working concentration of each nitrosamine, a series of working standard solutions containing different concentrations were derivatized and injected into the HPLC system with peroxyoxalate chemiluminescence detection. Linear least-squares regression was used to calculate the intercept, slope and correlation coefficient. The detection limits of the six dansyl nitrosamines were 0.31–1.20 pg (6.5–9.4 fmol) under the optimum conditions at a signal-to-noise ratio of 4. A solution containing 200 fmol of each nitrosamine was injected seven times to evaluate the repeatability of the assay system. The results are given in Table I.

The recoveries of six nitrosamines from a redistilled water sample were examined by measuring the peak height of the chemiluminescence intensity according to the above procedures. Table II shows the recoveries obtained by

spiking samples with six nitrosamines at 100 pmol.

The results show that the sensitivity of the proposed method is good, the detection limits are better than those reported for other methods [1,2,4–7] and the precision is satisfactory. It is expected to have wide applications in environmental analysis and biochemical and fundamental research.

REFERENCES

- 1 Q. Wan and C. Fu, *Chin. J. Chromatogr.*, 4 (1986) 238.
- 2 S.S. Hecht, R.M. Ornag and D. Hoffman, *Anal. Chem.*, 47 (1975) 2046.
- 3 P.E. Oettinger, F. Huffman, D.H. Fine and D. Lieb, *Anal. Lett.*, 6 (1973) 731.
- 4 J.K. Baker and C.Y. Ma, *IARC (Int. Agency Res. Cancer) Sci. Publ.*, No. 19 (1978) 19.
- 5 Z. Wang, H. Xu and C. Fu, in Zheng Chen (Editor), *1st Changchun International Symposium on Analytical Chemistry, China*, Jilin University Press, 1990, p. 57.
- 6 Z. Wang, H. Xu and C. Fu, *J. Chromatogr.*, 589 (1992) 349.
- 7 M. Zheng, C. Fu and H. Xu, in Dehe Zhang (Editor), *Proceedings of the 4th Asian Chemical Congress, Beijing*, Chinese Chemical Society Publishers, 1991, p. 346.
- 8 K. Imai and R. Wienberger, *Trends Anal. Chem.*, 4 (1985) 170.
- 9 K. Imai, A. Nishitani and Y. Tsukamoto, *Chromatographia*, 24 (1987) 77.
- 10 G.J. de Jong and P.J.M. Kwakman, *J. Chromatogr.*, 492 (1989) 319.
- 11 K. Kobayashi and K. Imai, *Anal. Chem.*, 52 (1980) 424.
- 12 L.M. Hwo and L.S. Ma, *Analytical Methods for N-Nitroso Compounds*, Science Publisher, Beijing, 1980.
- 13 A.G. Mohan and N. . Turro, *J. Chem. Educ.*, 51 (1974) 528.
- 14 C. Fu and Q. Wan, *Chin. J. Anal. Chem.*, 13 (1985) 595.

CHROMSYMP. 2683

Protein sorting by high-performance liquid chromatography

I. Biomimetic interaction chromatography of recombinant human deoxyribonuclease I on polyionic stationary phases[☆]

J. Cacia and C.P. Quan

Department of Medicinal and Analytical Chemistry, Genentech, Inc., 460 Point San Bruno Boulevard, South San Francisco, CA 94080 (USA)

M. Vasser

Department of Bioorganic Chemistry, Genentech, Inc., 460 Point San Bruno Boulevard, South San Francisco, CA 94080 (USA)

M.B. Sliwkowski

Department of Cell Culture and Fermentation Research and Development, Genentech, Inc., 460 Point San Bruno Boulevard, South San Francisco, CA 94080 (USA)

J. Frenz*

Department of Medicinal and Analytical Chemistry, Genentech, Inc., 460 Point San Bruno Boulevard, South San Francisco, CA 94080 (USA)

(First received September 30th, 1992; revised manuscript received December 22nd, 1992)

ABSTRACT

Chromatographic separations can be tailored to exploit specific interactions between a stationary phase ligand and a protein structural feature of interest. Variations in this feature then form the basis for sorting a mixture of closely related proteins into defined subpopulations. This report describes the sorting of variants of recombinant human deoxyribonuclease I (rhDNase) that differ in the occurrence of deamidation at a single residue. rhDNase, an enzyme that non-specifically hydrolyzes DNA, is glycosylated and exhibits considerable charge heterogeneity owing to the sialylation and phosphorylation of its N-linked oligosaccharides. This heterogeneity obscures the relatively subtle differences between deamidated and intact rhDNase, preventing separation on this basis in conventional ion-exchange HPLC. Published structural information on bovine DNase

* Corresponding author.

* Presented at the 16th International Symposium on Column Liquid Chromatography, Baltimore, MD, June 14–19, 1992. The majority of the papers presented at this symposium have been published in *J. Chromatogr.*, Vols. 631 + 632 (1993).

reveals that the analogous labile asparagine residue is involved in DNA binding, so stationary phases containing polyanionic ligands mimicking nucleic acids were employed to separate the deamidation variants of rhDNase. Electrostatically immobilized DNA, a “tentacle” cation exchanger (TCX) and immobilized heparin columns all resolved the deamidated and intact forms of rhDNase when operated at pH 4.5. The ligands of the TCX and heparin columns are sufficiently long, flexible and polyanionic to interact with rhDNase in a manner similar to DNA and to sort rhDNase variants on the basis of the charge difference of a single residue involved in that interaction. A non-hydrolyzable double-stranded oligonucleotide analogue of DNA was also synthesized and immobilized to an HPLC support. This column, operated at pH 6, where rhDNase is active, resolved the two isomeric products of deamidation of rhDNase, *i.e.*, variants of the enzyme containing either aspartate or isoaspartate in lieu of asparagine at the deamidation site in rhDNase. This is the first reported separation of intact variants of a glycoprotein differing on the basis of these isomeric products of deamidation through the common cyclic imide mechanism.

INTRODUCTION

Proteins are large, complex molecules containing a myriad of combinations of chemically distinct amino acid side chains. In addition, certain proteins bear post-translational modifications that further compound the intricacy of the molecule and that may, in the case of glycosylation, convert the protein into a variegated amalgam of species differing in the structures of the conjugate carbohydrates. The analytical characterization of a protein is, therefore, hampered by the multiplicity of chemical species that contribute to its physico-chemical behavior. The most prominent example of this approach to protein separations is affinity chromatography [1] that exploits a biological interaction between the protein and its natural ligand. The specificity of these interactions affords a powerful means of separating a protein from non-binding species.

Affinity chromatography is, however, just one example of a general approach to high resolution separations of proteins in which the chromatographic conditions are chosen to be selective for a specific feature of a protein, to give high selectivity for that feature, and to exhibit little or no selectivity for other characteristics. Hence, as in affinity separations, the chromatographic conditions are adjusted so that the stationary phase selectively interacts with a single or few chemical moieties of the protein, ignoring the remaining large number of distinct chemical species. The value of this approach to chromatographic separations is that a nonselective analytical system would be swamped by the variety of species present on a protein and yield little or no selectivity for any particular characteristic. The general approach to separating protein species

on the basis of a specific single characteristic is termed “protein sorting”, by analogy to the post-translational trafficking of proteins on the basis of specific structural motifs or “signals” on the protein that target it to particular intracellular or extracellular locations [2]. The power of chromatographic protein sorting is apparent when populations of closely related species are sorted, for instance according to the presence of particular carbohydrate groups on N-linked glycans [3] or, in the example described in this report, according to the occurrence of deamidation at a single site in a glycoprotein, recombinant human deoxyribonuclease I (rhDNase), that exhibits considerable charge heterogeneity engendered by glycosylation.

Deoxyribonuclease I (DNase) is an endonuclease that non-specifically hydrolyzes DNA. DNase isolated from bovine pancreatic tissue has been extensively characterized [4–6] and its crystal structure has been solved [7]. Human DNase has been cloned and expressed in mammalian cells for use as a therapeutic in the treatment of cystic fibrosis [8]. rhDNase has a high degree of charge heterogeneity arising from phosphorylation and sialylation of carbohydrate structures linked to both Asn-18 and Asn-106. The charge heterogeneity is manifested, for example, in isoelectric focusing (IEF) where rhDNase forms a ladder of six or more bands in a pI range of 3–4, as shown in Fig. 1. Additional charge complexity accrues to rhDNase through deamidation of the Asn-74 residue in the molecule. The deamidation of asparagine residues is well characterized in proteins [9]. Asparagine-serine sequences, such as that of residues 74 and 75 in rhDNase, are particularly prone to deamidate under alkaline conditions through a cyclic

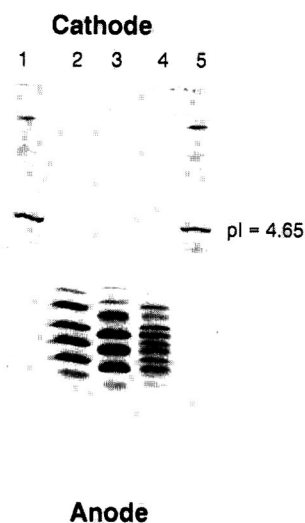


Fig. 1. Isoelectric focusing gel showing (lane 2) rhDNase, (lane 3) its deamidated variant and (lane 4) an equimolar admixture of the two components. Lanes 1 and 5 contained pI markers. The 0.2 mm thick IEF gel contained a 2% ampholyte mixture (Serva) in a pH range of 3–5 and was stained with Coomassie blue. Focusing was performed for 2 h with a voltage limit of 1600 V, and a power limit of 10 W.

imide intermediate [10] to yield two products, Asp-74 and iso-Asp-74. Fig. 2 shows the reaction pathway followed in this conversion of a neutral side chain to two isomeric residues with acidic side chains. The two isomeric products of deamidation differ in the lengths of both the side chain and the polypeptide backbone, with the iso-Asp form containing an added methylene

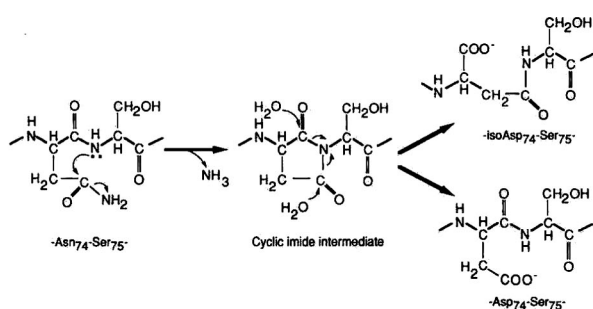


Fig. 2. Schematic of the base-catalyzed deamidation pathway for the Asn-Ser sequence in rhDNase. Asparagine residues deamidate under alkaline conditions by a mechanism that proceeds through a cyclic imide intermediate. The intermediate hydrolyzes to yield one of two isomeric products, containing either aspartic acid or isoaspartic acid residues in lieu of asparagine.

group in the backbone. rhDNase has been shown to undergo deamidation at Asn-74 under conditions of elevated pH and temperature, and to evince the reaction in tryptic mapping analysis [11]. IEF analysis of the deamidated variant of rhDNase, shown in Fig. 1, demonstrates that it retains the carbohydrate-related charge heterogeneity of the non-deamidated glycoprotein. IEF analysis of an admixture of the two variants, shown in lane 3 of Fig. 1, results in an IEF pattern with 12 or more bands, revealing the subtle acidic shift of the bands of the deamidated protein. The small difference between rhDNase and its deamidated variant—in terms of both the structural difference that is limited to conversion of an amide side chain to a carboxylic side chain as well as the small acidic shift noted in IEF—in the midst of a relatively large degree of charge heterogeneity of the glycoprotein, portends difficulties in resolving the variant from intact rhDNase by chromatographic methods. This report describes studies of the behavior of rhDNase and its deamidated variant in a variety of ion-exchange HPLC systems, including those designed to mimic the interaction of rhDNase with DNA, its natural substrate. The requirements for sorting of rhDNase variants on the basis of the occurrence of deamidation at Asn-74, and the protein structural basis for these requirements, are described.

EXPERIMENTAL

Chromatographic equipment

All chromatography was performed on a Hewlett-Packard (Palo Alto, CA, USA) Model 1090M liquid chromatograph equipped with a diode array detector, autosampler and Chemstation data collection and analysis software.

Materials

rhDNase and its deamidated variant were produced by mammalian cell culture and purified at Genentech. N-(2-hydroxyethyl)piperazine-N'-(2-ethanesulfonic acid) (HEPES), potassium phosphate and salmon testes DNA were obtained from Sigma (St. Louis, MO, USA) and sodium acetate and sodium chloride from Mallinckrodt (Paris, KY, USA). (2-N-Mor-

pholino)ethanesulfonic acid (MES) was obtained from ICN Biochemicals (Costa Mesa, CA, USA). Empty stainless-steel columns with dimensions of 50 mm × 4.6 mm I.D. were purchased from Alltech (Deerfield, IL, USA). Hydrosphere EP epoxide silica resin was obtained from Rainin (Woburn, MA, USA). The 5- μ m LiChrosphere SO₃⁻ packing with pore diameters of 1000 Å was obtained packed in glass cartridges that were unpacked, and the resin defined by suspending in 5 mM sodium acetate, pH 4.5. The fines remaining in the suspension after settling for 20 min were poured off. This procedure was repeated five times prior to packing the material into a steel column in the same buffer. The PL SAX, 150 × 4.6 mm I.D., 8 μ m, 1000 Å strong anion-exchange column was purchased from Polymer Labs. (Foster City, CA, USA). The TSK SP 5⁺ TSK Heparin 5PW columns both having dimensions of 75 mm × 7.5 mm I.D. were purchased from HP Genenchem (Palo Alto, CA, USA).

Methods

Strong anion-exchange chromatography. Column: Polymer Labs SAX, 150 × 4.6 mm. Flow-rate: 1.0 ml/min. Eluent A: 5 mM HEPES, 1 mM CaCl₂ pH 7.0. Eluent B: 1 M NaCl, 5 mM HEPES, 1 mM CaCl₂ pH 7.0. Gradient: 1-min hold at 0% B, followed by a linear gradient to 50% B over 40 min.

Strong cation-exchange chromatography. Column: TSK SP 5PW 75 × 7.5 mm. Flow-rate: 1.0 ml/min. Eluent A: 10 mM sodium acetate, 1 mM CaCl₂ pH 4.5. Eluent B: 1 M NaCl, 10 mM sodium acetate, 1 mM CaCl₂ pH 4.5. Gradient: 4-min hold at 0% B, followed by a linear gradient to 58% B over 26 min.

"Tentacle" cation-exchange chromatography. Column: LiChrosphere SO₃⁻, 5 μ m, 1000 Å packed into a 50 × 4.6 mm I.D. stainless-steel column as described above. The chromatographic conditions were identical to those described above for strong cation-exchange chromatography.

Heparin column chromatography. Column: TSK Heparin 5PW 75 × 7.5 mm. The chromato-

graphic conditions were identical to those described above for strong cation-exchange chromatography.

Electrostatically immobilized DNA affinity chromatography. Column: PL SAX 150 × 4.6 mm. Flow-rate: 1.0 ml/min. Eluent A: 10 mM sodium acetate, 1 mM CaCl₂ pH 4.5. Eluent B: 1 M NaCl, 10 mM sodium acetate, 1 mM CaCl₂ pH 4.5. The column was equilibrated with eluent A and 250- μ l aliquots of a 2 mg/ml solution of salmon testes DNA were injected until breakthrough was observed at UV 260 nm. An additional 10-mg amount of DNA was then injected to ensure adequate coating of anion-exchange sites in the column. Gradient: linear from 0% B to 70% B over 10 min, followed by a 2-min hold at 70% B.

Synthesis of non-hydrolyzable DNA analogue. Complementary phosphorothioate oligonucleotides with a sequence of 5'-GGCGCCT-CCAGCGTCGACGGCGNH₂-3' and 5'-CG-CCGTCGACGCTGGAGGCGCC-3' were synthesized on aminated controlled-pore glass (Clontech, Palo Alto, CA, USA) using H-phosphonate chemistry [12] on a Model 8600 DNA synthesizer (Milligen/Bioscience, South San Francisco, CA, USA). The non-hydrolyzable DNA analogue was synthesized with an amino group at the 3' end of one of the oligonucleotide strands to allow coupling to an activated packing material. The two strands were annealed by diluting the mixture to 0.2 mg/ml with 10 mM Tris-HCl, 1 mM EDTA, pH 7.5. The mixture was then boiled for 1 min and slowly cooled to room temperature. Three volumes of absolute ethanol and 100 mM NaCl were then added to precipitate the double-stranded oligonucleotide. The oligonucleotide was then centrifuged and lyophilized.

Immobilization of oligonucleotide analogue. A 10-mg amount of double-stranded oligonucleotide was mixed with 1 g of epoxy silica resin and resuspended to 5 ml with 100 mM KH₂PO₄, pH 7.0. The mixture was shaken for 24 h at room temperature and then slurry packed into a 50 × 4.6 mm stainless-steel HPLC column.

DNA-analogue affinity chromatography. Eluent A: 5 mM MES, 1 mM CaCl₂, pH 6.0.

Eluent B: 1 M NaCl, 5 mM MES, 1 mM CaCl₂, pH 6.0. Gradient: linear from 0 to 100% B over 20 min. Flow-rate: 1.0 ml/min.

RESULTS AND DISCUSSION

Deamidation is a relatively common degradation reaction [9] that increases the number of charged residues on a protein at physiological pH and therefore, in many cases, is readily detected. The charge difference between a deamidated protein and its intact parent provides the basis for separation and analysis of the occurrence of deamidation by anion-exchange HPLC [13], cation-exchange HPLC [14], capillary electrophoresis [13] and isoelectric focusing electrophoresis [13]. In addition, tryptic mapping [15], mass spectrometry [15], N-terminal sequencing [16] and enzymatic methyl-accepting capacity [17] can provide information on the occurrence of deamidation in peptides and proteins.

In many cases, chromatographic methods that separate deamidation variants of intact proteins are preferable, since they are relatively fast and quantitative, can be automated and can be scaled

up for preparative applications. The isoelectric point (*pI*) of the protein of interest often dictates the pH range of the mobile phase employed in ion-exchange HPLC and the choice of an anion or cation exchanger as the stationary phase. rhDNase is an acidic protein with a *pI* ranging between 3 and 4. Hence, anion-exchange chromatography is expected to provide strong retention under conditions near neutral pH where rhDNase is most stable. This mode of HPLC has been employed to resolve the deamidated variants of other acidic proteins [13]. A comparison of rhDNase and its deamidated variant run on anion-exchange chromatography is shown in Fig. 3A and B, respectively. Injection of an admixture of these two forms, shown in Fig. 3C, reveals no separation of the variants. Two fractions were collected from the admixture injection and run on an isoelectric focusing gel. The bands observed on the gel demonstrate that the column exhibits no selectivity for the deamidated form of rhDNase. Instead, the more acidic isozymes are retained longer on the anion exchanger, without resolving deamidation variants. The broad peaks obtained in the chromatograms shown in Fig. 3 probably reflect the charge heterogeneity con-

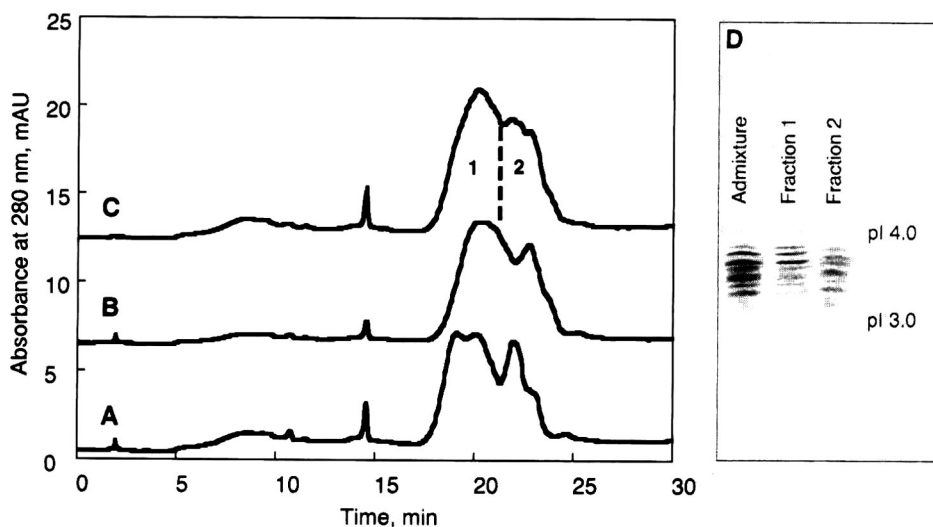


Fig. 3. Strong anion-exchange chromatography of (A) rhDNase, (B) its deamidated variant and (C) an admixture of the two variants. Fractions 1 and 2 were collected and run on a pH 3–5 isoelectric focusing gel shown in (D). Conditions are given in the text.

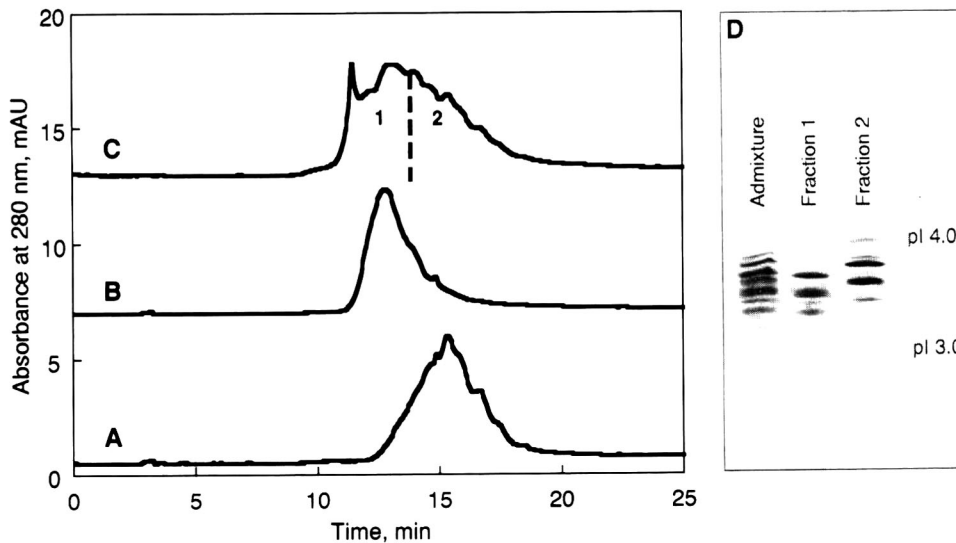


Fig. 4. Strong cation-exchange chromatography on a sulfopropyl column of (A) rhDNase, (B) its deamidated variant and (C) an admixture of the two variants. Fractions 1 and 2 were collected and run on a pH 3–5 isoelectric focusing gel shown in (D). Conditions are given in the text.

ferred on the protein by the presence of sialic acid and mannose phosphate on the glycans linked to rhDNase.

Cation-exchange HPLC has been employed to resolve the deamidated form of a glycoprotein that similarly exhibited a high degree of carbohydrate charge heterogeneity [14]. At pH 4.5, rhDNase, despite its low *pI*, can be retained on and recovered from a cation exchanger. Fig. 4 shows rhDNase and its deamidated variant injected on a sulfopropyl strong cation-exchange HPLC column. A slight resolution of these variants is observed when they are separately injected. rhDNase variants yield relatively broad peaks in these chromatograms, as on the anion exchange column, due to the charge heterogeneity of the population of N-linked oligosaccharides found on the glycoprotein. Injection of the admixture of the two variants reveals no useful separation with this column. Two fractions were collected from the admixture injection and run on an isoelectric focusing gel shown in Fig. 4D. As in anion-exchange chromatography, the separation is primarily based on carbohydrate charge heterogeneity with the more acidic species eluting earlier. The column exhibits a small selectivity for the deamidated rhDNase variant, but this selectivity is obscured by the contributions of

sialylation and phosphorylation of the molecule to retention.

The residue in rhDNase that is prone to deamidation has been identified as asparagine-74 (Asn-74). According to the published crystal structure [7], the corresponding residue in bovine DNase is known to be involved in binding of the DNA substrate. Fig. 5 shows the bovine DNase residues that are involved in binding DNA as determined by cocrystallization with a

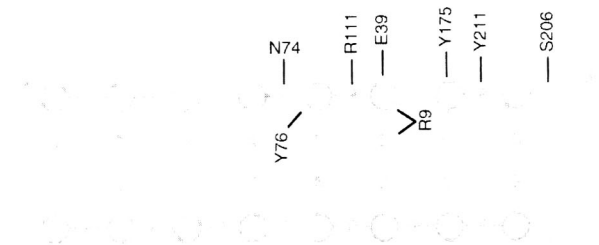


Fig. 5. Schematic of the DNA–DNase contacts determined from the crystal structure of the complex between a synthetic oligonucleotide and bovine DNase [7]. Asparagine-74 (N74) forms a hydrogen bond with a phosphate group in DNA. The other residues in the bovine enzyme involved in DNA-binding near the primary hydrolysis site on the substrate are arginines-9 and 111 (R9, R111), glutamate-39 (E-39), tyrosines-76, -175 and -211 (Y76, Y175, Y211) and serine-206 (S206).

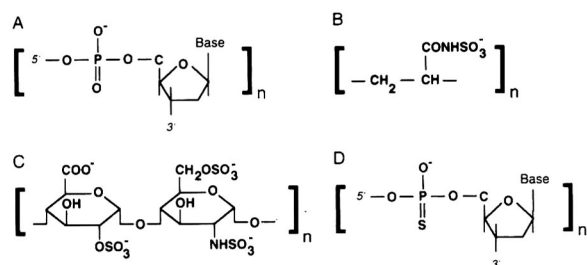


Fig. 6. Repeating units of the polyanionic ligands used for separation of rhDNase from its deamidated variant. (A) DNA, (B) tentacle SO_3^- (TCX), (C) heparin, (D) synthetic non-hydrolyzable DNA analogue.

synthetic oligonucleotide [7]. The Asn-74 residue, that is conserved between human and bovine DNases, is shown to hydrogen bond with a phosphodiester group in the oligonucleotide backbone. Since deamidation occurs in a portion of the molecule that is accessible to DNA, the separation of rhDNase from its deamidated variant may be achieved by exploiting the biomimetic interaction of a polyanionic ligand that similarly can gain access to the relevant portion of the molecule. Fig. 6A shows the repeating unit of the DNA biopolymer. The phosphodiester linkages between repeating units confer multiple negative charges to the DNA polymer

backbone. Fig. 6B–D shows the structures of polyionic ligands that were examined for the potential to imitate DNA by accessing the DNA binding site of rhDNase, and separate deamidation variants of the molecule.

The repeating unit of the “tentacle” strong cation-exchange (TCX) resin is shown in Fig. 6B. The TCX ligand contains sulfate groups as does the conventional sulfopropyl column discussed above. The TCX ligand, however, contains multiple cation-exchange moieties strung along the polymeric backbone creating a flexible polyanionic ligand. Each ligand is reported to consist of 5–50 repeating units [18]. The polymeric nature of the cation exchanger imparts certain characteristics of DNA to the ligand. Fig. 7A and B show the chromatograms obtained for rhDNase and its deamidated variant, respectively, on the TCX column. Injection of the admixture of the two variants, shown in Fig. 7C, results in baseline resolution of the two species. The two peaks were collected from the chromatogram shown in Fig. 7C and run on an isoelectric focusing gel, shown in Fig. 7D. The IEF analysis confirms that the TCX column recognizes the single charge difference at residue 74 between the two variants of rhDNase. Hence the TCX column biomimetically interacts with the

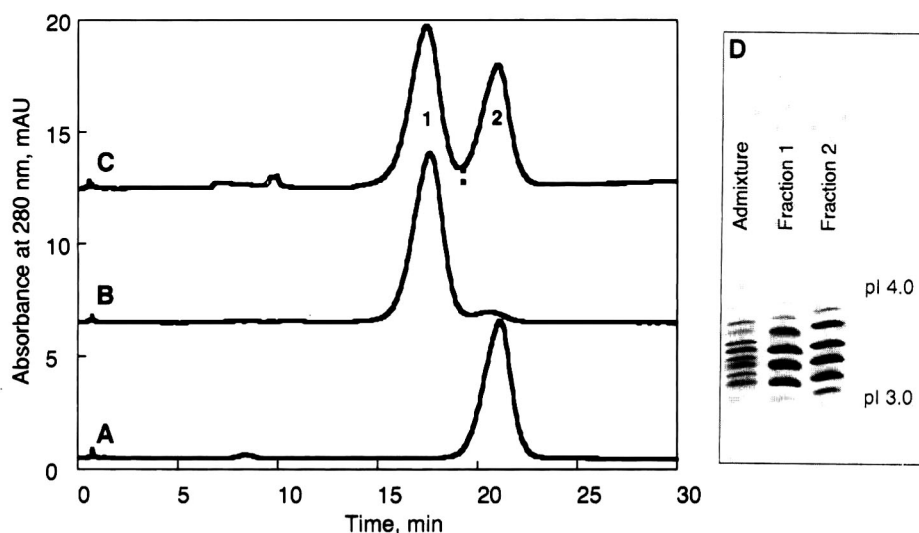


Fig. 7. Tentacle cation-exchange chromatography of (A) rhDNase, (B) its deamidated variant and (C) an admixture of the two variants. Fractions 1 and 2 were collected and run on a pH 3–5 isoelectric focusing gel shown in (D). Conditions were identical to those employed in Fig. 4.

same portion of the enzyme as the DNA substrate.

Another commercially available ligand containing a polymeric cation-exchange ligand, shown schematically in Fig. 6C, is the immobilized heparin column. Heparin is a sulfated glycosaminoglycan polysaccharide. Fig. 8A and B shows that the heparin column resolves rhDNase and its deamidated variant in a similar fashion to the TCX column. The efficiency of this separation is slightly less than that observed on the TCX column, although the interaction is still specific for the portion of the molecule containing the charge difference at residue 74. The two peaks resulting from injection of the admixture of the two variants (Fig. 8C) were collected and run on an isoelectric focusing gel shown in Fig. 8D. The resulting pattern demonstrates the selectivity exhibited by biomimetic interaction chromatography with this column despite the considerable carbohydrate-engendered charge heterogeneity of the two species.

The analyses of rhDNase variants on the TCX and heparin columns were carried out at pH 4.5 in order to obtain sufficient retention of the acidic glycoprotein. In order to demonstrate that the TCX and heparin ligands mimic DNA in the separations shown in Figs. 7 and 8, a DNA affinity column was prepared by electrostatic

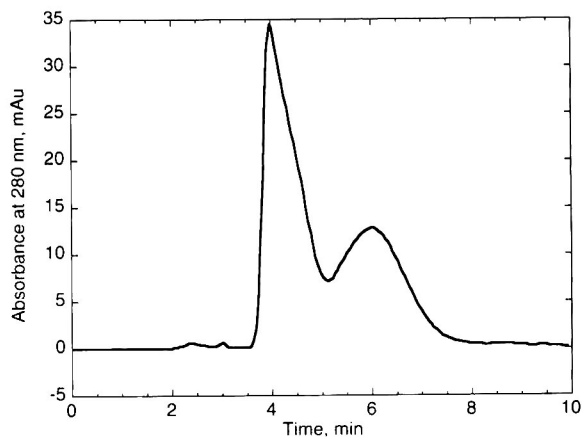


Fig. 9. Electrostatically immobilized DNA affinity chromatography of an admixture of rhDNase and its deamidated variant. Conditions are given in the text.

immobilization of salmon testes DNA on an anion-exchange HPLC column. The hydrolysis of DNA by DNase is negligible at pH 4.5, so under these conditions a practical DNA affinity column can be prepared. The strong anion-exchange column was coated with DNA at pH 4.5, effectively converting it to an affinity column for rhDNase. The admixture of rhDNase with its deamidated variant was injected, yielding the two peaks shown in the chromatogram in Fig. 9. The two peaks were shown to be the two charge

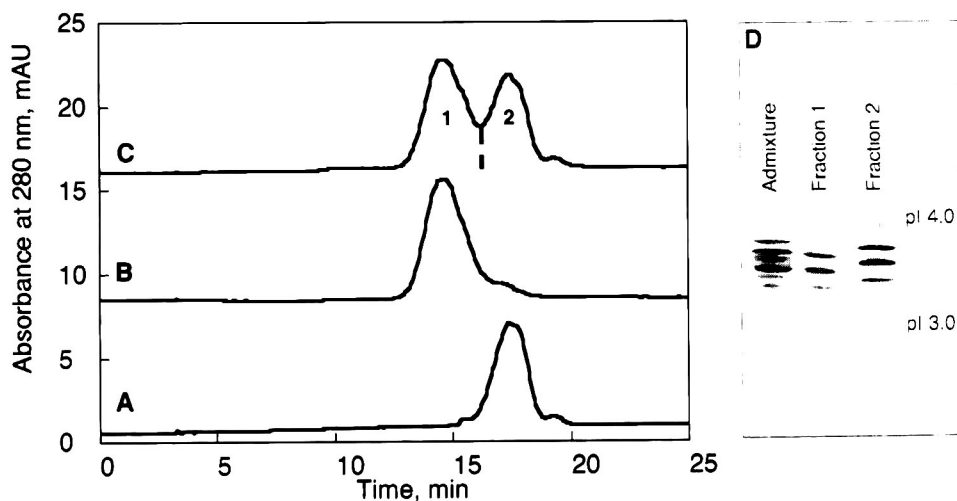


Fig. 8. Immobilized heparin chromatography of (A) rhDNase, (B) its deamidated variant and (C) an admixture of the two variants. Fractions 1 and 2 were collected and run on a pH 3–5 isoelectric focusing gel shown in (D). Conditions were identical to those employed in Fig. 4.

variants of rhDNase by collection and reinjection on the TCX column (data not shown), with the deamidated form eluting from the column earlier than intact rhDNase. This separation could not be obtained on the bare anion-exchange column prior to coating with DNA. The DNA affinity column exhibited relatively poor efficiency and reproducibility, owing to the poor stability of the electrostatic immobilization and the heterogeneity of the salmon testes DNA preparation. Nevertheless, the separation obtained on this column confirms the involvement of the labile Asn-74 residue in binding DNA, and the biomimetic behavior of the TCX and heparin ligands under these conditions.

Another way to investigate the interaction between DNA and rhDNase variants is to employ a column containing an immobilized synthetic oligonucleotide. In this study, complementary phosphorothioate analogues [12], having the linkage shown in Fig. 6D, were synthesized with the sequences given in the Experimental section. One strand was synthesized with a free amino group at the 3' end, and the annealed strands were covalently attached to activated silica particles through this group to make the immobilized double-stranded affinity column. At pH 4.5 the separation by this column was similar to that of the electrostatically immobilized DNA column (data not shown). The phosphorothioate DNA analog is refractory to hydrolysis by DNase [19], and so can be operated with a higher-pH mobile phase under conditions where the DNA affinity column is hydrolyzed. Fig. 10 shows the chromatograms of rhDNase, the deamidated form of rhDNase and the admixture of the two species on the oligonucleotide affinity column operated at pH 6. The column resolves the deamidated and intact forms of rhDNase, but also separates the deamidated form of the enzyme into two peaks. The two peaks were collected and characterized by tryptic mapping. Fig. 11 shows the tryptic maps of the two peaks of deamidated rhDNase collected from the oligonucleotide column, along with the map of intact rhDNase. The tryptic maps differ in the T6-7 and T7 peptides that contain the labile Asn-74 residue. The T7 peptide contains Asn as residue 74 and hence is an indicator of intact rhDNase, while

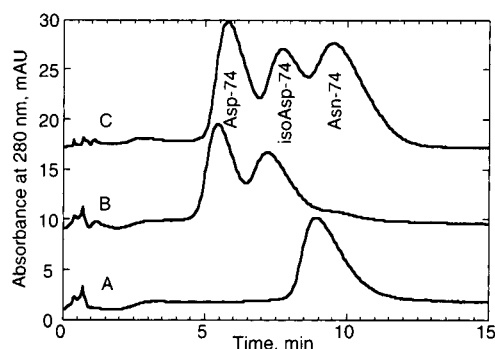


Fig. 10. Non-hydrolyzable DNA analogue affinity chromatography of (A) rhDNase, (B) its deamidated variant and (C) an admixture of the two variants. The peaks labeled "Asp-74", "isoAsp-74" and "Asn-74" were collected for characterization by tryptic mapping. The first peak was found to be rhDNase with aspartate at residue 74 (Asp-74 rhDNase), the second peak to be the isoAsp-74 isomer of the deamidated variant and the third peak to be intact rhDNase containing asparagine at position 74.

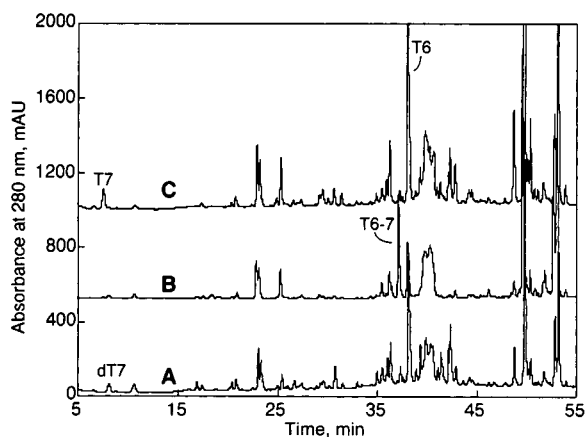


Fig. 11. Tryptic maps of the fractions collected from the DNA analogue affinity separation shown in Fig. 10C. (A) Chromatogram of the peptide mixture obtained on tryptic digestion of peak Asp-74, the deamidation variant containing aspartic acid at residue 74, as indicated by the peptide labeled dT7. (B) Chromatogram of the digest of peak isoAsp-74, the deamidation variant containing isoaspartic acid at residue 74, as indicated by the peptide T6-7. (C) Chromatogram of the digest of peak Asn-74, the intact form of rhDNase that contains asparagine at residue 74. The T7 peptide includes residues 74–77 of the digested protein, with asparagine at residue 74. The dT7 peptide similarly includes residues 74–77, but with aspartic acid at residue 74. The T6-7 peptide includes residues 51–77, with isoaspartic acid at residue 74 and no cleavage of the peptide bond after the arginine at residue 73.

the dT7 and T6-7 peptides are markers for the Asp-74 and isoAsp-74 containing deamidation variants, respectively. The tryptic maps thus reveal that the oligonucleotide analog column resolves the isomeric forms of deamidated rhDNase that contain either an aspartic acid or an isoaspartic acid residue in lieu of asparagine at position 74. The structural differences among these variants are shown in Fig. 2. The side chains of the two products of asparagine deamidation have essentially identical pK values, and so do not differ in charge, and rhDNase variants differing in these isomeric side chains are not resolved by isoelectric focusing gel electrophoresis. Nevertheless the two forms of deamidated rhDNase, that differ in both the length of the side chain and in the length of the polypeptide backbone, display sufficient differences in binding to the high-performance affinity column to allow their separation. This is apparently the first example of the separation of the two isomers of an intact glycoprotein resulting from deamidation through the cyclic imide pathway. The separation underscores the power of protein sorting and biomimetic interaction HPLC to yield high resolution of a specific characteristic of a protein that cannot be achieved by other analytical methods.

CONCLUSIONS

The physico-chemical interactions between the stationary phase surface and the surface of a protein provides the basis of separation in chromatography. Hence, knowledge of the structure of a protein can guide the selection of the conditions, including the choice of stationary phase, to obtain a particular separation. In this report the column selection for the separation of rhDNase from its deamidated variant was guided by the insight gained from the crystal structure of bovine DNase, that revealed that deamidation occurs at a residue involved in the binding of the enzyme to DNA. Conventional ion-exchange columns, with relatively short ligands, were unable to resolve rhDNase from its deamidated variant. Columns packed with polyanionic ligands—including a tentacle cation exchanger, immobilized heparin, immobilized DNA and an

immobilized synthetic DNA analogue—were able to achieve the separation of the two closely related proteins. The longer polyanionic ligands apparently can gain access to the relevant portion of the DNA binding site and mimic the interaction of DNase with its substrate and discriminate on the basis of deamidation at a single site in the glycoprotein. The physico-chemical interactions involved can themselves be studied by chromatographic methods. One example of such an interaction is suggested by the separation obtained on the oligonucleotide analogue column of the isomers of the deamidated form of rhDNase, that differ only in the geometry of the acidic residue resulting from deamidation of the asparagine at residue 74. The slight structural difference between the aspartate- and isoaspartate-containing variants of deamidated rhDNase provided sufficient selectivity to permit the isolation of the individual isomeric proteins from the oligonucleotide analog column for further characterization. The chromatographic separation of the two species on the biomimetic interaction column thus sheds new light on the biochemical interaction between variants of an enzyme and its substrate.

Both aspects of the surface interactions involved in chromatography—the column selection guided by protein structural considerations and the investigation of biochemical interactions by chromatographic methods—are examples of protein sorting, the high-resolution separation of proteins on the basis of a specific significant structural feature, without regard to the heterogeneity that may be present on the remainder of the protein. Since chromatographic resolution is essentially limited to the portion of the protein that interacts with the stationary phase, it is a powerful means of focusing the available separating power on the structural feature of interest, and sorting a population of proteins on the basis of characteristics of that feature. In this report, the structural feature of interest was Asn-74, and biomimetic interaction of the stationary phase ligands with the portion of the enzyme containing this residue was facilitated by the involvement of the residue in DNA binding. The chromatographic separation was focused on that portion of the molecule by the use of biomimetic

polyanionic ligands, and a mixture of rhDNase variants was sorted into subpopulations on the basis of the residue at the deamidation site in the protein. The subpopulations did not differ in other characteristics, including in the considerable charge heterogeneity associated with the oligosaccharides present at the two glycosylation sites on rhDNase.

ACKNOWLEDGEMENTS

The authors gratefully acknowledge the unstinting encouragement of and valuable discussions with Steve Spencer, Bryan Lawlis and Steve Shak of Genentech on this project. The authors also thank Professor Csaba Horváth of Yale University for many helpful discussions and insights into the protein sorting problem. Finally, the authors are also grateful to Loretta Benman of Genentech for her technical assistance in preparation of the graphics employed in this manuscript.

REFERENCES

- 1 S. Ostrove, *Methods Enzymol.*, 182 (1990) 357.
- 2 R.W. Compans (Editor), *Protein Traffic in Eukaryotic Cells; Selected Reviews (Current Topics in Microbiology and Immunology*, Vol. 170), Springer, Berlin, 1991.
- 3 J. Frenz, C.P. Quan, J. Cacia and C. Democko, in preparation.
- 4 M. Kunitz, *J. Gen. Physiol.*, 33 (1950) 349.
- 5 M. Laskowski, in P.D. Boyer (Editor), *The Enzymes*, Vol. 3, Academic Press, New York, 3rd ed., 1971, p. 289.
- 6 S. Moore, in P.D. Boyer (Editor), *The Enzymes*, Vol. 14, Academic Press, New York, 1981, p. 281.
- 7 A. Lahm and D. Suck, *J. Molec. Biol.*, 221 (1991) 645.
- 8 S. Shak, D.J. Capon, R. Hellmiss, S.A. Marsters and C.L. Baker, *Proc. Natl. Acad. Sci., U.S.A.*, 87 (1990) 9188.
- 9 H.T. Wright, *Crit. Rev. Biochem. Molec. Biol.*, 26 (1991) 1.
- 10 Y.C. Meinwald, E.R. Stimson and H.A. Scheraga, *Int. J. Pept. Protein Res.*, 28 (1986) 79.
- 11 C.P. Quan, J. Cacia, R. Chloupek, A. Guzzetta, W.S. Hancock, J. Gunson, M. Sliwkowski and J. Frenz, in preparation.
- 12 B.C. Froehler, P.G. Ng and M.D. Matteucci, *Nucleic Acid Res.*, 14 (1986) 5399.
- 13 J. Frenz, S.-L. Wu and W.S. Hancock, *J. Chromatogr.*, 480 (1989) 379.
- 14 G. Teshima, J. Porter, K. Yim, V. Ling and A. Guzzetta, *Biochemistry*, 30 (1991) 3916.
- 15 G.W. Becker, P.M. Tackitt, W.W. Bromer, D.S. Legeber and R.M. Riggin, *Biotechnol. Appl. Biochem.*, 10 (1988) 326.
- 16 D.G. Smyth, W.H. Stein and S. Moore, *Arch. Biochem. Biophys.*, 117 (1962) 1845.
- 17 A. Di Donato, P. Galletti and G. D'Alessio, *Biochemistry*, 25 (1986) 8361.
- 18 W. Müller, *J. Chromatogr.*, 510 (1990) 133.
- 19 S. Spitzer and F. Eckstein, *Nucleic Acids Res.*, 16 (1988) 11 691.

Semi-automated chromatographic procedure for the isolation of acetylated N-terminal fragments from protein digests[☆]

Dan L. Crimmins* and Richard S. Thoma

Howard Hughes Medical Institute, Core Protein/Peptide Facility, Washington University School of Medicine, 660 S. Euclid Avenue, Box 8022, St. Louis, MO 63110 (USA)

(Received November 19th, 1992)

ABSTRACT

Several published procedures have been combined to develop a general strategy for the specific identification and isolation of the acetylated-N-terminal fragment from all other proteolytic fragments. This ruse can be divided into four steps: (i) succinylation of the substrate to block lysine NH₂ groups; (ii) enzymatic digestion of the modified protein; (iii) automated phenylisothiocyanate derivatization of the protease derived fragments to block newly generated "free" N-termini; and (iv) reversed-phase high-performance liquid chromatography with on-line photodiode array spectroscopy. The individual phenylthiocarbonyl-peptide species exhibit an increased reversed-phase retention time and a greater UV (210–297 nm) profile compared to the corresponding control (–phenylisothiocyanate) digest. The N-terminal acetylated fragment shows neither a retention time shift nor an augmented UV profile. To validate each process step, synthetic peptides and acetylated-N-terminal proteins of known sequence were used as test samples. The desired fragment was isolated from three proteins and positively identified by electrospray mass spectrometry and amino acid composition. Proteins with other N-terminal blocking groups should be amenable to this procedure.

INTRODUCTION

Proteins, proteolytic fragments, and peptides blocked at the N-terminus are refractory to Edman degradation. It has been estimated that over 50% of soluble mammalian proteins are blocked at the N-terminus [1]. Considerable effort has therefore been devoted to deblocking schemes and subsequent sequence analysis. The target fragment is usually isolated from a digest and two distinct analytical procedures are then employed to obtain further structural information. In the first, removal of the blocking group

chemically [2], or enzymatic liberation of the N-acetyl (Ac) amino acid itself [3–8], can provide a substrate suitable for sequence determination. Mass spectrometry–mass spectrometry (MS–MS) analysis is the other approach and is a direct means of obtaining sequence information [9–15]. Recent studies have shown that the deblocked N-terminal fragment can be sequenced in the presence of all other appropriately modified digest fragments [5,6,16]. However, as these other fragments were not recovered during this procedure, potentially important structural information may be missed, particularly for unknown proteins [3–8,16].

In this study, we have combined several published procedures [5,17,18] to develop a general, semi-automated strategy that successfully identifies and isolates the Ac-N-terminal fragment from complex reversed-phase high-performance

* Corresponding author.

☆ Portions of this work have been presented at the 6th Symposium of The Protein Society, San Diego, CA, July 25, 1992.

liquid chromatography (RP-HPLC) peptide maps. Furthermore, since fractions from the entire chromatogram are collected, other protease-derived fragments are available for analysis if desired. We first present data using synthetic peptides of known composition as test samples to validate the procedure and then demonstrate that the overall method can be used to positively isolate the target fragment from proteolytic digests of three distinct proteins of known sequence. The strategy outlined in this report should be applicable to proteins with other N-terminal modifications, for the quality control of recombinant proteins, and in studies of homologous proteins from different sources.

EXPERIMENTAL

Chemicals and reagents

Peptides and proteins were purchased from Sigma (St. Louis, MO, USA) or Peninsula Labs. (Belmont, CA, USA) and used without further purification. For use, they were resuspended to a nominal concentration of 1–3 mg/ml with water or 0.1% trifluoroacetic acid (TFA) and stored at -20°C . Pierce (Rockford, IL, USA) supplied phenylisothiocyanate (PITC), triethylamine (TEA), TFA, and 8 M guanidinium chloride (GdmCl); succinic anhydride is a Fluka (Ronkonkoma, NY, USA) product; and chymotrypsin was obtained from Boehringer Mannheim (Indianapolis, IN, USA). Recovery studies used [^3H]leucine-enkephalin, 36.3 Ci/mmol, purchased from DuPont/NEN (Boston, MA, USA). The sources of HPLC columns and solvents, water purification, and additional materials have been described [19,20].

Succinylation

Slight modifications to established procedures were employed [5]. Amounts of 10–100 μg of the stock protein solution were taken to dryness in a Savant (Farmingdale, NY, USA) Speed-Vac, after which 200 μl of 0.1 M NH_4HCO_3 and 200 μl of 8 M GdmCl were added to the dried sample. The pH was adjusted to *ca.* 8 with 12% (v/v) TEA (*ca.* 20 μl) and then 0.5 mg of solid succinic anhydride added to the vial to start the reaction. The pH was monitored and maintained

between 8–9 by adding 20 μl aliquots of 12% TEA. After 30 min at room temperature, another portion of succinic anhydride was added and the reaction pH monitored as above, resulting in a final added TEA volume of *ca.* 200 μl . The mixture was incubated overnight at room temperature. Any remaining succinic anhydride was converted to succinic acid by adding 100 μl of 10% (v/v) TFA and the sample was transferred to a Millipore Ultrafree-MC 5000MW tube (Millipore, Boston, MA, USA) for spin-dialysis and solvent exchange (0.1 M $\text{NH}_4\cdot\text{HCO}_3$) at 10 000 rpm in a microfuge.

Proteolysis

Prior to digestion, the volume of the protein substrate was increased to *ca.* 140 μl with 0.1 M NH_4HCO_3 . A 10- μl volume of chymotrypsin at 0.5 mg/ml in water was added and the digestion mixture incubated for 4 h at 37°C . The reaction was quenched by adding 5 μl of 10% TFA and if desired, a small aliquot of this sample was injected on C_{18} RP-HPLC as the control (–PITC), with the remainder transferred to a Varian (Walnut Creek, CA, USA) 9090 auto-sampler conical vial and taken to dryness in a Savant speed-vac.

Automated PITC derivatization

To the dried, digested protein sample or dried synthetic peptide, were added 18 μl of ethanol–TEA–water (7:1:1, v/v/v) followed by 2 μl PITC. The liquids were mixed by four air displacement cycles and the reaction mixture was incubated for 20 min at room temperature [18]. Excess PITC and unwanted reaction by-products were extracted [18] by adding 90 μl heptane–ethyl acetate (2:1, v/v), after which 70 μl of 10 mM sodium phosphate pH 6.0 was added to increase the volume of the aqueous phase. The extraction liquid (90 μl heptane–ethyl acetate only) was added in two more portions and 75 μl of the aqueous layer were injected on C_{18} RP-HPLC.

RP-HPLC on-line photodiode array (PDA) analysis

Samples were chromatographed using standard RP-HPLC conditions (C_{18} Vydac 218TP54; solvent A is 0.1% TFA and solvent B is 0.095%

TFA in acetonitrile–water (90:10); 10% B to 60% B in 60 or 90 min at 1 ml/min and 37°C with fractions collected at 0.5-min intervals). On-line PDA analysis with a Varian Polychrom 9065 was used to identify the Ac-N-terminal fragment by the absence of phenylthiocarbonyl (PTC)-associated UV spectrum with the LC Star Polyview software library search routine supplied with the instrument. Basically, UV spectra (210–297 nm) of synthetic peptides containing known chromophores (aromatics, aromatics + PTC-peptide, PTC-peptide, and peptide only) are stored in the search library [21]. The chromatogram of the PITC derivatized, digested protein is then searched peak-by-peak against all spectra in the library to generate statistically relevant similarity indices for each peak. Positive matches of known fragments typically give values of 0.995 or greater. In this study, we are interested in that peak which is devoid of PTC attributes. In addition, this peak will not shift in retention time compared to the control (–PITC) chromatogram and is easily spotted in the three-dimensional PDA printout for the +PITC sample. Note also, that it is possible to tentatively assign the aromatic content of each peak through the library search routine. Data acquisition and analysis procedures, and additional chromatographic hardware have been described [19,20].

Analysis of RP-HPLC fractions

An aliquot of the desired fraction was subjected to standard 6 *m* HCl–Phenol hydrolysis for 1 h at 150°C and the hydrolysate manually derivatized with PITC for analysis [18]. Another aliquot was taken to dryness and resuspended in 15–30 μ l of 1% (v/v) NH₄OH prior to negative-ion electrospray (ES)–MS on a Sciex (Thornhill, Canada) API-III instrument (Dr. Kevin Duffin, Monsanto Corporate Research, St. Louis, MO, USA).

RESULTS AND DISCUSSION

Assessment of the procedure with synthetic peptides

Synthetic peptides were used as test substances to validate several steps of the overall process. Specifically, the peptides were subjected to automated PITC derivatization and RP-HPLC–PDA

analysis. For PITC modification both the completeness and specificity of the reaction were investigated. In addition, [³H]leucine-enkephalin provided a means of determining the recovery of the derivatized PTC-peptide after the heptane–ethyl acetate extraction procedure. In this case, greater than 97% of the tritiated peptide remained in the aqueous phase; a new RP-HPLC peak appeared with an increased retention time and less than 0.4% of the unreacted peptide was observed (data not shown).

Fig. 1 is a composite set of three-dimensional PDA chromatograms for DRVYIHPFLLVYS with either a “free” or acetylated N-terminus (panels A and B, respectively) and for pEQRLGNWAVGHLM(NH₂) and the lysine-3 [K³]-substituted peptide (panels C and D, respectively). Comparison of the PDA UV profile for the first peptide pair, –PITC (Fig. 1A) and +PITC (Fig. 1B), shows that covalent addition of PTC to “free” amines results in a retention time shift [17] and an augmented, distinct, and readily identifiable 210–297 nm spectrum for the derivatized species. Just as revealing, is the absence of a chromatographic shift and spectral change for the Ac-N-terminal peptide. This demonstrates the ability to identify PTC-peptides that contain aromatic residues in combination with non-PTC, aromatic containing, Ac-N-terminal peptides. The PTC chromophore of the adduct in this case dominates the 240–297 nm profile. The second peptide pair comprises species that are identical in every respect except for an arginine to lysine substitution at sequence position 3 ([R³] to [K³]). Each peptide is also blocked at the N-terminus in the form of a pyroglutamyl (pE) group so that only the [K³] variant is expected to react with PITC. These two peptides are not resolved by the standard C₁₈ RP-HPLC elution conditions (Fig. 1C), and as for the former test peptide pair, these pE-blocked peptides contain an even more intense aromatic-region absorbing residue, tryptophan. Nonetheless, the expected result is evident as the [K³] peptide increases in RP-HPLC retention time after PTC modification concomitant with a characteristic UV spectrum for this product (Fig. 1D). PTC modification of the [K³] variant produced a complete separation of this peptide pair where there originally was none.

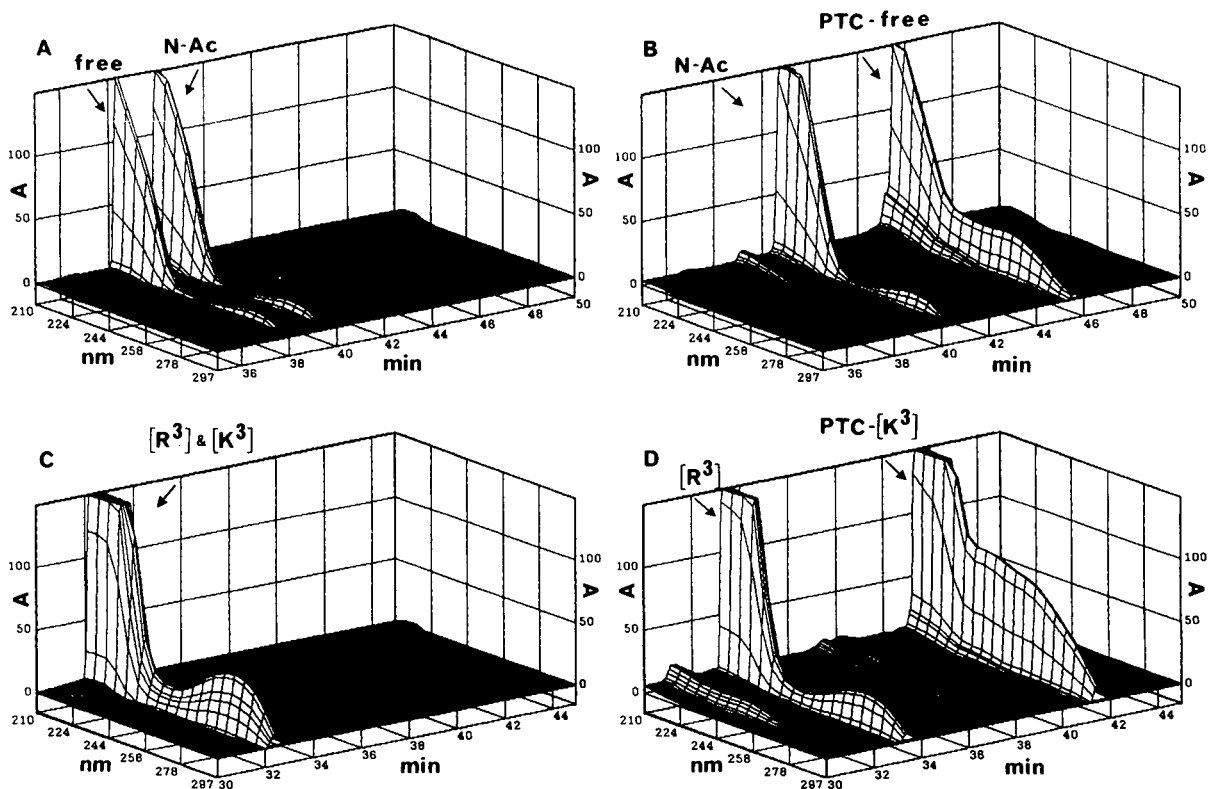


Fig. 1. C_{18} RP-HPLC of N-Ac and "free" renin substrate tetradecapeptide, and $[R^3]$ -Bombesin and $[K^3]$ -Bombesin. Three-dimensional PDA chromatogram of the mixtures displayed at the relevant retention times. (A) "Free" and N-Ac DRVYIHPFHLVYS mixture minus PITC at 150 mV full scale (mVFS); (B) "free" and N-Ac DRVYIHPFHLVYS mixture plus PITC at 150 mVFS; (C) $[R^3]$ - and $[K^3]$ -pEQRLGNWAVGHLM(NH_2) mixture minus PITC at 150 mVFS; (D) $[R^3]$ - and $[K^3]$ -pEQRLGNWAVGHLM(NH_2) mixture plus PITC at 150 mVFS. The HPLC gradient was for 60 min.

Assessment of the procedure with proteins and protein fragments

Three Ac-N-terminally blocked proteins of known sequence, calmodulin, cytochrome *c* and parvalbumin were subjected to each step of the overall procedure. The first step involves protein denaturation with GdmCl and succinylation of lysine residues. This is necessary because the desired N-terminal fragment may contain lysine residues which would react with PITC and thus produce a false negative assignment. For the present group of test proteins, cytochrome *c* and parvalbumin do contain lysine residues in the N-terminal fragment but calmodulin does not. Practically, this means for calmodulin succinylation can be omitted if one is interested in isolating the Ac-N-terminal fragment only. Several fragments will however, likely contain multi-

ple PTC reaction sites in the form of lysine residues. This streamlined process could be useful for example in isolating the blocked N-terminal, lysine deficient fragment from homologous proteins and then sequencing by the appropriate means. We were able to isolate the same proteolytic Ac-N-terminal peptide from calmodulin whether or not the protein was succinylated (data not shown).

Proteolytic digestion of the succinylated protein was the next step and in the majority of our reactions chymotrypsin was used. This was not an arbitrary choice on our part, and derives from the known primary specificity of chymotrypsin for aromatic residues. We wanted to minimize the possibility that the Ac-N-terminal peptide would contain multiple aromatic amino acids thereby obfuscating the UV spectral analysis.

The fact that for all three proteins the Ac-N-terminal fragment contained only one aromatic amino acid which was the C-terminal residue (see Tables I and II) speaks favorably for the above rationale.

A Varian 9090 autosampler with robotic automix routines was used previously to automate PITC derivatization of amino acid hydrolysates and liberated residues from exopeptidase digestions [18]. In that study, a heptane extraction step effectively removed excess PITC and reaction by-products from the aqueous sample prior to HPLC injection. For the present study, an empirically determined 2:1 ratio of heptane-ethyl acetate was found to be a compromise between high peptide recovery and acceptable removal of unwanted reaction products. Another aspect of the automated derivatization reaction is

TABLE I

AMINO ACID ANALYSIS OF THE ISOLATED Ac-N-TERMINAL PROTEOLYTIC FRAGMENTS

The fragments were isolated as indicated from the PDA chromatograms shown in Figs. 2–4.

Residue ^a	Protein					
	Calmodulin		Cytochrome <i>c</i>		Parvalbumin	
	Obs.	Exp.	Obs.	Exp.	Obs.	Exp.
Asx	1.0	1	1.0	1	1.8	2
Glx	4.4	5	1.1	1	2.0	2
Gly ^b	–	–	2.6	2	1.9	1
Thr ^c	1.1	1	–	–	1.5	1
Ala	2.1	2	–	–	4.0	4
Val	–	–	1.0	1	–	–
Met ^c	–	–	–	–	0.12	1
Ile	1.1	1	1.0	1	2.0	2
Leu	1.1	1	–	–	1.8	2
Phe	1.0	1	1.1	1	1.1	1
Lys ^b	–	–	2.4	3	1.7	2

^a The standard three letter code is used for the amino acids and the experimentally observed (Obs.) and the expected (Exp.) residue values for the predicted Ac-N-terminal fragment are listed.

^b Gly values are high and Lys values low due to incomplete hydrolysis of PTC-succinyl-Lys and co-elution of this derivative with PTC-Gly.

^c Met was oxidized to Met-sulfoxide during the hydrolysis. The *R* and *S* forms of PTC-Met-sulfoxide elute near PTC-Thr in our system, resulting in an inflated value for Thr.

that the free amino groups of the proteolytic fragments appeared to be quantitatively modified with PITC. This result derives from the observation that the peaks in the PDA chromatogram exhibit characteristic PTC spectral properties except for the blocked N-terminal fragment (see below).

Isolation and identification of C₁₈ RP-HPLC Ac-N-terminal proteolytic fragments

Calmodulin, cytochrome *c* and parvalbumin were each succinylated prior to protease treatment with chymotrypsin. After digestion, the resulting proteolytic fragments were reacted with PITC in an automated fashion and these modified samples were analyzed by C₁₈ RP-HPLC with on-line PDA spectroscopy (Figs. 2–4).

The three-dimensional PDA spectral plot of the +PITC C₁₈ RP-HPLC analysis for the calmodulin digest is shown in Fig. 2. Panel A represents the relevant chromatographic region from 15 to 55 min. The characteristic UV spectra of the PTC-adducts observed for the synthetic peptides (Fig. 1B and D) are readily apparent here also. Time axis expansion of panel A to 15 to 35 min (panel B) and 35 to 55 min (panel C) aided in the visual assignment of the N-terminal peptide. Simple inspection of these two plots allows one to immediately assign the peak at *ca.* 32 min (panel B, arrow) as the target fragment. The fraction containing this peak was subjected to amino acid analysis and negative-ion ES-MS to positively identify the peptide fragment. Table I lists the amino acid results for the calmodulin fraction. The agreement between the expected residues for the predicted Ac-N-terminal chymotryptic fragment of calmodulin with the experimentally determined values is good. ES-MS analysis of this fraction produced a clean spectrum (see Fig. 5A) with the tabulated molecular mass listed in Table II. These combined data (Tables I and II) unequivocally demonstrate that the fraction isolated from the three-dimensional PDA plot is the Ac-N-terminal chymotryptic fragment of calmodulin.

A similar representation of the three-dimensional PDA +PITC proteolytic digest chromatograms are shown for cytochrome *c* in Fig. 3 and for parvalbumin in Fig. 4. Again, time axis

TABLE II
MOLECULAR MASS ASSIGNMENT OF THE ISOLATED Ac-N-TERMINAL PROTEOLYTIC FRAGMENTS

The fragments were isolated as indicated from the PDA chromatograms shown in Figs. 2–4.

Predicted chymotryptic fragments

Calmodulin	N-Ac-Ala-Asp-Gln-Leu-Thr-Glu-Glu-Gln-Ile-Ala-Glu-Phe. Calculated $M_r = 1434.7$.
Cytochrome <i>c</i>	N-Ac-Gly-Asp-Val-Glu-Lys(X)-Gly-Lys(X)-Lys(X)-Ile-Phe. Calculated $M_r = 1461.7$. Lys(X) = succinyl-Lys.
Parvalbumin	N-Ac-Ala-Met-Thr-Glu-Leu-Leu-Asn-Ala-Glu-Asp-Ile-Lys(X)-Lys(X)-Ala-Ile-Gly-Ala-Phe. Calculated $M_r = 2176.1$. Lys(X) = succinyl-Lys.

ES-MS analysis of fragments^a

Protein	Mass peaks ^b	Species/charge	Observed M_r
Calmodulin	716.2	$(M - 2H^+)^{2-}$	1434.4
	727.4	$(M - 3H^+ + Na^+)^{2-}$	1434.8
	738.3	$(M - 4H^+ + 2Na^+)^{2-}$	1434.0
	1433.3	$(M - H^+)^-$	1434.3
	1455.6	$(M - 2H^+ + Na^+)^-$	1434.6
	Average		1434.5
Cytochrome <i>c</i>	486.2	$(M - 3H^+)^{3-}$	1461.6
	730.1	$(M - 2H^+)^{2-}$	1462.2
	741.0	$(M - 3H^+ + Na^+)^{2-}$	1462.0
	1460.8	$(M - H^+)^-$	1461.8
	1482.8	$(M - 2H^+ + Na^+)^-$	1461.8
	Average		1461.9
Parvalbumin	1087.3	$(M - 2H^+)^{2-}$	2176.6
	1144.1	$(M - H^+ + CF_3COO^-)^{2-}$	2176.2
	Average		2176.4

^a See Fig. 5 for the mass spectrum of each protein fragment.

^b The peaks were assigned as shown in Fig. 5A, calmodulin; B, cytochrome *c*; and C, parvalbumin.

expansion of the cytochrome *c* example (Fig. 3), originally displayed from 15 to 55 min (panel A), to 15 to 35 min (panel B) and 35 to 55 min (panel C) was used to identify the N-terminal fragment. Amino acid analysis of the isolated fraction at *ca.* 31 min (panel B, arrow) resulted in coincident values for the experimental and predicted residue compositions of the N-terminal fragment (Table I). This predicted chymotryptic peptide contains three Lys residues (Table II) which if not succinylated would yield a chromatographic species with a PDA UV spectrum characteristic of a PTC-peptide. The actual PDA UV spectrum containing the isolated fraction is

devoid of PTC attributes suggesting that this fragment is completely succinylated. The amino acid composition (Table I) supports this assertion but the definitive data in this case are derived from ES-MS analysis (see Fig. 5B). Molecular mass assignments for the mass peaks from this analysis given in Table II clearly indicate that the isolated fraction contains a completely succinylated species. The protease derived fragment under consideration is thus positively identified as the succinylated Ac-N-terminal chymotryptic fragment of cytochrome *c*.

Fig. 4A is an analogous C_{18} RP-HPLC-PDA

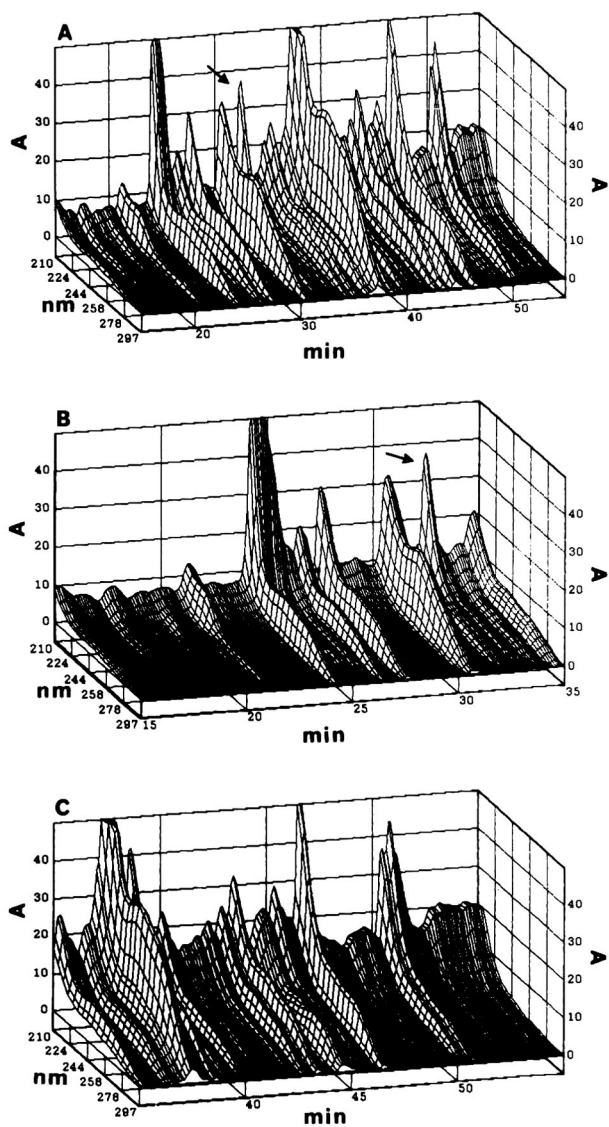


Fig. 2. C_{18} RP-HPLC-PDA three-dimensional display of the chymotryptic digest of calmodulin. (A) Chromatogram from 15 to 55 min, 210 to 297 nm at 50 mVFS; (B) expanded time axis from 15 to 35 min; (C) expanded time axis from 35 to 55 min. The arrow in A and B indicates the isolated Ac-N-terminal proteolytic fragment of calmodulin. The HPLC gradient was for 60 min.

three-dimensional profile of the region of interest at 20 to 80 min for the parvalbumin chymotryptic digest. This complex plot was expanded on the time axis into visually manageable blocks (panels B–D). The data in these three panels readily show the presence of many PTC-

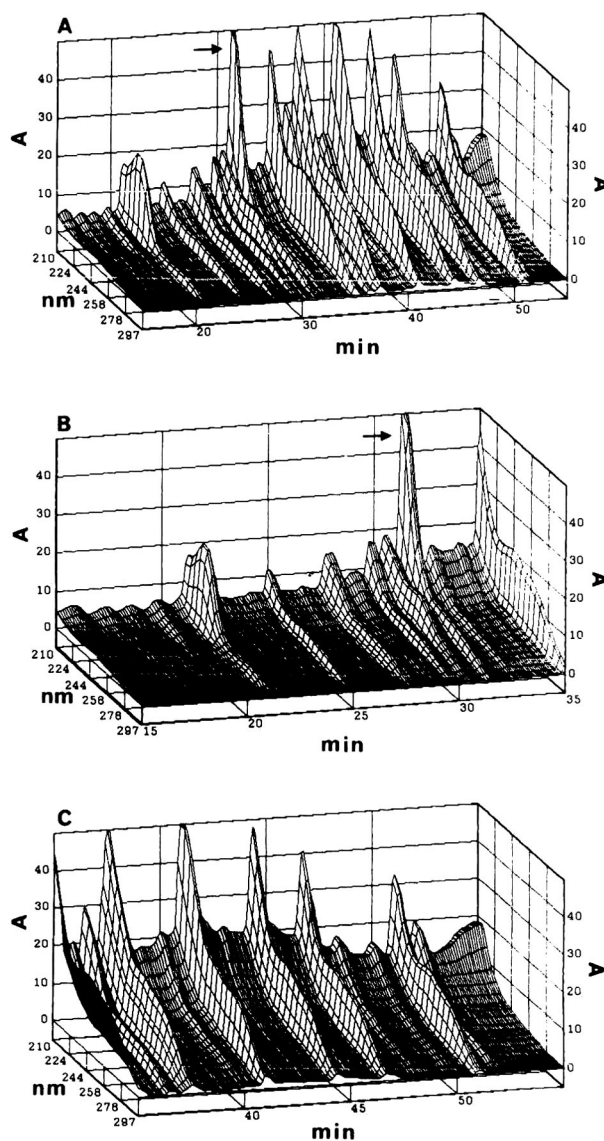


Fig. 3. C_{18} RP-HPLC-PDA three-dimensional display of the chymotryptic digest of cytochrome *c*. (A) Chromatogram from 15 to 55 min, 210 to 297 nm at 50 mVFS; (B) expanded time axis from 15 to 35 min; (C) expanded time axis from 35 to 55 min. The arrow in A and B indicates the isolated Ac-N-terminal proteolytic fragment of cytochrome *c*. The HPLC gradient was for 60 min.

peptide peaks, some of which additionally contain identifiable aromatic residues [21]. In this current study though, attention is focused on the triplet set of peaks near *ca.* 70 min (panel D, arrow). The latest eluting peak of this triplet group did not exhibit signature PTC UV spectral

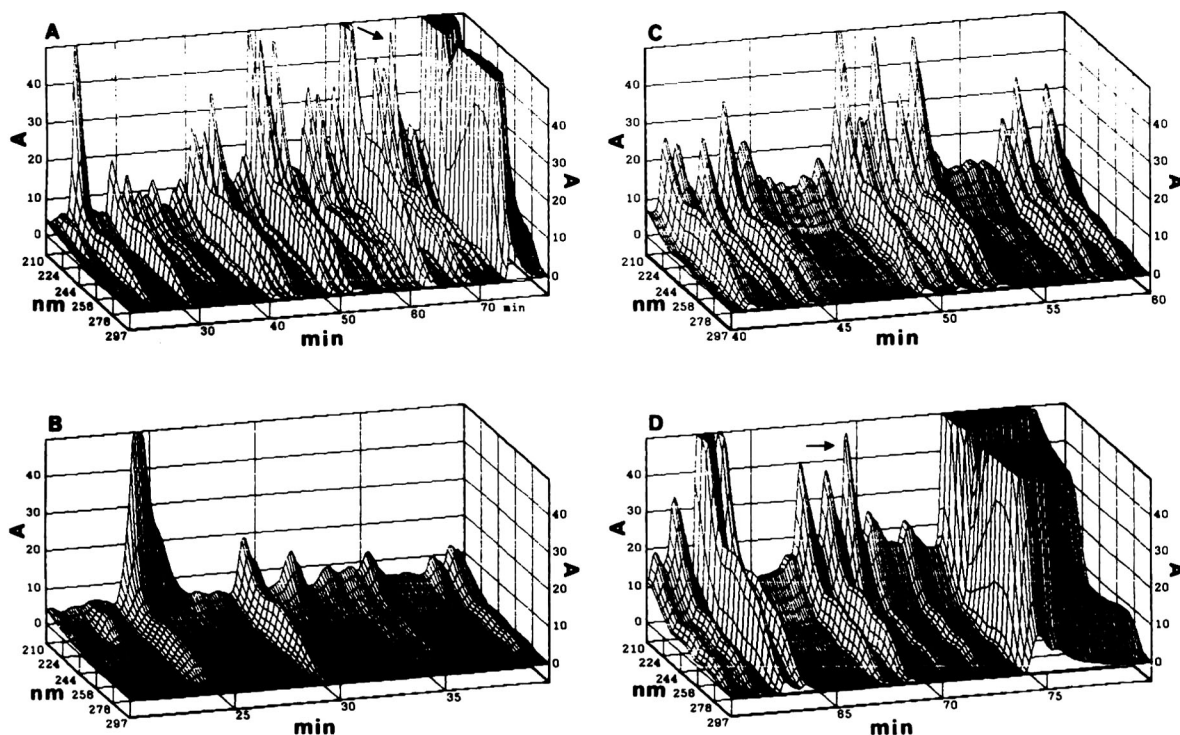


Fig. 4. C_{18} RP-HPLC-PDA three-dimensional display of the chymotryptic digest of parvalbumin. (A) Chromatogram from 20 to 80 min, 210 to 297 nm at 50 mVFS; (B) expanded time axis from 20 to 40 min; (C) expanded time axis from 40 to 60 min; (D) expanded time axis from 60 to 80 min. The arrow in A and D indicates the isolated Ac-N-terminal proteolytic fragment of parvalbumin. The HPLC gradient was for 90 min.

properties and was therefore selected for further analysis. The residue composition of this fraction was assessed from amino acid analysis (Table I) and was found to be consistent with the expected residue values. ES-MS analysis produced an acceptable spectrum (Fig. 5C) for which the species molecular mass of the indicated mass peaks were calculated and listed in Table II. Two Lys residues are present in the predicted Ac-N-terminal chymotryptic fragment of parvalbumin. A similar line of reasoning as expressed in the cytochrome *c* case, when applied here, results in the conclusion that the isolated parvalbumin peptide is the completely succinylated Ac-N-terminal chymotryptic peptide. One other aspect of the parvalbumin chromatogram is that the late C_{18} RP-HPLC elution of the N-terminal peptide could have been anticipated due to its high ratio (10:18) of hydrophobic amino acids and overall length.

We calculated the overall recovery for each proteolytic digest. This percentage is defined as the moles of the isolated Ac-N-terminal peptide fraction recovered from the PDA chromatogram relative to the initial moles of protein subjected to the four step procedure. These values were fairly constant for all three proteins, ranging from a high of 49% for cytochrome *c* to a low of 29% for parvalbumin. The recovery for calmodulin was intermediate at 42%. Several likely factors contributed to the ultimate recovery of the blocked peptide. These include: completeness of the succinylation step, recovery of these modified proteins after spin-dialysis and solvent exchange, the extent of protease digestion, and any losses due to the C_{18} RP-HPLC itself. In this initial investigation we did not attempt to optimize these individual processes for each protein but rather, sought to develop a scheme which we believe will have general applications. Clearly,

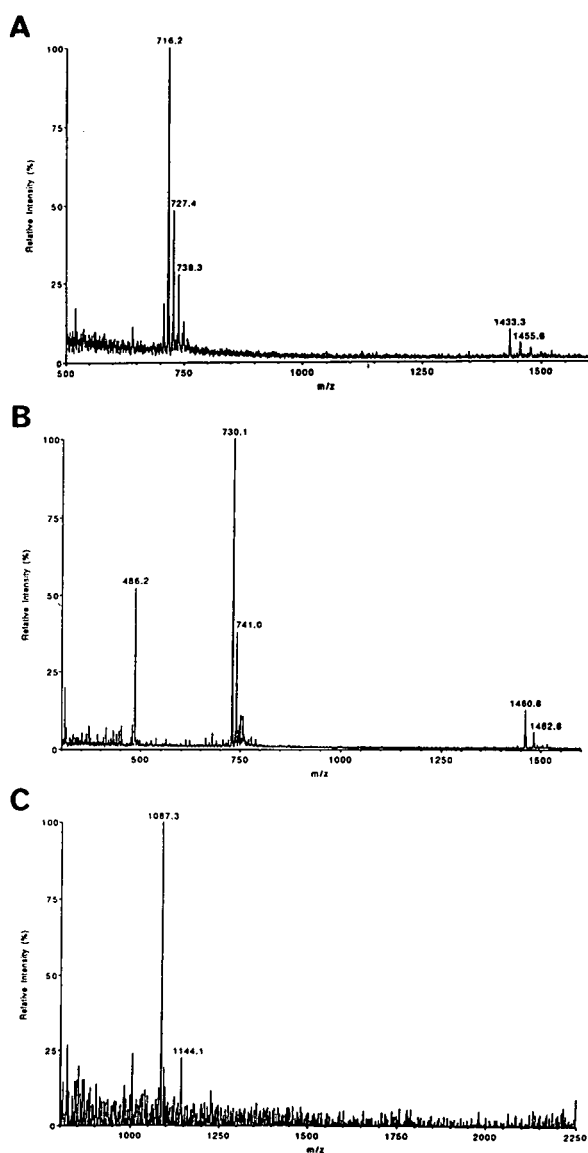


Fig. 5. ES-MS analysis of the isolated Ac-N-terminal proteolytic fragments from calmodulin, cytochrome *c* and parvalbumin. Spectra were recorded in the negative-ion mode. The species and charge states of the mass peaks, and the resulting molecular masses are listed in Table II. (A) Calmodulin fragment isolated from PDA chromatogram (Fig. 2); (B) cytochrome *c* fragment isolated from PDA chromatogram (Fig. 3); (C) parvalbumin fragment isolated from PDA chromatogram (Fig. 4).

each step could be selectively optimized for a given protein to increase the overall recovery of the isolated Ac-N-terminal fragment.

CONCLUSIONS

The blocked N-terminal peptide identification strategy presented in this report was successfully applied to complex proteolytic digests for the HPLC isolation of the Ac-N-terminal peptide from three distinct proteins. Since all HPLC peaks were collected in this procedure, they could be analyzed with the net result being an increase in HPLC information content.

On-line PDA spectroscopy provided some analytical advantages over conventional single or dual-wavelength detection. It was not absolutely necessary for instance, to perform a -PITC HPLC experiment for comparative purposes. This was evident from inspection of the PDA plot as the N-terminal peptide showed distinct (non-PTC) UV spectral properties. Preliminary work [21] indicates that as an added bonus, both the aromatic residue type and number can be assigned to several of the PTC-peptide peaks. We are currently [22] implementing the semi-automated strategy to develop an analogous C-terminal proteolytic fragment isolation procedure based on a variation of several C-terminal peptide isolation schemes [23–27]. It is anticipated that successful application of each, coupled with say MS-MS sequencing [28,29], would provide a novel and powerful polymerase chain reaction “anchoring” process.

ACKNOWLEDGEMENTS

We are grateful to Varian Instruments (John Simpson, Mari Wooldridge, Ron Lewis, Mark Johnson, Neil Lander and Maureen Joseph) for the loan of and the technical support for the Polychrom 9065 PDA system. We sincerely appreciate then efforts of Dr. Kevin Duffin for ES-MS analysis and data interpretation, Mr. Ned Siegel for his interest in this work, and Mr. Gary Lange for preliminary discussions (Monsanto Corporate Research).

REFERENCES

- 1 J. Brown and W. Roberts, *J. Biol. Chem.*, 251 (1976) 1009–1014.

- 2 D. Wellner, C. Panneerselvam and B. Horecker, *Proc. Natl. Acad. Sci. U.S.A.*, 87 (1990) 1947–1949.
- 3 W. Jones, L. Manning and J. Manning, *Biochem. Biophys. Res. Commun.*, 139 (1986) 244–250.
- 4 T. Farries, A. Harris, D. Auffret and A. Aitken, *Eur. J. Biochem.*, 196 (1991) 679–685.
- 5 R. Krishna, C. Chin and F. Wold, *Anal. Biochem.*, 199 (1991) 45–50.
- 6 R. Krishna, in R. Houge-Angeletti (Editor), *Techniques in Protein Chemistry III*, Academic Press, San Diego, CA, 1992, pp. 77–84.
- 7 R. Krishna and F. Wold, *Prot. Sci.*, 1 (1992) 582–589.
- 8 *Methods for N-Terminal Sequence Analysis of N-Terminally Blocked Proteins; Technical Guide 1*, Takara Biochemical, Berkeley, CA, 1992.
- 9 K. Eckhart, H. Schwarz, M. Chorev and C. Gilon, *Eur. J. Biochem.*, 157 (1986) 209–216.
- 10 K. Biemann, *Biomed. Environ. Mass Spectrom.*, 16 (1988) 99–111.
- 11 B. Gibson, Z. Yu, B. Gillece-Castro, W. Aberth, F. Walls and A. Burlingame, in T. Hugli (Editor), *Techniques in Protein Chemistry*, Academic Press, San Diego, CA, 1989, pp. 135–151.
- 12 J. Gorman, G. Corino and B. Shiell, *Biomed. Environ. Mass Spectrom.*, 19 (1990) 646–654.
- 13 B. Egestad, M. Estonius, O. Danielsson, B. Persson, E. Cederlund, R. Kaiser, B. Holmquist, B. Vallee, X. Pares, J. Jefferey and H. Jornvall, *FEBS Lett.*, 269 (1990) 194–196.
- 14 J. Smith, G. Thevenon-Emeric, D. Smith and B. Green, *Anal. Biochem.*, 193 (1991) 118–124.
- 15 D. Hunt, J. Alexander, A. McCormack, P. Martino, H. Michel, J. Shabanowitz, N. Sherman, M. Moseley, J. Jorgenson and K. Tomer, in J. Villafranca (Editor), *Techniques in Protein Chemistry II*, Academic Press, San Diego, CA, 1991, pp. 441–454.
- 16 H. Hirano, S. Komatsu, H. Takakura, F. Sakiyama and S. Tsunasawa, *J. Biochem.*, 111 (1992) 754–757.
- 17 F. Colilla, S. Yadav, K. Brew and E. Mendez, *J. Chromatogr.*, 548 (1991) 303–310.
- 18 R. Thoma and D. Crimmins, *J. Chromatogr.*, 537 (1991) 153–165.
- 19 D. Crimmins, J. Gorka, R. Thoma and B. Schwartz, *J. Chromatogr.*, 443 (1988) 63–71.
- 20 D. Crimmins, R. Thoma, D. McCourt and B. Schwartz, *Anal. Biochem.*, 176 (1989) 255–260.
- 21 D. Crimmins, R. Thoma and M. Joseph, in preparation.
- 22 R. Thoma and D. Crimmins, in preparation.
- 23 P. Hargrave and F. Wold, *Int. J. Peptide Protein Res.*, 5 (1973) 85–89.
- 24 T. Isobe, T. Ichimura and T. Okuyama, *Anal. Biochem.*, 155 (1986) 135–140.
- 25 L. Johnson and G. Tarr, in K. Walsh (Editor), *Methods of Protein Sequence Analysis —1986*, Humana Press, Clinton, NJ, 1987, pp. 351–358.
- 26 K. Ikura, H. Yokota, R. Sasaki and H. Chiba, *Biochemistry*, 28 (1989) 2344–2348.
- 27 J. Dixon, B. Gildea and J. Coull, presented at the 6th Symposium of The Protein Society, San Diego, CA, July 25, 1992, abstract T93.
- 28 K. Biemann, *Ann. Rev. Biochem.*, 61 (1992) 977–1010.
- 29 A. Tsugita, K. Takamoto, M. Kamo and H. Iwadata, *Eur. J. Biochem.*, 206 (1992) 691–696.

Separation of isomeric compounds by reversed-phase high-performance liquid chromatography using Ag^+ complexation

Application to *cis*–*trans* fatty acid methyl esters and retinoic acid photoisomers

A. Baillet*, L. Corbeau, P. Rafidison and D. Ferrier

Centre d'Études Pharmaceutiques, Laboratoire de Chimie Analytique, Rue J.B. Clément, F-92296 Chatenay-Malabry Cédex (France)

(First received January 17th, 1992; revised manuscript received December 10th, 1992)

ABSTRACT

The improvement of the chromatographic efficiency using Ag^+ complexing reversed-phase liquid chromatography for the analysis of geometric isomers was studied. The influence of the nature and concentration of silver salts on π -complex formation was investigated with two types of sample, fatty acid methyl esters and *trans*-retinoic acid photoisomers. First, the separations of *cis*–*trans*-linoleic acids and *cis*–*trans*-oleic acids were confirmed. Second, the π -complexation was shown to occur with more complex chemical structures such as *trans*-retinoic acid and its photoisomers. The chromatographic separation of seven geometric isomers of *trans*-retinoic acid was then carried out with good efficiency in half the time required in previous work.

INTRODUCTION

Argentation chromatographic methods are useful for the analysis of unsaturated compounds. Many publications have described the use of metal ions to improve the separation of analytes by thin-layer chromatography [1], gas-liquid chromatography [2] and high-performance liquid chromatography (HPLC) [3], especially for *cis*–*trans* geometric isomers [1,4–6].

First, silver ion complexing liquid chromatography was performed using adsorption chromatographic systems with silica gel impregnated with various amounts of silver salts as stationary

phases [7,8]. This technique was then transposed successfully to reversed-phase liquid chromatographic systems for the separation of various compounds such as vitamin D, estrogenic derivatives, unsaturated hydrocarbons, triglycerides and fats [9–11], but a strong interaction takes place in the mobile phase. It was shown previously [9] that the presence of a silver salt in the mobile phase leads to the formation of a π -complex. The bonding is considered to involve an interaction between very electrophilic silver ions and filled π orbitals of unsaturated compounds.

Two conclusions on the behaviour of π -complexes in reversed-phase liquid chromatography were drawn by Schomburg and co-workers [10,11]: the polarity of the Ag^+ π -complex is

* Corresponding author.

higher than the polarity of the initial compound, so its elution is quicker and a decrease in its capacity factor is observed with silver salt in the mobile phase; and the retention times depend on the number, type and position of the unsaturations, according to the complexation equilibrium constants. *Cis* complexes, generally more stable than *trans* complexes, show a greater affinity with the mobile phase and elute earlier. This explains the high separation efficiencies observed with argentation chromatographic systems in the analysis of geometric isomers.

In this study, we first confirmed the previously published data on the chromatographic separation of fatty acid isomers. We then investigated the potential of this method for improving the separation of photoisomers of retinoic acid. The photodegradation of *trans*-retinoic acid leads to the formation of numerous isomers. Until now, their separation has been carried out by reversed-phase liquid chromatography [12–16], but the methods showed poor resolution and/or very long analysis times. With regard to the presence of conjugated double bonds in the structure of retinoic acid, we also studied the behaviour of the *cis*–*trans* isomer mixture in argentation liquid chromatography and the benefits obtained in terms of resolution and analysis time.

EXPERIMENTAL

Chemicals

Fatty methyl esters and silver and potassium salts were purchased from Sigma (La Verpillière, France). *trans*-Retinoic acid was kindly donated by Laboratories Roche (Neuilly sur Seine, France). HPLC-grade methanol was purchased from Prolabo (Paris, France) and perchloric acid from Merck (Nogent sur Marne, France). Water for HPLC was doubly distilled.

The photoisomers of retinoic acid were obtained by irradiation of a 0.05 g per 100 ml solution of *trans*-retinoic acid in ethanol solution. Aliquots of 5 ml of this solution were poured into a Pyrex crystallizing dish (50 mm diameter), then irradiated with a Biotronic UV crystallizing

dish (50 mm diameter), then irradiated with a Biotronic UV system (Vilber Lourmat, Torcy, France) controlled by a microcomputer. Irradiations were performed at 365 nm (UVA) and 312 nm (UVB) simultaneously.

HPLC of fatty acid methyl esters

The chromatograph consisted of a solvent-delivery pump from Altex (Touzart et Matignon, Vitry sur Seine, France), a Rheodyne injection valve (20- μ l loop), a Shimadzu SPD-2A variable-wavelength detector (Touzart et Matignon) operating at 210 nm and a Kipp & Zonen BD-40 recorder (Cunow, Cergy St. Christophe, France). The column was 300 mm \times 4 mm I.D. stainless-steel packed with Nucleosil C₁₈ stationary phase (7 μ m particle size) from Touzart et Matignon. The initial eluent was methanol–water–perchloric acid (85:15:0.01, v/v/v) with the addition of either silver perchlorate (concentration range $1 \cdot 10^{-4}$ – $5 \cdot 10^{-3}$ M) or potassium perchlorate (concentration range $1 \cdot 10^{-4}$ – $1 \cdot 10^{-3}$ M). These mobile phases were degassed by sonication and filtered through a 0.22- μ m membrane (Millipore, St. Quentin en Yvelines, France). The flow-rate was set at 1 ml min⁻¹.

HPLC of retinoic acid isomers

HPLC was performed using a Knauer pump (Cunow) equipped with a Rheodyne injection valve (5- μ l loop). Detection was carried out with a Shimadzu SPD-2A variable-wavelength detector (Touzart et Matignon) set at 345 nm and connected with a Perkin-Elmer (Z.I. de Courtaboeuf, France) LCI 100 computing integrator. A column (150 mm \times 4.6 mm I.D.) packed with a Spherisorb ODS-2 stationary phase (3 or 5 μ m particle size) from SFCC (Neuilly Plaisance, France) was used. The mobile phases consisted of methanol–water–perchloric acid (80:0:0.02, v/v/v) containing either a silver salt (nitrate or perchlorate) (concentration range $1 \cdot 10^{-3}$ – $5 \cdot 10^{-2}$ M) or a potassium salt (nitrate or perchlorate) (concentration range $1 \cdot 10^{-3}$ – $5 \cdot 10^{-2}$ and $1 \cdot 10^{-3}$ – $1 \cdot 10^{-2}$ M, respectively). The flow-rate was set at 1 ml min⁻¹.

RESULTS AND DISCUSSION

 π -Complex formation

The effectiveness of π -complexation was demonstrated by comparing the behaviour of saturated and unsaturated fatty acid methyl esters with silver salts and by comparing the behaviour of the retinoic acid photoisomers with both potassium and silver salts. The chemical structures are illustrated in Fig. 1.

Fig. 2 shows the variation of the capacity factors of the saturated and unsaturated fatty acid methyl esters with the silver perchlorate concentration in the mobile phase. At low concentrations ($<10^{-3}$ M) no significant change is observed in the capacity factors for either saturated or unsaturated compounds. Indeed, the ionic strength remains very weak. Using silver perchlorate concentrations higher than 10^{-3} M in the mobile phase, a significant decrease in the capacity factors is observed for unsaturated compounds since the retention times of saturated

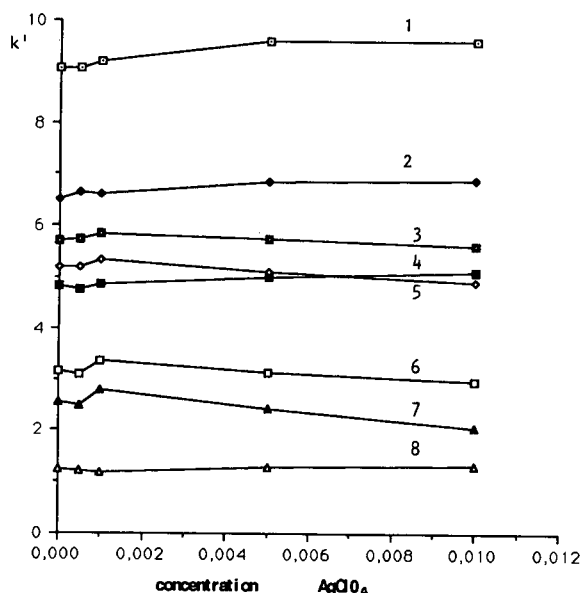


Fig. 2. Effect of the silver perchlorate concentration in the mobile phase on the capacity factors of unsaturated and saturated fatty acid methyl esters: 1 = methyl stearate; 2 = methyl heptadecanoate; 3 = methyl *trans*-9-octadecenoate; 4 = methyl palmitate; 5 = methyl oleate; 6 = methyl *trans*-9,*trans*-12-octadecadienoate; 7 = methyl linoleate; 8 = methyl laurate.

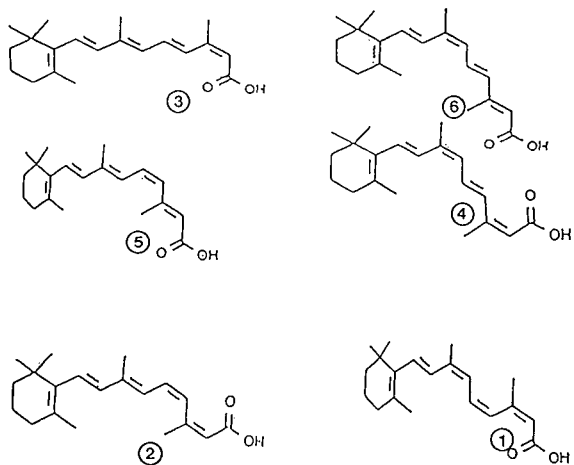
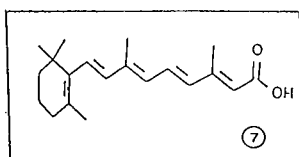


Fig. 1. Structures of *trans*-retinoic acid (7) and its photoisomers 13-*cis* (3), 9-*cis* (6), 11-*cis* (5), 9,13-di-*cis* (4), 11,13-di-*cis* (2) and 9,11,13-tri-*cis* (1).

methyl esters increase owing to the stronger “salt” effect.

The chromatographic elution of retinoic acid photoisomers was studied using a mobile phase containing either potassium nitrate or perchlorate (Fig. 3A) or with silver nitrate or perchlorate (Fig. 3B). As expected, only the presence of silver salts led to a decrease in the capacity factors of the seven compounds, whereas the retention times increased with potassium salts. The phenomenon is more important than with the fatty acid methyl esters because of the wider concentration range used.

Two phenomena occur when a silver salt is added in the mobile phase: a “salt” effect, *i.e.*, a simple increase in the ionic strength of the medium, which was observed for low concentrations of silver perchlorate in the fatty acid methyl esters study and for potassium salts in the retinoic acid photoisomers study; and a π -complexation effect due to $[\text{Ag-molecule}]^+$ form-

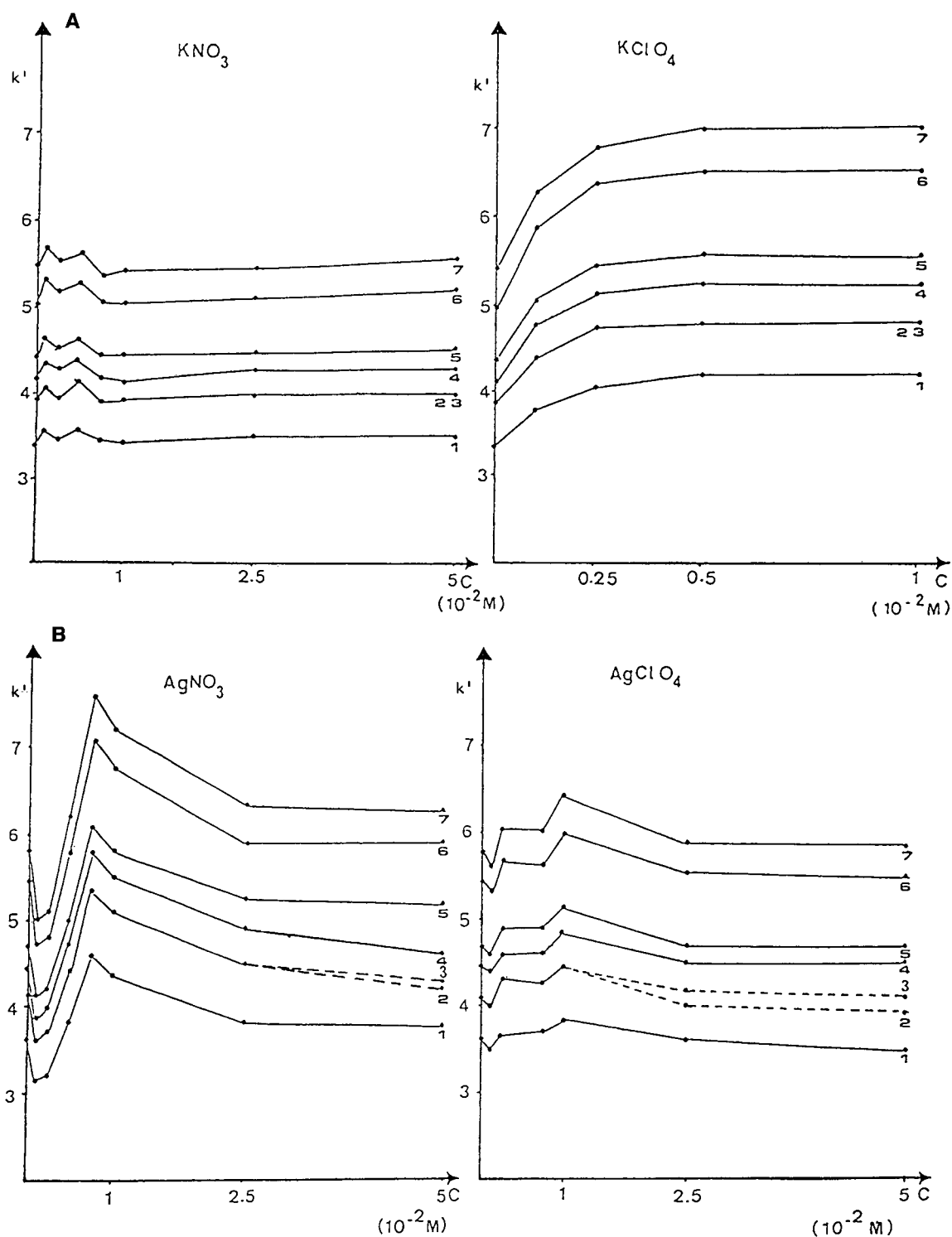


Fig. 3. Effect of (A) potassium salt and (B) silver salt concentrations in the mobile phase on the capacity factors of *trans*-retinoic acid photoisomers: 1 = 9,11,13-*tri-cis*-retinoic acid; 2 = 11,13-*di-cis*-retinoic acid; 3 = 13-*cis*-retinoic acid; 4 = 9,13-*di-cis*-retinoic acid; 5 = 11-*cis*-retinoic acid; 6 = 9-*cis*-retinoic acid; 7 = *trans*-retinoic acid.

ation, which was observed only with silver salts at a defined concentration and with compounds containing π -electrons of various origins, particularly double bonds. This effect is observed not only with the fatty acid methyl esters but also with more complex chemical structures such as *trans*-retinoic acid and its photoisomers.

Influence of the kind and concentration of silver salts

Figs. 2 and 3B show that a defined silver salt concentration has to be reached to induce the complexation. This critical salt concentration changes with the chemical nature of both the analytes and silver salt used: using silver perchlorate, the complexation was observed for a lower silver concentration with fatty acid methyl esters ($5 \cdot 10^{-3} M$) than with retinoic acid photoisomers ($1 \cdot 10^{-2} M$).

The comparison between silver nitrate and perchlorate was performed only with retinoic acid photoisomers. The chromatographic analysis of fatty acid methyl esters using silver nitrate was not carried out because there was too much noise at the detection wavelength (210 nm). The decrease in retention times related to the π -complexation is amplified with silver nitrate but the phenomenon is more selective with silver

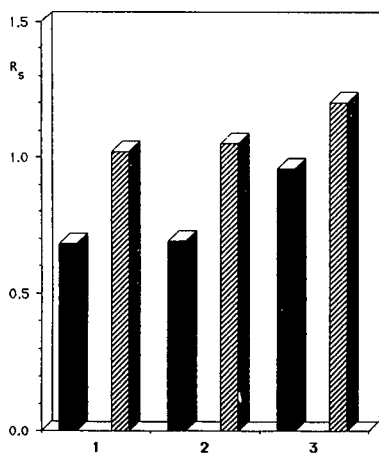


Fig. 4. Variation of R_s with silver perchlorate concentration in the mobile phase in chromatographic separations of the *cis-trans*-linoleic acid methyl esters and the *cis-trans*-oleic acid methyl esters. Mobile phase (1) without salt, (2) containing $5 \cdot 10^{-3} M$ KClO₄ and (3) containing $5 \cdot 10^{-3} M$ AgClO₄. Black bars, C'_{18c}/C'_{18t} ; hatched bars, C''_{18c}/C''_{18t} .

perchlorate. When the silver salt concentration in the mobile phase is higher, the “salt” effect increases with increasing ionic strength and compensates for the “complexation” effect (Fig. 3B). The retention times of the compounds become constant.

Improvement of the separation of retinoic acid photoisomers

The chromatographic analysis of a *cis-trans*-linoleic acid and *cis-trans*-oleic acid mixture shows the improvement of the resolution, R_s , in the presence of silver perchlorate by a factor of 1.4 for C''_{18c}/C''_{18t} and 1.2 for C'_{18c}/C'_{18t} (Fig. 4). These results confirm those previously published for oleic and elaidic acid isomers [10]. As the capacity factor seems to be a function of the number of double bonds, the improvement in

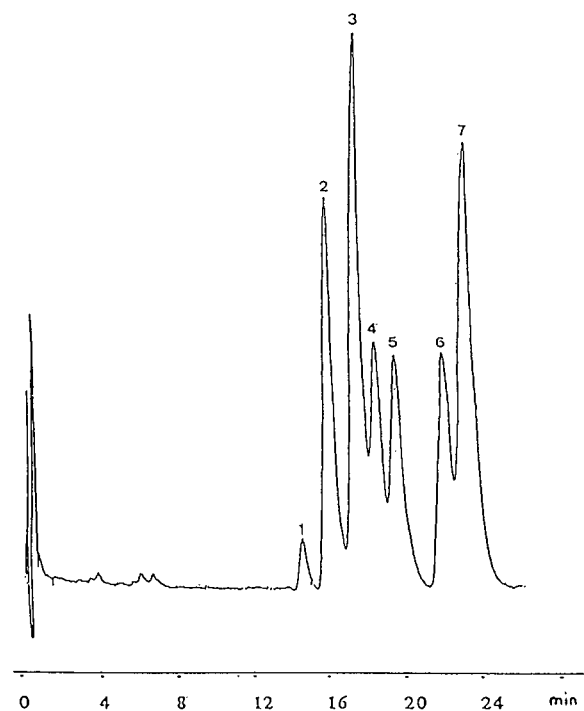


Fig. 5. Ag⁺ complexation reversed-phase liquid chromatogram of *trans*-retinoic acid photoisomers: 1 = 9,11,13-tri-*cis*-retinoic acid; 2 = 11,13-di-*cis*-retinoic acid; 3 = 13-*cis*-retinoic acid; 4 = 9,13-di-*cis*-retinoic acid; 5 = 11-*cis*-retinoic acid; 6 = 9-*cis*-retinoic acid; 7 = *trans*-retinoic acid. For chromatographic conditions, see Experimental (particle size of stationary phase = 3 μm).

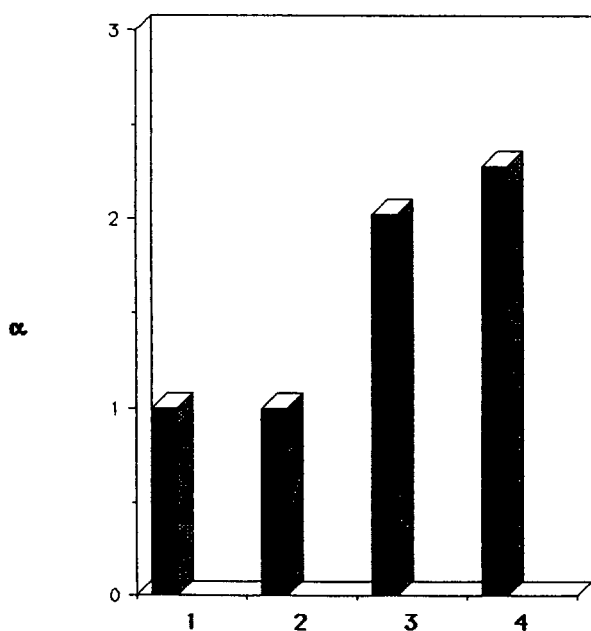


Fig. 6. Dependence of selectivity (α) for 13-*cis* and 11,13-di-*cis* photoisomers on silver salt concentration. Mobile phase (1) without salt, (2) containing $1 \cdot 10^{-2}$ M KClO_4 and (3 and 4) containing $1 \cdot 10^{-2}$ M AgClO_4 . Particle size of the stationary phase (1,2,3) $5 \mu\text{m}$ and (4) $3 \mu\text{m}$.

the separation depends on the steric configuration.

Likewise, the separation of the seven geometric isomers was achieved with the addition of silver salts to the mobile phase (Fig. 5). For example, Fig. 6 illustrates the twofold improvement in selectivity obtained between the 13-*cis* and the 11,13-di-*cis* isomers using mobile phases of similar ionic strength but containing Ag^+ ions instead of K^+ ions.

All these results demonstrate the improvement of the efficiency of the silver ion complexing liquid chromatographic system. Compared with the previously published data, the present analysis provides efficient separations of *trans*-retinoic acid and its photoisomers in half the time. The selectivity per unit time is enhanced with respect to the other proposed chromatographic separations.

CONCLUSIONS

This work confirmed the chromatographic behaviour of fatty acid methyl esters with silver

salts. We showed that the formation of π -complexes with *trans*-retinoic acid photoisomers can occur. A comparison of the behaviour of these molecules with similar chemical structures showed the necessity to determine accurately two critical parameters, the nature and the concentration of the silver salt added to the mobile phase. Moreover, this method leads to very efficient separations and is able to resolve a complex mixture of retinoic acid photoisomers. This method is particularly adapted for the study of *trans*-retinoic acid photodegradation.

REFERENCES

- 1 L.J. Morris, *J. Lipid Res.*, 7 (1966) 717.
- 2 H.B.S. Conacher, *J. Chromatogr. Sci.*, 14 (1976) 405.
- 3 R.M. Smith, S.J. Bale, S.G. Westcott and M. Martin-Smith, *Analyst*, 112 (1987) 1209.
- 4 C.R. Vogt, J.T. Baxter and T.R. Ryan, *J. Chromatogr.*, 150 (1978) 93.
- 5 R.P. Evershed, E.D. Morgan and L.D. Thompson, *J. Chromatogr.*, 237 (1982) 350.
- 6 I. Mitsushi, T. Fuminaro, N. Yoshikata and S. Masaki, *Anal. Biochem.*, 125 (1982) 197.
- 7 F. Mikes, V. Schurig and E. Gil-Av, *J. Chromatogr.*, 83 (1973) 91.
- 8 R. Battaglia and D. Frohlich, *Chromatographia*, 13 (1980) 428.
- 9 R.J. Tscherne and G. Capitano, *J. Chromatogr.*, 136 (1977) 337.
- 10 B. Vonach and G. Schomburg, *J. Chromatogr.*, 149 (1978) 417.
- 11 G. Schomburg and K. Zegarski, *J. Chromatogr.*, 114 (1975) 174.
- 12 R.M. McKenzie, D.M. Hellwege, M.L. McGregor, N.L. Rockley, P.J. Riquetti and E.C. Nelson, *J. Chromatogr.*, 155 (1978) 379.
- 13 B.A. Halley and E.C. Nelson, *J. Chromatogr.*, 175 (1979) 113.
- 14 R.W. Curey and J.W. Fowble, *Photochem. Photobiol.*, 47 (1988) 831.
- 15 P.A. Lehman and A.M. Malany, *J. Invest. Dermatol.*, 93 (1989) 595.
- 16 M.G. Motto, K.L. Facchine, P.F. Hamburg, D.J. Burinsky, R. Dunphy, A.R. Oyler and M.L. Cotter, *J. Chromatogr.*, 481 (1989) 255.

Comparative study of liquid chromatographic methods for the determination of cefadroxil

C. Hendrix, Yongxin Zhu, C. Wijsen, E. Roets and J. Hoogmartens*

Katholieke Universiteit Leuven, Laboratorium voor Farmaceutische Chemie, Instituut voor Farmaceutische Wetenschappen, Van Evenstraat 4, B-3000 Leuven (Belgium)

(First received September 22nd, 1992; revised manuscript received December 8th, 1992)

ABSTRACT

A comparative study of two isocratic liquid chromatographic methods for the determination of cefadroxil is described. The first method, prescribed in the monograph of the European Pharmacopoeia for the assay of cefadroxil, uses a classical alkyl-bonded phase (C_{18}) as the stationary phase. This method is very similar to that prescribed by the United States Pharmacopoeia. The other method uses poly(styrene–divinylbenzene). Poor reproducibility of the selectivity towards cefadroxil and related substances was observed when the first method was examined on different C_{18} columns. Copolymer columns, on the other hand, gave the same elution order on stationary phases from different manufacturers and of different age. Four bulk samples of cefadroxil were analysed following both methods and the results were compared.

INTRODUCTION

It has been described that classical alkyl-bonded phases (C_{18}) can suffer from poor reproducibility of the selectivity during liquid chromatography (LC) of cephalosporins [1]. This type of reversed phase is, nevertheless, widely prescribed in pharmacopoeial methods. For the assay of cefadroxil, the European Pharmacopoeia (Ph. Eur.) prescribes an LC method using a C_{18} stationary phase [2]. The selectivity of this method for cefadroxil and related substances was examined on six stationary phases. The United States Pharmacopoeia (USP) XXII prescribes nearly the same method for the assay of cefadroxil [3]; only the pH and concentration of the buffer of the mobile phase are slightly different. The influence of these differences on the selectivity was examined.

On four columns, four bulk samples were analysed following the Ph. Eur. method. The

results were compared with those obtained by an isocratic LC method using poly(styrene–divinylbenzene) (PS–DVB) as stationary phase. This PS–DVB method was proved to give very reproducible selectivity [4].

EXPERIMENTAL

Reference substances and samples

The European Pharmacopoeia Chemical Reference Standard (Ph. Eur. CRS; 94.2%) was used as the standard.

Bulk samples of different origin and age were chosen in order to have samples of variable purity.

Related substances

Related substances present as impurities in cefadroxil can originate from the semi-synthesis and from degradation. The structures and origin of potential impurities of cefadroxil have been given previously [4]. 7-Aminodesacetoxycephalosporanic acid (VII) and D-4-hydroxyphenylglycine (VIII) are the basic constituents of the

* Corresponding author.

cefadroxil molecule. L-Cefadroxil (II), Δ^2 -cefadroxil (VI), 4-hydroxyphenylglycylcefadroxil (IX) and the pivalamide of 7-ADCA (XI) can arise from the semi-synthesis of cefadroxil. The other related substances are decomposition products. 3-Hydroxymethylene-6-(4-hydroxyphenyl)piperazine-2,5-dione (III) and 3-hydroxy-4-methyl-2(5H)-thiophenone (IV) are formed in acidic medium. III and 3-aminomethylene-6-(4-hydroxyphenyl)piperazine-2,5-dione (V) are formed in neutral medium and the cefadroxil Δ^4 -cephalosporoates (X) are formed in alkaline medium. X was never isolated but was prepared *in situ* by dissolving cefadroxil in 0.1 M NaOH (1 mg/ml) and storing the solution at room temperature for 10 min.

Solvents and reagents

Acetonitrile (99%) (Janssen Chimica, Beerse, Belgium) was distilled before use. Phosphoric acid (85%) and potassium dihydrogenphosphate (analytical-reagent grade) were obtained from Merck (Darmstadt, Germany) and sodium 1-oc-tanesulphonate (NaOS) from Janssen Chimica. Water was distilled twice.

LC apparatus and operating conditions

Isocratic elution was always used. The equipment consisted of an L-6200 pump (Merck-Hitachi, Darmstadt, Germany), a Model D 254-nm fixed-wavelength UV monitor (LDC/Milton Roy, Riviera Beach, FL, USA) and a Model 3396 A integrator (Hewlett-Packard, Avondale, PA, USA). For the examination of peak homogeneity the UV detector was replaced with a Model 990 photodiode-array detector (Waters, Milford, MA, USA). The samples were injected by a Marathon autosampler (Spark Holland, Emmen, Netherlands) with sample cooling (6°C) equipped with a fixed 20- μ l loop and a Julabo C and F10 Cryomat (Julabo Labortechnik, Seelbach, Germany). The columns (250 \times 4.6 mm I.D.) were packed in the laboratory with (A) Hypersil ODS, 5 μ m (Shandon, Runcorn, UK), (B) Partisil ODS-3, 10 μ m (Whatman, Clifton, NJ, USA), (C) Spherisorb ODS-1, 10 μ m (Phase Separations, Queensferry, UK), (D) RSIL C₁₈ HL, 10 μ m (Bio-Rad, Eke, Belgium), (E) Nucleosil 100 C₁₈, 5 μ m (Macherey-Nagel,

Düren, Germany), (F) Bio-Sil C₁₈ LL, 90 Å, 5 μ m (Bio-Rad), (G) PLRP-S, 100 Å, 8 μ m (Polymer Labs., Church Stretton, Shropshire, UK) or (H) PRP-1, 7–9 μ m (Hamilton, Reno, NV, USA). The columns were immersed in a water-bath heated by a Julabo EM thermostat. The column temperature was 30°C for the alkyl-bonded phases and 50°C for the PS–DVB phases. For both methods the flow-rate was 1 ml/min.

Mobile phase

The Ph. Eur. method prescribes acetonitrile–0.272% (w/v) KH₂PO₄ solution (4:96, v/v). The USP XXII method prescribes acetonitrile–buffer (pH 5.0) (4:96, v/v). The buffer is prepared by dissolving 13.6 g of KH₂PO₄ in water to make 2000 ml. The pH of the solution is then adjusted to 5.0 with 10 M KOH. The PS–DVB method uses acetonitrile–0.02 M sodium 1-oc-tanesulphonate–0.2 M phosphoric acid–water (12.5:20:5:up to 100, v/v).

Mobile phases were degassed by ultrasonication before use.

Sample preparation

Samples for quantitative analysis following the Ph. Eur. method were prepared by weighing 50 mg of cefadroxil into a 100-ml volumetric flask. Mobile phase was used as the solvent. For the PS–DVB method 30 mg of cefadroxil were weighed into a 20-ml volumetric flask and mobile phase containing 30% of 0.02 M sodium 1-oc-tanesulphonate solution was used as the solvent.

The chemical reference substance was dissolved in the same way as the samples.

RESULTS AND DISCUSSION

Examination of the selectivity of the LC methods

In the USP method the pH of the mobile phase is controlled by phosphate buffer (pH 5.0). The Ph. Eur. method uses a phosphate solution at pH 4.7. These very similar mobile phases were compared on the same C₁₈ column by analysing a mixture of cefadroxil and related substances. The small difference in pH did not influence the selectivity, so it was decided that

both mobile phases gave the same result. A shortcoming of the USP method was the lack of a resolution test. The capacity factor and the number of plates of the cefadroxil peak were used as criteria for the adjustment of the mobile phase. These criteria are obviously not indicative for the selectivity of a stationary phase. The USP method was not considered further in the experiments because of its similarity with the Ph. Eur. method.

The selectivity of the Ph. Eur. method was examined on six C₁₈ columns (A–F) by the determination of the capacity factors of cefadroxil and related substances. For each column the composition of the mobile phase was adapted to obtain the required resolution of at least 5.0 between cefadroxil and amoxicillin. Table I shows that only two of the columns examined (A and E) complied with this requirement. The resolution on the other columns was insufficient, even after complete elimination of the organic modifier from the mobile phase. Nevertheless, the selectivity was investigated on each column.

TABLE I
COMPOSITION OF THE MOBILE PHASE FOR EACH COLUMN FOLLOWING THE PH EUR. METHOD, WITH THE CORRESPONDING RESOLUTION BETWEEN CEFADROXIL AND AMOXICILLIN

Column	Mobile phase composition		Resolution
	CH ₃ CN (vol.)	0.272% KH ₂ PO ₄ (vol.)	
A	4	96	5.4 ^a
	1.5	98.5	10.1 ^a
B	3	97	1.8
	0	100	3.2
C	4	96	1.5
	0.6	99.4	3.1
	0	100	3.7
D	3	97	2.4
	0.6	99.4	3.6 ^a
	0	100	4.0
E	4	96	5.4 ^a
	0.9	99.1	9.6 ^a
F	0.3	99.7	2.9 ^a

^a Mobile phases used for quantitative analysis.

Because columns A and E complied with the resolution test when using a fast-eluting mobile phase, the selectivity was also checked using a mobile phase with a lower content of acetonitrile. The results are shown in Fig. 1. X, which is a complex mixture of diastereoisomers, is not shown. This polar mixture eluted close to the dead volume of the chromatogram. IV was eluted at k' close to 10 or more. IX and XI were always eluted much later than cefadroxil ($k' > 30$). Using a mobile phase containing 4% of acetonitrile columns A and E complied with the resolution test ($R_s = 5.4$); nevertheless, cefadroxil was not separated from all related substances. Complete separation was achieved using columns A (1.5% CH₃CN), D (0.6% CH₃CN), column E (0.9% CH₃CN) and F (0.3% CH₃CN). The resolution test gave $R_s = 10.1, 3.6, 9.6$ and 2.9 , respectively. Obviously, there is insufficient relationship between this resolution test and the

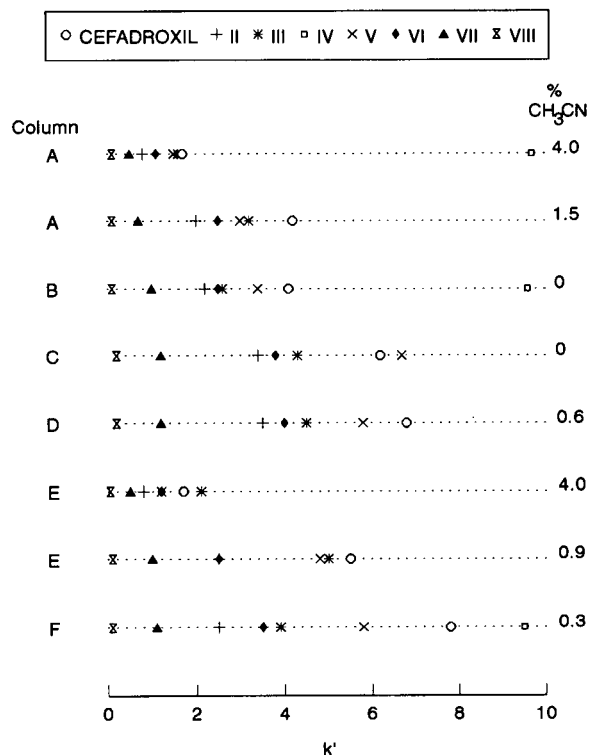


Fig. 1. Capacity factors of cefadroxil and related substances on different C₁₈ columns following the Ph. Eur. method. Mobile phase: CH₃CN–0.272% KH₂PO₄ [$x:(100-x)$, v/v], where x is given on the right of the figure.

selectivity of the LC method when applied to different columns. Also, differences in elution order can be observed for the different columns, e.g., the elution order of cefadroxil and V is column dependent. The separation of cefadroxil from decomposition products formed in alkaline medium was examined by analysis of an *in situ* prepared solution of X under the best LC conditions for each column. The homogeneity of the cefadroxil peak was examined by normalization at 230 nm of the UV spectra taken at the left slope, the maximum and the right slope. Only columns D (0.6% CH₃CN) and F (0.3% CH₃CN) gave a homogeneous cefadroxil peak. It can be concluded that the selectivity is column dependent and that the method does not guarantee a selective determination of cefadroxil.

The selectivity of the PS–DVB method has already been examined and reported previously [4]. This method is able to separate cefadroxil from all known related substances and performs equally well on different commercially available brands of PS–DVB. The age and the history (former use) of the columns were observed to have a limited influence on the selectivity. These

characteristics are an important improvement compared with the pharmacopoeial method.

Quantitative analysis of bulk samples by two LC methods

Four bulk samples were analysed following the pharmacopoeial method and the PS–DVB method. The Ph. Eur. CRS for cefadroxil was used as the standard.

The analyses following the Ph. Eur. were performed on four C₁₈ columns, A, D, E and F. The mobile phase compositions were those marked with superscript *a* in Table I. Columns A and E were used under both non-separating (4% CH₃CN) and separating (1.5 and 0.9% CH₃CN) conditions. The results are given in Table II. The relative standard deviation (R.S.D.) calculated on the peak area of six subsequent injections of cefadroxil was well below the prescribed limit of 1.0% [2]. Each sample was analysed four times. For all the LC conditions nearly identical results were obtained. The R.S.D. did not exceed 1.0%.

The analyses by the LC method developed on PS–DVB were performed on columns G and H. Using the mobile phase described under Ex-

TABLE II
RESULTS OF THE ASSAY FOLLOWING THE PH. EUR. METHOD

Values in % (w/w) with R.S.D. values (%) in parentheses (*n* = 4).

Column	CH ₃ CN in mobile phase (%)	Sample no.			
		1	2	3	4
A	4.0	93.32 (0.3)	93.94 (0.4)	90.36 (0.4)	90.93 (1.1)
	1.5	93.45 (0.2)	94.16 (0.2)	90.19 (0.8)	90.77 (0.3)
D	0.6	93.28 (0.5)	94.28 (0.1)	90.13 (0.5)	90.15 (0.2)
E	4.0	93.71 (0.2)	94.29 (0.4)	90.59 (0.3)	91.00 (0.4)
	0.9	93.73 (0.5)	93.85 (0.6)	90.46 (0.3)	91.09 (0.2)
F	0.3	93.70 (0.2)	94.49 (0.1)	90.84 (0.2)	90.77 (0.8)
Mean		93.53 (0.4) (<i>n</i> = 24)	94.17 (0.4) (<i>n</i> = 24)	90.46 (0.5) (<i>n</i> = 24)	90.78 (0.5) (<i>n</i> = 24)

TABLE III
RESULTS OF THE ASSAY FOLLOWING THE PS–DVB
METHOD

Values in % (w/w) with R.S.D. values (%) in parentheses and number of analyses (*n*).

Column	Sample no.			
	1	2	3	4
G	93.72 (0.2) (<i>n</i> = 7)	94.21 (0.5) (<i>n</i> = 6)	90.50 (0.4) (<i>n</i> = 5)	91.13 (0.5) (<i>n</i> = 6)
H	93.43 (0.4) (<i>n</i> = 4)	93.96 (0.3) (<i>n</i> = 4)	90.11 (0.2) (<i>n</i> = 4)	90.21 (0.2) (<i>n</i> = 4)
Mean	93.62 (0.3) (<i>n</i> = 11)	94.11 (0.4) (<i>n</i> = 10)	90.31 (0.3) (<i>n</i> = 9)	90.67 (0.7) (<i>n</i> = 10)

perimental, a resolution of 4.3 for column G and 4.7 for column H was obtained between cefadroxil and amoxicillin, which is better than the required resolution of 4.0 [4]. The results are given in Table III. Both columns gave nearly identical results.

The results of the assay of four bulk samples by the pharmacopoeial method using four different C₁₈ columns and by the LC method using two different PS–DVB columns were compared. The test of significance of differences of means [5] was performed using the grand means of both methods. The resulting figures were less than the tabulated limits ($t_{0.80}$), so the difference was not significant even at the 20% level.

CONCLUSIONS

The results might lead to the conclusion that both methods are equivalent. However, this can

be confirmed only for the samples examined, which apparently did not contain impurities that were co-eluted with cefadroxil in the pharmacopoeial method. It should also be mentioned that the resolution test prescribed by the pharmacopoeial method did not guarantee the complete separation of cefadroxil from related substances. Even when complying with this resolution test, the mobile phase still needed adaptation in order to obtain complete separation.

In general, it can be concluded that the poor reproducibility of the selectivity of the classical alkyl-bonded phases was again demonstrated here. Therefore, these methods are less suitable as official methods. The PS–DVB method, on the other hand, offers more reliable results because of its reproducible selectivity.

ACKNOWLEDGEMENTS

The National Fund for Scientific Research (Belgium) is acknowledged for financial support. The gifts of samples by the Belgian Ministry of Health and by different manufacturers are gratefully acknowledged. The authors thank A. Decoux and I. Quintens for editorial assistance.

REFERENCES

- 1 I. Wouters, S. Hendrickx, E. Roets, J. Hoogmartens and H. Vanderhaeghe, *J. Chromatogr.*, 291 (1984) 59.
- 2 Cefadroxilum, *Pharmeuropa*, 2 (1990) 184.
- 3 *United States Pharmacopeia XXII*, 3rd Suppl., United States Pharmacopoeial Convention, Rockville, MD, 1989.
- 4 C. Hendrix, C. Wijzen, Li Ming Yun, E. Roets and J. Hoogmartens, *J. Chromatogr.*, 628 (1993) 49.
- 5 *Theory and Problems of Statistics in SI Units*, McGraw-Hill, New York, 1st ed., 1972, p. 189.

Combined high-performance aqueous size-exclusion chromatographic and pyrolysis–gas chromatographic–mass spectrometric study of lignosulphonates in pulp mill effluents

Erik R.E. van der Hage*, Willem M.G.M. van Loon and Jaap J. Boon

Unit for Mass Spectrometry of Macromolecular Systems, FOM-Institute for Atomic and Molecular Physics, Kruislaan 407, 1098 SJ Amsterdam (Netherlands)

Henk Lingeman and Udo A.Th. Brinkman

Department of Analytical Chemistry, Free University, De Boelelaan 1083, 1081 HV Amsterdam (Netherlands)

(First received January 23rd, 1992; revised manuscript received December 24th, 1992)

ABSTRACT

An aqueous high-performance size-exclusion chromatographic (HPASEC) method for lignosulphonates was developed and optimized using a TSK G3000SW column. Curie-point pyrolysis–gas chromatography–mass spectrometry (Py–GC–MS) was used to characterize the lignosulphonates on the molecular level. Combined HPASEC and Py–GC–MS results showed that a sodium lignosulphonate standard, prepared under mild conditions, was a relatively polydisperse polymer that still contained features of a natural lignin polymer. Lignosulphonates discharged by pulp mills are more monodisperse macromoles of a relatively low molecular mass and are structurally modified to a greater extent than the sodium lignosulphonate standard. A relationship was established between the molecular mass distributions of the various lignosulphonate macromolecules and the fraction of preserved phenylpropane structural units.

INTRODUCTION

Lignosulphonates are formed during sulphite pulping processes of wood chips by substitution of α - or γ -hydroxy groups on the side-chains of the 4-propanol-2-methoxyphenol and 4-propanol-2,6-dimethoxyphenol structural units of lignin [1]. The aim of sulphite pulping is to extract lignins from wood by sulphonation, yielding a brighter wood pulp [1]. Although the toxicity of lignosulphonates is probably low, this class of

compounds may significantly contribute to the sulphur content of river and drinking waters [2]. In modern sulphite pulp mills, the emission of lignosulphonates has been strongly reduced by recovery and commercial use or incineration of these compounds [3]. However, significant residual amounts of lignosulphonates are still discharged by modern sulphite pulp mills and very large amounts may still be discharged by older sulphite pulp mills [3,4].

The molecular mass distribution, as measured by size-exclusion chromatography (SEC), is an important parameter for characterizing this class of lignin-derived compounds. Lignosulphonates

* Corresponding author.

are largely composed of macromolecules having molecular masses of more than 1000 g mol^{-1} . Molecular mass distributions are used to characterize these water-soluble polymers and monitor structural changes during physical, chemical or biological degradation processes.

Aqueous SEC of lignosulphonates has been performed with organic polysaccharide-based Sephadex gels [5]. Over the past decade, silica-based high-performance aqueous SEC (HPASEC) gels have been developed which give higher plate numbers and increased analysis speed compared with polymeric gels [6–8]. A major advantage of HPASEC is that derivatization of water-soluble polymers is not necessary. This leaves macromolecular structures unchanged and allows the direct analysis of aqueous samples. An SEC study of aquatic humic substances using a TSK G3000SW column has been reported by Vartiainen *et al.* [9]. Up to now, no studies have been reported on aqueous SEC of lignosulphonates using this column.

The structural analysis of dissolved macromolecular lignosulphonates and chlorolignosulphonates in natural and waste waters has been reviewed recently [4]. Although chemical degradation techniques have frequently been used to identify substructures of lignosulphonates [10,11], these methods are time consuming and various chemical modifications of the phenylpropane structural units occur owing to the severe chemical conditions used in these methods.

Curie-point pyrolysis–gas chromatography–mass spectrometry (Py–GC–MS) is a rapid microanalytical method for the structural analysis of lignin polymers on a molecular level [12,13]. The technique requires minimum sample preparation and preserves side-chain information of the phenylpropane structural units. Py–GC–MS has been applied to pulp mill effluents [4,14], chlorolignins in xylan [15] and plastic contaminants in pulp [16].

The objectives of this study were to develop an optimized HPASEC method to determine molecular mass distributions of lignosulphonates using the TSK G3000SW column. Curie-point Py–CG–MS was used to obtain detailed structural information on a molecular level. The rela-

tionship between the molecular mass of the various lignosulphonate macromolecules and the preservation of phenylpropane structural units was investigated.

EXPERIMENTAL

Chromatographic conditions

The SEC system consisted of an Applied Biosystems (Ramsey, NJ, USA) Model 400 isocratic pump, a Rheodyne (Berkeley, CA, USA) Model 7125 injection valve with a $20\text{-}\mu\text{l}$ sample loop and an Applied Biosystems Model 783 UV detector (280 nm), which was connected in series with a Spectra-Physics (San Jose, CA, USA) Model SP 6040 XR refractive index (RI) detector. The system was operated at ambient temperature. The use of a Waters TCM column oven (50°C) did not improve the chromatographic performance of the system.

A TSK G3000SE_{XL} precolumn ($750 \text{ mm} \times 7.5 \text{ mm I.D.}$) was used in combination with a TSK G3000SW_{XL} analytical column ($300 \text{ mm} \times 7.5 \text{ mm I.D.}$) (Toyo Soda Manufacturing, Tokyo, Japan). Its theoretical plate number, determined with ethylene glycol (Merck, Darmstadt, Germany), was 41 400. The void volume (V_0), determined with a pullulan standard (molecular mass $853\,000 \text{ g/mol}$), was 5.74 ml. The permeation volume (V_i), determined with ethylene glycol, was 12.71 ml. Molecular mass determinations were obtained using a 0.2 M sodium acetate (Merck) mobile phase at a flow-rate of 1 ml/min . The mobile phase was adjusted to pH 7 with nitric acid (J.T. Baker, Deventer, Netherlands), filtered ($0.45\text{-}\mu\text{m}$ filter, Millipore) and purged with helium.

Data were processed using a Nelson 760 series interface and Nelson Analytical software (Version 5.1) and laboratory-made SEC software (FOM-Amolf, Amsterdam, Netherlands).

Curie-point pyrolysis mass spectrometry

Curie-point pyrolysis was performed with a FOM 4-LX pyrolysis unit [12]. Sample solutions of $20 \mu\text{g}$ ($5 \mu\text{l}$ of aqueous solution of 4 mg/ml) were applied to a ferromagnetic wire and dried under reduced pressure. The wire was inserted in a glass liner, flushed with argon to remove air

and subsequently placed into the pyrolysis unit. The ferromagnetic wire was inductively heated within 0.1 s to its Curie-point temperature (610°C), at which it was held for 4 s. Pyrolysis fragments were flushed to a 25 m × 0.32 mm I.D. CP-SIL-5 CB fused-silica capillary column (film thickness 0.41 μm) using helium as a carrier gas. Py-GC-MS was performed using a Packard 438 S chromatograph coupled to a Jeol DX-303 double-focusing (EB) mass spectrometer. The GC oven was kept at 30°C during pyrolysis and was subsequently programmed to 300°C at 4°C/min. The interface was kept at 200°C and the ion source at 180°C. Compounds were ionized at 70 eV under electron impact conditions and mass analysed over the range m/z 35–500. Data were processed using the Kratos (Manchester, UK) analytical MACH3 software package.

Materials

Sodium polystyrenesulphonate (NaPSS) of molecular mass 1 200 000, 400 000, 46 000, 18 000, 8000, 4600 and 1800 g/mol and pullulan standards of molecular mass 853 000, 380 000, 100 000, 48 000, 23 700 and 5800 g/mol were obtained from Polymer Laboratories (Church Stretton, UK). Maltoheptaose of molecular mass 1152 (Boehringer, Mannheim, Germany) and maltotriose of molecular mass 504 (Serva, Heidelberg, Germany) were used as low-molecular mass polysaccharide standards.

Sodium lignosulphonate was purchased from Roth (Karlsruhe, Germany). Deionized water obtained with a Milli-Q system (Millipore, Bedford, MA, USA) was used throughout.

Samples from German sulphite pulp mill effluents were collected in January 1989 from PWA Aschaffenburg, Holtzmann (Karlsruhe) and PWA Mannheim. The samples were stored in high-density polyethylene containers (Nalgene, Rochester, NY, USA) with a low phthalate content and refrigerated at –20°C.

RESULTS AND DISCUSSION

Owing to the heterogeneous composition of lignosulphonates, no universal monodisperse calibration standards are available. Molecular mass calibration with polymer standards which

are structurally different from the polymers under investigation requires the assumption that the chromatographic separation is governed by the hydrodynamic volume ($[\eta]M$) only. The structural resemblance between the sample solutes and the calibration standards essentially determines the accuracy of the calibration results. Although ultrafiltration fractions of lignosulphonates probably give more representative calibration standards [17], this method is time consuming and apparently less reproducible, owing to differences in the selected samples and ultrafiltration systems. Therefore, well defined NaPSS standards which show an acceptable structural resemblance to lignosulphonates were preferred in this study.

Rigid, porous silica-based hydrophilic gels such as TSK type SW gels are known to contain residual silanol groups as a result of incomplete derivatization [6,7]. These anionic groups ($pK_a \approx 7$ [18]) give rise to secondary separation effects of polar and ionized solute molecules and lead to deviations in calibration results [7,8,19].

Ion-exclusion effects caused by repulsion of negatively charged solutes from the pores of the TSK SW gel by dissociated silanol groups were investigated by comparing the calibration graphs of NaPSS and pullulan using different eluent ionic strengths. Fig. 1 shows the linear part of the calibration graphs (3500–100 000 g/mol) at various ionic strengths of sodium acetate. Apparently, the pullulan calibration graph is independent of the ionic strength, *i.e.*, this linear uncharged polymer is not subject to ion exclusion. However, the NaPSS calibration graph is strongly dependent on the eluent ionic strength. This demonstrates strong electrostatic interactions between sulphonate functional groups and the packing surface. As a result, earlier elution of NaPSS relative to a non-ionized pullulan standard of the same molecular mass is observed.

A theoretical ion-exclusion graph can be derived from the Debye–Hückel theory [19]:

$$V_e = kI^{-1/2} \quad (1)$$

where V_e is the ion-exclusion volume, k is a fitting factor and I is the ionic strength of the mobile phase. By choosing an appropriate value for k (*i.e.* 2.34 for molecular mass 1800), the

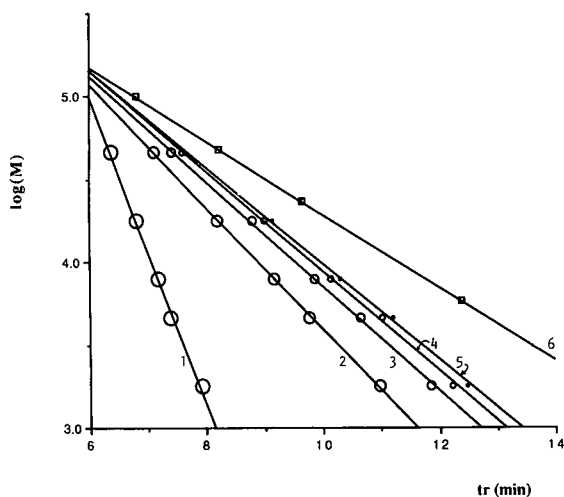


Fig. 1. Optimization of the mobile phase ionic strength using pullulan (6) and sodium polystyrenesulphonate standards. Mobile phase: 0.01 *M* sodium acetate (1); 0.05 *M* sodium acetate (2); 0.1 *M* sodium acetate (3); 0.15 *M* sodium acetate (4); 0.2 *M* sodium acetate (5). pH = 7.

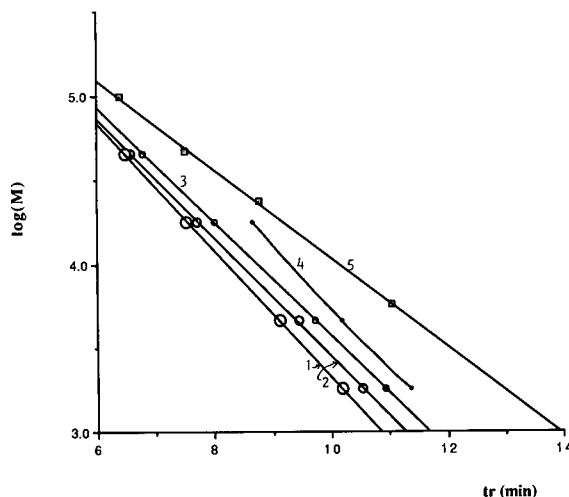


Fig. 2. Optimization of the mobile phase pH using pullulan (5) and sodium polystyrenesulphonate standards. Mobile phase: 0.05 *M* sodium acetate, pH 7 (1), pH 6 (2), pH 5 (3) and pH 3.8 (4).

Debye–Hückel graph can be fitted very well on to the experimental data. As significant deviations from this theoretical graph usually indicate adsorption effects, it can be concluded that ion exclusion is the only secondary separation effect of NaPSS using the present type of column at pH 7. Fig. 1 shows that this effect is minimized at high ionic strengths.

The effect of cations on the separation was investigated with eluents containing 0.01 *M* sodium acetate, potassium acetate or ammonium acetate. The type of cations in the eluent did not influence the calibration graph of NaPSS or the chromatography of the lignosulphonate samples. This indicates that the hydrodynamic volume of the cations plays an insignificant role in the shielding of the ionized silanol and sulphonate groups.

The effect of eluent pH is shown in Fig. 2. The mobile phase pH was optimized using 0.05 *M* sodium acetate buffers with pH values of 3.8, 5, 6 and 7. Interestingly, the calibration graph of NaPSS shifts towards the pullulan calibration graph when the eluent pH is lowered. This can be explained by reduced ion exclusion, due to protonation of silanol groups. Barth [7] reported that below pH 4 the ionization of silanol groups

is suppressed. When an eluent pH of 3.8 was used, irreversible adsorption of high-molecular mass NaPSS standards on the stationary phase was observed in our study. This indicates strong hydrophobic interactions between NaPSS and the TSK G3000SW gel, probably as a result of hydrogen bonding of free phenolic hydroxyl groups with protonated silanol groups. Protonation of the sulphonate groups is unlikely at pH 3.8 because lignosulphonates are strongly acidic macromolecules ($pK_a \approx 0.5$ [20]). The decrease in ion-exclusion effects on decreasing the eluent pH from 7 to 5 is comparable to the increase in the ionic strength from 0.05 to 0.1 *M*. Changing the pH may also lead to deviations in measured molecular mass distributions as a result of the formation of association complexes. This effect is minimized at pH 7–9 and at low dissolved organic carbon concentrations (<100 mg/l) [21,22].

In general, improved chromatographic resolution is observed when an eluent of low ionic strength is used. The best resolution was obtained using 0.01 *M* sodium acetate. In Fig. 3, characteristic HPASEC traces are shown which allow “fingerprinting” of the lignosulphonate samples. Decreasing the electrolyte concentration will also lead to an increase in intramolecu-

lar expansion of polyanionic lignosulphonates [7]. As a result of these inter- and intramolecular electrostatic effects at low electrolyte concentrations, a dramatic decrease in retention volume of most compounds is observed (Fig. 3) compared with the chromatograms obtained at 0.2 M sodium acetate (Fig. 4), and no accurate molecular mass determinations are obtained. Gupta and McCarthy [23] showed that the effective hydrodynamic radius of lignosulphonates was approximately doubled when the electrolyte concentration was changed from 1.0 M NaCl to zero in water.

It appears from the present data that by using an eluent ionic strength of 0.2 M, sodium acetate ionic effects are strongly reduced. To avoid the possibility of increasing adsorption and association at low eluent pH (<4), the increase in ionic strength was preferred to suppress secondary separation effects. Thus, an eluent of 0.2 M

sodium acetate and pH 7 was used for molecular mass determinations.

The reproducibility of the system was investigated with respect to retention time, peak height and peak area by seven injections of an NaPSS standard (molecular mass 1800). The relative standard deviations were 0.2, 2 and 5%, respectively.

HPASEC traces of the sodium lignosulphonate and pulp mill effluent samples recorded by UV absorption are shown in Fig. 4. The corresponding number-average molecular masses (M_n) and mass-average molecular masses (M_w) are listed in Table I. The sodium lignosulphonate standard shows a relatively high M_w value compared with the lignosulphonates discharged by pulp mill effluents, whereas the M_n values obtained are comparable. A useful procedure is to define the ratio M_w/M_n as a measure of the polydispersity of the sample. The corresponding

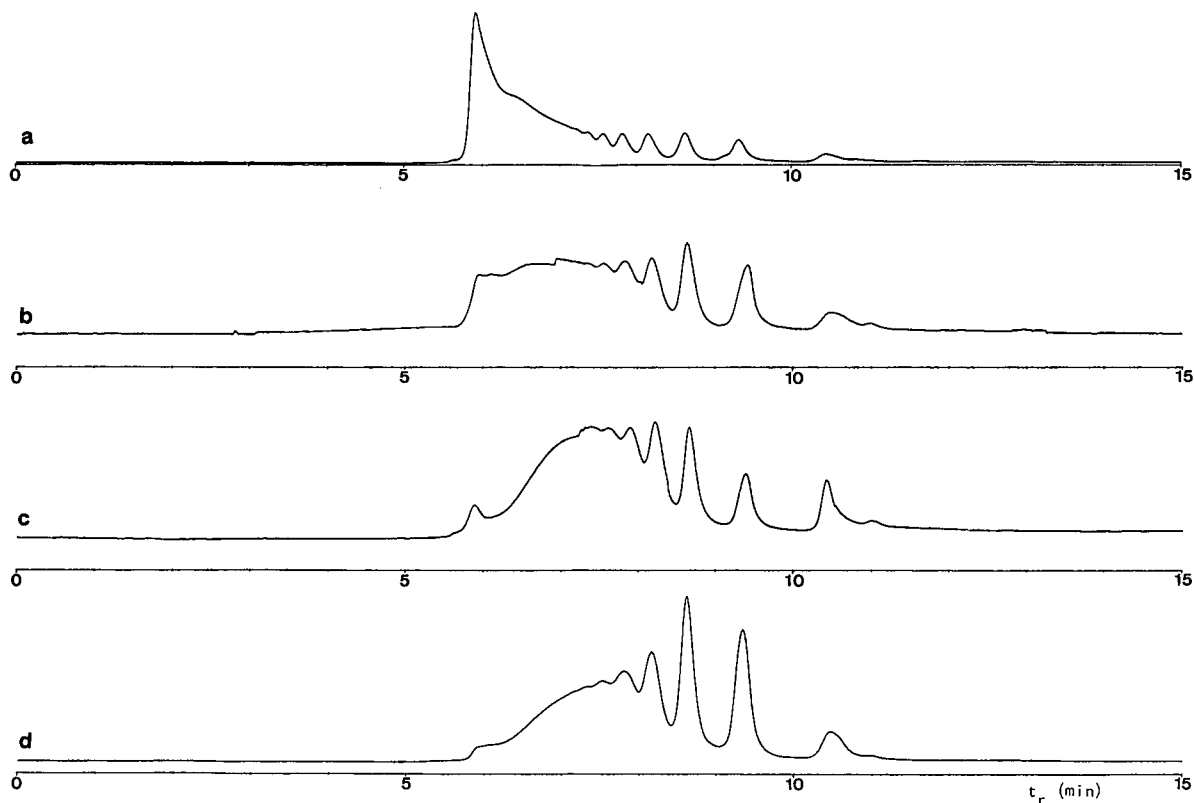


Fig. 3. Molecular mass distributions of (a) sodium lignosulphonate, (b) effluent from PWA Mannheim, (c) effluent from Holtzmann and (d) effluent from PWA Aschaffenburg. Eluent: 0.01 M sodium acetate (pH 7).

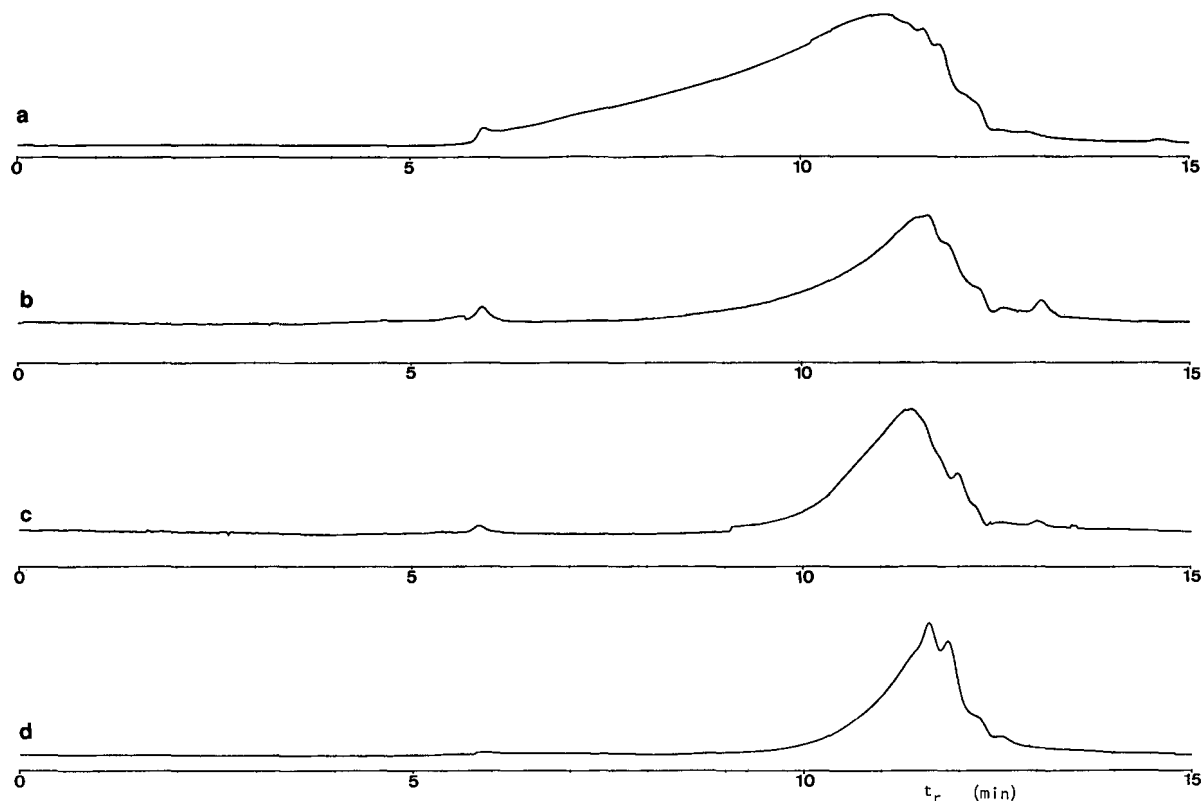


Fig. 4. Molecular mass distributions of (a) sodium lignosulphonate, (b) effluent from PWA Mannheim, (c) effluent from Holtzmann and (d) effluent from PWA Aschaffenburg. Eluent: 0.2 M sodium acetate (pH 7).

polydispersity index values (PD) [24] are given in Table I.

Large PD values, indicating a wide polydispersity of molecular mass, are characteristic of non-linear polymers [25]. The PD value of 6.12 obtained for the sodium lignosulphonate stan-

dard indicates that a wide range of molecular sizes is obtained in the sulphonation process but that depolymerization is not taken to the stage at which the product consists of monomer and low-molecular-mass oligomers. The pulp mill effluent samples show much lower PD values than the

TABLE I

HPASEC AND Py-GC-MS RESULTS FOR SODIUM LIGNOSULPHONATE AND LIGNOSULPHONATES DISCHARGED BY PWA MANNHEIM, HOLTZMANN AND PWA ASCHAFFENBURG

Sample	M_w (g/mol)	M_n (g/mol)	Max. M_w (g/mol)	PD^a	DP^b	>5000 ^c (%)	$C_6C_3^d$ (%)
Sodium lignosulphonate	16 700	2700	144 300	6.12	75	57	49
PWA Mannheim	8400	3300	20 700	2.55	38	43	38
Holtzmann Karlsruhe	4900	3000	9700	1.67	22	29	33
PWA Aschaffenburg	4100	2600	11 300	1.61	18	27	32

^a Polydispersity, M_w/M_n .

^b Degree of polymerization (average structural unit masses 223 g/mol).

^c Cumulative fraction >5000 g/mol.

^d Cumulative fraction of phenylpropane structural units as determined by Py-GC-MS.

sodium lignosulphonate standard, indicating more monodisperse distributions of lignosulphonates formed during the sulphite pulping processes. Large differences in the maximum molecular mass (Table I) which could be observed in the HPASEC traces are also reflected in the polydispersity factors. The calibration results listed in Table I clearly show that the sodium lignosulphonate standard mainly consists of macromolecules of molecular mass above 5000 g/mol, whereas the pulp mill effluents appear to be composed of more depolymerized lignosulphonates. The approximate degree of polymerization (*DP*) was calculated (Table I) by taking into account that lignosulphonates usually contain one $-\text{SO}_3\text{Na}$ functional group for each two structural units [1], and the average molecular mass of one monomer unit is consequently about 223 g/mol for softwood-derived lignosulphonates.

Differences in aliphatic side-chain types are an important criterion for the degree of modification of the original phenylpropane (C_6C_3) structural units during sulphite pulping. Analytical flash pyrolysis was used to dissociate lignosulphonates thermally into cleavage products which reflect the structure of the original polymer [12]. The Py-GC-MS trace of sodium lignosulphonate is shown in Fig. 5. The distributions of the

2-methoxyphenol structural units obtained on pyrolysis are given in Table II. The major peaks observed in the chromatogram are assigned to 2-methoxyphenol (1), 2-methoxy-4-vinylphenol (4), *trans*-2-methoxy-4-(prop-2-enyl)phenol (9), 2-methoxy-4-(propan-2-one)phenol (13) and 2-methoxy-4-(propanol) phenol (16). Sulphonate groups which occupy the α - or γ -position of the aliphatic side-chain of the lignin structural units are readily eliminated during pyrolysis. Hence a relatively high abundance of pyrolysis products with unsaturated aliphatic side-chains is observed.

The lignosulphonate pyrolysis products with preserved C_6C_3 structural units, listed in Table I, show a definite trend with respect to the molecular mass distributions. A total amount of 49% of intact phenylpropane structural units was obtained on Py-GC-MS analysis of sodium lignosulphonate. Lower fractions of preserved C_6C_3 structural units are obtained on pyrolysis of the lignosulphonates discharged by pulp mills (Table I). This indicates that a large proportion of the propane side-chains is dissociated during the pulping processes as a result of the cleavage of the interunit linkages in lignin. Small amounts (<1%) of 2,6-dimethoxyphenol derivatives are detected in the lignosulphonates discharged by PWA Mannheim and Holtzmann, which indi-

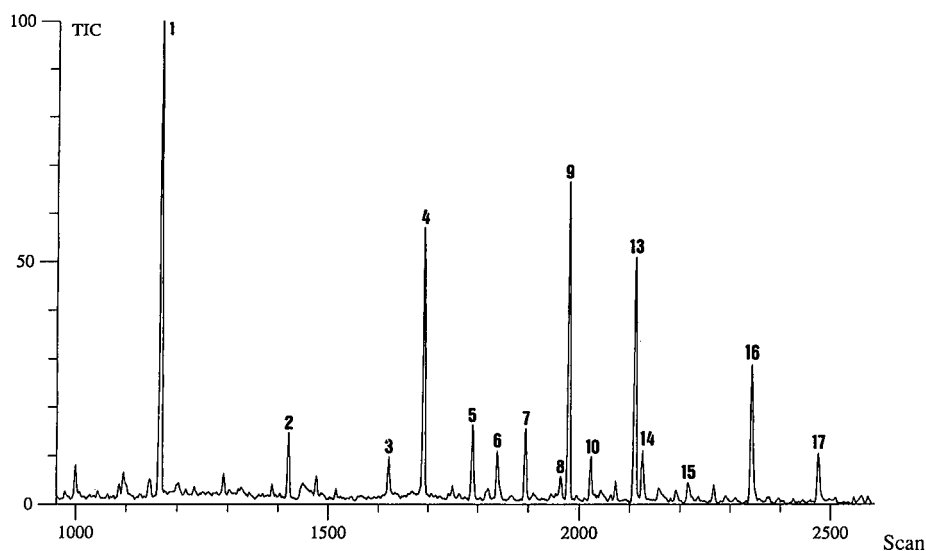


Fig. 5. Curie-point pyrolysis Py-GC-MS trace of sodium lignosulphonate. Peak numbers refer to Table II.

TABLE II

CURIE-POINT Py-GC-MS DATA FOR 2-METHOXYPHENOL PYROLYSIS PRODUCTS OF SODIUM LIGNOSULPHONATE (NaLS) AND LIGNOSULPHONATES DISCHARGED BY PWA MANNHEIM (A), HOLTZMANN KARLSRUHE (B) AND PWA ASCHAFFENBURG (C)

Peak No. ^a	Retention time (min)	Compound	Abundance (%)			
			NaLS	A	B	C
1	19.21	2-Methoxyphenol	23.6	19.7	18.0	17.4
2	23.38	2-Methoxy-4-methylphenol	3.2	8.9	12.4	12.2
3	27.02	2-Methoxy-4-ethylphenol	2.8	6.5	9.9	8.6
4	28.10	2-Methoxy-4-vinylphenol	12.7	11.8	20.4	17.5
5	29.50	2-Methoxy-4-(prop-1-enyl)phenol	3.9	4.5	4.9	3.0
6	30.41	2-Methoxy-4-formylphenol	2.8	12.1	4.1	10.2
7	31.36	2-Methoxy-4-(prop-2-enyl)phenol (<i>cis</i>)	3.6	2.1	2.4	3.4
8	32.40	2-Methoxy-4-(ethanal)phenol	1.1	—	—	—
9	33.02	2-Methoxy-4-(prop-2-enyl)phenol (<i>trans</i>)	14.9	8.9	10.3	12.9
10	33.47	2-Methoxy-4-acetylphenol	2.2	2.9	2.1	2.6
11	33.54	2-Methoxyphenol-4-(C ₃ H ₃) derivative	—	5.3	5.9	3.5
12	34.08	2-Methoxyphenol-4-(C ₃ H ₃) derivative	—	4.0	4.3	4.2
13	35.15	2-Methoxy-4-(propan-2-one)phenol	13.1	5.9	5.2	3.3
14	35.26	2-Methoxy-4-(ethanol)phenol	2.6	0.4	—	—
15	37.05	2-Methoxy-4-(propanal)phenol	1.6	1.8	—	1.2
16	39.05	2-Methoxy-4-(propanol)phenol	8.7	2.5	—	—
17	41.26	2-Methoxy-4-(prop-2-enal)phenol	3.2	2.7	—	—

^a See Fig. 5.

cates that only softwood is used in the pulping process. Only the lignosulphonates discharged by PWA Aschaffenburg contain a mixture or copolymer of 2-methoxyphenol and 2,6-dimethoxyphenol lignin. A 2-methoxyphenol/2,6 dimethoxyphenol ratio of 0.7 was calculated from the Py-GC-MS data by summing all 2-methoxyphenol and 2,6-dimethoxyphenol pyrolysis products. The lignosulphonates present in the effluent of PWA Aschaffenburg contain 31% of 2-methoxyphenol derivatives with intact propane side-chains and 38% of 2,6-dimethoxyphenol derivatives with intact C₆C₃ structural units such as 2-methoxy-4-(prop-1-enyl)phenol, *trans*-2-methoxy-4-(prop-2-enyl)phenol and 2-methoxy-4-(propan-2-one)phenol. These results suggest that the 2-methoxyphenol structural units are more reactive towards sulphonation and hydrolysis reactions than 2,6-dimethoxyphenol structural units. A total amount of 32% of preserved phenylpropanoid structural units was calculated for the lignosulphonates present in the effluent of PWA Aschaffenburg.

Phenol and dihydroxybenzene derivatives are

also detected in the pyrolysates of the lignosulphonates discharged by pulp mills such as phenol, 4-methylphenol, 4-ethylphenol, 4-vinylphenol, dihydroxybenzene and 4-methyldihydroxybenzene. These compounds are not detected in the mildly isolated sodium lignosulphonate standard used in this study. The relatively high abundance of these compounds in combination with the low abundance of preserved phenylpropane structural units clearly indicates that the original lignin polymer has been structurally changed as a result of demethylation, demethoxylation and condensation reactions which occur during the pulping processes. A detailed list of all the pyrolysis products observed on Py-GC-MS analysis of lignosulphonates in the pulp mill effluents used in this study has recently been published by Van Loon *et al.* [4].

Residual polysaccharides are detected in all effluent samples. Small amounts of chlorinated phenolic pyrolysis products are observed in the effluents of PWA Mannheim and Holtzmann such as 2-methoxy-6-chlorophenol, 2-methoxy-

4-methyl-6-chlorophenol, 2-methoxy-4-vinyl-6-chlorophenol, 2-methoxy-4-(prop-2-enyl)-6-chlorophenol, 2-methoxy-4-(propan-2-one)-6-chlorophenol and 2-methoxy-4-(chloropropyl)phenol. These chlorinated lignin structural units are formed during the bleaching sequences which are applied to the paper pulp in order to remove residual lignins.

CONCLUSIONS

Several secondary separation effects, which occur when using the TSK G3000SW column, were investigated and could be strongly reduced using a mobile phase of 0.2 M sodium acetate at pH 7. The molecular mass distributions show distinct differences between the various lignosulphonate samples and can be used to characterize structural modifications.

HPASEC traces obtained with 0.01 M sodium acetate as the eluent are characteristic and allow "fingerprinting" of sulphite pulp mill effluents. The relatively high chromatographic resolution makes this system potentially useful for fractionation and subsequent spectrometric analysis of lignosulphonates.

The combined HPASEC and Py-GC-MS data show that the sodium lignosulphonate standard, which is prepared under relatively mild conditions, is a relatively polydisperse polymer with a large proportion of preserved phenylpropane structural units. This water-soluble macromolecule still contains features of a natural lignin polymer. The lignosulphonates discharged by paper pulp mills are more monodisperse macromolecules of a lower molecular mass which are modified to a greater extent.

ACKNOWLEDGEMENTS

The Water Transport Company Rijn-Kennemerland (WRK), Nieuwegein, Netherlands, and the Dutch Organization for Scientific Research (NWO) are gratefully acknowledged for their financial support. This work is part of the research program of the Foundation for Fundamental Research of Matter (FOM).

REFERENCES

- 1 D.W. Glennie, in K.V. Sarkanen and C.H. Ludwig (Editors), *Lignins*, Wiley, New York, 1971, pp. 597–631.
- 2 K. Kummerer and P. Krauss, *Gewässerschutz, Wasser, Abwasser*, 114 (1990) 109–136.
- 3 L. Huber and H. Baumung, *Water Sci. Technol.*, 20 (1988) 19.
- 4 W.M.G.M. van Loon, J.J. Boon and B. de Groot, *J. Anal. Appl. Pyrol.*, 20 (1991) 275–302.
- 5 D. Budin and L. Susa, *Holzforchung*, 36 (1982) 17–22.
- 6 P.L. Dubin (Editor), *Aqueous Size-Exclusion Chromatography (Journal of Chromatography Library, Vol. 40)*, Elsevier, Amsterdam, 1988.
- 7 H.G. Barth, *J. Chromatogr. Sci.*, 18 (1980) 409–429.
- 8 E. Pfannkoch, K.C. Lu, F.E. Regnier and H.G. Barth, *J. Chromatogr. Sci.*, 18 (1980) 430–441.
- 9 T. Vartiainen, A. Liimatainen and P. Kauranen, *Sci. Total Environ.*, 62 (1987) 75–84.
- 10 K. Lindström and F. Österberg, *Holzforchung*, 38 (1984) 201.
- 11 F. Österberg and K. Lindström, *Holzforchung*, 39 (1985) 149.
- 12 J.J. Boon, in A. Chesson and E.R. Ørskov (Editors), *Physico-Chemical Characterisation of Plant Residues for Industrial and Feed Use*, Elsevier Applied Science, London, 1989, pp. 25–49.
- 13 J.J. Boon, A.D. Pouwels and G.B. Eijkel, *Biochem. Soc. Trans.*, 15 (1987) 170.
- 14 W.M.G.M. van Loon, A.D. Pouwels, P. Veenendaal and J.J. Boon, *Int. J. Environ. Anal. Chem.*, 38 (1990) 255–264.
- 15 A.D. Pouwels and J.J. Boon, *J. Wood Chem. Technol.*, 7 (1987) 197.
- 16 N. Dunlop-Jones and L.H. Allen, *Tappi J.*, 2 (1988) 109.
- 17 N.G. Lewis and W.Q. Yean, *J. Chromatogr.*, 331 (1985) 419–424.
- 18 K.K. Unger, *Porous Silica*, Elsevier, Amsterdam, 1979, pp. 130–141.
- 19 S. Mori, *Anal. Chem.*, 61 (1989) 530–534.
- 20 R.C. Weast (Editor), *Handbook of Chemistry and Physics*, 56th ed., CRC Press, Cleveland, OH, 1975, p. D-150.
- 21 G.R. Aiken, D.M. McKnight and R.L. Wershaw (Editors), *Humic Substances in Soil, Sediment, and Water*, Wiley, New York, 1985, pp. 477–492.
- 22 G.L. Amy, M.R. Collins, C.J. Kuo and P.H. King, *Proc. AWWA Annu. Conf.*, (1985) 1347–1361.
- 23 P.R. Gupta and J.L. McCarthy, *Macromolecules*, 1 (1968) 236.
- 24 H. Hassi, P. Tikka and E. Sjöström, *Tappi (Proc. Int. Sulphite Pulping Conf.)*, (1982) 165–170.
- 25 D.A.I. Goring, in K.V. Sarkanen and C.H. Ludwig (Editors), *Lignins*, Wiley, New York, 1971, pp. 695–768.

Comparison of high-performance liquid and gas chromatography in the determination of organic acids in culture media of alkaliphilic bacteria

Sari Paavilainen* and Timo Korpela

Department of Biochemistry, University of Turku, SF-20500 Turku (Finland)

(First received October 14th, 1992; revised manuscript received December 21st, 1992)

ABSTRACT

Volatile and non-volatile organic acids were analysed by high-performance liquid chromatography (HPLC) on an Aminex HPX-87H, gas–solid chromatography (GSC) on a Porapak Q and gas–liquid chromatography (GLC) on a fused-silica capillary column. The results were compared by using standard acid solutions and with culture media of two strains of alkaliphilic *Bacillus*. Whereas the resolution of acids was excellent with GLC, the quantitative reproducibility was better with HPLC. Identification of complex culture mixtures was accomplished by GC–MS. Applicability of the methods for different purposes is discussed.

INTRODUCTION

The identification and determination of acidic fermentation products formed in culture media of microbes are useful for many purposes; for example, monitoring of microbial media during the industrial preparation of various food products is important for their quality control. In addition, acids formed in microbial culture media are analysed in clinical chemistry. The third main field is in studying the metabolic pathways in bacteria.

The methods used to determine acidic metabolites in the cultivation media of microbes include thin-layer (TLC) [1], gas–solid (GSC) [2], gas–liquid (GLC) [3] and high-performance liquid chromatography (HPLC) [4]. At present, GLC and HPLC are the most popular as identification and determination are more straightforward and precise than the other available methods.

The GC procedures require separate treatments of the samples for volatile and non-volatile acids. The volatile acids can be assayed in the acidified cultural media directly [2] or after extraction with an organic solvent, whereas non-volatile acids require derivatization [5–7]. With HPLC all acids can be analysed in one sample whenever the column resolution allows [8–10]. In recent years HPLC has become more widespread owing to the improved column selectivity and detector sensitivity. Analyses of short-chain acids using HPLC and packed GC columns have been compared previously [8,11]. In this work, volatile and non-volatile acids were analysed by HPLC, GSC with a packed column and GLC with a capillary column.

EXPERIMENTAL

Bacteria and culture conditions

Bacillus circulans var. *alkalophilus* (ATCC 21783) and alkaliphilic *Bacillus* sp. 17-1 (ATCC 31007) were cultivated in a basal carbonate medium containing 1% starch, 0.5% bacto-pan-

* Corresponding author.

tone (Difco, Detroit, MI, USA), 0.5% yeast extract (Difco) and mineral salts [12]. Sodium carbonate (10%) was separately sterilized and added to obtain a 1% concentration in the final medium. The medium (200 ml) was inoculated with 10 ml of preculture in a 500-ml erlenmeyer flask on a shaker at 37°C. Samples (5 ml) were taken automatically with a sampling device at intervals of 4 h [13]. Bacterial cells were removed by centrifugation and the supernatants were stored at –20°C until used.

High-performance liquid chromatography

Organic acids were separated on an Aminex HPX-87H organic acid analysis column (300 mm × 7.8 mm I.D.; 9 μm particle size) (Bio-Rad Labs., Richmond, CA, USA) equipped with an Aminex HPX-87H Micro-Guard column (30 mm × 4.6 mm I.D.) and holder (Bio-Rad Labs.). The HPLC column was connected to a Waters (Milford, MA, USA) Model 510 pump equipped with a Rheodyne (Cotati, CA, USA) Model 7125 injector (20-μl sample loop) and to a Model 2142 refractive index detector (LKB, Bromma, Sweden) with a Model C-R3A integrator (Shimadzu, Kyoto, Japan). The mobile phase was 0.004 M sulphuric acid. The column was operated at the room temperature and the flow-rate of the mobile phase was 0.6 ml/min.

Bacterial cultures were centrifuged at 5000 g for 30 min to remove cells. A 1-ml volume of supernatant was transferred into a 5-ml capped tube. A 0.25-ml volume of 9.0 M sulphuric acid, 0.6 g of sodium chloride and 5 ml of diethyl ether were added to the tube. The samples were treated with a vortex mixer for 1 min and centrifuged at 1000 g for 5 min. The ether phases were transferred into clean glass tubes and 1.0 ml of 0.1 M NaOH solution was added. The ether phase was extracted with a vortex mixer and the turbid mixture was centrifuged at 1000 g for 5 min. The diethyl ether phases were then removed. The residual diethyl ether in the aqueous phase was allowed to evaporate from the open tubes overnight at room temperature [10]. The standards for HPLC and GLC were the same and they were treated in the same way as culture samples. No internal standard was necessary with HPLC.

Gas chromatography

Volatile and non-volatile acids were analysed on a fused-silica capillary column coated with nitroterephthalate-modified polyethylene glycol NB-351 (25 m × 0.32 mm I.D., $d_f = 0.2 \mu\text{m}$) (HNU-Nordion, Helsinki, Finland). Volatile acids were also analysed on a glass column (2.20 m × 2.0 mm I.D.) packed with Porapak Q (80–100 mesh) [2]. A Varian (Palo Alto, CA, USA) Model 3700 gas chromatograph equipped with a flame ionization detector connected to an HP 3388A integrator (Hewlett-Packard, Avondale, PA, USA) was used. The operating conditions for the capillary column were injector temperature 200°C, detector temperature 230°C and column temperature programmed from 60 to 200°C at 6°C/min. The flow-rates were 1.2 ml/min for the carrier gas (nitrogen), 300 ml/min for air and 30 ml/min for hydrogen. The splitting ratio was 50:1. The conditions for the packed column were injector temperature 230°C, detector temperature 250°C and column temperature programmed from 150 to 240°C at 10°C/min.

Volatile fatty acids were extracted into diethyl ether [6] with a slight modification. A 0.4-ml volume of 10 M sulphuric acid, 1 g of sodium chloride and 2 ml of diethyl ether were added to 2 ml of culture supernatant. The amples were treated with a slowly rotating mixer for 30 min. Two phases were separated by centrifugation for 5 min at 1000 g and the ether layer was transferred into another tube with a Pasteur pipette. The standard mixture contained formic, acetic, propionic, butyric, valeric and caproic acid (2 mg/ml of each in water). Evaporation of the sample and the injection volume (0.5 μl) were corrected using hexadecane as an internal standard (20 μl/l of diethyl ether). Standard solutions were treated in the same way as the supernatants from bacterial cultivations. Volatile acids were also analysed using a packed glass column directly from culture samples which were made acidic with oxalic acid [2].

For analysis of non-volatile acids, methanol (4 ml) and 10 M sulphuric acid (0.75 ml) were added to 2 ml of culture supernatant or of the standard mixture [6]. The tubes were stoppered and stirred with a vortex mixer and kept at 60°C for 30 min. Then 2 g of sodium chloride, 2 ml of

water and 2 ml of chloroform were added and the tubes were blended and centrifuged. The chloroform layers were transferred into other tubes. The standard mixture contained pyruvic, oxalic, lactic, fumaric, malonic and benzoic acid (3 mg/ml of each in water). A small amount of sodium hydroxide was added to get all of the acids into solution.

Gas chromatography–mass spectrometry

The GC–MS system consisted of a VG Analytical (Wythenshawe, UK) Model 7070E organic mass spectrometer equipped with a VG Model 11-250 data system and a Dani (Monza, Italy) Model 3800 HR gas chromatograph. The capillary GC operating conditions were as above except that the programming rate was 4°C/min and the carrier gas was helium.

RESULTS

Analyses of standard mixtures

Results for standard mixtures of organic acids

obtained by HPLC and GLC are given in Tables I and II. Relative retention times (*RRT* values) and response factors (*RF* values) of volatile acids are expressed with respect to caproic acid (Table I), whereas *RRT*s and *RF*s of non-volatile acids are compared with fumaric acid (Table II). The theoretical plate numbers (*N*) for the HPLC, GLC and GSC columns were calculated with the “Sigma 5” method for peaks of Gaussian shape and were 10 000, 200 000–300 000 and 6000–10 000, respectively.

With HPLC all volatile standard acids were separated at room temperature (Table I) with 0.004 *M* sulphuric acid as the mobile phase. However, the retention times (*t_R* values) were fairly long. For example, that of caproic acid was about 60 min which is three times longer than with GLC. The precision of the *RRT* values of acids with HPLC was usually very high (R.S.D. <1%, *n* = 5; results not shown). Among the non-volatile acids pyruvic, malonic, lactic and fumaric acid separated as individual peaks. Oxalic acid eluted immediately after the solvent peak and was broad compared with the other

TABLE I

RELATIVE RETENTION TIMES (*RRT*) AND RESPONSE FACTORS (*RF*) OF VOLATILE ACIDS WITH RESPECT TO CAPROIC ACID

The extraction recoveries are shown for HPLC. The reproducibilities of the *RF* values of HPLC and GLC analyses are expressed as the standard deviation (S.D.; *n* = 5) and the relative standard deviation (R.S.D.). The concentration of each of the acids in aqueous solution was 0.2–1.0 mg/ml for HPLC and 2 mg/ml for GLC.

Acid	HPLC				GLC		
	<i>RRT</i> ^a	<i>RF</i> ^{b,c}	R.S.D. (%)	Extraction efficiency (%)	<i>RRT</i> ^a	<i>RF</i> ^{b,c}	R.S.D. (%)
Formic	0.24	0.33 ± 0.01	3.0	64	–	–	–
Acetic	0.27	0.48 ± 0.01	2.1	70	0.60	0.33 ± 0.01	3.0
Propionic	0.32	0.80 ± 0.23	28.8	84	0.69	0.88 ± 0.03	3.4
Butyric	0.40	0.88 ± 0.04	4.5	100	0.78	0.99 ± 0.06	6.1
Valeric	0.61	0.89 ± 0.01	1.1	100	0.89	0.91 ± 0.07	7.7
Caproic	1.00	1.00		100	1.00	1.00	

^a *RRT* = relative retention time with respect to caproic acid.

$$^b \text{RF} = \text{response factor} = \frac{(\text{area})_{\text{acid}}(\text{mass})_{\text{caproic}}}{(\text{area})_{\text{caproic}}(\text{mass})_{\text{acid}}}$$

^c ± Values are standard deviations (S.D.) of five independent measurements including extractions of standard mixtures compared with caproic acid, which was assigned a value of *RF* = 1.00 in each run.

TABLE II

RELATIVE RETENTION TIMES (*RRT*) AND RESPONSE FACTORS (*RF*) OF NON-VOLATILE ACIDS WITH RESPECT TO FUMARIC ACID

The extraction recoveries are shown for HPLC. The reproducibilities of the *RF* values are expressed as in Table I. The concentration of each of the acids in aqueous solution was 3 mg/ml.

Acid	HPLC				GLC		
	<i>RRT</i> ^a	<i>RF</i> ^{b,c}	R.S.D. (%)	Extraction efficiency (%)	<i>RRT</i> ^a	<i>RF</i> ^{b,c}	R.S.D. (%)
Oxalic	0.42	0.69 ± 0.09	13.0	35	0.79	0.69 ± 0.05	7.2
Pyruvic	0.54	0.41 ± 0.04	9.8	47	0.55 ^d 0.75 ^d	0.57 ± 0.08 ^d	14.0
Malonic	0.61	0.38 ± 0.01	2.6	42	0.94	0.97 ± 0.02	2.1
Lactic	0.76	0.27 ± 0.01	3.7	28	0.65	0.69 ± 0.10	14.5
Fumaric	1.00	1.00	—	100	1.00	1.00	—
Benzoic	—	—	—	—	1.12	0.84 ± 0.01	1.2

^a *RRT* with respect to fumaric acid.

$${}^b RF = \frac{(\text{area})_{\text{acid}}(\text{mass})_{\text{fumaric}}}{(\text{area})_{\text{fumaric}}(\text{mass})_{\text{acid}}}$$

^c Standard deviation (S.D.) of five independent measurements including extractions of standard mixtures compared with fumaric acid, which was assigned a value of *RF* = 1.00 in each run.

^d Pyruvic acid decomposed under the conditions used and yielded two peaks. The areas of the two peaks were summed and compared with fumaric acid.

standard acid peaks. Benzoic acid was not eluted from the column with 0.004 *M* sulphuric acid (Table II).

Volatile acids were analysed by GLC directly from diethyl ether phases of acidified samples and non-volatile acids from chloroform after derivatization with methanol–sulphuric acid. All the volatile and methyl esters of non-volatile standard acids were separated well. The acids showed sharp, symmetrical peaks with baseline resolution, except pyruvic acid, which appeared as two peaks. The *RF* of formic acid was near to zero when using flame ionization detection (FID). The R.S.D. (*n* = 5) of the *RRT* values was < 1% with GLC.

With GLC the *RF* values of volatile acids were higher than with HPLC, except for formic and acetic acid. The R.S.D.s (*n* = 5) of the *RF* values with HPLC ranged from 1.1% (valeric acid) to 4.5% (butyric acid), but for propionic acid it was 28.8% (Table I). This high R.S.D. was due to a “negative” peak near the signal from the acid.

Generally, the variation of *RF* values of compounds other than propionic acid with GLC was higher (from 3.0 to 7.7%) than with HPLC (Table I). The *RF* values of methyl esters of non-volatile compounds were also higher with GLC than the *RF* values of the free acids with HPLC (Table II). The *RF* values of non-volatile compounds had more variation than volatile acids when analysed with both methods.

The amounts of extracted acids were compared with unextracted standards using HPLC (Table I). The recoveries were *ca.* 60, 70, and 80% for formic, acetic and propionic acid, respectively, and 100% for butyric, valeric and caproic acid when the concentration of each acid was 1 mg/ml or less. The extraction recovery of butyric and longer chain volatile acids decreased with increasing chain length and acid concentration. The extraction recoveries were smaller for non-volatile acids, ranging from *ca.* 30% (lactic acid) to 50% (pyruvic acid), with the exception of fumaric acid, for which the recovery

was 100%. The increased concentration did not interfere with the extraction of non-volatile compounds.

Analyses of fermentation media

GLC and HPLC results for the culture media of alkaliphilic *Bacillus* sp. 17-1 are illustrated in Fig. 1. Acetic acid was the most abundant (Fig.

1A and B). The culture sample also contained other volatile acids such as propionic, isobutyric, butyric and isovaleric acid, detected by both GLC and HPLC (Fig. 1A and B).

The standard solution of volatile acids (Fig. 2A) and culture samples of *Bacillus circulans* var. *alkalophilus* were subjected to GSC with a column of Porapak Q (Fig. 2B). Whereas little

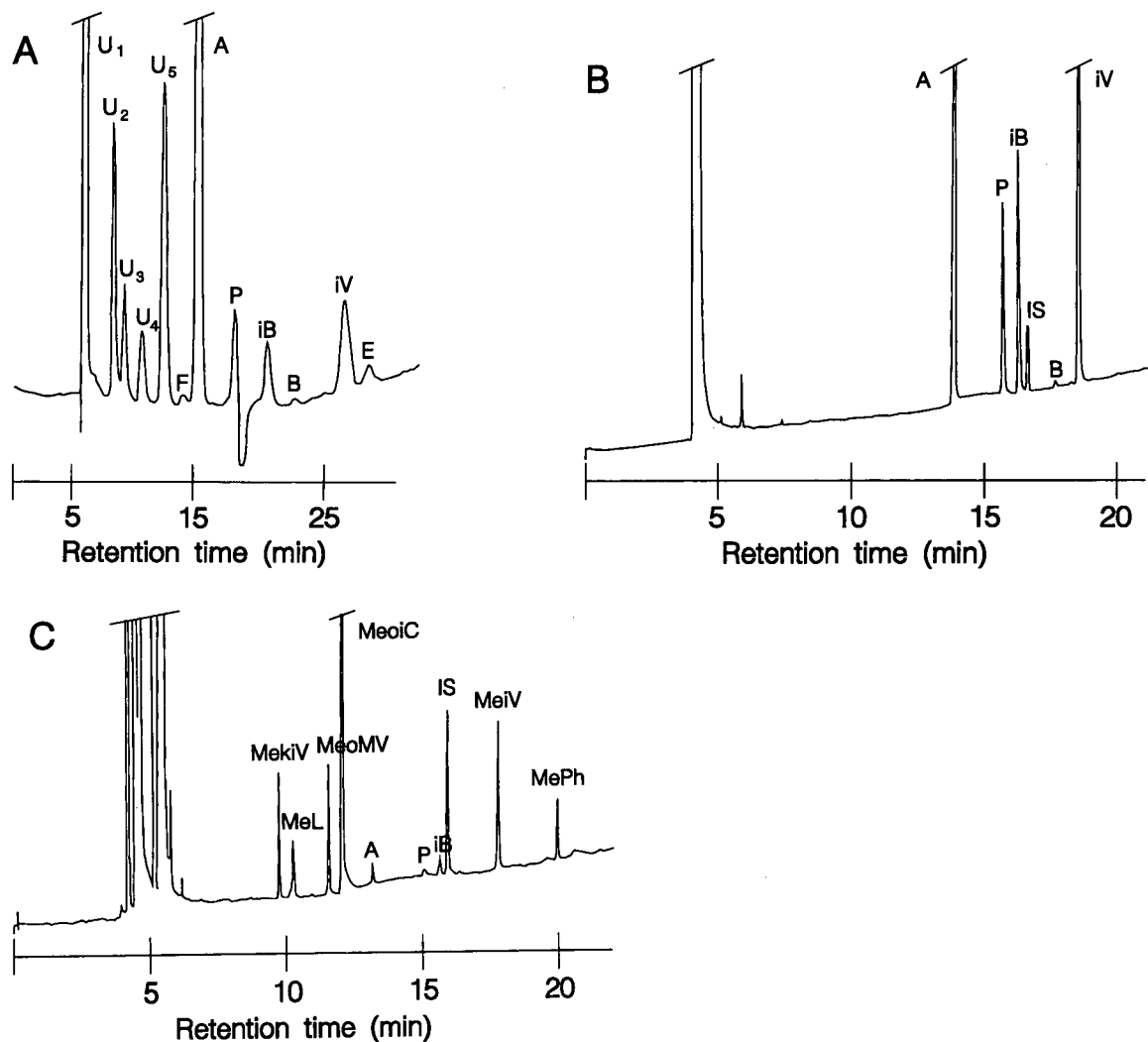


Fig. 1. Separation of short-chain acids from culture medium of alkaliphilic *Bacillus* sp. 17-1 (A) by HPLC as free acids, (B) by GLC as free acids and (C) by GLC as methyl esters. The compounds are abbreviated as follows: A = acetic acid; B = butyric acid; F = formic acid; iB = isobutyric acid; iV = isovaleric acid; MeiV = methyl isovalerate; MekIV = methyl α -ketoisovalerate; MeL = methyl lactate; MeoiC = methyl α -oxoisocaproate; MeoMV = methyl D - α -oxo- β -methylvalerate; MePh = methyl phenylacetate; IS = internal standard = hexadecane (20 μ l/l); U₁–U₅ = unidentified components; E = diethyl ether. Concentrations of identified compounds (mg/ml) in selected peaks: (A) F = 0.02, A = 3.40, P = 0.30, iB = 0.20, B = 0.01, iV = 0.35; (B) A = 3.45, P = 0.27, iB = 0.24, B = 0.01, iV = 0.40; and (C) MekIV = 0.30, MeL = 0.17, MeoMV = 0.32, MeoiC = 1.50 and MePh = 0.13. Injection volumes: (A) 20; (B) 0.5; and (C) 2 μ l.

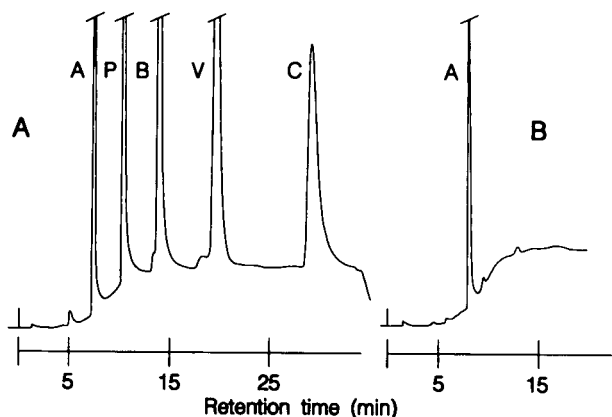


Fig. 2. GSC of (A) standard volatile short-chain acids and (B) culture medium of *Bacillus circulans* var. *alkalophilus* with Porapak Q. Standard solution contained (A) acetic, (P) propionic, (B) butyric, (V) valeric and (C) caproic acid. Formic acid was included in the standard mixture and the small peak (F) before acetic acid may represent it. Concentrations of the standard acids (A–C) were 2 mg/ml. The calculated concentration of A in (B) was 1.7 mg/ml. Injection volume, 1 μ l.

or no response was observed from formic acid, acetic acid was readily detected. Two small unknown peaks in the chromatogram after acetic acid (Fig. 2B) were already present in the uninoculated medium. Such compounds did not appear with the diethyl ether-extracted samples. Because there is no necessity for sample preparation, chromatography with Porapak Q is a valuable method when only a low resolution of volatile acids is required.

More detailed analyses of volatile and non-volatile acids of the bacterial culture media were done using GC–MS. The MS data bank system (see Experimental) was very helpful in the identification of methyl esters of unknown GLC peaks, showing the presence of α -ketoisovaleric, D - α -oxo- β -methylvaleric, α -oxoisocaproic and phenylacetic acid (MekIV, MeoMV, MeoiC and MePh, respectively, in Fig. 1C). These acids are also produced by several anaerobic bacteria [14].

The culture media of alkaliphilic *Bacillus* sp. 17-1 contained lactic acid. Its concentration was lower when analysed by GLC (MeL in Fig. 1C) than HPLC (U_5 in Fig. 1A). Succinic acid eluted at the same retention time as lactic acid with

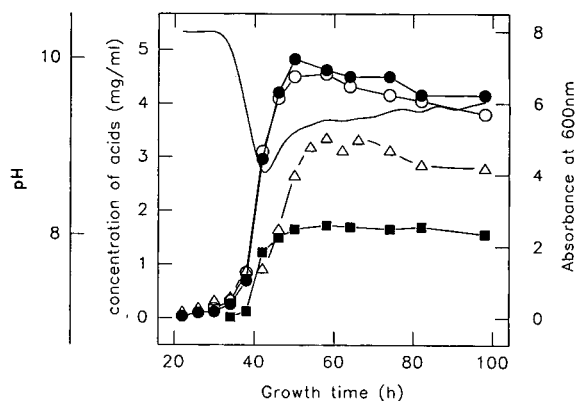


Fig. 3. Production of acetic and formic acid in cultivation medium of *Bacillus circulans* var. *alkalophilus*. Acetic acid was determined using (○) HPLC and (●) GLC and formic acid was determined using (■) HPLC. The growth (Δ) and pH (line without symbols) curves are included.

HPLC. However, succinic acid did not exist in the culture medium of this bacterium as it was not detected by GLC. The large lactic acid peak in HPLC may contain other acids, *e.g.* oxo-acids, which were identified by GC–MS. In the HPLC trace there were four other peaks (U_1 , U_2 , U_3 and U_4 , Fig. 1A) which were not identified. Two of them (U_3 and U_4) eluted close to pyruvic and malonic acid, but these acids were not detected with GLC. One peak (U_2) may belong to a sugar. Peak U_1 that comes with the solvent peak was much higher than the normal solvent peak and hence the media contain substances that are not separated with this column.

The kinetics of the appearance of acetic and formic acid in the culture medium with variation in pH during the growth of the alkaliphilic *Bacillus* are shown in Fig. 3. Acetic acid measured by GLC and HPLC correlated well with each other (Fig. 3). The formic acid curve was drawn according to the HPLC results because there was no FID response.

DISCUSSION

HPLC with an Aminex HPX-87H column has certain definite advantages over GLC for the separation of organic acids. All of the resolved acids can be analysed in one sample without derivatization. Filtered culture media can be

used without extraction [8], but this procedure may leave potentially interfering compounds in the samples [9]. Especially for the assay of formic acid with other readily evaporating acids and tricarboxylic acids, which are difficult to derivatize, HPLC is beneficial. In addition, the determination of carbohydrates from unextracted culture samples simultaneously with acids is possible with the Aminex-87H column when a refractive index detector is used [8]. However, some procedures are needed to decrease the t_R values or to improve the resolution of some acids. The t_R values of acids shorten on increasing the temperature of the eluent [15] or on increasing the proportion of acetonitrile from 5 to 11% for fumaric acid and certain aromatic carboxylic acids [9]. A higher column temperature (50°C) and 10% acetonitrile separated succinic and lactic acid, in addition to benzoic acid, although the retention time of the latter was still long [10].

The recovery of acids was studied in sodium hydroxide extracts of the HPLC samples (see Experimental). The recovery from standard mixtures ranged from 28% to 100% (Table I), which was higher than that reported previously [10] for diethyl ether extracts of pyruvic, lactic, acetic, propionic, butyric, valeric and caproic acid. The efficiency of extraction of volatile fatty acids increased with increasing carbon chain length when the concentration of acids was ≤ 1.0 mg/ml (Table I). When the concentration of each volatile acids was > 1.0 mg/ml the extraction recovery decreased for butyric and longer chain acids. Related results were also obtained after double extractions with diethyl ether–sodium hydroxide from water [16].

The GLC samples were prepared according to the method of Drucker [6]. Other methods such as derivatization with boron trifluoride–butanol [7] have many steps and boron halides in methanol have a very limited shelf-life [6]. Methylation with methanol and sulphuric acid is a simple and rapid technique, especially for large numbers of samples. The disadvantage of the methanol–sulphuric acid method is that not all of the tricarboxylic acid-cycle acids, *e.g.*, citric acid, are detected and two peaks appeared from pyruvic acid after derivatization. For identifica-

tion of TCA-cycle acids and for avoiding multiple peak formation from double bonds or from oxo-groups, trimethylsilyl derivatization has been used [17,18].

There was no FID response to formic acid and in general methyl esters of volatile acids were difficult to analyse because of the ease of evaporation and retention near the solvent peak. For example, the boiling point of methyl formate is only 31.8°C. These problems can be overcome by using another kind of detector or by using derivatization with butanol–sulphuric acid [19].

Poor resolution can bring about not only difficulties in identification of the chromatographic peaks but also errors in quantitative results. An advantage of GLC is the extremely high resolution of modern capillary columns. In this study, both volatile and methyl esters of non-volatile acids were separated well and the retention times remained reasonable (Fig. 1B and C). It has been stated that a stationary phase of very polar character allows the resolution of the largest number of methyl esters of acids [14].

With HPLC the relatively low resolution may produce problems. Parallel tests with high-resolution GLC can exclude possible errors. For example, the absence of succinic acid (peak U₅) in Fig. 1A was readily excluded with the aid of the results in Fig. 1C. Despite the generally much lower resolution of HPLC, aromatic acids are well separated with high k' values on commonly used HPLC columns [9]. For aromatic acids, an advantage of HPLC is the feasibility of utilizing the high sensitivity and selectivity of UV detectors [9]. Unfortunately, the detection of non-aromatic acids does not permit many alternatives.

An advantage of GC is the ease of the simultaneous use of MS for the identification of peaks in the chromatograms. MS combined with HPLC is a less advanced and not readily available method. However, the use of HPLC in the analysis of acids from microbial culture samples has become more common in recent years, apparently because of the facility of sample preparation and because different types of short-chain acids can be determined in a single analysis. The reproducibility of HPLC at the quantitative level is also better than that of GLC. However, when

the definite identity of various acids from bacteria is required, GC–MS is the method of choice.

REFERENCES

- 1 J.R. Norris and D.W. Ribbons (Editors), *Methods in Microbiology*, Vol. 6A, Academic Press, London, 1971.
- 2 M.H. Henderson and T.A. Steedman, *J. Chromatogr.*, 244 (1982) 337.
- 3 D.B. Drucker, *Microbiological Applications of Gas Chromatography*, Cambridge University Press, Cambridge, 1981.
- 4 D.B. Drucker, *Microbiological Applications of High-Performance Liquid Chromatography*, Cambridge University Press, Cambridge, 1987.
- 5 A.F. Rizzo, *J. Clin. Microbiol.*, 11 (1980) 418.
- 6 D.B. Drucker, *J. Chromatogr.*, 208 (1981) 279.
- 7 C.W. Moss and O.L. Nunez-Montiel, *J. Clin. Microbiol.*, 15 (1982) 308.
- 8 G.G. Ehrlich, D.F. Goerlitz, J.H. Bourell, G.V. Eisen and E.M. Godsy, *Appl. Environ. Microbiol.*, 42 (1981) 878.
- 9 G.O. Guerrant, M.A. Lambert and C.W. Moss, *J. Clin. Microbiol.*, 16 (1982) 355.
- 10 R.F. Adams, R.L. Jones and P.L. Conway, *J. Chromatogr.*, 336 (1984) 125.
- 11 W.H. Loh, N. Santoro, R.H. Miller and O.H. Tuovinen, *J. Gen. Microbiol.*, 130 (1984) 1051.
- 12 M.J. Mäkelä, S.K. Paavilainen and T.K. Korpela, *Can. J. Microbiol.*, 36 (1990) 176.
- 13 M. Mäkelä, S. Paavilainen and T. Korpela, *Lab. Pract.*, 37 (1988) 69.
- 14 J.P. Carlier and N. Sellier, *J. Chromatogr.*, 493 (1989) 257.
- 15 W.K. Chong, G.A. Mills, G.P. Weavind and V. Walker, *J. Chromatogr.*, 487 (1989) 147.
- 16 C. Lucarelli, L. Radin, R. Corio and C. Eftimiadi, *J. Chromatogr.*, 515 (1990) 415; see also ref. 50 cited therein.
- 17 A. Pinelli and A. Colombo, *J. Chromatogr.*, 118 (1976) 236.
- 18 H. Rosenqvist, H. Kallio and V. Nurmikko, *Anal. Biochem.*, 46 (1972) 224.
- 19 J.P. Salanitro and P.A. Muirhead, *Appl. Microbiol.*, 29 (1975) 374.

Series-coupled capillary columns for the separation of N,(O)-trifluoroacetyl isopropyl derivatives of D,L-aspartic acid and L-hydroxyproline by gas chromatography

Xianwen Lou, Xueliang Liu and Liangmo Zhou*

Dalian Institute of Chemical Physics, Chinese Academy of Sciences, 129 Street, Dalian 116012 (China)

(First received July 16th, 1992; revised manuscript received December 3rd, 1992)

ABSTRACT

N-Trifluoroacetyl (TFAc)-D,L-aspartic acid (Asp) isopropyl ester and N,O-TFAc-L-hydroxyproline (Hpr) isopropyl ester, which give overlapping peaks when a single chiral capillary column is used, were separated with a cross-linked polycyanoethyl vinyl siloxane-L-Val-*tert.*-butylamide capillary column coupled in series with either a cross-linked polyethylene glycol 20M capillary column or a wall-coated OV-101 capillary column. A method for calculating the appropriate lengths of the coupled columns was developed. D,L-Asp and L-Hpr in real samples were also separated using the series-coupled column systems.

INTRODUCTION

Most amino acids in nature are of L configuration. However, in tissues such as bone [1,2], tooth [3], eye lens [4] and brain [5], all of them have a slow turnover rate. Therefore, D-amino acids tend to accumulate and increase in concert with ageing [6]. The racemization in living cells, which do not exhibit renewal processes, is of importance in the study of ageing phenomena. The racemization of amino acids in dead, fossilized materials can be employed as a dating parameter [7]. Among the amino acids, aspartic acid (Asp) is the most frequently used for age estimation [8]. Unfortunately, the N-trifluoroacetyl (TFAc) isopropyl ester of Asp is seriously overlapped by the N,O-TFAc isopropyl ester of

L-hydroxyproline (Hpr), a common component in living tissues and fossilized materials, when a cross-linked polycyanoethyl vinyl siloxane-L-Val-*tert.*-butylamide capillary column is used.

Several methods, such as stationary phase tuning, mixed-phase columns and series-coupled columns, for selectivity tuning have been reported [9]. The series-coupled column systems are the most important because they are convenient and can present a general applicable technique for optimizing selectivities when capillary columns are to be used [10]. Selectivity can be obtained with the coupled columns by using different lengths or phase ratios of the columns, by adjusting the flow-rate through each column or by operating each column at different temperatures [11]. This technique has been studied and applied by several groups [9–17]. However, the use of this approach has not been fully investigated in the separation of enantiomers.

In this work, two different capillary columns,

* Corresponding author.

polyethylene glycol (PEG) 20M and OV-101, were series-coupled to a cross-linked polycyanoethyl vinyl siloxane–L-Val-*tert.*-butylamide capillary. The lengths of the coupled columns needed for the separation of the derivatives of D,L-Asp and L-Hpr were calculated and optimized.

THEORY

There is general agreement among several workers that the effective capacity factor, $k'(\text{eff})$, for a system of series-coupled columns can be calculated by

$$k'(\text{eff}) = \sum_{i=1}^n \phi(i)k'(i) \quad (1)$$

$$\phi(i) = t(mi)/t(m) = t(mi) / \sum_{i=1}^n t(mi) \quad (2)$$

$$t(mi) = L(i)/\overline{u(i)} \quad (3)$$

where $k'(i)$, $t(i)$, $\phi(i)$, $L(i)$ and $\overline{u(i)}$ are the capacity factor, carrier gas hold-up time, fractional carrier gas hold-up time, length and average carrier gas velocity of the i th column, respectively [10].

For a two-column system:

$$\begin{aligned} k'(\text{eff}) &= \phi(1)k'(1) + \phi(2)k'(2) \\ &= [t(m1)k'(1) + t(m2)k'(2)]/t(m) \\ &= [L(1)k'(1)/\overline{u(1)} + L(2)k'(2)/\overline{u(2)}]/t(m) \end{aligned} \quad (4)$$

The separation factor (α) of a pair of components (a and b) is defined as

$$\begin{aligned} \alpha &= k'(a)/k'(b) \\ &= \frac{L(1)k'(a1)/\overline{u(1)} + L(2)k'(a2)/\overline{u(2)}}{L(1)k'(b1)/\overline{u(1)} + L(2)k'(b2)/\overline{u(2)}} \end{aligned} \quad (5)$$

According to Guiochon and co-workers [12,18] $\overline{u(1)}$ and $\overline{u(2)}$ can be written as

$$\overline{u(1)} = j(1)u(a) \quad (6)$$

$$\overline{u(2)} = j(2)u(o) \quad (7)$$

$$j(1) = \frac{3}{2} \cdot \frac{p^2(i) - p^2(a)}{p^3(i) - p^3(a)} \cdot p(a) \quad (8)$$

$$j(2) = \frac{3}{2} \cdot \frac{p^2(a) - p^2(o)}{p^3(a) - p^3(o)} \cdot p(o) \quad (9)$$

$$p^2(a) = \frac{L(2)p^2(i) + L(1)p^2(o)}{L(1) + L(2)} \quad (10)$$

$$u(a)p(a) = u(o)p(o) \quad (11)$$

Let

$$t = \overline{u(1)}/\overline{u(2)} \quad (12)$$

Combining eqns. 6–12, we have

$$t = \frac{L(1)[p(a) - p(o)]}{L(2)[p(i) - p(a)]} \quad (13)$$

Let

$$x = \frac{t(m2)}{t(m1)} = \frac{L(2)/\overline{u(2)}}{L(1)/\overline{u(1)}} \quad (14)$$

Then eqn. 5 can be written as

$$\alpha = \frac{k'(a1) + xk'(a2)}{k'(b1) + xk'(b2)} \quad (15)$$

For a certain separation factor and resolution (R), the minimum effective plate number needed can be calculated from

$$N = \left(\frac{4R\alpha}{\alpha - 1} \right)^2 \quad (16)$$

The effective plate number is defined as

$$N = \left(\frac{t(R)}{\sigma} \right)^2 \quad (17)$$

$$\frac{1}{N} = \left(\frac{\sigma}{t(R)} \right)^2 \quad (18)$$

$$\begin{aligned} t(R) &= t(1) + t(2) \\ &= \frac{k'(1)L(1)}{u(1)} + \frac{k'(2)L(2)}{u(2)} \end{aligned} \quad (19)$$

If the extra-column effect can be ignored, then σ^2 can be written as

$$\begin{aligned} \sigma^2 &= \sigma^2(1) + \sigma^2(2) \\ &= \left(\frac{\sigma(1)t(1)}{t(1)} \right)^2 + \left(\frac{\sigma(2)t(2)}{t(2)} \right)^2 \end{aligned}$$

$$= \frac{[t(1)]^2}{N(1)} + \frac{[t(2)]^2}{N(2)} \quad (20)$$

$$N(i) = L(i)n(i) \quad (21)$$

Combining eqns. 14, 18, 19 and 20 yields

$$\frac{1}{N} = \frac{[k'^2(1)/N(1) + x^2k'^2(2)/N(2)]}{[k'(1) + xk'(2)]^2} \quad (22)$$

The ranges of x , $L(1)$ and $L(2)$ values can be calculated by an iterative technique by combining eqns. 12, 14, 15 and 22. In the first step, the effect of the velocity gradient along the column was ignored, and the columns used in our experiments had the same inner diameter (0.25 mm), hence $u(1) = u(2)$

$$x = \frac{L(2)/\overline{u(2)}}{L(1)/\overline{u(1)}} = \frac{L(2)}{L(1)} \quad (23)$$

After obtaining the ranges of L , $L(1)$ and $L(2)$ values, the approximate inlet pressure [$p(i)$] can be easily presumed for a practical average carrier gas velocity. Substituting these values into eqns. 10 and 13, the t value [$u(1)/u(2)$] can be calculated. Using this t value, more concise values of L , $L(1)$ and $L(2)$ can be obtained by combining eqns. 14, 15 and 22. Even more concise values of L , $L(1)$ and $L(2)$ can be reached by iteration of t several times. From a practical point of view, iteration of t twice is sufficient.

EXPERIMENTAL

Chromatographic conditions

The preparations of the fused-silica capillary columns, cross-linked polycyanoethyl vinyl siloxane-*L*-Val-*tert*-butylamide (column C), cross-linked PEG 20M (column P) and wall-coated OV-101 (column O), have been described previously [19–21].

Fused-silica tubing (2 cm × 0.53 mm I.D.) and two silicone rubber septa were used to connect columns in the two-column system (Fig. 1). The chromatographic separations were carried out with a GC R1A gas chromatograph equipped with a split injector and a flame ionization detector.

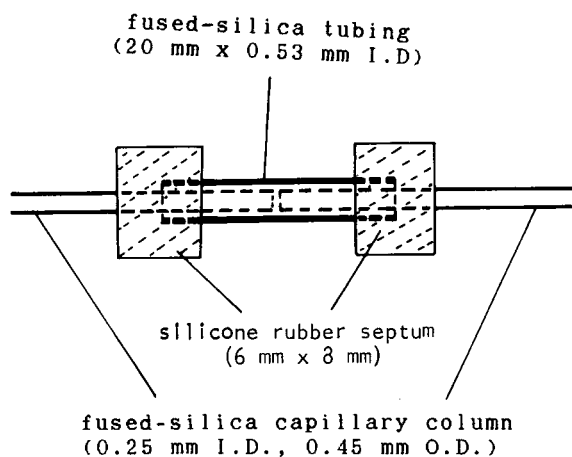


Fig. 1. Connection of the series-coupled columns.

Samples and derivatization

Aspartic acid (Asp) was obtained from Sigma. *L*-Hydroxyproline (Hpr) was kindly supplied by Professor X. Xu (Shanghai Institute of Materia Medica, Academia Sinica, Shanghai, China) and the tooth and bone samples by Ms. Y. Shun (Shanghai Institute of Expert Testimony, Shanghai, China). According to Wang *et al.* [8], the samples were hydrolysed in 6 *M* HCl at 110°C for 24 h and the hydrolysis products were treated with a column of Dowex AG 50W-X8, 100–200 mesh (Bio-Rad Labs., Munich, Germany), in the H⁺ form, eluted with 2 *M* aqueous ammonia. The amino acids were derivatized as *N*,(*O*)-trifluoroacetyl (TFAC) isopropyl esters according to McKenzie and Tenaschuk [22].

Calculations

An IBM-AT compatible microcomputer and software written in Quick-Basic Ver. 4.0 (Microsoft) were used for the calculations.

RESULTS AND DISCUSSION

The capacity factors (k') and separation factors (α) of the solutes are given in Tables I–III.

The *D/L* ratio of Asp is a widely used value for age estimation of living cells and fossilized materials. However, the peak of TFAC-*L*-Asp isopropyl ester is seriously overlapped by that of *N*,*O*-TFAC-*L*-Hpr isopropyl ester when using a cross-linked polycyanoethyl vinyl siloxane-*L*-

TABLE I

k' AND α VALUES OF THE SOLUTES ON CROSS-LINKED POLYCYANOETHYL VINYL SILOXANE-L-VAL-*TERT.*-BUTYLAMIDE COLUMN

Solute	120°C		130°C		140°C		150°C	
	k'	α	k'	α	k'	α	k'	α
D-Asp	11.98		7.18		4.48		2.84	
		1.051		1.040		1.031		1.025
L-Asp	12.59		7.47		4.62		2.91	
L-Hpr	12.72		7.50		4.64		2.91	

TABLE II

k' VALUES OF THE SOLUTES ON CROSS-LINKED PEG 20M COLUMN

Solute	120°C	130°C	140°C	150°C
D,L-Asp	15.84	9.36	5.63	3.50
L-Hpr	13.06	7.68	4.60	2.83

TABLE III

k' VALUES OF THE SOLUTES ON WALL-COATED OV-101 COLUMN

Solute	120°C	130°C	140°C	150°C
D,L-Asp	10.41	6.66	4.43	3.02
L-Hpr	7.82	5.04	3.37	2.30

Val-*tert.*-butylamide column (column C), and this situation cannot be improved simply by changing the column temperature (Table I). The use of series-coupled columns is the method of choice for selectivity tuning. The derivatives of Asp and L-Hpr can be readily separated with either a PEG 20M (column P) or an OV-101 column (column O) (Tables II and III). Therefore, it is possible that the derivatives of D,L-Asp and L-Hpr might be separated with column P or column O series-coupled to column C.

It is well known that direct chiral separations can only be carried out with chiral columns. The coupling of an achiral column will decrease the enantioselectivity of a chiral column (eqn. 15). Asp is an amino acid with low α values when using most diamide chiral stationary phases (CSPs) [23]. Therefore, the lengths of the cou-

pled columns must be carefully calculated and optimized.

The plots of α versus x [$L(2)\overline{u(1)}/L(1)\overline{u(2)}$] at 130°C are shown in Fig. 2. With a certain α value, the range of x values can be easily calculated from eqn. 15.

In order to obtain a satisfactory resolution between N-TFAC-D,L-Asp isopropyl ester and N,O-TFAC-L-Hpr isopropyl ester with reasonable column lengths, the minimum α values were set as 1.025 and the R values as 1.5. By an iterative technique and combining eqns. 13, 15 and 22, the range of x values, the column length ratios [$L(2)/L(1)$] and the minimum column lengths (L) can be obtained. Some results are given in Table IV.

Fig. 3 shows how $\overline{u(1)}/\overline{u(2)}$ changes with the column length ratio [$L(2)/L(1)$]. It is found that, with values of $p(i)/p(o) < 2.0$, the variation of $\overline{u(1)}/\overline{u(2)}$ is not significant over a wide range of $L(2)/L(1)$. In most open-tubular column

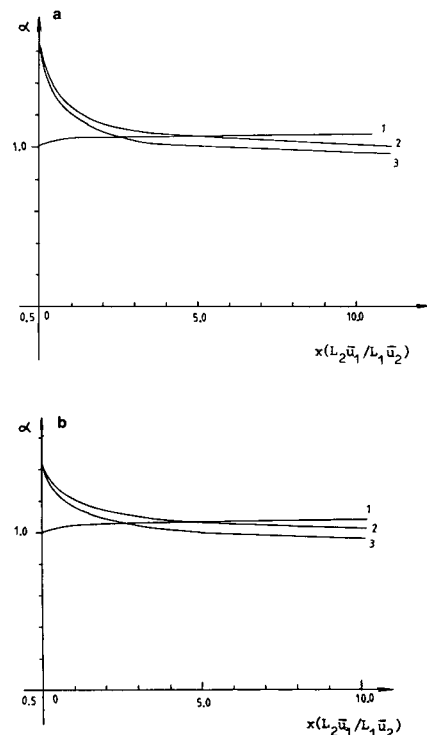
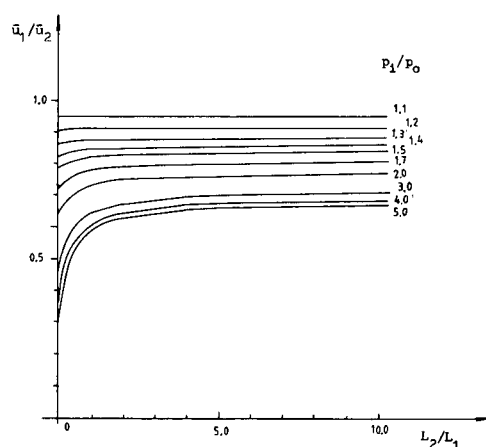


Fig. 2. Plots of α versus x at 130°C. (a) Column O-coupled to column C; (b) column P-coupled to column C. 1 = L-Asp/D-Asp; 2 = L-Asp/L-Hpr; 3 = D-Asp/L-Hpr.

TABLE IV

RANGES OF x , α AND $L(2)/L(1)$ OF THE SERIES-COUPLED COLUMN SYSTEMS UNDER ISOTHERMAL CONDITIONS [$p(i) = 0.15$ MPa, $p(o) = 0.10$ MPa]

Column coupling	Parameter ^a	120°C	130°C	140°C ^b	150°C ^b	
C-P	x	1.3–2.3	2.2–2.9			
	$\alpha(L/D\text{-Asp})$	1.025–1.032	1.025–1.028			
	$\alpha(D\text{-Asp}/L\text{-Hpr})$	1.061–1.025	1.040–1.026			
	First iteration					
	$L(2)/L(1)$	1.3–2.3	2.2–2.9			
	$t\{u(1)/u(2)\}$	0.82–0.83	0.83–0.83			
	Second iteration					
	$L(2)/L(1)$	1.6–2.8	2.7–3.5			
	$t\{u(1)/u(2)\}$	0.83–0.83	0.83–0.83			
	Third iteration					
	$L(2)/L(1)$	1.6–2.8	2.7–3.5			
C-O	x	0.9–2.2	1.6–2.9			
	$\alpha(L/D\text{-Asp})$	1.026–1.036	1.026–1.031			
	$\alpha(D\text{-Asp}/L\text{-Hpr})$	1.100–1.027	1.065–1.026			
	First iteration					
	$L(2)/L(1)$	0.9–2.2	1.6–2.9			
	$t\{u(1)/u(2)\}$	0.82–0.83	0.83–0.83			
	Second iteration					
	$L(2)/L(1)$	1.1–2.7	1.9–3.5			
	$t\{u(1)/u(2)\}$	0.83–0.83	0.83–0.83			
	Third iteration					
	$L(2)/L(1)$	1.1–2.7	1.9–3.5			

^a x is the ratio $L(2)\overline{u(1)}/L(1)\overline{u(2)}$.^b Dashes indicate no suitable values.Fig. 3. Variation of $\overline{u(1)/u(2)}$ with $L(2)/L(1)$.

systems, the values of $p(i)/p(o)$ are <2.0 because of their high permeability. Hence for calculating the ranges of $L(2)/L(1)$, $L(1)$ and $L(2)$, iteration of t twice is sufficient in most instances.

From Table IV, it can be seen clearly that at column temperatures of 120 and 130°C, the requirement of the α values can be met with certain ranges of x values with both series-coupled column systems, P-C and O-C. The achiral columns were used as the first column. Considering the analysis speed and the carrier gas velocity gradient, a total column length $L = 21.3$ m, $p(i)/p(o) = 1.5$, $x = 2.5$ [$L(2)/L(1) = 3$] and a column temperature of 130°C were selected for both systems. The α values of the systems were calculated and compared with the experimental results (Table V).

The chromatograms of N-TFAC-D,L-Asp isopropyl ester and N,O-TFAC-L-Hpr isopropyl ester obtained using column C and the series-coupled column systems are shown in Fig. 4. With the optimized lengths of the coupled columns, both pairs of solutes, Asp and Hpr and D,L-Asp, can be baseline separated. Fig. 5 shows

TABLE V

COMPARISON OF α VALUES FROM CALCULATION AND EXPERIMENT $L(1) = 5.3$ m, $L(2) = 16$ m, temperature = 130°C, $p(i) = 0.15$ MPa, $p(o) = 0.10$ MPa.

Solutes	Column O–column C		Column P–column C	
	Experimental	Calculated	Experimental	Calculated
D-Asp/L-Hpr	1.036	1.034	1.034	1.033
L-Asp/D-Asp	1.030	1.029	1.028	1.027

typical chromatograms of amino acids in tooth and bone samples obtained using column C and the series-coupled column systems.

CONCLUSIONS

A method for calculating the appropriate lengths of series-coupled columns was developed. With this method, good results for the separation of N-TFAC-D,L-Asp isopropyl ester and N,O-TFAC-L-Hpr isopropyl ester were obtained with two systems of series-coupled columns.

SYMBOLS

i Column index
 $j(i)$ James–Martin pressure correction factor (eqns. 6–9)
 $k(\text{eff})$ Effective capacity factor (eqn. 1)

$k(ai)$ Capacity factor of solute a on i th column
 $k(bi)$ Capacity factor of solute b on i th column
 L Total column length of the series-coupled system
 $L(i)$ Length of i th column
 N Effective plate number of the series-coupled system
 $N(i)$ Effective plate number of i th column
 n Effective plate number per metre of the system
 $n(i)$ Effective plate number per metre of i th column
 $p(a)$ Intermediate pressure
 $p(i)$ Inlet pressure
 $p(o)$ Outlet pressure
 R Resolution
 t Relative average velocity $\overline{u(1)}/\overline{u(2)}$ of the carrier gas
 $t(i)$ Adjusted retention time for a retained solute in i th column

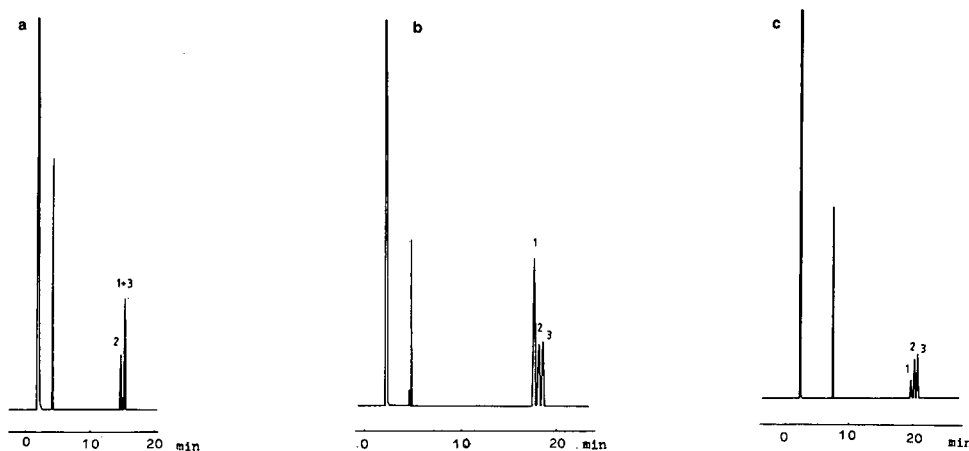


Fig. 4. Chromatograms of D,L-Asp and L-Hpr. Columns: (a) column C (16 m \times 0.25 mm I.D.); (b) column O (5.3 m \times 0.25 mm I.D.)–column C (16 m \times 0.25 mm I.D.) [$p(i) = 0.15$ MPa, $p(o) = 0.10$ MPa]; (c) column P (5.3 m \times 0.25 mm I.D.)–column C (16 m \times 0.25 mm I.D.) [$p(i) = 0.15$ MPa, $p(o) = 0.10$ MPa]. Temperature, 130°C; carrier gas, nitrogen; detector, flame ionization. Peaks: 1 = L-Hpr; 2 = D-Asp; 3 = L-Asp.

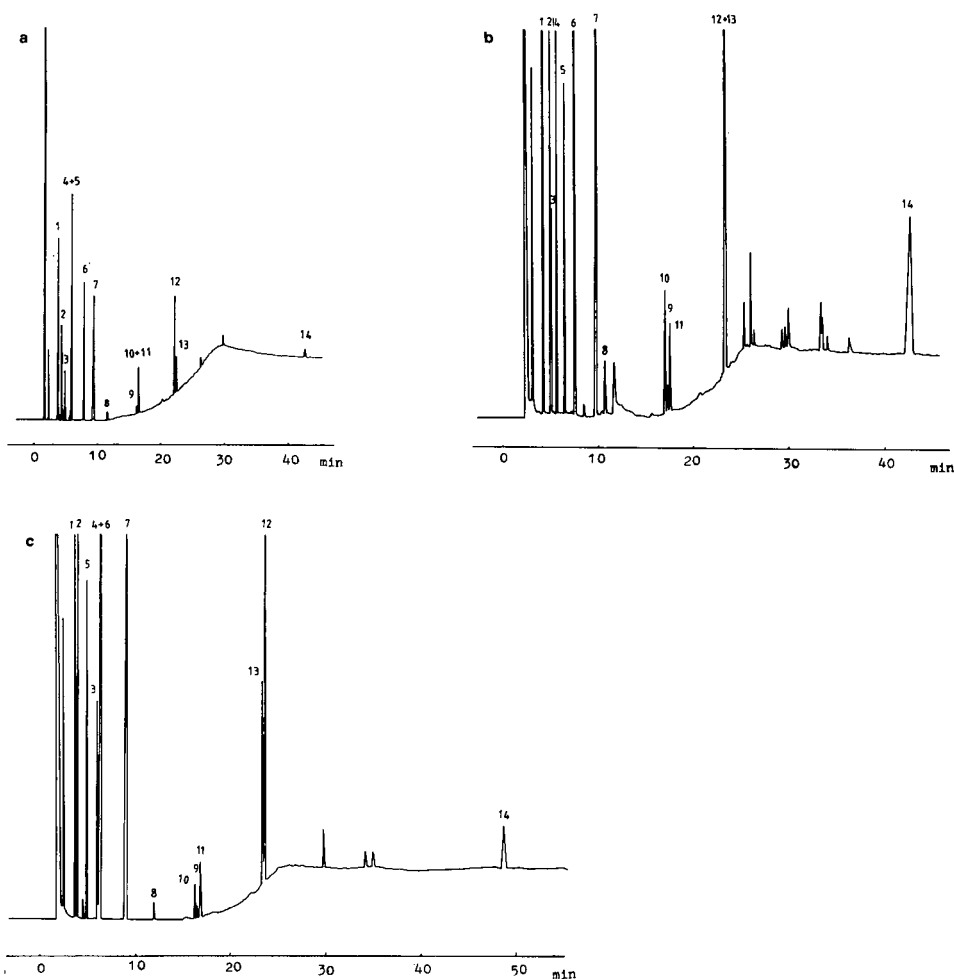


Fig. 5. Chromatograms of amino acids in real samples. (a) Sample, bone; column, C (16 m \times 0.25 mm I.D.); temperature, 120°C (10 min), then increased at 4°C/min to 190°C. (b) Sample, tooth; column, O (5.3 m \times 0.25 mm I.D.)–C (16 m \times 0.25 mm I.D.) [$p(i)$ = 0.15 MPa, $p(o)$ = 0.10 MPa]; temperature, 130°C (15 min), then increased at 6°C/min to 190°C. (c) Sample, bone; column, P (5.3 m \times 0.25 mm I.D.)–C (16 m \times 0.25 mm I.D.) [$p(i)$ = 0.15 MPa, $p(o)$ = 0.10 MPa]; temperature, 130°C (15 min), then increased at 6°C/min to 190°C. In all instances the carrier gas was nitrogen and a flame ionization detector was used. Peaks: 1 = L-Ala; 2 = L-Val; 3 = L-Thr; 4 = Gly; 5 = L-Ile; 6 = L-Leu; 7 = L-Pro; 8 = L-Ser; 9 = D-Asp; 10 = L-Hpr; 11 = L-Asp; 12 = L-Glu; 13 = L-Phe; 14 = L-Lys.

$t(m)$	Total carrier gas hold-up time
$t(mi)$	Carrier gas hold-up time of i th column
$t(R)$	Adjusted retention time for a retained solute in the system
$\overline{u(i)}$	Average carrier gas velocity of i th column
$u(a)$	Carrier gas velocity at the connection point of the system
$u(o)$	Carrier gas velocity at the outlet of the system
x	Ratio of carrier gas hold-up time, $t(m2)/t(m1)$

α	Separation factor
$\phi(i)$	Fractional carrier gas hold-up time of i th column
σ	Standard deviation of the system
$\sigma(i)$	Standard deviation of i th column

ACKNOWLEDGEMENTS

We thank Professors Qinghai Wang, Daoqian Zhu, Yafeng Guan and Dr. Hongxing Huang for valuable discussions. This work was supported by the National Natural Science Foundation of

China and the Youth Science Foundation of Dalian Institute of Chemical Physics.

REFERENCES

- 1 K. King, Jr., and J.L. Bada, *Nature*, 281 (1977) 135.
- 2 S. Matsuura and N. Ueta, *Nature*, 286 (1980) 883.
- 3 P.M. Helfman and J.L. Bada, *Nature*, 262 (1976) 279.
- 4 P.M. Masters, J.L. Bada and J.S. Zigler, Jr., *Nature*, 268 (1977) 71.
- 5 E.H. Man, M.E. Sandhouse, J. Burg and G.H. Fisher, *Science*, 220 (1983) 1407.
- 6 S. Ohtani and K. Yamamoto, *Jpn. J. Legal Med.*, 45 (1991) 119.
- 7 V. Schurig, *Angew. Chem., Int. Ed. Engl.*, 23 (1984) 747.
- 8 G. Wang, L. Zhou, S. Chen, H. Luo and J. Wang, *Fenxi Huaxue*, 15 (1987) 783.
- 9 P. Sandra, F. David, M. Proot, G. Diricks, M. Verstappe and M. Verzele, *J. High Resolut. Chromatogr. Chromatogr. Commun.*, 8 (1985) 782.
- 10 H.T. Mayfield and S.N. Chesler, *J. High Resolut. Chromatogr. Chromatogr. Commun.*, 8 (1985) 595.
- 11 R.E. Kaiser and R.I. Reider, *J. High Resolut. Chromatogr. Chromatogr. Commun.*, 1 (1978) 201.
- 12 J. Krupčík, G. Guiochon and J.M. Schmitter, *J. Chromatogr.*, 213 (1981) 189.
- 13 J. Krupčík, J. Mocak, A. Simova, J. Garaj and G. Guiochon, *J. Chromatogr.*, 238 (1982) 1.
- 14 D.F. Ingraham, C.F. Schoemaker and W. Jennings, *J. Chromatogr.*, 239 (1982) 39.
- 15 M.F. Mehran, W.J. Cooper and W. Jennings, *J. High Resolut. Chromatogr. Chromatogr. Commun.*, 7 (1984) 215.
- 16 T.B. Buys and T.W. Smuts, *J. High Resolut. Chromatogr. Chromatogr. Commun.*, 4 (1981) 317.
- 17 R.E. Kaiser, R.I. Rieder, L. Leming, L. Blomberg and P. Kusz, *J. High Resolut. Chromatogr. Chromatogr. Commun.*, 8 (1985) 580.
- 18 G. Guiochon, *Chromatogr. Rev.*, 8 (1966) 1.
- 19 X. Lou, Y. Liu and L. Zhou, *J. Chromatogr.*, 552 (1991) 153.
- 20 L. Zhou, M. Huang, G. Wang and D. Zhu, *Fenxi Huaxue*, 15 (1987) 542.
- 21 L. Zhou, G. Wang, T. Zhang, E. Xia and D. Zhu, *Fenxi Huaxue*, 13 (1985) 406.
- 22 S.L. McKenzie and D. Tenaschuk, *J. Chromatogr.*, 173 (1979) 53.
- 23 R.W. Souter, *Chromatographic Separation of Stereoisomers*, CRC Press, Boca Raton, FL, 1985, p. 19.

Gas chromatographic determination of sodium monofluoroacetate as the free acid in an aqueous solvent

Bruce A. Kimball* and Elizabeth A. Mishalanie[☆]

United States Department of Agriculture, Animal and Plant Health Inspection Service, Denver Wildlife Research Center, Building 16, Denver Federal Center, Denver, CO 80225 (USA)

(First received August 14th, 1992; revised manuscript received December 15th, 1992)

ABSTRACT

A procedure was developed for the determination of sodium monofluoroacetate as the free acid by capillary gas chromatography with mass-selective detection. Commercially available polyethylene glycol capillary columns were compatible with injections of highly acidic aqueous solutions which were required for this relatively strong acid. Using monochloroacetic acid as an internal standard, a coefficient of variation of less than 2% was routinely obtained from replicate injections of a 100 µg/ml solution of sodium monofluoroacetate in 1 M HCl. The monofluoroacetic acid/monochloroacetic acid detector response ratio was a linear function of sodium monofluoroacetate concentration from 5 to 200 µg/ml. Since derivatization is not required and mass spectrometric identification of monofluoroacetic acid is obtained, the method offers advantages over previously described chromatographic methods for the determination of sodium monofluoroacetate. The average analyte recovery from 30 to 40 g biological samples fortified with between 2.5 and 100 mg of sodium monofluoroacetate was 81% with relative standard deviation typically less than 7%. The instrument limit of detection was 200 pg sodium monofluoroacetate when the detector was operated in the selected ion monitoring mode.

INTRODUCTION

Sodium monofluoroacetate (CH₂FCO₂Na) has been used as a vertebrate pesticide for more than 40 years, and is commonly known as Compound 1080. Its use has been widespread throughout North America, Australia and New Zealand with peak usage in the 1960s. Sodium monofluoroacetate is extremely toxic. The oral LD₅₀ (*Rattus*

fuscipes) is 1.13 mg/kg [1]. It has been administered for the control of vertebrate pests through several baiting techniques and as a liquid formulation for the protection of livestock from predators. The US Environmental Protection Agency required data concerning sodium monofluoroacetate residues on sheep wool and skin after the liquid formulation was released from livestock protection collars during coyote attacks on sheep.

Because of the extreme toxicity of sodium monofluoroacetate, there has been a need for monitoring low levels of this compound in a variety of matrices. Numerous methods have been developed for the determination of sodium monofluoroacetate in pesticide formulations, tissues, and environmental samples. Since 1980,

* Corresponding author.

[☆] Present address: United States Environmental Protection Agency, Office of Enforcement, National Enforcement Investigations Center, Building 45, Denver Federal Center, Denver, CO 80225, USA.

methods have been published based on non-chromatographic techniques such as indirect fluorometric detection [2], ^{19}F nuclear magnetic resonance [3,4], and direct measurement of the fluoride ion [5–7]. Many gas [8–21] and liquid [22,23] chromatographic determinations require pre-column derivatization of monofluoroacetic acid. Although some of these chromatographic techniques are capable of detecting low levels of monofluoroacetic acid, the derivatization procedures are generally complex and time consuming. Esterification is particularly difficult due to the presence of water in the sample extract. Time-consuming drying steps are required and low analyte recoveries are often obtained [17]. An analytical method using ion chromatography was developed in this laboratory for the determination of sodium monofluoroacetate based on the separation and detection of the monofluoroacetate ion [24]. This method has been used to assay sodium monofluoroacetate technicals, manufacturing use products, and aqueous formulations containing sodium monofluoroacetate. A reversed-phase liquid chromatographic method for the determination of the free acid has recently been reported [25]. However, a procedure for the gas chromatographic determination of sodium monofluoroacetate as the free acid has not been reported to date.

Commercially available capillary columns have been shown to be compatible with injections of aqueous samples because of their bonded and crosslinked phases. J & W Scientific presented data [26] describing the DB-FFAP (free fatty acid phase) column's ability to perform the separation of weak fatty acids ($\text{C}_2\text{--}\text{C}_7$) in water with $\text{p}K$ values ranging from 4.7 to 4.9. Using these types of capillary columns with minor procedural modifications, we have developed a procedure for the determination of monofluoroacetic acid, a stronger acid with a $\text{p}K_a$ of 2.7. This procedure requires the use of 1 *M* HCl as the sample solvent, which minimizes adsorption problems commonly encountered with the chromatographic determination of free acids in aqueous solutions. The gas chromatographic procedure described below does not require a derivatization procedure, provides high-resolution separations, and allows for selective detection of monofluoroacetic acid.

EXPERIMENTAL

Apparatus

A Hewlett-Packard Model 5890 gas chromatograph equipped with a Hewlett-Packard 5970 series mass-selective detector was used for this work. The mass-selective detector was equipped with a Model 270 Granville-Phillips ion gauge and controller to monitor pressure in the ion source which was typically $4 \cdot 10^{-5}$ Torr (1 Torr = 133.322 Pa). The electron impact ionization energy was 70 eV.

Octadecyl silane solid-phase extraction (SPE) columns (J.T. Baker, Phillipsburg, NJ, USA) were used for sample clean-up.

A capillary guard column was required when solutions of 1 *M* HCl were injected into the gas chromatograph. The guard column was prepared from a fused-silica capillary column identical to the analytical column.

The capillary columns were 15 m \times 0.25 mm I.D. with 0.25 μm bonded phases of acidified polyethylene glycol (DB-FFAP; J & W Scientific, Folsom, CA, USA, and Nukol; Supelco, Bellefonte, PA, USA). A helium carrier was used at a linear velocity of 47 cm/s. The use of a lower, more optimum linear velocity was prevented by the pressure drop across the short column created by the capillary direct interface.

Reagents

Sodium monofluoroacetate (97%) and nigrosine black dye were provided by Tull Chemical Co. (Oxford, AL, USA). Tartrazine dye (FD&C Yellow No. 5) was obtained from Ingredient Technology Corp. (Des Plaines, IL, USA). Deionized water was produced in the laboratory and used to prepare all aqueous solutions.

The following solutions were prepared for GC analysis: 10 and 1000 $\mu\text{g}/\text{ml}$ acetic, propionic and isocaproic acids in water; 100 $\mu\text{g}/\text{ml}$ acetic, propionic and isocaproic acids in ethyl acetate; 100 $\mu\text{g}/\text{ml}$ sodium monofluoroacetate in water; 2500 $\mu\text{g}/\text{ml}$ sodium monofluoroacetate in 1 *M* HCl; and 100 $\mu\text{g}/\text{ml}$ sodium monofluoroacetate in 200 *mM* trifluoroacetic acid (TFA). The calibration standards were 5, 10, 50, 100, 150 and 200 $\mu\text{g}/\text{ml}$ sodium monofluoroacetate in 1 *M* HCl with monochloroacetic acid added as an internal standard at a concentration of 50 $\mu\text{g}/\text{ml}$.

To prepare a solution of monofluoroacetic acid in an organic solvent, 1 ml of the 2500 $\mu\text{g/ml}$ sodium monofluoroacetate in 1 M HCl solution was subjected to a liquid–liquid extraction with 10 ml of ethyl acetate. Solutions containing only 1 M HCl were treated similarly to serve as reagent blanks. Acetic acid was added to the ethyl acetate extracts as an internal standard to give a final acetic acid concentration of 50 $\mu\text{g/ml}$.

Preparation of capillary guard column

The guard column was prepared by removing 3 cm of the polyimide coating from one end of a capillary column which was identical to the analytical column. A glassblowing torch burning methane and compressed air was used for this procedure. The exposed fused silica was deactivated with a 5% dichlorodimethyl silane in toluene solution and the guard column was cut to a length of 0.5 m. The end of the guard column with the polyimide removed was positioned in the injector so that only deactivated fused silica was exposed in the injection port. Connection to the analytical column was made by a fused-silica low-dead-volume connector (Restek Corp., Bellefonte, PA, USA).

Procedure

Biological samples consisting of sheepskin with attached wool were fortified with an aqueous

sodium monofluoroacetate formulation. The formulation consisted of 10 mg/ml sodium monofluoroacetate, 0.05 mg/ml nigrosine black dye and 5 mg/ml tartrazine dye in water. A control formulation (containing no sodium monofluoroacetate) was also prepared and replicate samples were fortified with this solution. The sheepskin/wool samples were cut into 100- cm^2 pieces (approximate mass 30–40 g) prior to fortification and each piece was extracted with 500 ml 1 M HCl. Since the samples were fortified with at least 2.5 mg, concentration of the 500-ml extracts was not required. Aliquots (10 ml) of the extracts were then cleaned-up by passing through octadecyl SPE columns. Monochloroacetic acid was added to a known volume of the treated extract as an internal standard to produce a final concentration of 50 $\mu\text{g/ml}$.

The injection port temperature was 200°C and the transfer line to the mass-selective detector source was maintained at 230°C. The injection mode, oven temperature programs and mass-selective detector parameters are summarized in Table I. Injections were either 1 μl split (100:1) or 1 μl splitless (purge time 0.6 min, split vent flow 80 ml/min). Injections (1 μl) of 7.4 M phosphoric acid were made every 5 to 10 injections when solutions of 1 M HCl were injected into the gas chromatograph. Sample extracts were filtered through 0.45- μm nylon filters prior to injection. Single point calibrations were used

TABLE I
SUMMARY OF GC AND DETECTOR PARAMETERS

SIM = Selected ion monitoring.

Condition	Injection mode	Oven program	Mass-selective detector
A	Split	135°C isothermal	SIM, m/z 41, 43, 45, 55, 57, 60, 74, 87
B	Splitless	85°C (0.5 min) $\xrightarrow{15^\circ\text{C}/\text{min}}$ 245°C	SIM, m/z 41, 43, 45, 55, 57, 60, 74, 87
C	Splitless	85°C (0.5 min) $\xrightarrow{15^\circ\text{C}/\text{min}}$ 230°C	SIM, m/z 61, 78
D	Splitless	60°C (0.5 min) $\xrightarrow{15^\circ\text{C}/\text{min}}$ 215°C	SIM, m/z 41, 43, 45, 55, 57, 60, 74, 87
E	Splitless	60°C (0.5 min) $\xrightarrow{15^\circ\text{C}/\text{min}}$ 215°C	Scan, m/z 15 \rightarrow 80 SIM, m/z 60, 78
F	Splitless	110°C (0.5 min) $\xrightarrow{15^\circ\text{C}/\text{min}}$ 240°C	SIM, m/z 61, 78
G	Splitless; guard column	110°C $\xrightarrow{15^\circ\text{C}/\text{min}}$ 200°C	SIM, m/z 50, 78

for the quantitation of sodium monofluoroacetate in the sample extracts.

RESULTS AND DISCUSSION

Various solvent systems were investigated to identify a solvent that would (1) convert the sodium salt to the free acid, (2) provide for adequate chromatographic performance of monofluoroacetic acid and (3) be useful as an extraction solvent for complex matrices. Each solvent system is described and discussed below.

Free acid–water solutions

Aqueous solutions of acetic, propionic and isocaproic acids were used to verify the performance of the capillary columns under the conditions recommended by the column manufacturers. The columns from two manufacturers exhibited good resolution of the three acids under isothermal conditions when split injections were made (Table I, condition A). Injection of a water reagent blank after the sample solutions did not result in chromatographic responses from these acids.

Splitless injections of these solutions were then investigated. In order to retain chromatographic performance of the free acids, adjustment of the oven temperature program was required (Table I, condition B). Injections of a 10- $\mu\text{g}/\text{ml}$ solution of the acids under these conditions resulted in a chromatographic separation similar to that observed in the split mode. However, injections of water after the sample solutions produced chromatographic responses for each of the acids. These “ghost peak” responses may have been the result of adsorption and desorption processes in the injection port. Polar compounds such as free acids exhibit an affinity for active sites in the injection port. Adsorption may also occur at active sites on the head of the column. Highly polar solvents such as water can then desorb the acids from the active sites. Consequently, the performance of the chromatographic system was acceptable under the conditions specified by the column manufacturers, but was not acceptable under conditions that would be needed for residue determinations.

Because less than 1% of the monofluoroace-

tate is protonated in a 100 $\mu\text{g}/\text{ml}$ sodium monofluoroacetate in water solution, sodium monofluoroacetate in water solutions could not be chromatographed under conditions similar to the free acid in water solutions (Table I, condition C). No chromatographic responses were observed after numerous injections of a 100 $\mu\text{g}/\text{ml}$ sodium monofluoroacetate in water solution. However, when a single injection of 1 M HCl was made after injection of the sodium monofluoroacetate in water solution, a monofluoroacetic acid response was observed. Repeat injections of the sodium monofluoroacetate in water solution following injection of 1 M HCl resulted in a chromatographic response for monofluoroacetic acid, but the peak shape rapidly deteriorated with subsequent injections. Apparently, the injection of HCl resulted in the formation of the free acid from the non-volatile salt remaining in the injection port. This also produced an acidic environment which promoted the formation of the free acid in subsequent injections of sodium monofluoroacetate in water. As more injections of sodium monofluoroacetate/water solution were made, the effect of the acid diminished until a monofluoroacetic acid response was no longer observed.

Free acid–ethyl acetate solutions

Splitless injections of the 100- $\mu\text{g}/\text{ml}$ standard solution of acetic, propionic and isocaproic acids in ethyl acetate were followed by splitless injections of water or ethyl acetate (Table I, condition D). Only the injection of water resulted in ghost peak responses for the three acids. Similar to previous observations, split injections of the free acids–ethyl acetate solution followed by split injections of water did not result in chromatographic responses. These observations indicate that the increased residence time of the analyte and solvent in the injection port during splitless injections and solvent polarity lead to the appearance of the ghost peaks.

In addition to the solvating power and residence time of the solvent, the adsorption/desorption behavior of weak acids is also a function of the analytes' acid strength and the rate of gas–solid collisions which lead to adsorption. For example, the splitless injection of water pro-

duced larger ghost peak responses for monofluoroacetic and monochloroacetic acids relative to the weaker acetic acid. The rate of adsorption of a gas to a solid surface is determined by the sticking coefficient and the rate of gas–solid collisions. This collision rate has an inverse square root relationship with molecular mass. This influence is exhibited in the splitless injection of water induced desorption responses of acetic (pK_a 4.7), propionic (pK_a 4.9) and isocaproic (pK_a 4.8) acids. Although they are similar in acid strength, the ghost peak response of acetic acid is larger in relation to the ghost peak responses of the more massive propionic acid which is in turn larger than the response of isocaproic acid.

Monofluoroacetic acid–ethyl acetate solutions

In an effort to eliminate the adsorption/desorption behavior observed with the water solvent system, an organic solvent was investigated. Monofluoroacetic acid was partitioned into ethyl acetate by liquid–liquid extraction of a sodium monofluoroacetate–1 M HCl solution, resulting in a solution of monofluoroacetic acid in acidified ethyl acetate. Based on calculations using the pK_a of monofluoroacetate, 1 M HCl should protonate >99.9% of the monofluoroacetate. Splitless injections of the monofluoroacetic acid–ethyl acetate solutions (Table I, condition E), resulted in a good chromatographic response for monofluoroacetic acid. Acetic acid was added to the ethyl acetate solution for use as an internal standard and also exhibited good chromatographic behavior. However, when reagent blanks (ethyl acetate extract of 1 M HCl) containing the internal standard were injected, a monofluoroacetic acid response was observed. This ghost peak response persisted for numerous subsequent injections of the reagent blank. The signal was identified as a monofluoroacetic acid response by its mass spectrum (Fig. 1). Syringe carryover was eliminated as the source of the ghost peak by use of separate syringes for injecting standard solutions and blanks. Since the only source of monofluoroacetic acid was the standard solutions, it was apparent that the free acid was being desorbed from the injection port and/or the head of the column as described

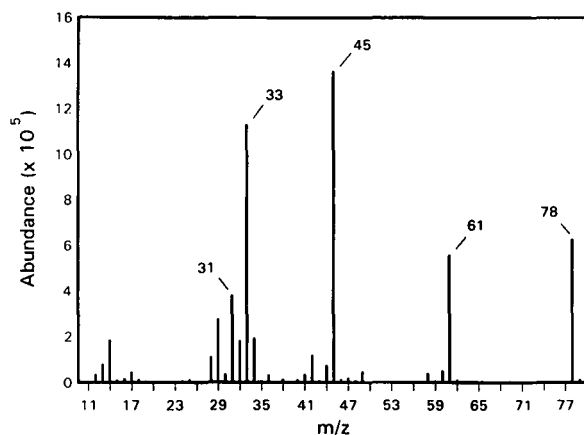


Fig. 1. Mass spectrum of monofluoroacetic acid. m/z 31 = fragment FC^+ ; m/z 33 = FH_2C^+ ; m/z 45 = $HO-C=O^+$; m/z 61 = $FH_2C-C=O^+$; m/z 78 = M^+ .

previously. Injection port liners were silanized or phosphorylated in an attempt to eliminate the liner as the source of active sites in the injection port. These procedures did not eliminate observance of ghost peak responses. However, phosphorylation of the stainless steel seal in the injection port did temporarily eliminate the ghost peak responses. Apparently, the small amount of water which partitioned into the ethyl acetate promoted desorption of the acids from the injection port. Attempts to dry the ethyl acetate extract by centrifugation or addition of sodium sulfate did not eliminate the ghost peaks.

Sodium monofluoroacetate–TFA solutions

The monofluoroacetic acid–ethyl acetate data indicated that neither physical nor chemical attempts to eliminate water from ethyl acetate produced the desired effect. A TFA (pK_a 0.3) solvent system was pursued in an attempt to eliminate or minimize the adsorption/desorption behavior of monofluoroacetic acid. TFA could provide a sufficiently acidic environment to protonate monofluoroacetate and also buffer sample extracts. However, since it is also a free acid, TFA caused a chromatographic interference during injections of a 100 $\mu g/ml$ sodium monofluoroacetate in 200 mM aqueous TFA solution (Table I, condition F), and this approach was not pursued further.

Sodium monofluoroacetate–1 M HCl solutions

Since 1 M HCl was an effective solvent for desorbing monofluoroacetic acid present in the injector system, it was investigated for use as an injection solvent. As a sample extraction solvent, this solution was also sufficiently acidic to provide sample extracts with a pH similar to the standard solutions. This would allow for direct quantitative comparison of standard and sample solutions.

The corrosive nature of this solvent necessitated some procedural changes which were designed to protect the analytical column. In addition to keeping the initial oven temperature above 100°C to prevent condensation of the corrosive solvent on the head of the column, the guard column was used to further prevent permanent damage to the analytical column. Removal of the polyimide coating from the capillary column was necessary because the 1 M HCl reacted with the polyimide exposed in the hot injection port. These procedures allowed for prolonged use of 1 M HCl as an injection solvent. The chromatographic performance of monofluoroacetic acid was retained with these changes (Table I, condition G). However, elimination of the solvent effect deteriorated the chromatographic performance of the internal standard, acetic acid. Monochloroacetic acid was chosen to replace acetic acid as the internal standard. Fig. 2 shows a typical chromatogram of a 1 M HCl solution containing sodium monofluoroacetate and monochloroacetic acid under these conditions.

Although the use of 1 M HCl as the injection solvent resulted in excellent chromatography, the desorption of the free acid continued to produce ghost peaks. Following 20 to 30 injections of a solution of 100 µg/ml sodium monofluoroacetate and 50 µg/ml monochloroacetic acid in 1 M HCl, a decreasing trend was observed in the monofluoroacetic acid/monochloroacetic acid detector response ratio. The injection of reagent blanks also resulted in chromatographic responses from the two acids.

Since phosphoric acid had previously been shown to deactivate the injection port, a 1-µl injection of 7.4 M H₃PO₄ was made after every 5 to 10 injections of standard solutions or sam-

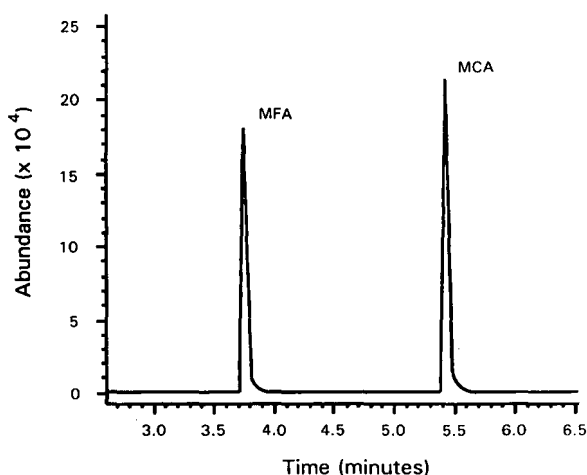


Fig. 2. Monofluoroacetic acid (MFA) and the internal standard monochloroacetic acid (MCA) in 1 M HCl (Table I, condition G).

ples. This procedure prevented the occurrence of ghost peaks in reagent and matrix blanks. H₃PO₄ was an excellent solvent for desorbing weak acids which had been previously adsorbed and prevented the adsorption of weak acids in subsequent injections. As expected, phosphoric acid (or pyrophosphoric acid which is present at the injection port temperature of 200°C) damaged the guard column. Typically, we observed deterioration of chromatographic performance after approximately 50 injections of H₃PO₄. Replacement of the guard column restored chromatographic performance. No visible corrosion or other damage to the mass-selective detector source was evident after several hundred injections of acidic aqueous solutions. In addition, the quadrupole tuning parameters did not indicate damage to the source components.

Selectivity, bias and repeatability

Three replicate sheepskin/wool samples fortified with the control formulation and nine sheepskin/wool samples fortified with the sodium monofluoroacetate containing formulation were extracted with 1 M HCl to remove the sodium monofluoroacetate residues. The pH values of the sample extracts were less than 0.5 which allowed for direct quantitative comparison to standard solutions of sodium monofluoroacetate in 1 M HCl. No chromatographic interfer-

ences were observed from the extraction of the control samples. Recoveries of sodium monofluoroacetate from samples fortified at 2.5, 50 and 100 mg were 85.5% (S.D. = 2.2%, $n = 3$), 80.0% (S.D. = 5.8%, $n = 3$) and 76.7% (S.D. = 2.5%, $n = 3$) respectively. An analysis of variance performed on these data demonstrated that recovery did not vary significantly at the three fortification levels. The lack of available wool and skin samples precluded the analysis of more than three replicate fortified samples.

Response linearity and limit of detection

Repeated injection of a 100 $\mu\text{g}/\text{ml}$ sodium monofluoroacetate and 50 $\mu\text{g}/\text{ml}$ monochloroacetic acid in 1 M HCl solution typically produced detector response ratios with a relative standard deviation of less than 2% from 5 consecutive injections. Response linearity was demonstrated with two sets of six calibration standards. The sodium monofluoroacetate concentration in the calibration standards ranged from 5 to 200 $\mu\text{g}/\text{ml}$, and the internal standard concentration was held constant at 50 $\mu\text{g}/\text{ml}$. Each solution was injected in triplicate. The monofluoroacetic acid/monochloroacetic acid detector response ratio was plotted as a function of sodium monofluoroacetate concentration and a linear regression analysis was performed on the 36-point data set.

Regression analysis generated a y -intercept of 0.002 and a slope of 0.007. The standard error of

the y -intercept was 0.003 and the standard error of the slope was 0.00002. The coefficient of determination (r^2) was 0.9996 which indicates a linear relationship. Applying a 95% confidence interval to the y -intercept data, it is found that the y -intercept is not significantly different from zero. Therefore, these data demonstrate that a linear relationship exists between detector response ratio and sodium monofluoroacetate concentration and that the ratio can be assumed to be directly proportional to concentration over the investigated range. As a result, a single-point calibration was used to quantitate solutions containing 5–200 $\mu\text{g}/\text{ml}$ sodium monofluoroacetate.

The instrument limit of detection (ILOD) was estimated from a monofluoroacetic acid chromatographic response which was approximately 10 times greater than the peak-to-peak noise in the baseline of a chromatogram from a standard solution. The ILOD was defined as the amount of monofluoroacetic acid which would produce a response corresponding to three times the peak-to-peak noise. The instrument limit of detection was determined to be 200 pg sodium monofluoroacetate (200 ng/ml) when the mass-selective detector was operated in the SIM mode (Table I, condition G).

Quality control results from sample analysis

This methodology was used for the determination of sodium monofluoroacetate residues on sheepskin/wool samples collected during a pes-

TABLE II
RECOVERY OF SODIUM MONOFLUOROACETATE FROM QUALITY CONTROL SAMPLES

30- to 40-g wool and skin samples fortified with 50 mg sodium monofluoroacetate.

Replicate	Run							
	1 (%)	2 (%)	3 (%)	4 (%)	5 (%)	6 (%)	7 (%)	8 (%)
1	83.2	81.6	88.3	76.8	79.8	76.3	89.4	85
2	85.7	79.5	87.7	97.3	79.7	76.4	91.8	77
3	87.6	82.0	85.1	85.8	—	84.5	87.2	82
4	—	—	—	—	—	—	101	—
Mean %	85.5	81.0	87.0	86.6	79.8	79.1	92.4	81
S.D. (%)	2.2	1.3	1.7	10.3	—	4.7	6.1	4
R.S.D. (%)	2.6	1.6	2.0	11.9	—	5.9	6.6	5

ticide registration study. Each time a set of samples was analyzed, replicate quality control samples were fortified with 50 mg sodium monofluoroacetate. Analyte recovery for these samples is presented in Table II. Mean recoveries of sodium monofluoroacetate from the quality control samples were in good agreement with the recovery observed during method development. The increased variability in the quality control data from run 4 was attributed to deterioration of the guard column. Replacement of the guard column led to improved precision. The cause of one high recovery value (run 7) was not identified.

ACKNOWLEDGEMENTS

The authors wish to thank Dr. Peter J. Savarie for providing the biological samples and Margaret Goodall and Doreen McHugh for providing the quality control data.

Mention of commercial products is for identification only and does not constitute endorsement by the USA Government.

REFERENCES

- 1 Hazardous Substances Databank (*Database Online*). National Library of Medicine, Bethesda, MD, 1991, sodium fluoroacetate; unique identifier: HSDB 743; p. 10 of 16.
- 2 T. Sakai, A. Fujimoto and T. Miyahara, *Eisei Kagaku*, 27 (1981) 45–49.
- 3 M.L. Baron, C.M. Bothroyd, G.I. Rogers, A. Staffa and I.D. Rae, *Phytochemistry*, 26 (1987) 2293–2295.
- 4 R.L. Frost, R.W. Parker and J.V. Hanna, *Analyst (London)*, 114 (1989) 1245–1248.
- 5 C.L. Batcheler and C.N. Challies, *N.Z.J. For. Sci.*, 18 (1988) 109–115.
- 6 G. Livanos and P.J. Milham, *J. Assoc. Off. Anal. Chem.*, 67 (1984) 10–12.
- 7 H.M. Stahr, J. Kinker and D. Nicholson, *Proc. Annu. Meet. Am. Assoc. Vet. Lab. Diagn.*, 26 (1984) 145–154.
- 8 W.J. Allender, *J. Anal. Toxicol.*, 14 (1990) 45–49.
- 9 L.W. Bennett, G.W. Miller, M.H. Yu and R.I. Lynn, *Fluoride*, 16 (1983) 111–117.
- 10 D.G. Burke, D.K.T. Lew and X. Cominos, *J. Assoc. Off. Anal. Chem.*, 72 (1989) 503–507.
- 11 H.H. Casper, T.L. McMahon and G.D. Paulson, *J. Assoc. Off. Anal. Chem.*, 68 (1985) 722–725.
- 12 H.H. Casper, M.E. Mount, R.E. Marsh and R.H. Schmidt, *J. Assoc. Off. Anal. Chem.*, 69 (1986) 441–442.
- 13 J.J.L. Hoogenboom and C.G. Rammell, *J. Anal. Toxicol.*, 11 (1987) 140–143.
- 14 E.J. Huggins, H.H. Casper and C.D. Ward, *J. Assoc. Off. Anal. Chem.*, 71 (1988) 579–581.
- 15 I. Okuno, G.E. Connolly, P.J. Savarie and C.P. Breidenstein, *J. Assoc. Off. Anal. Chem.*, 67 (1984) 549–553.
- 16 I. Okuno, D.L. Meeker and R.R. Felton, *J. Assoc. Off. Anal. Chem.*, 65 (1982) 1102–1105.
- 17 H. Ozawa and T. Tsukioka, *Anal. Chem.*, 59 (1987) 2914–2917.
- 18 H. Ozawa and T. Tsukioka, *J. Chromatogr.*, 473 (1989) 251–259.
- 19 H. Tietjen, F. Deines and W. Stephensen, *Bull. Environ. Contam. Toxicol.*, 40 (1988) 707–710.
- 20 T. Vartiainen and J. Gynther, *Food Chem. Toxicol.*, 22 (1984) 307–308.
- 21 T. Vartiainen and P. Kauranen, *Anal. Chim. Acta*, 157 (1984) 91–97.
- 22 D.M. Collins, J.P. Fawcett and C.G. Rammell, *Bull. Environ. Contam. Toxicol.*, 26 (1981) 669–673.
- 23 A.C. Ray, L.O. Post and J.C. Reagor, *J. Assoc. Off. Anal. Chem.*, 64 (1981) 19–24.
- 24 B.A. Kimball, unpublished results, June 1989.
- 25 W.J. Allender, *J. Liq. Chromatogr.*, 13 (1990) 3465–3471.
- 26 J & W Scientific, *The Separation Times*, 2 (1988) 4–5.

Comparison of hydrodistillation and supercritical fluid extraction for the determination of essential oils in aromatic plants

Steven B. Hawthorne*

Energy and Environmental Research Center, University of North Dakota, Box 8213, Grand Forks, ND 58202 (USA)

Marja-Liisa Riekkola and Katariina Serenius

Department of Chemistry, University of Helsinki, Vuorikatu 20, SF-00100 Helsinki (Finland)

Yvonne Holm and Raimo Hiltunen

Department of Pharmacy, Pharmacognosy Division, University of Helsinki, Fabianinkatu 35, SF-00170 Helsinki (Finland)

Kari Hartonen

Department of Chemistry, University of Helsinki, Vuorikatu 20, SF-00100 Helsinki (Finland)

(First received October 9th, 1992; revised manuscript received December 10th, 1992)

ABSTRACT

Supercritical fluid extraction (SFE) and hydrodistillation were compared as methods to extract essential oils from savory, peppermint and dragonhead. Despite the high solubilities of essential oil components in supercritical CO₂, the extraction rates were relatively slow with pure CO₂ (ca. 80% recovery after 90 min). However, a 15-min static extraction with methylene chloride as modifier followed by a 15-min dynamic extraction with pure CO₂ yielded high recoveries which agreed well with the results of hydrodistillation performed for 4 h. Spike recovery studies demonstrated that compounds as volatile as monoterpenes can be quantitatively (>90%) collected off-line from the SFE effluent. SFE recovered some organic compounds from each of the samples that were not extracted by hydrodistillation, most notably C₂₇, C₂₉, C₃₁, and C₃₃ *n*-alkanes.

INTRODUCTION

Supercritical fluids are receiving increasing attention for performing analytical-scale extractions of samples ranging from environmental matrices to food products because of the potential to perform rapid (often <30 min) extractions, to reduce the use of hazardous solvents,

and to couple the extraction step with gas, liquid or supercritical fluid chromatography [1–3]. Recently, supercritical fluid extraction (SFE) has been applied to the determination of essential oil components using both off-line SFE and SFE coupled with GC [4–8]. While the majority of reports have focussed on qualitative analysis, SFE and SFE–GC have been demonstrated to yield reasonable recoveries of spiked essential oil compounds and reproducible recoveries of native (not spiked) compounds [6,9]. However, high

* Corresponding author.

recoveries of spiked compounds from aromatic plants do not necessarily indicate high recoveries of native compounds, since spiked compounds are likely only associated with surface sites on the plant matrix, while the native essential oils are distributed throughout the plant material.

To further investigate the ability of SFE to yield quantitative extractions of native essential oil compounds, SFE recoveries from three aromatic plants, savory [9], peppermint [10] and dragonhead [11,12], were compared to those obtained using hydrodistillation [13–15]. Both the absolute quantities of each major essential oil component (as mg extracted per gram of plant tissue) and the distribution of the individual compounds (as % composition of the extracted essential oil) are compared in the SFE and hydrodistillation extracts using capillary GC. The use of organically modified CO₂ to increase SFE rates is also described.

EXPERIMENTAL

Sample extractions

Three aromatic plants, savory (*Satureja hortensis* L.), dragonhead (*Dracocephalum moldavica* L.) and peppermint (*Mentha x piperita* L.), were used as received (air dried and coarsely ground). All hydrodistillations were performed using triplicate 25-g portions of each sample for 4 h using 500 ml of water per extraction as previously described [13–15]. Following hydrodistillation, the extracted essential oils were quantitatively transferred into a volumetric flask using several rinses of methylene chloride and diluted as appropriate for gas chromatographic analysis.

SFE was performed on replicate portions of each sample using “SFE-grade” CO₂ (Scott Specialty Gases, Plumsteadville, PA, USA) supplied to an ISCO SFX-210 extraction unit by a Model 260D syringe pump (ISCO, Lincoln, NE, USA). All extractions were performed at 400 atm (1 atm = 101 325 Pa) and a temperature of 70°C. Stainless-steel extraction cells (2.5 ml) supplied with the extraction unit were filled with each sample (500 mg) for all SFE studies. SFE flow-rates were maintained at *ca.* 0.7 ml/min (measured as liquid CO₂ at the pump) using outlet restrictors made from 12 cm lengths of 32

μm I.D. fused-silica tubing (Polymicro Technologies, Phoenix, AZ, USA) which were attached to the extractor using a short (*ca.* 2 cm) length of 1/16 in. (1 in. = 2.54 cm) O.D. stainless-steel tubing and a “Swagelok” tubing union. Since preliminary studies demonstrated that unheated restrictors frequently plugged (both from water freezing at the restrictor outlet and from extracted organic material at the restrictor inlet), the restrictor heater previously described by Burford *et al.* [16] was used at 100°C for all extractions reported here. (The restrictor heater sold with the ISCO unit was not available for this study.) Except as otherwise noted, extracted analytes were collected into 4 ml methylene chloride placed in an 7-ml glass screw-top vial.

All extractions with pure CO₂ were performed in the dynamic (continual flow) mode. The extraction rates of individual compounds were determined by collecting fractions at specific time intervals during SFE, and analyzing in a manner identical to that used for the other extracts. All of the extractions performed with the addition of organic modifier (either pesticide-grade hexane, acetone or methylene chloride) were performed by adding 0.5 ml of the modifier to the sample in the 2.5 ml extraction cell and immediately inserting the cell into the SFE unit and pressurizing to 400 atm. The extraction was then performed in the static mode for 15 min (*i.e.*, the outlet valve on the SFE unit was left closed when the inlet valve was opened), then the outlet valve was opened and the cell was swept for an additional 15 min with CO₂ in the dynamic mode. For the modifier experiments, the extracted analytes were collected in 4 ml of the same solvent as was used for the modifier.

Gas chromatographic analysis

All GC analyses were performed using a 12.5 m HP Ultra 1 column having a 0.2 mm I.D. and a 0.33 μm film thickness (Hewlett-Packard, Avondale, PA, USA). GC-flame ionization detection (FID) analyses were performed using a Hewlett-Packard Model 5890 gas chromatograph in the split mode with a temperature program of 50°C (hold for 2 min) followed by a temperature ramp at 8°C min to 300°C. Quantitations were based on the addition of dodecane as the internal

TABLE I

CONCENTRATIONS OF ESSENTIAL OIL COMPONENTS IN SAVORY BASED ON HYDRODISTILLATION AND SFE

Species	Peak no. ^a	Hydrodistillation		SFE, set 1		SFE, set 2	
		mg/g (%R.S.D.) ^b	Composition (%) ^c	mg/g (%R.S.D.) ^b	Composition (%) ^c	mg/g (%R.S.D.) ^b	Composition (%) ^c
C ₁₀ H ₁₆ ^d	1	0.13 (10)	0.8 ± 0.1	0.15 (7)	0.7 ± 0.0	0.13 (7)	0.6 ± 0.0
α-Pinene ^e	2	0.19 (9)	1.1 ± 0.1	0.21 (6)	1.0 ± 0.1	0.19 (8)	0.9 ± 0.1
β-Pinene ^e	3	0.09 (10)	0.5 ± 0.0	0.11 (8)	0.5 ± 0.0	0.10 (7)	0.4 ± 0.0
C ₁₀ H ₁₆ ^d	4	0.28 (7)	1.6 ± 0.1	0.33 (7)	1.5 ± 0.1	0.29 (7)	1.3 ± 0.1
C ₁₀ H ₁₆ ^d	5	0.46 (8)	2.6 ± 0.1	0.40 (14)	1.8 ± 0.3	0.41 (5)	1.9 ± 0.1
ρ-Cymene ^e	6	1.25 (7)	7.0 ± 0.2	1.46 (3)	6.6 ± 0.2	1.31 (8)	5.9 ± 0.5
γ-Terpinene ^e	7	4.40 (8)	24.6 ± 1.1	5.08 (6)	22.9 ± 1.1	4.46 (8)	20.3 ± 1.6
C ₁₀ H ₁₂ O ₂ ^d	8	0.06 (51)	0.3 ± 0.1	1.15 (7)	4.5 ± 0.4	1.30 (8)	5.2 ± 0.4
Carvacrol ^e	9	12.14 (4)	59.5 ± 1.5	14.31 (1)	55.9 ± 1.0	14.85 (0.2)	59.3 ± 0.9
C ₁₅ H ₂₄ ^d	10	0.21 (9)	1.0 ± 0.1	0.30 (5)	1.2 ± 0.1	0.31 (4)	1.2 ± 0.0
C ₁₅ H ₂₄ ^d	11	0.22 (4)	1.1 ± 0.2	0.42 (3)	1.6 ± 0.1	0.44 (3)	1.7 ± 0.0
C ₁₀ H ₁₄ O ₂ ^d	12	0.01 (7)	0.1 ± 0.0	0.49 (12)	1.9 ± 0.2	0.48 (9)	1.9 ± 0.2
Total		19.44	100	24.41	100	24.27	100

^a Peak numbers refer to the chromatogram in Fig. 1.

^b Concentrations and percent relative standard deviations (%R.S.D.) were based on triplicate hydrodistillations performed on the same day, and two triplicate sets of SFE extractions performed on two different days.

^c Compositions of each component were calculated for each individual extract, as the % (w/w) of the species listed in the table.

^d Tentative identification based on MS.

^e Identification based on comparison of mass spectra and chromatographic retention times with those of standard compounds.

TABLE II

CONCENTRATIONS OF ESSENTIAL OIL COMPONENTS IN PEPPERMINT BASED ON HYDRODISTILLATION AND SFE

Species	Peak no. ^a	Hydrodistillation		SFE, set 1		SFE, set 2	
		mg/g (%R.S.D.) ^b	Composition (%) ^c	mg/g (%R.S.D.) ^b	Composition (%) ^c	mg/g (%R.S.D.) ^b	Composition (%) ^c
α-Pinene ^e	1	0.04 (4)	0.7 ± 0.0	0.04 (8)	0.7 ± 0.1	0.04 (4)	0.8 ± 0.0
β-Pinene ^e	2	0.09 (7)	1.4 ± 0.0	0.07 (18)	1.3 ± 0.2	0.08 (18)	1.4 ± 0.2
1,8-Cineole ^d	3	0.53 (12)	7.3 ± 0.2	0.46 (4)	7.9 ± 0.3	0.49 (8)	7.9 ± 0.3
cis-Sabinenehydrate ^d	4	0.15 (18)	2.1 ± 0.2	0.23 (6)	3.9 ± 0.2	0.26 (12)	4.1 ± 0.2
Menthone ^d	5	2.07 (5)	28.7 ± 1.5	1.60 (6)	27.5 ± 1.2	1.70 (5)	27.4 ± 1.4
Menthol ^e	6	3.33 (12)	46.0 ± 1.5	2.59 (2)	44.7 ± 0.9	2.76 (8)	44.4 ± 1.1
Methylacetate ^e	7	0.31 (3)	4.3 ± 0.3	0.27 (11)	4.3 ± 0.3	0.28 (5)	4.5 ± 0.5
β-Carophyllene ^e	8	0.29 (10)	4.0 ± 0.1	0.22 (12)	3.8 ± 0.5	0.24 (10)	3.9 ± 0.1
C ₁₅ H ₂₄ ^d	9	0.26 (11)	3.6 ± 0.1	0.23 (4)	3.9 ± 0.2	0.26 (16)	4.2 ± 0.4
C ₁₅ H ₂₄ ^d	10	0.14 (13)	1.9 ± 0.1	0.10 (14)	1.7 ± 0.2	0.11 (23)	1.8 ± 0.3
Total		7.21	100	5.81	100	6.22	100

^a Peak numbers refer to the chromatogram in Fig. 2.

^b Concentrations and percent relative standard deviations (%R.S.D.) were based on triplicate hydrodistillations performed on the same day, and two triplicate sets of SFE extractions performed on two different days.

^c Compositions of each component were calculated for each individual extract, as the % (w/w) of the species listed in the table.

^d Tentative identification based on MS.

^e Identification based on comparison of mass spectra and chromatographic retention times with those of standard compounds.

TABLE III

CONCENTRATIONS OF ESSENTIAL OIL COMPONENTS IN DRAGONHEAD BASED ON HYDRODISTILLATION AND SFE

Species	Peak no. ^a	Hydrodistillation		SFE	
		mg/g (%R.S.D.) ^b	Composition (%) ^c	mg/g (%R.S.D.) ^b	Composition (%) ^c
Neral ^e	1	0.015 (46)	2.9 ± 0.3	0.024 (2)	2.7 ± 0.3
Geraniol ^e	2	0.014 (40)	2.5 ± 0.1	0.030 (11)	3.3 ± 0.1
Geranial ^e	3	0.021 (39)	3.8 ± 0.4	0.063 (4)	7.1 ± 0.8
Thymol ^e	4	0.038 (40)	7.0 ± 0.6	0.091 (11)	10.2 ± 2.0
Carvacrol ^e	5	0.081 (48)	14.9 ± 1.6	0.123 (8)	13.7 ± 2.0
Neryl acetate ^d	6	0.017 (34)	3.1 ± 0.3	0.062 (5)	6.9 ± 0.6
Geranylacetate ^e	7	0.360 (45)	65.8 ± 1.1	0.511 (22)	56.1 ± 5.6
Total		0.75	100	1.27	100

^a Peak numbers refer to the chromatogram in Fig. 3.^b Concentrations and percent relative standard deviations (%R.S.D.) were based on triplicate hydrodistillations and triplicate SFE extractions.^c Compositions of each component were calculated for each individual extract, as the % (w/w) of the species listed in the table.^d Tentative identification based on MS.^e Identification based on comparison of mass spectra and chromatographic retention times with those of standard compounds.

standard to each extract and on standard curves generated from the pure standard compounds. [When the pure compounds were not available (as indicated in Tables I–III), the FID relative response factors were estimated based on the FID responses of the pure standards having the same molecular formula.] GC–MS analyses were performed using identical GC conditions on a Hewlett-Packard Model 5989A GC–MS system. Except as otherwise noted, all identifications were based on comparisons of the mass spectra and retention times of the pure standards with those of the sample species.

RESULTS AND DISCUSSION

As noted above, the initial supercritical fluid extractions were hampered by plugging of the outlet restrictor which occurred intermittently during SFE of each of the three samples. However, when the restrictor heater [16] was used to heat the restrictor to 100°C, plugging from matrix components was eliminated, although it was important to ensure that the inlet end of the restrictor (and not just the middle portion of the restrictor) was heated. This arrangement heated all of the restrictor except the outlet end of the

restrictor (ca. 4 cm) that was inserted into the collection vial. Plugging at the restrictor outlet (presumably from extracted water freezing at the end of the restrictor) also occasionally occurred as the solvent temperature dropped below 0°C from the cooling effect of the expanding CO₂. This was easily avoided by simply placing the collection solvent vial in a small beaker containing ca. 15 ml of room temperature water at the beginning of the extraction.

The GC–FID chromatograms of the SFE and hydrodistillation extracts from savory, peppermint, and dragonhead are shown in Figs. 1–3 (peak identities are given in Tables I–III) and, in general, show the same major components as would be expected from earlier reports [9–12]. Qualitatively, the chromatograms of the SFE extracts were very similar to those from the hydrodistillation extracts for all three samples, although SFE did extract some additional species from each of the samples (none of which were present in SFE blanks). Most notably, all of the SFE extracts contained plant wax odd-numbered *n*-alkanes (primarily C₂₇, C₂₉, C₃₁ and C₃₃), while none of these alkanes were detected in significant quantities in any of the hydrodistillation extracts. (The presence of *n*-alkanes in the

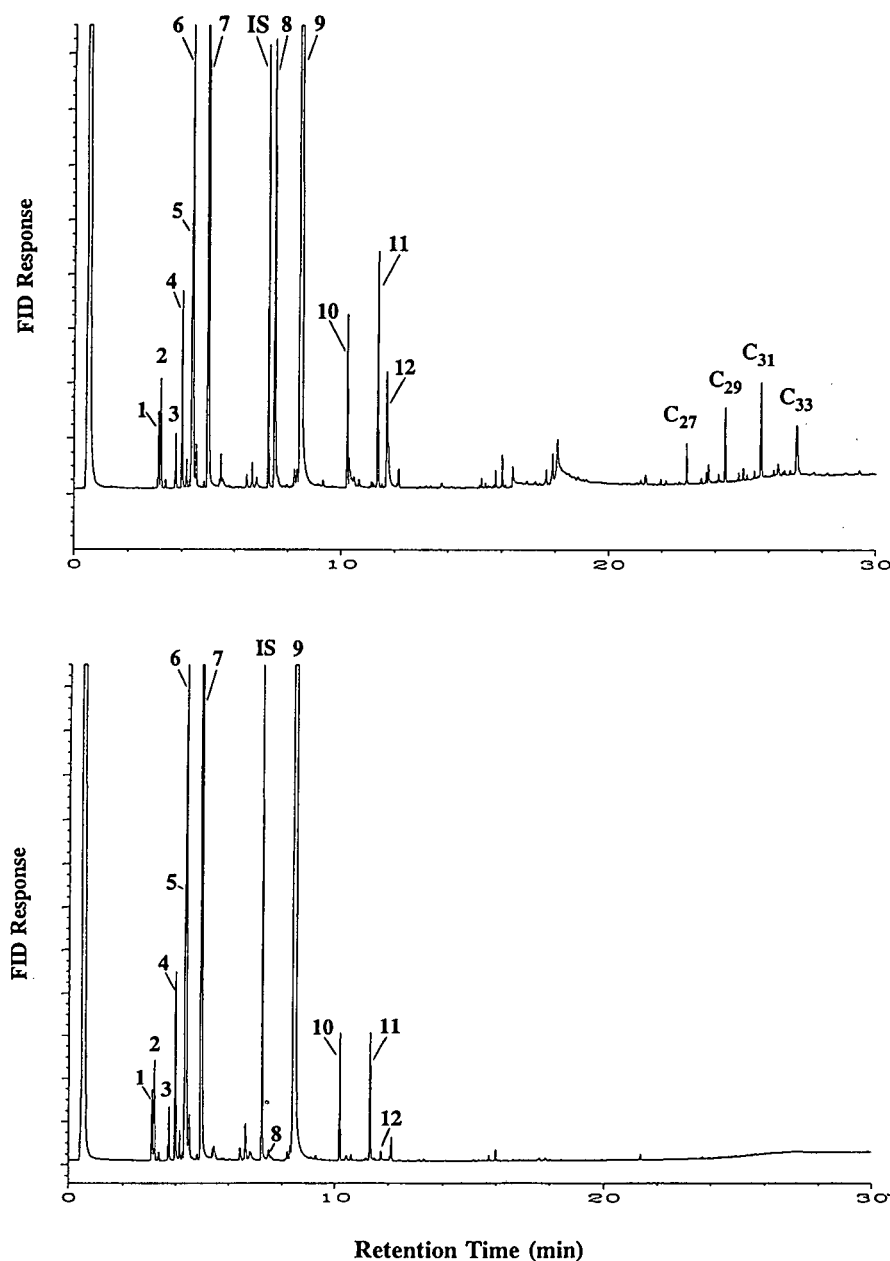


Fig. 1. GC-FID chromatograms of the SFE (top) and hydrodistillation (bottom) extracts of savory. Individual peaks are identified in Table I (IS designates the internal standard). Chromatographic conditions are given in the text.

SFE extracts was also confirmed by the presence of *n*-alkanes in liquid methylene chloride extracts of the same plant materials.) While nearly all of the additional species extracted by SFE were relatively non-volatile and eluted much later than the primary essential oil components (*i.e.*, several minutes after the sesquiterpenes), the

SFE extract from savory contained significant concentrations of two species (peaks 8 and 12 in Fig. 1) which eluted with the primary essential oil components (discussed later in the text).

Extraction with pure CO₂

Preliminary development of the SFE condi-

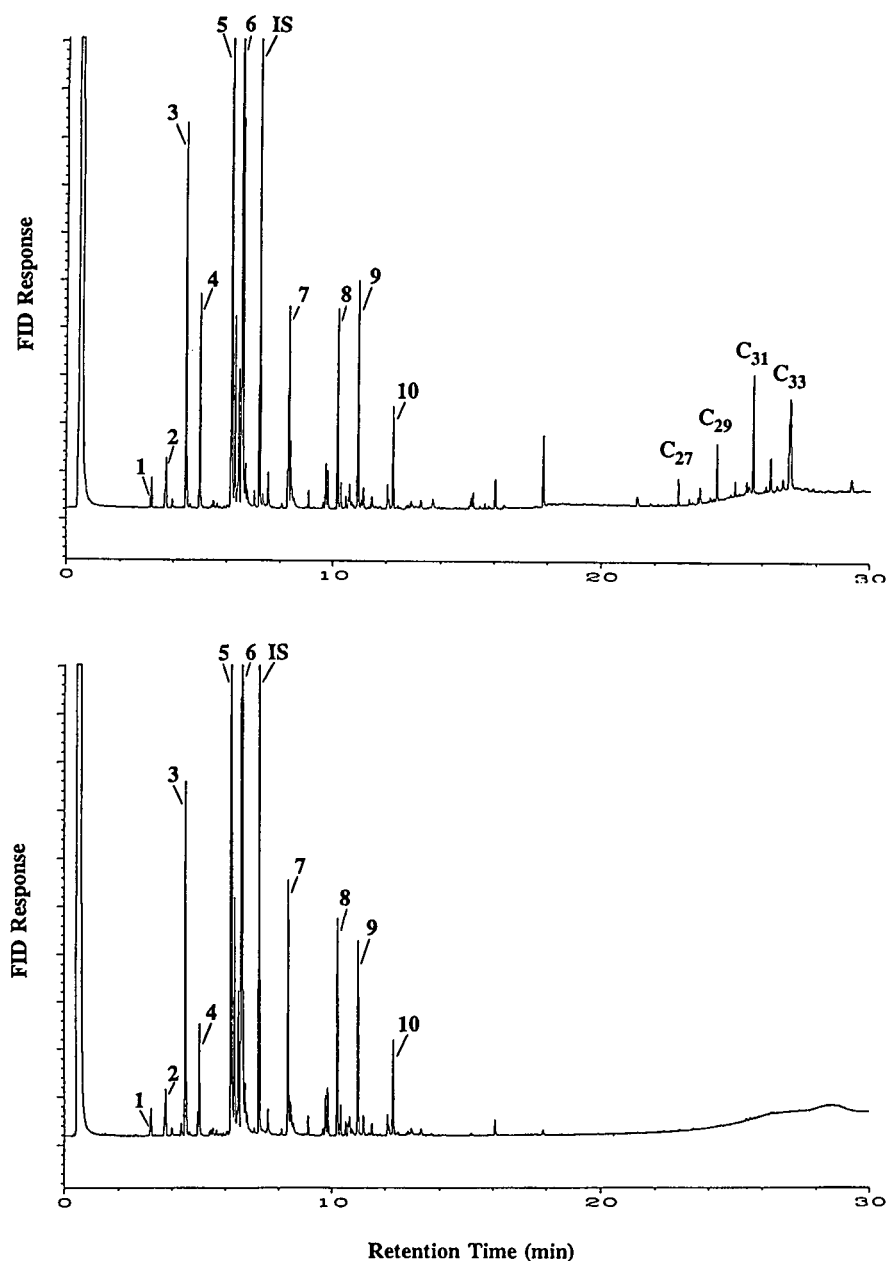


Fig. 2. GC-FID chromatograms of the SFE (top) and hydrodistillation (bottom) extracts of peppermint. Individual peaks are identified in Table II (IS designates the internal standard). Chromatographic conditions are given in the text.

tions were performed using savory, with the goal of obtaining quantitative (>95%) extraction of the essential oils with an extraction time of 30 minutes. Since individual essential oil components typically have high solubilities in supercritical CO₂ under the conditions used in this study,

it was hoped that pure CO₂ could be used for quantitative SFE extractions. However, as shown in Fig. 4 by the extraction rates of carvacrol and γ -terpinene, SFE with pure CO₂ at 400 atm for 30 min only recovered *ca.* 75% of the total extractable essential oil components.

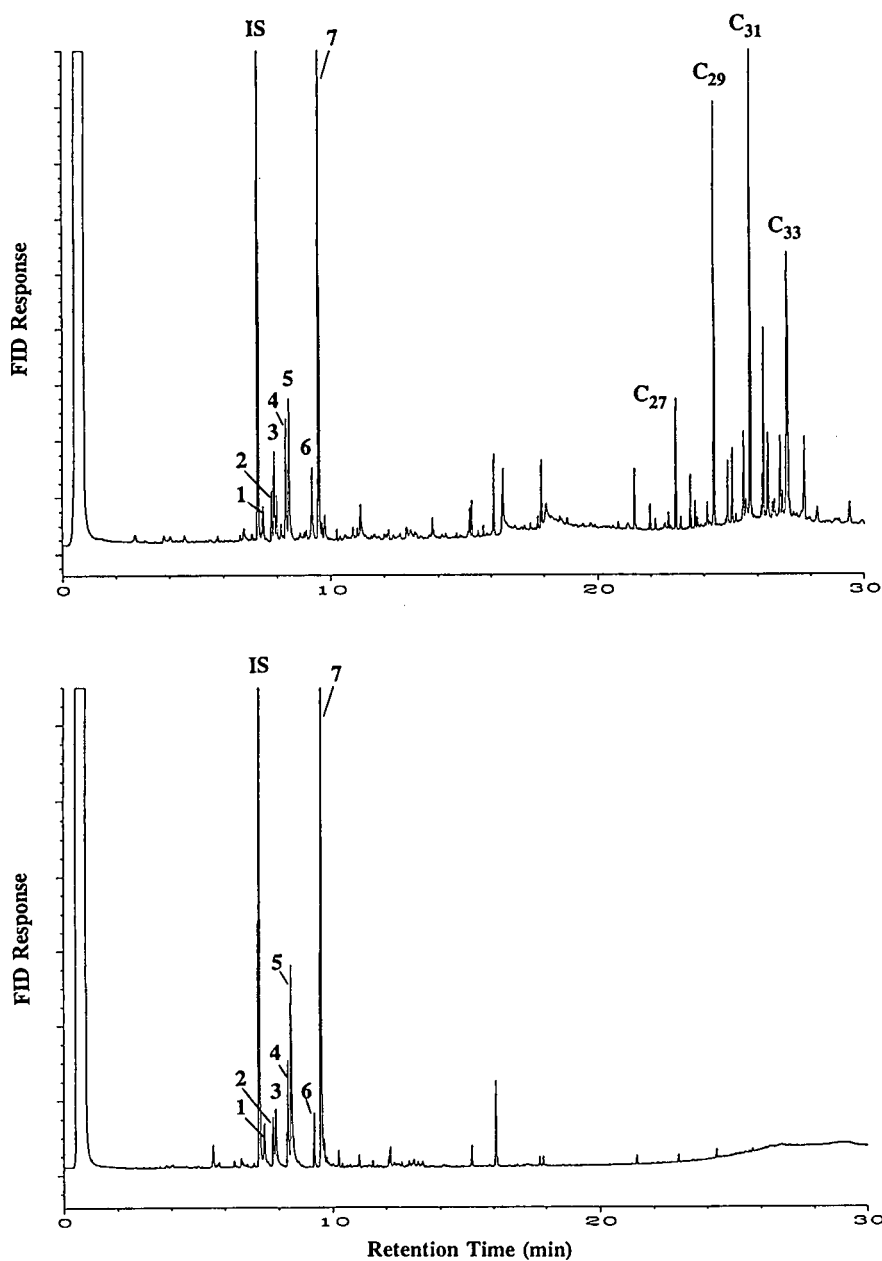


Fig. 3. GC-FID chromatograms of the SFE (top) and hydrodistillation (bottom) extracts of dragonhead. Individual peaks are identified in Table III (IS designates the internal standard). Chromatographic conditions are given in the text.

Even after 90 min of extraction with pure CO_2 , ca. 15% of additional extractable components remained in the savory matrix. Since the solubility of individual essential oil components is very high (typically several %, w/w, ref. 17) and since a 30-min extraction would utilize ca. 20 ml

of the supercritical CO_2 , the extraction rates appear to be kinetically limited (rather than solubility limited) in a manner similar to that previously described by a diffusion model for SFE [18]. (Note that while the extraction rates are described by the mathematics of the diffusion

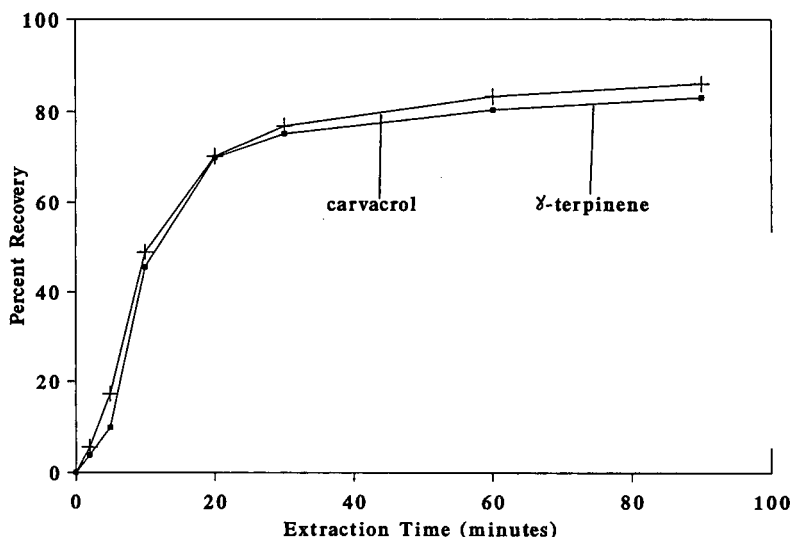


Fig. 4. Extraction rates of carvacrol and γ -terpinene using pure CO_2 . Quantitative recovery (100%) was defined as the total quantities of each component extracted by a combination of SFE for 90 min with pure CO_2 followed by an additional extraction with methylene chloride modified CO_2 (15 min static followed by 15 min dynamic as described in the text).

model, matrix-analyte interactions and the related kinetics of the desorption process are likely to fit the same mathematics, and appear more likely to control SFE rates than diffusion of the analytes in the matrix alone.) Because a primary goal of the extraction method was to achieve quantitative recovery with an extraction time of no more than 30 min, the addition of organic modifiers to the CO_2 was therefore evaluated.

Comparison of organic modifiers

The addition of organic modifiers to CO_2 can be achieved either by utilizing a dual pumping system, or by purchasing the modified CO_2 as a pre-mixed fluid. A much simpler (and less expensive) alternative is to simply add a measured volume (0.5 ml in this study) of the modifier directly to the extraction cell, an approach that only requires one pump filled with pure CO_2 . To ensure that the modifier was not rapidly swept out of the extraction cell upon pressurization, the initial extraction was performed in the static mode (no flow out of the cell) after pressurization with the CO_2 pump. After the 15-min static extraction step, the outlet valve of the extractor was opened and the extracted analytes were then swept out of the cell with pure CO_2 for an

additional 15-min dynamic extraction (performed in a manner identical to that used for the pure CO_2 extractions discussed above).

While selection criteria for SFE modifiers are not clear [3], we hoped to obtain high extraction efficiencies using a modifier that has good characteristics for subsequent GC injections, as well as for efficient collection of the SFE-extracted analytes (19). Therefore, three modifiers (hexane, acetone and methylene chloride) were chosen for the initial modifier survey. To avoid any potential GC injection problems that might occur with mixed solvent systems, the SFE extracts from the modifier survey were collected in the same solvent as that used for the modifier. Replicate samples of savory were sequentially extracted three times with each modifier.

The relative extraction efficiencies (compared to the yields from triplicate hydrodistillation extractions) obtained after one and after three sequential extractions with the three modifiers are shown in Fig. 5. A single extraction with hexane-modified CO_2 yielded poor recoveries (ca. 40 to 60%), although three sequential extractions (a total extraction time of 90 min) yielded recoveries similar to those obtained from four hours of hydrodistillation. While the recoveries with acetone modifier were superior to

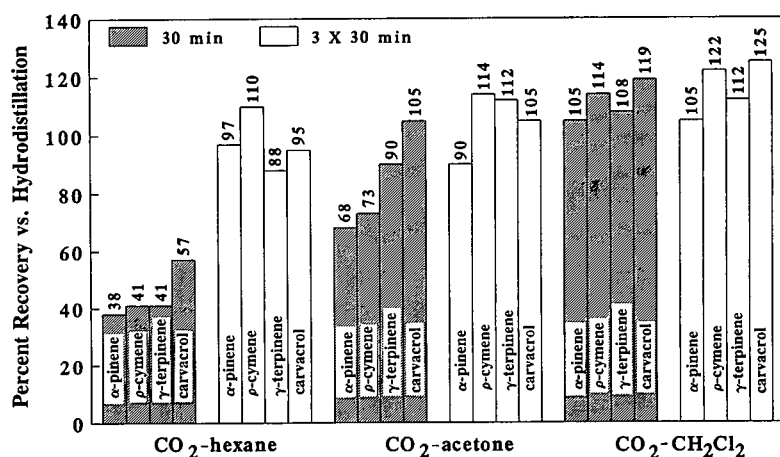


Fig. 5. Relative extraction efficiencies of representative essential oil components from savory using hexane, acetone and methylene chloride modifiers in CO₂. Three sequential extractions were performed with each modifier of replicate savory samples. The bars indicate the quantity of the components extracted after one 15 min static/15 min dynamic extraction ("30 min") and after three sequential 15/15 min extractions ("3 × 30 min"). Extraction efficiencies are based on the amounts extracted using hydrodistillation of triplicate samples.

the hexane modifier, three sequential extractions were still required to obtain extraction efficiencies similar to those achieved using hydrodistillation. However, a single 30-min extraction (15 min static/15 min dynamic) with the methylene chloride-modified CO₂ was sufficient to obtain extraction efficiencies even higher than those obtained using hydrodistillation. In addition, three sequential extractions with methylene chloride modifier failed to yield any significant increase in the amounts of the essential oil components that were extracted (Fig. 5). Since a single extraction with methylene chloride-modified CO₂ yielded essentially quantitative extraction efficiencies with a total extraction time of only 30 min, this method was used for all subsequent extractions.

Collection efficiencies of volatile compounds

Many of the more volatile flavor and fragrance compounds (e.g., monoterpenes) of interest in this study have previously been shown to be lost during off-line SFE when the extracted organics are collected in liquid solvents, although with careful choice of collection solvent conditions the collection efficiencies of species such as α-pinene have been increased to 90% [19]. If such losses

occurred during the dynamic SFE step because of poor collection efficiencies, the resultant low recoveries could mistakenly be blamed on poor extraction (rather than poor collection) efficiencies. Therefore, the recoveries of spiked organics (*i.e.*, added to the sample rather than a native component) using the methylene chloride-modified CO₂ procedure were measured to determine if the extracted analytes were efficiently removed from the extraction cell and efficiently trapped in the collection solvent. Approximately 25 to 30 μg each of several representative flavor compounds were spiked onto a savory sample that had previously been exhaustively extracted (*i.e.*, no detectable analytes remaining in the SFE extracts) using four sequential methylene chloride modified CO₂ extractions. The spiked samples were then immediately extracted using methylene chloride-modified CO₂ in the same manner as that used for the normal samples (15 min static followed by 15 min dynamic SFE). The average recoveries from three spiked samples were α-pinene (92%), γ-terpinene (97%) thymol (98%), eugenol (102%), geranyl acetate (97%) and β-caryophyllene (102%), which demonstrates that collection in 4 ml of methylene chloride was sufficient for the compounds of interest in this study.

Comparison of SFE and hydrodistillation extracts

Although the focus of this study was to develop SFE conditions for essential oil components, some interesting differences in the SFE versus the hydrodistillation extracts were readily apparent. First, the hydrodistillation extracts were light yellow, while the SFE extracts were dark green indicating the extraction of chlorophyll along with the essential oils (this was not the case when using pure CO₂, as the dark green extracts only resulted from the modified CO₂ extractions). Examination of the GC–FID chromatograms also showed the presence of odd-numbered plant wax *n*-alkanes in the SFE extracts that were not detected in the hydrodistillation extracts (Figs. 1–3). The concentrations found for these alkanes from the three test samples are shown in Table IV, and are generally lower than the major essential oil components of savory and peppermint, however the *n*-alkanes have concentrations similar to the most concentrated flavor compound (geranial acetate) from dragonhead (Table III). Kinetic plots similar to those shown in Fig. 4 demonstrate that these alkanes are extracted more rapidly with pure CO₂ than the essential oil components, which might be expected since plant waxes are found on the tissue surface. While these alkanes do not interfere with the determination of the essential oil components by GC–FID, their presence in the SFE extracts requires that higher final chromatographic temperatures be used to ensure their removal from the GC column.

TABLE IV

CONCENTRATIONS OF *n*-ALKANES EXTRACTED BY SFE FROM SAVORY, PEPPERMINT AND DRAGONHEAD

	Concentration (mg/g plant tissue)		
	Savory	Peppermint	Dragonhead
Heptacosane (C ₂₇)	0.09	0.05	0.13
Nonacosane (C ₂₉)	0.17	0.11	0.48
Untriacontane (C ₃₁)	0.33	0.22	0.77
Tritriacontane (C ₃₃)	0.35	0.32	0.61

The quantities of each of the major flavor and fragrance compounds extracted using hydrodistillation and SFE are shown in Tables I–III. The quantitative reproducibilities of the two extraction techniques were similar for savory and peppermint (Tables I and II), however, SFE yielded much better quantitative reproducibilities for the dragonhead sample. (It must be noted that the relative standard deviations shown in Tables I–III are based on the mg/g tissue of each extracted species, and not on the percent composition data. RSDs based on the percent composition for each extract are typically lower, *e.g.*, 2 to 11% for the hydrodistillation extracts of dragonhead compared to *ca.* 40% for the mg/g data.) Initially there was concern that the relatively small samples used for SFE (0.5 g) might not be representative of the bulk sample. However, the RSDs obtained using SFE clearly demonstrate that the 0.5-g samples were sufficiently large to be representative of the bulk sample, since SFE obtained similar (or better) reproducibilities than hydrodistillation performed using 20-g samples. In addition, since the RSDs obtained from replicate GC analyses of single extracts were typically <2%, these results demonstrate that the quantitative variations shown in Tables I–III result from the extraction processes, and are not a result of sample inhomogeneity or the GC analysis.

SFE extracted slightly higher quantities of all of the species from savory than hydrodistillation (Table I), while SFE extracted slightly lower quantities from peppermint (Table II). The average amounts of the essential oil components extracted from dragonhead were much higher using SFE. However, the total quantity of essential oils available in dragonhead for extraction is much lower (*ca.* 1 mg/g tissue) than those available from savory and peppermint (*ca.* 20 and 6 mg/g, respectively), which makes quantitative recovery of the extracted oils from the hydrodistillation apparatus difficult. Although care was taken to recover all of the oil from the hydrodistillation (using solvent washes), it is likely that the lower apparent recoveries (and the poorer quantitative reproducibility based on the mg/g data) shown for the hydrodistillation of dragonhead is a result of an inability to quantita-

tively recover the relatively small amounts of essential oil from the hydrodistillation apparatus.

When the extraction results are compared based on percent composition of the extracted essential oil, all three samples showed good agreement between the SFE and hydrodistillation extracts (Tables I–III), with the exception of some very low concentration species (*e.g.*, <0.1 mg/g) such as geranial and neryl acetate (from dragonhead, Table III) which showed *ca.* two times higher concentrations in the SFE extracts. The most significant difference found between the SFE and hydrodistillation extracts from all three samples used in this study was the relative concentrations of peaks 8 and 12 in the savory extracts [tentatively identified by MS as a hydroxy- and methoxy-substituted phenyl propene isomer, C₁₀H₁₂O₂ (*M_r* = 164), and a C₁₀H₁₄O₂ (*M_r* = 166) isomer, respectively]. Both of these species were found at concentrations 15 to 20 times higher in the SFE extracts than in the hydrodistillation extracts (Table I), possibly because hydrodistillation was not effective for their extraction (as was the case for the *n*-alkanes). Alternatively, hydrodistillation has been shown to cause degradation of some essential oil components from exposure to high temperatures and atmospheric oxygen [13] resulting in poor recoveries. To determine whether these two species were poorly extracted or degraded during hydrodistillation, a 0.5-g portion of the savory residue (after hydrodistillation) was extracted by SFE. The SFE extract contained both species (as well as small amounts of carvacrol and the two sesquiterpenes, and all of the *n*-alkanes). However, the quantities of the two species that were recovered were < 1/3 of those expected based on SFE of the original savory samples, indicating that some degradation of those species during hydrodistillation may have occurred.

The similarity in composition seen for the more volatile compounds (*e.g.*, monoterpenes) in Tables I–III was particularly interesting since it was initially suspected that the hydrodistillation technique could result in significant losses of such volatile species during the four hour extraction. However, since the spike recovery study discussed above demonstrated the ability of SFE to quantitatively collect monoterpenes, and since

the SFE and hydrodistillation extracts showed very similar distributions of the volatile components, the results of this study suggest that hydrodistillation does not result in significant losses of the more volatile essential oil components.

CONCLUSIONS

SFE provides a rapid and quantitative method for extracting essential oils from aromatic plants that compares favorably with the results of hydrodistillation. While essential oil components generally have high solubility in pure supercritical CO₂, the addition of an organic modifier (methylene chloride) greatly increased the extraction rates indicating that matrix-analyte interactions are more important than bulk solubility for controlling SFE extraction rates and recoveries.

ACKNOWLEDGEMENTS

The authors would like to thank the Academy of Finland for financial support. The loan of the SFE unit by ETEK (Helsinki, Finland) and ISCO (Lincoln, NE, USA) is also appreciated.

REFERENCES

- 1 J.L. Veuthey, M. Caude and R. Rosset, *Analisis*, 18 (1990) 103.
- 2 R.W. Vannoort, J.-P. Chervet, H. Lingeman, G.J. de Jong and U.A.Th. Brinkman, *J. Chromatogr.*, 505 (1990) 45.
- 3 S.B. Hawthorne, *Anal. Chem.*, 62 (1990) 633A.
- 4 E. Stahl and K.W. Quirin, *Pharm. Res.*, 5 (1984) 189.
- 5 K. Sugiyama and M. Saito, *J. Chromatogr.*, 442 (1988) 121.
- 6 S.B. Hawthorne, M.S. Krieger and D.J. Miller, *Anal. Chem.*, 60 (1988) 472.
- 7 R.M. Smith and M.D. Burford, *J. Chromatogr.*, 600 (1992) 175.
- 8 K. Hartonen, M. Jussila, P. Manninen and M.-L. Riekola, *J. Microcol. Sep.*, 4 (1992) 3.
- 9 V.M.v. Schantz, Y. Holm, R. Hiltunen and B. Galambosi, *Dtsch. Apoth.-Z.*, 127 (1987) 2543.
- 10 J.P. Sang, *J. Chromatogr.*, 253 (1982) 109.
- 11 Y. Holm, R. Hiltunen and I. Nykänen, *Flavour Fragrance J.*, 3 (1988) 109.
- 12 Y. Holm, B. Galambosi and R. Hiltunen, *Flavour Fragrance J.*, 3 (1988) 113.
- 13 G. Schmaus and K.-H. Kubeczka, in A. Baerheim

- Svendsen and J.J.C. Scheiffer (Editors), *Essential Oils and Aromatic Plants*, Martinus Nijhoff/Dr. W. Junk Publishers, Dordrecht, 1985, p. 127.
- 14 A. Koedam, in N. Margaris, A. Koedam and D. Vokou (Editors), *Aromatic Plants: Basic Applied Aspects*, Martinus Nijhoff Publishers, The Hague, 1982, p. 229.
- 15 A. Koedam, *Comparative Study of Isolation Procedures for Essential Oils—Hydrodistillation vs. Solvent Extraction*, Drukkerij J.H. Pasmans, The Hague, 1980, pp. 7–36.
- 16 M.D. Burford, S.B. Hawthorne, D.J. Miller and T. Braggins, *J. Chromatogr.*, 609 (1992) 321.
- 17 E. Stahl and G. Gerard, *Perfum. Flavor*, 10 (1985) 29.
- 18 K.D. Bartle, A.A. Clifford, S.B. Hawthorne, J.J. Langenfeld, D.J. Miller and R. Robinson, *J. Supercrit. Fluids*, 3 (1990) 143.
- 19 J.J. Langenfeld, M.D. Burford, S.B. Hawthorne and D.J. Miller, *J. Chromatogr.*, 594 (1992) 297.

Peroxyoxalate chemiluminescence detection in capillary electrophoresis

Nian Wu and Carmen W. Huie*

Department of Chemistry, State University of New York at Binghamton, Binghamton, NY 13902-6000 (USA)

(First received October 15th, 1992; revised manuscript received December 14th, 1992)

ABSTRACT

The feasibility of employing peroxyoxalate chemiluminescence (PO-CL) detection in capillary electrophoresis (CE) was demonstrated using a two-step approach for the CE separation and dynamic elution (elution under pressure) of the analytes. In this approach, potential problems associated with incompatibilities between mixed aqueous–organic solvent and electrically driven separation systems were avoided by switching off the CE power supply at an appropriate time and connecting the CE capillary to a syringe pump to effect dynamic elution. The effects of dynamic flow-rate and PO-CL reagent concentration on the CL signal intensity and/or peak width were examined for the measurements of three dansylated amino acids. The average limit of detection for these analytes using this PO-CL method is about 1.2 fmol (*ca.* 85 nM) which is approximately 35-fold lower than UV absorption methods.

INTRODUCTION

Due to the small sample volume requirement in capillary electrophoresis (CE), the development of new detection methods capable of providing improvements in limits of detection (LOD) is an important area of research. A wide range of method based on well-known detection principles have been demonstrated to be quite useful for CE, including UV absorption [1–3], fluorescence [4–6], mass spectrometry [7,8], conductivity [9] and electrochemistry [10,11]. Among these methods UV absorption is the most popular because most organic analytes possess high molar absorptivities at the 210-nm region; nevertheless, UV absorption method lacks sensitivity primarily due to the short optical path-length available across the capillary column. To achieve significant gain in LOD, detection methods based on phenomena of high inherent sensitivity, such as fluorescence, should be used. For

example, using a laser for fluorimetric excitation, detection of zeptomole (10^{-21} mol) quantities of analytes has been reported [5,6]. However, laser-induced fluorescence methods possess some disadvantages, such as the presence of significant background noise, *e.g.*, Rayleigh and Raman scattering generated by the high-intensity laser, and the high price and complexity of most laser systems. These particular disadvantages could be, however, largely overcome by performing fluorescence measurements via chemical excitation, *i.e.*, the generation of fluorescence in which the electronically excited state of the molecule is provided by a chemical reaction (chemiluminescence).

Chemiluminescence (CL) has been shown to be a highly sensitive method for detection in conventional [12,13] and microcolumn [14] high-performance liquid chromatography (HPLC). Recently the feasibility of using CL as a detection scheme in CE has been demonstrated as well using the luminol CL system for the sensitive detection of two luminol derivatives [15]. It should be noted that, however, among the most

* Corresponding author.

common CL systems, *e.g.*, luminol, lucigenin and the peroxyoxalate (PO)-CL reaction, the PO-CL system has been most widely used for post-column detection in HPLC [16]. The popularity of the PO-CL reaction, which is based on the oxidation of an oxalate derivative in the presence of a suitable fluorophore, is in part due to its high quantum efficiency and, perhaps more importantly, its ability to excite a wide range of different fluorophores when compared to other CL systems. Although the use of organic solvents is required in most common applications of PO-CL detection in HPLC involving reversed-phase columns due to the low solubility and instability of most oxalate derivatives in aqueous solutions, the post-column addition of PO-CL reagents to the column effluent containing the fluorophores to generate CL emission can be achieved with excellent sensitivity while maintaining good separation performance under optimized experimental conditions [17]. The involvement of mixed aqueous–organic solvent systems, however, could present some major difficulties in the use of PO-CL reaction as a detection scheme in CE due to, for examples, the influence of organic solvents on the migration behaviors of the analytes, which are strongly dependent on their mobilities in the aqueous electrophoretic buffer, and the possible effect of high electric field strength on the stability of the PO-CL reagents [18].

Camilleri *et al.* [19] have recently demonstrated that CE separation of proteins and peptides followed by elution under pressure (dynamic elution) can be achieved with little loss of resolution, thus allowing the possible use of CE as a micropreparative technique. In this paper a similar two-step approach, involving switching off the CE power supply at an appropriate time and connecting the capillary to a syringe pump to effect dynamic flow, was demonstrated for the post-column detection of analytes in CE using the PO-CL reaction. Using dynamic elution, potential problems associated with incompatibilities between mixed aqueous–organic solvent and electrically driven separation systems are avoided. The effects of dynamic flow-rate and PO-CL reagent concentration on the CL signal intensity and/or peak width were ex-

amined for the measurements of three dansylated (Dns)-amino acids. LOD obtained using the present PO-CL method were compared to those of UV absorption method.

EXPERIMENTAL

Chemicals

Bis-(2,4,6-trichlorophenyl)oxalate (TCPO) was prepared using the procedures described by Mohan and Turro [20]. Dns-Glycine, Dns-L-arginine and Dns-L-leucine were purchased from Sigma (St. Louis, MO, USA). Hydrogen peroxide (30%) and all other chemicals were of analytical grade from Aldrich (Milwaukee, WI, USA). TCPO was dissolved in ethyl acetate and hydrogen peroxide was diluted with acetonitrile. All buffer solutions were made with distilled and deionized water.

Apparatus

CE separation was performed with a laboratory-built instrument consisting of an acrylic box designed with a safety-interlocked door to prevent operator contact with a +30 kV high-voltage power (Glassman High Voltage, Whitehouse Station, NY, USA), which was connected to the buffer reservoirs with platinum electrodes to effect CE separation. For on-line UV absorption detection, a detection window was created by burning off a small section of the polyimide coating at 40 cm from the anodic end of the electrophoretic capillary (55 cm × 75 μm I.D. × 144 μm O.D.) purchased from Polymicrotech (Phoenix, AZ, USA). Absorption of analytes which migrate pass the detection window was measured using a Spectra 100 UV–Vis detector set at 210 nm (Spectra-Physics, San Jose, CA, USA). For post-column CL detection, a post-column reactor which consisted of various fused-silica capillaries held within a Swagelock stainless-steel tee and a detection cell was constructed.

Fig. 1 shows a schematic diagram of the post-column reactor. One arm of the tee contained the electrophoretic capillary which was inserted into the reaction capillary (10 cm × 200 μm I.D. × 400 μm O.D.; Supelco, Bellefonte, PA, USA) situated at the opposite arm of the tee.

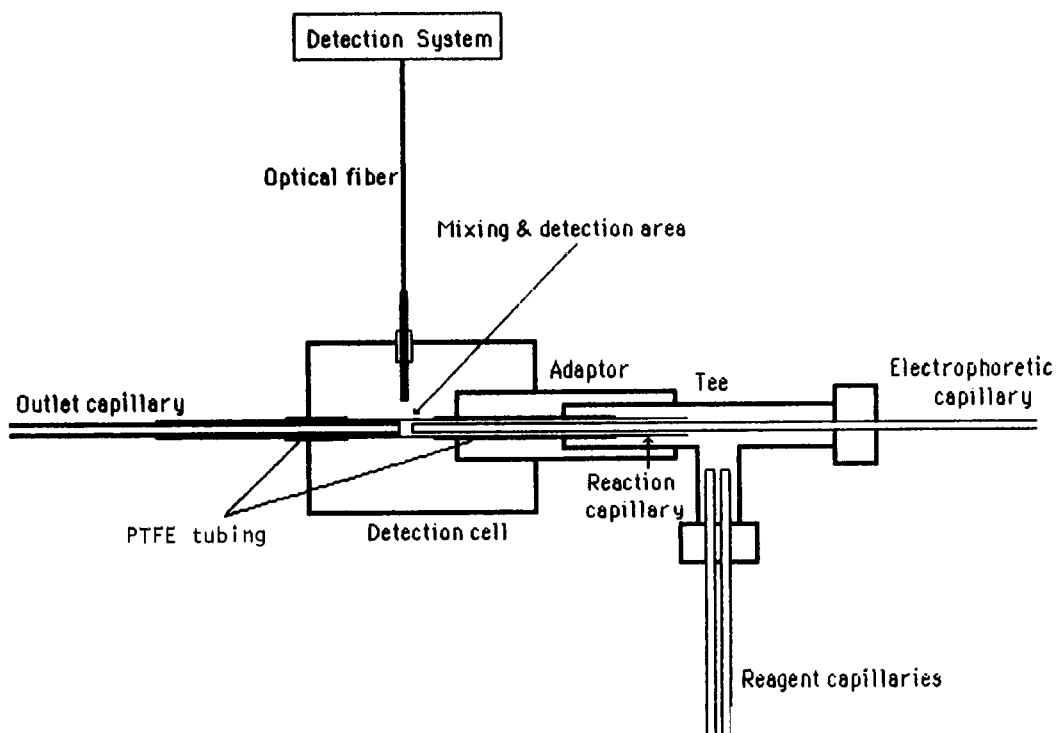


Fig. 1. Cross-sectional view of the post-column reactor.

The tee was connected to the detection cell via an adaptor and both the electrophoretic and reaction capillaries were inserted into the detection cell through the inner core of a PTFE tubing ($400\ \mu\text{m}$ I.D. \times $1.5\ \text{mm}$ O.D.), which served to protect the thin and fragile wall of the fused-silica capillaries. The reaction capillary extended from the tee through the entire length of the detection cell whereas the electrophoretic capillary terminated at a fixed distance near the center of the detection cell; an outlet capillary with smaller dimensions ($20\ \text{cm} \times 100\ \mu\text{m}$ I.D. \times $195\ \mu\text{m}$ O.D., Polymicrotech) was inserted into the opposite end of the reaction capillary to create a restricted area adjacent to the terminating end of the electrophoretic capillary to allow for mixing of the PO-CL reagents and column effluent containing analytes to occur within this post-column region. Two reagent capillaries ($15\ \text{cm} \times 75\ \mu\text{m}$ I.D. \times $144\ \mu\text{m}$ O.D., Polymicrotech) inserted into the central arm of the tee were used to deliver the PO-CL reagents (TCPO and H_2O_2) into the mixing area through the

small gaps that exist between outer surface of the electrophoretic capillary and inner surface of the reaction capillary. Dynamic elution of electrophoretic buffer and transport of the PO-CL reagents under pressure were achieved using two Sage syringe pumps (Model 341B; Orion, Boston, MA, USA).

To detect CL emission generated within the post-column mixing region, a detection window on the reaction capillary was made by burning off $2\ \text{mm}$ length of the polyimide coating. The CL emission was collected via one end of an optical fiber bundle: $61\ \text{cm}$ long \times $1.6\ \text{mm}$ diameter with a numerical aperture of 0.55 and an acceptance angle of 68° (Part No. 77520; Oriel, Stratford, CT, USA) situated directly above the detection window, and the other end of the fiber bundle was interfaced to the detection system. The CL emission was isolated by a 10-nm band-pass filter centered at $520\ \text{nm}$ (Corion, Holiston, MA, USA) and was detected using a photomultiplier tube (Model 9558B; EMI, Plainview, NY, USA) operated at voltage between 700 and 800

V. The photocurrent was fed to a picoammeter (Model 7080, Oriel) and the signal was recorded on an integrator (Chromjet, Spectra-Physics).

Procedures

The CE separations were performed with a 20 mM sodium borate buffer (pH 8.9). Dns-amino acid stock solutions were prepared by dissolving appropriate amounts of the analytes into the buffer solutions. After making serial dilutions to obtain the desired concentrations, the sample solutions were electrokinetically injected into the CE system at the anodic end by applying 9 kV for 5 s. The electrophoretic capillary was treated by purging with 0.05 M NaOH for about 0.5 h and then rinsed with the run buffer for 2 h before use.

The CE separation of analytes followed by dynamic elution was accomplished by first turning on the power supply at 16.5 kV for 3.2 min. During this time, the syringe pump connected to the reagent capillaries was turned on momentarily to provide a fresh supply of PO-CL reagents into the post-column mixing region. After 3.2 min, both the reagent supply pump and high-voltage power supply were turned off. The anodic and cathodic ends of the electrophoretic

capillary were then removed from buffer reservoirs and attached to a syringe pump and one arm of the tee as shown in Fig. 1, respectively. Immediately afterward, delivering of the PO-CL reagents was resumed and dynamic elution of the analytes was started by turning on the two separate syringe pumps that were adjusted to the appropriate flow rates.

RESULTS AND DISCUSSION

One of the most important factors which limits detectabilities in PO-CL based HPLC systems is that without the presence of fluorescent analytes, a relatively low background CL signal can be detected when the column effluent is mixed with the PO-CL reagents [13,21]. Recent evidence suggests that this background signal may arise from reaction intermediates and/or products of the PO-CL reaction, and its intensity can be influenced by various experimental factors [17,22]. We found that the flow-rate of the PO-CL reagents (TCPO and H_2O_2) affected the background signal intensity as follows: at 2.5 $\mu\text{l}/\text{min}$ or lower, the background current was found to remain relatively constant at 2.5 nA, and it increased by a factor of about 2 at flow-

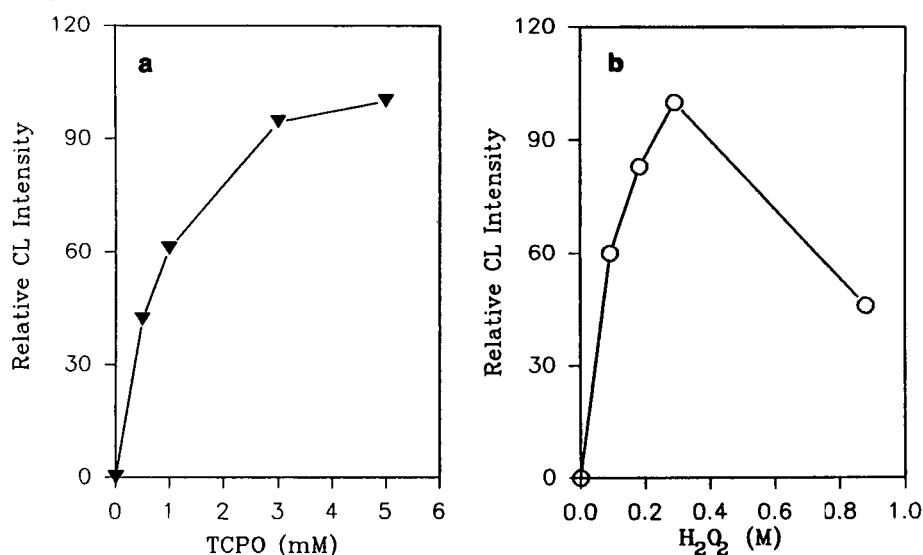


Fig. 2. Effects of (a) TCPO and (b) H_2O_2 concentrations on the relative CL intensity of 54 μM of Dns-L-leucine. The corresponding concentrations of TCPO and H_2O_2 in (a) and (b) were fixed at 5 mM and 0.29 M, respectively. Dynamic elution and PO-CL reagents flow-rate were set at 1.7 $\mu\text{l}/\text{min}$.

rates higher than $4 \mu\text{l}/\text{min}$ (dynamic flow-rate of the CE running buffer was kept at an optimum rate of $1.7 \mu\text{l}/\text{min}$, see below). Using a flow-rate of $1.7 \mu\text{l}/\text{min}$ for both the CL reagents and running buffer, Fig. 2a and b shows that the concentrations of TCPO and H_2O_2 which produced the highest CL intensity for the post-column detection of Dns-L-leucine were found to be 5 mM and 0.3 M , respectively.

A major concern in using the present approach is that after CE separation, peak broadening due to diffusion and/or other processes may occur, resulting in loss of resolution during the dynamic elution process. Fig. 3 shows the effects of flow-rate due to dynamic elution on the relative peak width (measured at the baseline) of three Dns-amino acids after CE separation. When compared to the normalized peak width of these analytes separated by CE without the influence of dynamic elution and detected by UV absorption detection method (Fig. 3: relative peak width = 1, at flow-rate = 0), it can be seen that broadening of the peak widths indeed occurred at a flow-rate of $1.2 \mu\text{l}/\text{min}$. This broadening effects were reduced significantly as a result of an increase in the flow-rate, with the peak widths approaching those obtained without dynamic elution after

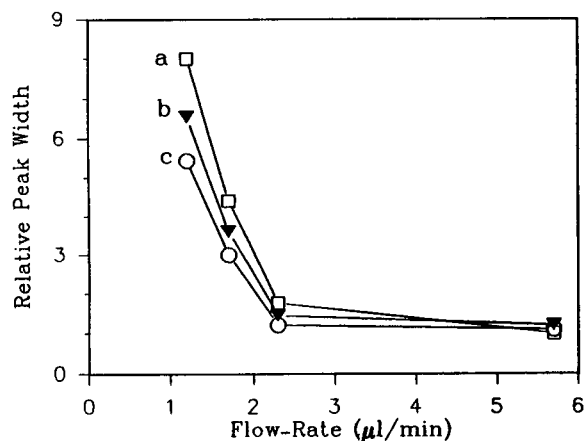


Fig. 3. Effects of flow-rate due to dynamic elution on relative peak width (at baseline) of three Dns-amino acids: (a) Dns-L-arginine = $1.24 \mu\text{M}$; (b) Dns-L-leucine = $1.08 \mu\text{M}$ and (c) Dns-glycine = $1.26 \mu\text{M}$. Flow-rate for the PO-CL reagents was $1.7 \mu\text{l}/\text{min}$ and the respective concentrations for TCPO and H_2O_2 were 4.5 mM and 0.29 M .

about $2 \mu\text{l}/\text{min}$; however, it should be noted that in conjunction with the decrease in peak broadening a loss in separation selectivity was found at higher flow-rates. Fig. 4 shows the effects of flow-rate due to dynamic elution on the relative CL intensity of three Dns-amino acids. It is clear that optimal CL intensity occurred at lower flow-rates ($<1.5 \mu\text{l}/\text{min}$) and started to decrease significantly, in particular for Dns-L-leucine and Dns-glycine, at flow-rates higher than *ca.* $1.7 \mu\text{l}/\text{min}$. Importantly the results obtained in Figs. 3 and 4 indicated that in choosing a flow-rate for dynamic elution of the three Dns-amino acids, a compromise has to be made between separation and detection performance, and it appears that the optimum flow-rates fall in the range between *ca.* 1.5 and $2.0 \mu\text{l}/\text{min}$.

Using the optimized conditions that have been determined for the flow-rates and PO-CL reagent concentrations, the separation and detection characteristics of the three Dns-amino acids after CE separation followed by dynamic elution and post column PO-CL detection are shown in Fig. 5a. For comparison purposes, Fig. 5b shows the CE separation and detection of the same Dns-amino acids without the influence of elution under pressure and using on-line UV absorption method. It can be seen that although the peak widths of the three analytes were broadened as a result of dynamic elution and post-column CL

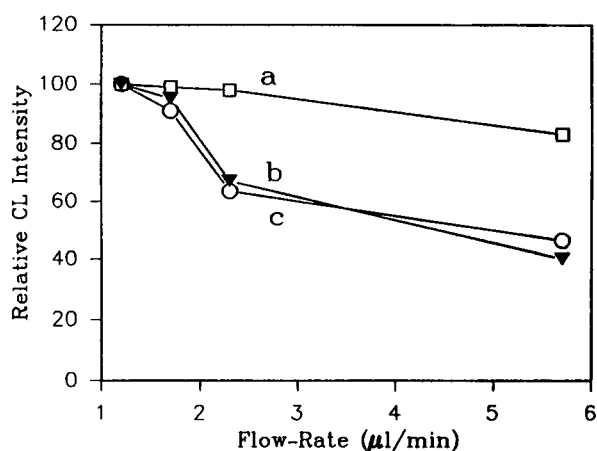


Fig. 4. Effects of flow-rate due to dynamic elution on the relative CL intensity of (a) Dns-L-arginine, (b) Dns-L-leucine and (c) Dns-glycine. Experimental conditions were as in Fig. 3.

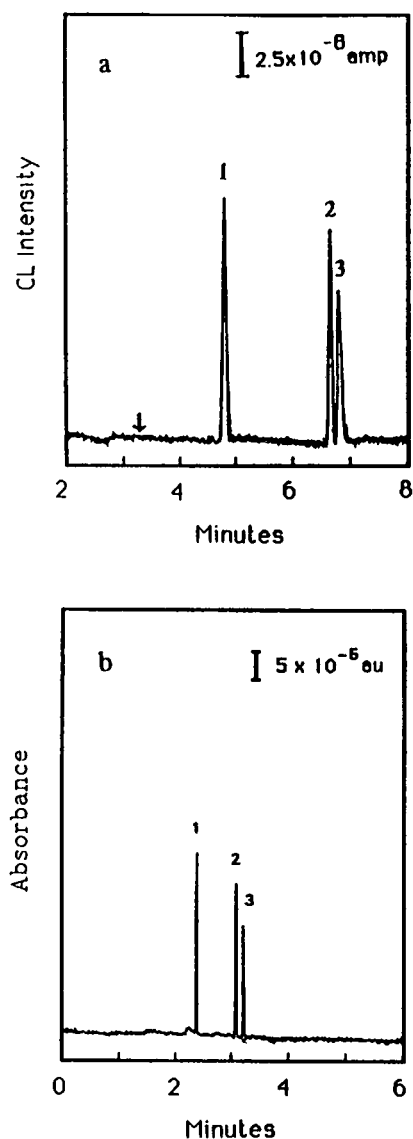


Fig. 5. (a) CE separation of (1) $1.24 \mu\text{M}$ of Dns-L-arginine; (2) $1.08 \mu\text{M}$ of Dns-L-leucine and (3) $1.26 \mu\text{M}$ of Dns-glycine followed by dynamic elution and PO-CL detection. Dynamic elution and PO-CL reagents flow-rate were set at $1.7 \mu\text{l}/\text{min}$. Concentrations of TCPO and H_2O_2 were 4.5 mM and 0.29 M , respectively. The arrow indicates the time at which the high-voltage power supply was turned off. (b) CE separation of (1) $62 \mu\text{M}$ Dns-L-arginine; (2) $54 \mu\text{M}$ of Dns-L-leucine and (3) $63 \mu\text{M}$ of Dns-glycine and detected using on-line UV absorption method.

reaction (baseline peak widths increased by a factor of about 3 to 4 at a flow-rate of $1.7 \mu\text{l}/\text{min}$ as shown in Fig. 3), the separation of all the

Dns-amino acids can still be achieved with baseline resolution. The advantage of the present method is in the improvement of LOD using the PO-CL system for sensitive detection. When compared to UV absorption detection, Table I shows an improvement factor of 1 to 2 order of magnitude in mass or concentration LOD was achieved for the measurements of the three Dns-amino acids using the present method. Average relative standard deviation ($n = 3$) on peak height for the three dansyl amino acids measured using the PO-CL method as shown in Fig. 5a was about 4.1%.

In conclusion we have demonstrated the feasibility of using the PO-CL system for the post-column detection of analytes after CE separation followed by elution under pressure. Clearly, more investigations are needed to optimize the various experimental factors which affect detection and separation performance using the present method. For examples, the use of deuterated running buffer may minimize the loss of resolution due to slower rate of analyte diffusion within the higher viscosity buffer solution [19]; modifications of the volume and geometry of the detection cell and connecting hardware may lead to less dispersion and/or higher degree of mixing between analytes and reagents; and also, the change in temperature, pH and the addition of catalyst and organic modifiers may affect CL efficiency and/or kinetics. Many of these factors have already been investigated in detail for the optimal determination of analytes in post-column HPLC systems involving the PO-CL reaction [12,17] and the knowledge gain in this area could be directed toward the improvements of separa-

TABLE I

COMPARISON OF CONCENTRATION AND MASS DETECTION LIMITS BETWEEN ABSORBANCE AND CHEMILUMINESCENCE DETECTION METHODS

Dns-Amino acid	LOD ($S/N = 3$)	
	UV absorption	PO-CL
Dns-L-Arginine	42 fmol ($2.4 \mu\text{M}$)	1.2 fmol (71 nM)
Dns-L-Leucine	32 fmol ($2.3 \mu\text{M}$)	1.0 fmol (69 nM)
Dns-Glycine	50 fmol ($3.8 \mu\text{M}$)	1.5 fmol (114 nM)

tion and detection performance using dynamic elution and PO-CL detection in CE.

ACKNOWLEDGEMENTS

The authors thank Dr. Richard A. Hartwick for the use of his research facilities and Spectra-Physics for financial assistance.

REFERENCES

- 1 Y. Walbroehl and J.W. Jorgenson, *J. Chromatogr.*, 315 (1984) 135.
- 2 M. Krejčí, K. Tesařík and J. Pajurek, *J. Chromatogr.*, 191 (1980) 17.
- 3 T. Tsuda and G. Nakagawa, *J. Chromatogr.*, 268 (1983) 369.
- 4 J.W. Jorgenson and K.D. Lukacs, *Anal. Chem.*, 53 (1981) 1298.
- 5 S. Wu and N.J. Dovichi, *J. Chromatogr.*, 480 (1989) 141.
- 6 J.V. Sweedler, J.B. Shear, H.A. Fishman, R.W. Zare and R. Scheller, *Anal. Chem.*, 63 (1991) 496.
- 7 R.A. Smith, J.A. Olivares, N.T. Nguyen and H.R. Udseth, *Anal. Chem.*, 60 (1989) 436.
- 8 M. Moseley, L. Deterding, K. Torner and J.W. Jorgenson, *J. Chromatogr.*, 480 (1989) 197.
- 9 X. Huang and R.N. Zare, *Anal. Chem.*, 63 (1991) 2193.
- 10 F.E.P. Mikkers, F.M. Everaerts and Th.P.E.M. Verheggen, *J. Chromatogr.*, 169 (1979) 11.
- 11 R.A. Wallingford and A.G. Ewing, *Anal. Chem.*, 59 (1987) 1763.
- 12 S. Kobayashi and K. Imai, *Anal. Chem.*, 52 (1980) 424.
- 13 K.W. Sigvardson and J.W. Birks, *Anal. Chem.*, 55 (1983) 432.
- 14 M.L. Grayeski and A. Weber, *Anal. Lett.*, 17 (1984) 1953.
- 15 R. Dadoo, L.A. Colón and R.N. Zare, *J. High Resolut. Chromatogr.*, 15 (1992) 133.
- 16 K. Robards and P.J. Worsfold, *Anal. Chim. Acta*, 266 (1992) 147.
- 17 P.J.M. Kwakman and U.A.Th. Brinkman, *Anal. Chim. Acta*, 266 (1992) 175.
- 18 R. Brina and A.J. Bard, *J. Electroanal. Chem.*, 238 (1987) 277.
- 19 P. Camilleri, G.N. Okafo and C. Southan, *Anal. Biochem.*, 196 (1991) 178.
- 20 A.G. Mohan and N.J. Turro, *J. Chem. Educ.*, 51 (1974) 528.
- 21 R. Weinberger, C.A. Mannan, M. Cerchio and M.L. Grayeski, *J. Chromatogr.*, 288 (1984) 445.
- 22 N. Hanaoka, H. Tanaka, A. Nakamoto and M. Takado, *Anal. Chem.*, 63 (1991) 26.

Automated preseparation derivatization on a capillary electrophoresis instrument

R.J.H. Houben, H. Gielen and Sj. van der Wal*

DSM Research, P.O. Box 18, 6160 MD Geleen (Netherlands)

(First received August 4th, 1992; revised manuscript received December 3rd, 1992)

ABSTRACT

Fully automated derivatization prior to separation and the separation conditions were established for the determination of D-valine in an excess of L-valine by preseparation derivatization with *o*-phthalaldehyde and N-acetylcysteine, separation of the resulting diastereomers by micellar electrokinetic capillary chromatography and absorbance detection. The precision and detection limit with absorbance detection are a factor of three worse than those achieved with HPLC and fluorimetric detection. The application of the method at high enantiomeric excess or with chemically impure samples is limited by the detector of the instrument.

INTRODUCTION

High-voltage capillary electrophoresis (CE) is a very efficient separation technique that suffers from a lack of detector sensitivity, but derivatization is a means of improving this. Postcolumn derivatization in CE has been shown to be feasible, but peak broadening in the reactor diminishes the efficiency benefit of CE [1]. Precolumn (preseparation) derivatization is an alternative that does not affect the efficiency.

In high-performance liquid chromatography (HPLC) the introduction of instrumentation for fully automated sample handling brought both the precision and the ease of use of precolumn derivatization within acceptable levels. This made precolumn derivatization in HPLC a popular technique and numerous suitable reagents for several functional groups are now available.

An analysis that is routinely performed in our laboratories by HPLC with automated pre-

column derivatization is the determination of the enantiomeric purity of amino acids and their derivatives. The enantiomers are made to react with a chiral reagent and the resulting diastereomers are separated by reversed-phase HPLC. Several of these diastereomeric derivatives can be separated with equivalent resolution in a shorter time by micellar electrokinetic capillary chromatography (MECC) on a CE instrument [2]. Therefore, it can be expected that in CE the automation of preseparation derivatization will be at least as important as in HPLC. A prerequisite is that the instrumentation and reagents are generally available in sufficiently pure form and do not have to be assembled or synthesized, respectively.

The benefits of fully automated preseparation derivatization on a CE instrument are not limited to derivatization with chiral reagents or analyses of chiral compounds but stem from the increased precision and convenience of automation of the derivatization compared with manual operation on the one hand and the resolution that can be obtained when separating on a

* Corresponding author.

capillary system with voltage instead of pressure as a driving force on the other.

In this paper we focus, as an example, on the determination of D-valine in an excess of L-valine by pre-separation derivatization, separation by MECC and absorbance detection.

EXPERIMENTAL

A P/ACE System 2050 (Beckman, Palo Alto, CA, USA) performed both the precolumn derivatizations and the separations and detection. To verify the concentrations used for the calibration graph of the P/ACE detector, the absorbance at 470 nm of solutions of potassium dichromate of different concentrations were measured in a 1-mm cell on a Lambda 15 spectrophotometer (Perkin-Elmer, Norwalk, CT, USA). The calibration graph was then obtained, based on the assumption of a negligible effect of stray light for the lowest concentrations used.

The HPLC system used to determine the absorptivity of derivatives of several reagents at the wavelengths available with the P/ACE system, consisted of Gilson (Villiers-le-Bel, France) Model 305/302 pumps, a Rheodyne (Cotati, CA, USA) Model 7125 injector, a 50 × 4 mm I.D. Nucleosil 120-5-C₁₈ column (Macherey-Nagel, Düren, Germany) and a Waters Model 990 diode-array detector (Millipore, Bedford, MA, USA). The eluent was a gradient from 10 to 90% acetonitrile in 10 mM phosphoric acid in 18 min at a flow-rate of 1 ml/min. L-Serine was employed as a test compound.

The reagents used in the absorptivity experiment were 1,2-phthalic dicarboxaldehyde (OPA) (Janssen, Beerse, Belgium) with N-acetylcysteine (NAC) (Janssen) [3] or N-acetyl-D-penicillamine (NAP) (Fluka, Buchs, Switzerland) [4] as a chiral thiol, 2,3,4,6-tetra-O-acetyl-β-D-glucopyranosyl isothiocyanate (GITC) (Polysciences, Warrington, PA, USA) [5], 1-fluoro-2,4-dinitrophenyl-5-D-alanineamide (Marfey's reagent) (Pierce, Rockford, IL, USA) [2] and (+)-1-(9-fluorenyl)ethyl chloroformate (Flec) (Fluka) [6]. Each reagent was added sub-stoichiometrically to prevent interference from unreacted reagent.

The sample solution consisted of the indicated concentration of (total) amino acid in 0.12 M

boric acid adjusted to pH 9.4 with 1 M sodium hydroxide solution.

The reagent solution was made by addition of 14 mg of OPA and 17 mg of NAC to a solution of 17% (v/v) ethanol and 83% aqueous 0.12 M boric acid. This reagent solution was adjusted to pH 9.4 with 1 M sodium hydroxide solution.

All other chemicals were of analytical-reagent grade (Merck, Darmstadt, Germany). All water was filtered through a Milli-Q apparatus (Millipore) and all solutions were filtered through a 0.22-μm nylon filter before use.

The eluting buffer for MECC was prepared by dissolving 0.1% (w/w) methylhydroxyethylcellulose 30 000 (MEC) (Serva, Heidelberg, Germany) and sodium dodecyl sulphate (SDS) to a 0.1 M concentration in 0.58 M acetic acid and adjusting the pH to 3.7 with 1 M tris(hydroxymethyl)aminomethane (Tris) (USB, Cleveland, OH, USA).

Owing to the high limit of detection with the UV detector, a high concentration of analyte has to be used, which necessitates a high buffer capacity during the derivatization, which in turn demands a high ionic strength of the separation buffer. The low mobility of Tris keeps the conductivity-to-buffer-capacity ratio of the eluent to a minimum. The peak symmetry and selectivity for the OPA–NAC derivatives is excellent at pH 3.7. A benefit of using 0.1% MEC and buffering at pH 3.7 is the stability of the retention times: the electroosmotic flow is suppressed and the (negative) electrophoretic mobility of the derivatives dictates the retention.

Each new capillary was conditioned by a 10-min rinse with 1 M sodium hydroxide solution followed by several elongated blank runs. When the retention times of the derivatives do not decrease in consecutive runs the capillary is ready for use (if the electroosmotic flow is still too large, no peaks may be detected at all).

RESULTS AND DISCUSSION

Detector linearity

The sensitivity of an absorbance detector is approximately proportional to the path length of the incident radiation in the detector. In CE this

path length is the diameter of the separation capillary, which is about 1% of the path length in a standard HPLC detector. This limits the dynamic range on the low absorbance side; stray light is the limiting parameter in the high absorbance region.

The percentage of stray light, S , can be calculated with the equation

$$\log\left(\frac{P_0}{P'}\right) = \log\left[\frac{1+S}{(P/P_0)+S}\right]$$

where P_0 = power of the incident beam, P = power of the exit beam, without stray light, and P' = power of the exit beam.

A calibration graph with potassium dichromate was obtained using the P/ACE system, a 50 μm I.D. capillary and a detector wavelength of 340 nm (Fig. 1). About 18% of stray light is present and correction for non-linearity is necessary above 0.1 absorbance. (The wide absorbance bands of potassium dichromate make the effect of band width on the non-linearity of the detector negligible.)

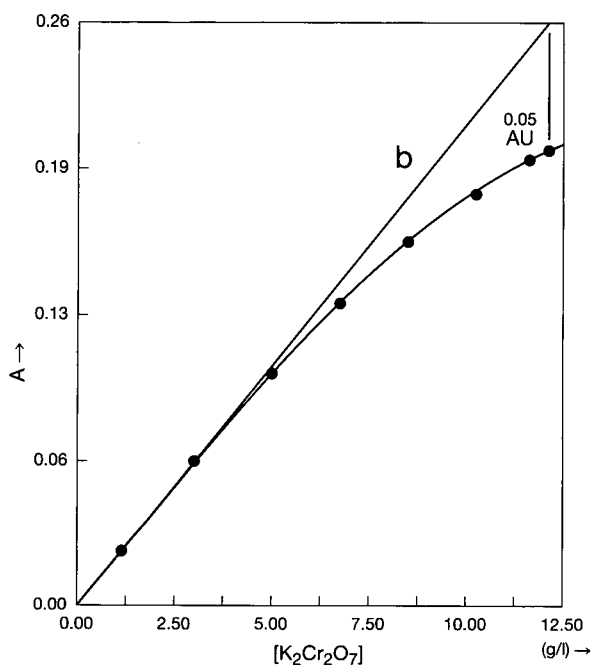


Fig. 1. Calibration graph to test the linearity of the absorbance detector. (b) Graph without stray light; (●) other experimental data.

Derivatization reagent

An increasing number of chiral reagents are commercially available. To make a selection we determined the absorptivity at five wavelengths of five reagents for derivatization of (primary) amines that are available to us. The results are given in Table I. Several derivatives show considerable absorptivity at 214 nm; unfortunately, possible interferences are likely to absorb in this low-UV region also. Marfey's reagent has the most favourable spectral characteristics. Moreover, this reagent has been shown to result in exceptionally good enantioselectivities on MECC separation systems [2]. However, with the present P/ACE system the implementation of the automated derivatization with Marfey's reagent requires elevated temperature or very lengthy derivatization times, so to demonstrate the feasibility of precolumn derivatization the fast

TABLE I
ABSORPTIVITY OF DIFFERENT DERIVATIVES

Reagent	Molar absorptivity $\times 10^{-3}$ ($\text{l mol}^{-1} \text{cm}^{-1}$)				
	200 nm	214 nm	254 nm	280 nm	340 nm
OPA-NAC	23.7	31.7	10.7	4.0	10.6
OPA-NAP	26	31.5	13.3	4.7	13.3
GITC	17	7.7	3.8	1.6	0.5
Marfey's reagent	19	10	5.7	5.7	25
Flec	38	36	16	9.5	0

reaction of D,L-valine with OPA-NAC was chosen [3,7].

Reaction conditions

The full programme used for automatic derivatization and separation is given in Table II.

First a capillary volume of sample is taken (step 3), analogous to the precise method of complete loop filling in HPLC [8]. Then a timed amount of reagent is flushed backwards at fixed pressure together with the sample into a microvial (step 5) and a stream of nitrogen is used to mix the contents of the microvial during the reaction (step 7). The electrophoresis buffer is

introduced into the separation capillary (step 9), injection takes place (step 10) and in addition to the separation (step 11) the capillary is cleaned to prevent memory effects (step 12). In between several steps carryover is eliminated by a dip in water of the possibly contaminated capillary end. The vial caps are constructed so that dilution by liquid adhering to the outside of the capillary is prevented.

The yield of the derivatization reaction is dependent on the pH and the excess of reagent in the microvial. Therefore, in addition to the reagent the sample solutions were buffered at the optimum pH of 9.4. At a reagent to sample ratio of 6.0-6.7 the excess of reagent has no significant influence on the result.

TABLE II

PROGRAM FOR AUTOMATED DERIVATIZATION FOLLOWED BY SEPARATION OF THE DERIVATIVES

Inlet vial ^a	Contents	Outlet vial	Contents
11	Separation buffer	1	Separation buffer
12-x	Analyte	2	Water
(x + 1)-31	Empty microvial	3	Reagent
33	Water	4	Water
34	Water	8	Empty
		10	Empty

Display Channel A with grid lines
Time: 0.00 to 10.00 Minutes
Channel A: -0.005 to 0.040 Absorbance

STEP	PROCESS	DURATION	INLET	OUTLET	CONTROL SUMMARY
1	SET DETECTOR				UV: 340 nm Rate: 10 Hz Normal Rise Range: 0200 -10% Zero 2.0 min.
2	SET TEMP				Temp: 25 °C
3	RINSE	2.0 min	12	8	Forward: High Pressure
4	WAIT	0.0 min	33	2	
5	RINSE	1.5 min	22	3	Reverse
6	WAIT	0.0 min	22	4	
7	RINSE	1.0 min	22	10	Reverse
8	WAIT	0.0 min	34	10	
9	RINSE	1.9 min	11	10	Forward: High Pressure
10	INJECT	25.0 s	22	10	Pressure
11	SEPARATE	10.0 min	11	1	Constant Voltage: 30.00 kV Current Limit: 100.0 uA Integrator On/Off
12	RINSE	3.5 min	11	10	Forward: High Pressure

^a x = 21 for single analysis of ten samples; x = 16 for triplicate analysis of five samples, etc.

Quantitative analysis

The method of Table II was investigated for the determination of the enantiomeric composition of pure valine at a high enantiomeric excess of L-valine using external standard methods. When the chemical purity of the analyte is known, only the peak of the D-valine derivative has to be measured, which can be done at good signal-to-noise ratios using concentrations of the major derivative that may overload the phase system.

Four different concentrations of D-valine in an approximately constant total valine concentration were analysed in quadruplicate (see Table III and Fig. 2). The calibration graph indicates that the percentage of D-valine in this range can be determined with a 0.1% precision (95%

TABLE III

CALIBRATION GRAPH FOR D-VALINE

Experiment No.	Area of D-valine peak ^a			
	A	B	C	D
1	20.88	33.65	71.93	106.52
2	19.50	33.22	74.12	107.61
3	17.17	39.23	72.62	106.80
4	19.60	38.71	71.61	

^a Total valine concentration and D-valine to L-valine ratio: (A) 36.0 mM and 0.0050; (B) 35.9 mM and 0.0097; (C) 35.9 mM and 0.0191; (D) 36.7 mM and 0.0283.

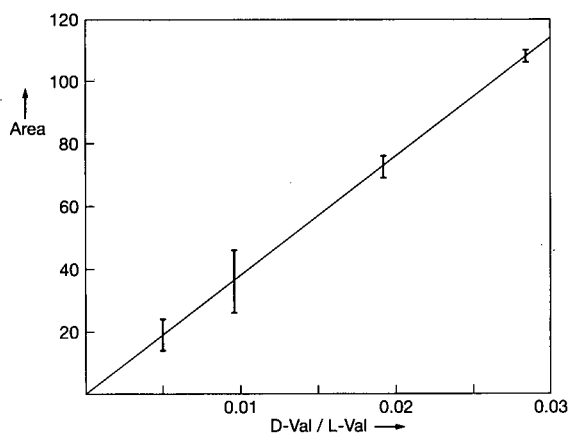


Fig. 2. Calibration graph for D-valine in excess of L-valine. Data are shown at the 95% confidence interval.

confidence interval) and a limit of detection of 0.3% D-valine in L-valine. A simpler one-point calibration gives a relative standard deviation (R.S.D.) of 6% at the 1% D-valine in L-valine level.

Improvement of the method

The precision and detection limit with absorbance detection obtained here are a factor of three worse than those achieved with HPLC and fluorimetric detection [7]. The precision could be improved by using the D/L ratio of the analyte. The ratio method also allows chemically impure analytes to be analysed. The validity of the

improvement by the ratio method was tested on a racemic mixture (see Table IV). It is clear that this is a significant advance.

At a concentration of 34 mM L-valine elutes under overload conditions: the local pH is not well defined and the analyte peak is distorted and absorbs in the non-linear range of the detector (see Fig. 3A). To eliminate the distortion the concentration must be decreased to 13 mM (Fig. 3B), which gives an unacceptable increase in the limit of detection with the detector used.

A different buffer during the reaction with less capacity can give some extension of the linearity of the calibration graph at high analyte concentrations (e.g., by detection of the main component in a less sensitive way at a different wavelength than the trace component). While this is a minor improvement, a laser-induced fluorescence detector is likely to offer the sensitivity needed, with additional selectivity [9]. Such a detector with a helium-cadmium laser is being constructed in our laboratory.

Other means of improving the precision such as standard additions or reagent addition by capillary volume instead of a timed constant pressure can be investigated when this detector is installed

The promising results of this investigation (i.e., the better resolution and a shorter separation time with MECC compared with HPLC) in

TABLE IV

COMPARISON OF AREA AND AREA RATIO FOR PRECISION OF RESULTS

Experiment No.	Area 1	Area 2	Area 1/area 2	Retention time (s)	
				t_{r1}	t_{r2}
1	302.698	322.966	0.9372	6.649	7.075
2	298.328	321.499	0.9279	6.551	6.968
3	306.909	321.108	0.9558	6.570	6.989
4	298.574	320.887	0.9305	6.572	6.992
5	307.495	326.802	0.9409	6.575	6.998
6	278.609	297.657	0.9360	6.592	7.018
7	302.348	319.821	0.9454	6.600	7.027
8	318.416	340.876	0.9341	6.589	7.020
9	298.680	314.274	0.9504	6.615	7.049
10	309.527	330.771	0.9358	6.609	7.044
R.S.D. (%)	3.4	3.5	1.0	0.4	0.5

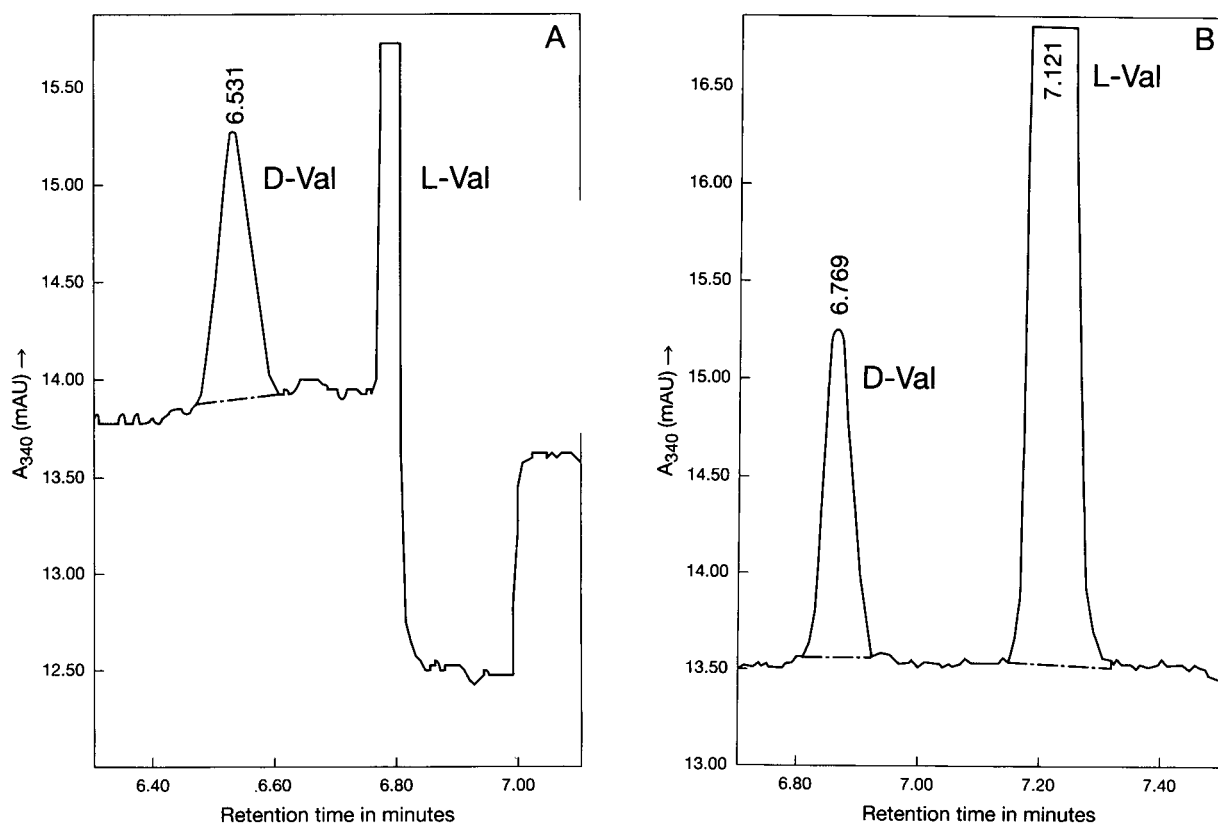


Fig. 3. Chromatogram of D,L-valine derivatives at the (A) 34 mM and (B) 13 mM levels.

our opinion warrant the research effort and increased instrumental expense. With the instrument manufacturers being aware of these developments, even more versatile software will become available to suit user-specific applications.

ACKNOWLEDGEMENT

We appreciate the opportunity given by the Higher Institutes for Professional Education at Heerlen and Venlo to their students R.J.H.H. and H.G. to complete their graduation work at DSM Research.

REFERENCES

1 D.J. Rose and J.W. Jorgenson, *J. Chromatogr.*, 447 (1988) 117.

- 2 A.D. Tran, T. Blanc and E.J. Leopold, *J. Chromatogr.*, 516 (1990) 241.
- 3 R.H. Buck and K. Krummen, *J. Chromatogr.*, 387 (1984) 279.
- 4 R.H. Buck and K. Krummen, *J. Chromatogr.*, 387 (1987) 255.
- 5 A. Jegorov, V. Matha, T. Trnka and M. Cerpy, *J. High Resolut. Chromatogr.*, 13 (1990) 718.
- 6 S. Einarsson and B. Josefsson, *Anal. Chem.*, 59 (1987) 1191.
- 7 A. Duchateau, M. Crombach, J. Kamphuis, W.H.J. Boesten, H.E. Schoemaker and E.M. Meijer, *J. Chromatogr.*, 471 (1989) 263.
- 8 *Technical Note No. 5*, Rheodyne, Cotati, CA, December 1983.
- 9 B. Nickerson and J.W. Jorgenson, *J. High Resolut. Chromatogr. Chromatogr. Commun.*, 11 (1988) 878.

Determination of salbutamol-related impurities by capillary electrophoresis

K.D. Altria

Pharmaceutical Analysis, Glaxo Group Research, Park Road, Ware, Herts. SG12 0DP (UK)

(First received May 22nd, 1992; revised manuscript received December 28th, 1992)

ABSTRACT

This paper describes the use and capabilities of capillary electrophoresis (CE) in the determination of two dimeric impurities present in salbutamol sulphate drug substance. Acceptable measures of detector linearity of response over the typical impurity range, detection limits, precision of peak area and migration times were obtained. The results obtained by CE were directly compared to those obtained by HPLC and TLC. The data shows agreement between the three techniques.

INTRODUCTION

Capillary electrophoresis (CE) has previously been used for the determination of drug-related impurities [1–5]. In addition there have also been a number of reports [5,6–9] of the separation of pharmaceuticals by the associated technique of micellar electrokinetic capillary chromatography (MECC). Elegant separations have been published showing the resolution of relatively low-concentration test mixtures of specific drug related compounds. However, there has been little emphasis on showing that these methods are capable of use in working analytical environments.

Salbutamol sulphate is a bronchodilator widely used for the treatment of asthma, which is sold under the Glaxo tradename of Ventolin. There are a range of well characterised potential, and actual, synthetic and degradative impurities possible [10]. HPLC methods have been developed and reported for the determination of these impurities [10,11]. There are several dimeric impurities, largely arising from degradation. These impurities are late eluters (>30 min) using the HPLC methods employed which makes quantitation of trace levels difficult. Two of these

late eluting dimeric compounds of particular interest are the “bis ether” impurity and “side-by-side” impurity. The structures of these impurities and salbutamol itself are given in Fig. 1.

This paper describes the preliminary validation experiments, and application of a free zone CE method, for the determination of selected salbutamol-related impurities present at low levels in drug substance.

EXPERIMENTAL

Sodium citrate (20 mM, pH 2.5) was obtained from Applied Biosystems (San Jose, CA, USA). Water was obtained from a Milli-Q system (Millipore, Watford, UK). A P/ACE 2000 CE instrument (Beckman, Palo Alto, CA, USA) which was connected to a Hewlett-Packard (Bracknell, UK) data collection system was used for CE analysis. The fused-silica capillaries used in this study were purchased from Beckman. Samples were obtained from within Glaxo.

Drug substance sample solutions were prepared by accurately weighing 12 ± 1.2 mg into 10 ml of distilled water. Bis ether standards were prepared by diluting accurately weighed amounts of bis ether standard to 10.0 ml of distilled

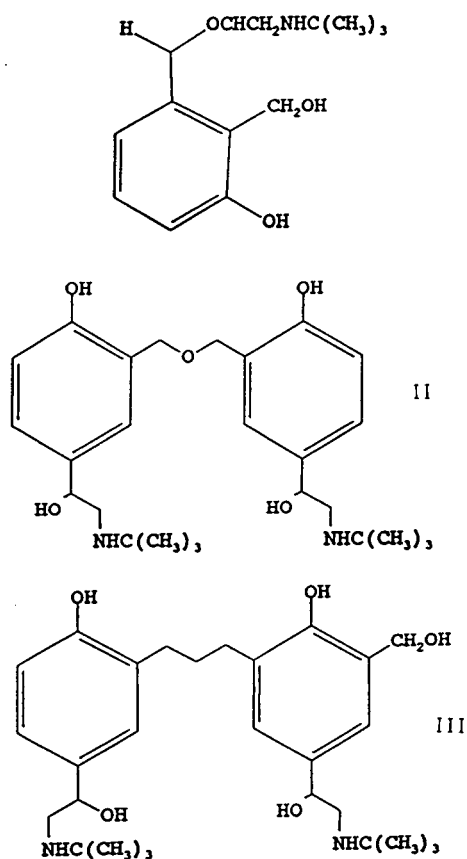


Fig. 1. Structures of salbutamol and dimeric salbutamol impurities. I = Salbutamol; II = bis ether; III = side-by-side.

water. Both samples and standards were prepared in duplicate.

The separation conditions are described in

TABLE I
CAPILLARY ELECTROPHORESIS SEPARATION METHOD

Step No.	Conditions
I	Rinse cycle 1: 0.5 M NaOH, 2 min
II	Rinse cycle 2: run buffer, 4 min
III	Set detector 0.02 AUFS
IV	5.0-s hydrodynamic sampling
V	Operating voltage: +30 kV
	Operating temperature: 25°C
	Capillary dimensions: 57 cm × 75 μm fused silica
	Run time: 10 min
	Wavelength: 200 nm

Table I, the method consisting of five automated steps.

RESULTS AND DISCUSSION

Optimization of the CE separation procedure

The principal CE variable is carrier electrolyte pH as this affects both solute mobility and electroendosmotic flow (EOF) velocity [12]. An electrolyte pH range of 2.5 to 11.0 was evaluated and a low pH (pH 2.5) electrolyte was selected which gave adequate separation with a run-time of 10 min.

To minimise the analysis time the maximum applicable voltage of +30 kV was used to perform the separation. This presented no problem in terms of joule heating whilst employing the relatively low electrolyte concentration (20 mM).

The limits of detection are generally poorer in CE compared to those obtained in HPLC. However, it is possible with CE to employ detection wavelengths as low as 190 nm where many solutes have an enhanced absorptivity. For example salbutamol has an eight-fold increase in signal when monitoring at 200 nm compared to the HPLC wavelength of 276 nm.

Viscosity influences the amount of solute introduced in both electrokinetic and hydrodynamic sampling [13,14]. Therefore, both samples and calibrations solutions were prepared in water to match the viscosities of the solutions. Injection of aqueous samples and calibrations also gives rise to a focussing, or pre-separation concentration [15] of sample ions in the initial portion of the separation capillary.

The use of rinse cycles is strongly advocated by CE instrument manufacturers as these cycles have been shown [16] to improve peak area and migration time reproducibility. Standard cycles used are an alkaline or acid wash followed by a pre-separation rinse with the carrier electrolyte.

System performance assessment

Selectivity. Test mixtures containing known amounts of authentic working standards for both salbutamol and the related impurities were prepared and analysed under the conditions given in

Table I. Good resolution between the bis ether impurity and side-by-side impurity from each other and salbutamol was obtained within a run-time of 10 min. Fig. 2 shows the migration order and relative impurity levels in a typical salbutamol sample. The order of elution being side-by-side, bis ether and lastly salbutamol.

This migration order can be explained in terms of the charges and sizes of the individual solutes. Electrophoretic mobility is related to the ratio of the charge and hydrated ionic radius (HIR) of an ion [17]. In this separation the dimeric species have twice the charge of the salbutamol ion but less than double its HIR. This gives them a higher charge/HIR ratio and they therefore elute before the salbutamol. The spatial orientation of the side-by-side in solution may be such that its HIR is smaller than bis ether which may explain the separation observed between these dimeric species.

It is anticipated that variation in the method parameters such as capillary type and coatings, addition of organic modifier, additives, temperature increase, and the electrolyte nature and concentration may have a beneficial effect upon the separation. Nielen [18] has reported the effect of varying such parameters upon the separation of aminobenzoic acid positional isomers. However, the separation conditions given

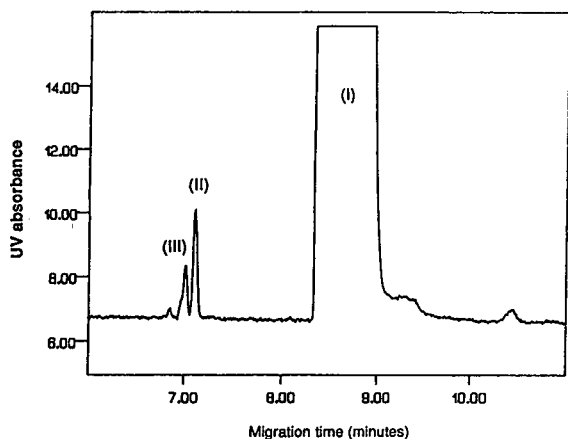


Fig. 2. Typical electropherogram of a salbutamol sample. Separation conditions: 20 mM sodium citrate pH 2.5, +30 kV, 25°C, 57 cm \times 75 μ m fused silica (50 cm to detector), 200 nm, sample concentration 1 mg/ml in water, injection time 5 s. Peaks: I = salbutamol; II = bis ether; III = side-by-side.

above gave a robust, selective, relatively uncomplicated analytical method with adequate resolution, within an acceptable analysis time.

Sensitivity. A limit of detector (LOD) of 0.02% (w/w) of the salbutamol loading (1 mg/ml) was obtained with a signal-to-noise ratio of greater than 3. This is equivalent to an LOD of 200 ng/ml in solution. This figure is in line with those reported previously [19].

Precision. To measure the performance of the system in terms of reproducibility a variety of tests were performed. Initially a single sample solution was analysed sequentially six times. The acceptable data obtained for the various measurements of operating performance are given in Table II.

External standardisation was also used to quantify bis ether levels. This method consists of preparing bis ether calibration solutions and obtaining appropriate response factors. To assess the repeatability of this method, four individual calibration solutions were prepared, and injected in duplicate, obtaining a mean overall R.S.D. of 4.0% for response factors. One of these calibration solutions was then injected seven times and a R.S.D. figure of 2.45% was obtained for response factor. This performance was considered acceptable given the low levels being quantified.

Separation efficiencies. Separation efficiencies as measured by theoretical plate count values can be exceptional in CE. However, there is a marked reduction in peak efficiency with increased sample concentration. In this specific example, salbutamol at a concentration of 1 mg/ml gave an average plate count of 1600 whilst the bis ether at ca. 0.3% (w/w) of the salbutamol loading (equivalent to 0.3 μ g/ml) gave an average plate count of 163 284.

This reduction of separation efficiency with sample loading is largely due to increased distortion of the conductivity profile along the capillary with increased sample loading [20].

Migration times. Table II shows relative migration times to have good reproducibility. The larger variation for the impurity peak times relative to salbutamol can be explained by the poorer peak shape of the salbutamol peak giving increased variability in measuring the peak apex.

TABLE II
ANALYSIS OF SIX REPLICATE INJECTIONS OF A
SALBUTAMOL DRUG SUBSTANCE SAMPLE

	Peak area data		
	Salbutamol	Dimer	Bis ether
Maxima	583658	3056	2347
Minima	571094	2889	2238
Mean	578520	2967	2293
R.S.D. (%)	0.76	2.2	2.0
	%area/area with respect to salbutamol		
	Dimer	Bis ether	
Maxima	0.525	0.406	
Minima	0.502	0.387	
R.S.D. (%)	1.6	1.8	
	Relative retention time data		
	Dimer wrt salbutamol ^a	Bis ether wrt salbutamol ^a	Bis ether wrt dimer ^a
Maxima	0.890	0.903	0.987
Minima	0.884	0.898	0.985
Mean	0.888	0.901	0.986
R.S.D. (%)	0.30	0.32	0.07
	Theoretical plates count data		
	Salbutamol	Dimer	Bis ether
Maxima	1830	172530	195061
Minima	1319	148214	173506
Mean	1594	163284	185350
R.S.D. (%)	12.1	5.2	4.5

^a wrt = with reference to.

This variability can be reduced by calculating the effective mobility [21] of the solute peaks.

Quantitation. There have been several reports [22–26] concerning the reproducibility of peak areas on automated instruments. Instrument manufacturers typically quote that R.S.D.s of less than 2% can be routinely obtained. Use of rinsing routines can assist in reducing levels of error to a level comparable to HPLC. By employing an internal standard, variability can be reduced still further with typical R.S.D.s of below 1% being obtained [26].

The %area/area data for both the bis ether and side-by-side (Table II) indicates good reproducibility with R.S.D.s below 2%. The results obtained for the salbutamol peak area are comparable to HPLC system performance. The R.S.D.s obtained for the impurity peaks acceptable given the variations obtained in measuring such small peaks.

It is recognised [27] that in CE, peak areas are directly proportional to both the sample concentration and migration time. The latter is related to the residence time that the peak spends in the detection window *i.e.* for a sample injection containing two solutes with identical UV response and concentration the slower moving peak will give a larger peak area. The extent of the peak area increase is directly related to the ratio of the two migration times.

Therefore it is necessary to normalise peak areas to their migration times to quote %area/area ratios. This normalisation simply consists of dividing the peak area obtained by the migration time of the peak [28].

The bis ether content was calculated for a particular batch of salbutamol drug substance using both the external standard calibration and standard addition approaches. The result obtained from the standard addition method (0.34%, w/w) was in good agreement with that calculated by external calibration (0.32%, w/w).

Linearity. Standard solutions of bis ether equivalent to between 0.05 and 1.4% (w/w) of a 1 mg/ml salbutamol sample were prepared and analysed in duplicate. A linear detector response (peak area) with bis ether content was obtained with a correlation coefficient of 0.999 and intercept of less than 1% of typical values, the gradient of the line was 7972. Typical levels of these impurities in samples are in the region of 0.1 to 0.5 (as determined by TLC).

In addition a 1 mg/ml salbutamol sample was spiked with known amounts of bis ether [between 0.1 and 1.4% (w/w) of the salbutamol loading] using a standard addition type method. A linear increase in detector response (peak area), with bis ether content, was obtained using this approach with a correlation coefficient of 0.993. The slope of this line was 7581. An intercept value of 3120 was obtained as the batch

of salbutamol used contained a residual amount of dimeric impurities.

QUANTITATIVE ANALYSIS

Comparison of CE with HPLC and TLC

Bis ether levels were quantified (in duplicate) in a range of batches by both HPLC and CE employing external standards of the bis ether compound. The results obtained (Table III) agree well. A paired *t*-test at a 95% confidence interval indicates that no significant difference exists between the CE and HPLC bis ether results.

Side-by-side levels were quantified by CE employing response factors from the bis ether standards. Side-by-side levels were generated by HPLC using side-by-side external standards.

TABLE III

COMPARISON OF BIS ETHER AND SIDE-BY-SIDE LEVELS IN EXPERIMENTAL SALBUTAMOL SULPHATE DRUG SUBSTANCE BATCHES AS DETERMINED BY CE, HPLC AND TLC

Batch	Bis ether (% , w/w)			Dimer (% , w/w)		
	CE	HPLC	TLC	CE	HPLC	TLC
1	0.14	0.16	0.18	0.08	0.08	0.09
	0.14	0.16		0.08	0.08	
2	0.10	0.11	0.19	0.06	0.07	0.12
	0.10	0.11		0.07	0.06	
3	0.20	0.19	0.24	0.13	0.11	0.16
	0.20	0.19		0.14	0.10	
4	0.12	0.13	0.20	0.07	0.06	0.13
	0.15	0.14		0.08	0.05	
5	0.13	0.14	0.12	0.08	0.06	0.08
	0.12	0.13		0.07	0.05	
6	0.31	0.28	0.32	0.18	0.17	0.23
	0.31	0.26		0.19	0.15	
7	0.07	0.09	0.12	0.05	0.04	0.06
	0.08	0.10		0.06	0.03	
8	0.38	0.38	0.45	0.20	0.18	0.28
	0.44	0.38		0.22	0.19	
9	0.37	0.38	0.36	0.19	0.17	0.30
	0.37	0.35		0.19	0.17	
10	0.75	0.66	0.69	0.39	0.33	0.45
	0.77	0.67		0.40	0.35	

Analysis of residuals indicates that the CE side-by-side data is typically 0.02 higher than that obtained by HPLC. This is explained by the different calibration procedures employed and the level of discrepancy does not unduly impact on the experimental results given the relatively low levels of impurities being determined.

TLC results are the mean of four individual analyses. TLC impurity levels were compared against salbutamol standards as detected at 254 nm. This procedure may explain significant differences between the results obtained by TLC and those generated by CE and HPLC. However the TLC results do serve to confirm the ranking of the batches in terms of relative impurity levels within this sample set.

CONCLUSIONS

This report demonstrates the use of a CE based method for the determination of drug related impurities in a working analytical environment. Acceptable levels of precision in terms of both migration time and peak area were obtained. The limit of detection for the related impurities was found to be 0.02% of the salbutamol loading (equivalent to 200 ng/ml of the impurity in solution) which is at least comparable to that achieved by HPLC. Linearity of the method was demonstrated by the use of both external standardisation and a standard addition method. Good cross-correlation for related impurity levels was obtained between HPLC, TLC and CE. It is strongly suggested that the complementary nature of CE based methods to HPLC will increase their application in pharmaceutical analysis for the quantitative determination of drug related impurities.

ACKNOWLEDGEMENTS

Thanks are extended to Dr. R.P. Munden of Glaxo Group Research (GGR) for helpful discussions, Mr. R.E. Bland of Glaxo Manufacturing Services for kindly supplying the TLC and HPLC data and to Mr. C. Luscombe for assistance with statistical evaluation of the data.

REFERENCES

- 1 K.D. Altria and C.F. Simpson, *J. Biomed. Pharm. Anal.*, 6 (1988) 801.
- 2 M.C. Roach, P. Gozel and R.N. Zare, *J. Chromatogr.*, 426 (1988) 129.
- 3 A.M. Hoyt and M.J. Sepaniak, *Anal. Lett.*, 22 (1989) 861.
- 4 K.D. Altria, M.M. Rogan and G. Finlay, *Chromatogr. Anal.*, Aug. (1990) 9.
- 5 K.D. Altria and N.W. Smith, *J. Chromatogr.*, 538 (1991) 506.
- 6 S. Fujiwara and S. Honda, *Anal. Chem.*, 59 (1987) 2773.
- 7 D.F. Swaile, D.E. Burton, A.T. Balchunas and M.J. Sepaniak, *J. Chromatogr. Sci.*, 26 (1988) 406.
- 8 H. Nishi, N. Tsumagari, T. Kakimoto and S. Terabe, *J. Chromatogr.*, 477 (1989) 259.
- 9 T. Nagawaka, Y. Oda and A. Shibukawa, *Chem. Pharm. Bull.*, 37 (1989) 707.
- 10 R.P. Munden, *Ph.D. Thesis*, University of East Anglia, 1991.
- 11 M. Mulholland and J. Waterhouse, *Chromatographia*, 25 (1988) 769.
- 12 K.D. Altria and C.F. Simpson, *Chromatographia*, 24 (1987) 527.
- 13 R.A. Wallingford and A.G. Ewing, *Anal. Chem.*, 60 (1988) 259.
- 14 D. Rose and J.W. Jorgenson, *Anal. Chem.*, 60 (1988) 643.
- 15 S.E. Moring, J.C. Colburn, P.D. Grossman and H.H. Lauer, *GC Int.*, 3 (1990) 46.
- 16 S.C. Smith, J.K. Strasters and M.G. Khaledi, *J. Chromatogr.*, 559 (1991) 57.
- 17 C.J.O.R. Morris and P. Morris, *Methods in Biochemistry*, Wiley, New York, 1976, Ch. 12.
- 18 M.W.F. Nielen, *J. Chromatogr.*, 542 (1991) 173.
- 19 M.T. Ackermans, J.L. Beckers, F.M. Everaerts and I.G.J.A. Seelen, *J. Chromatogr.*, 590 (1992) 341.
- 20 F.E.P. Mikkers, F.M. Everaerts and Th.P.E.M. Verheggen, *J. Chromatogr.*, 169 (1979) 11.
- 21 M.T. Ackermans, F.M. Everaerts and J.L. Beckers, *J. Chromatogr.*, 606 (1992) 229.
- 22 P.C. Rahn, *Am. Biotechnol. Lab.*, Jan. (1990) 22.
- 23 H.E. Schwartz, M. Melera and R.G. Brownlee, *J. Chromatogr.*, 480 (1989) 129.
- 24 D.J. Rose and J.W. Jorgenson, *Anal. Chem.*, 60 (1988) 642.
- 25 S. Honda, S. Iwase and S. Fujiwara, *J. Chromatogr.*, 404 (1987) 313.
- 26 E.V. Dose and G.A. Guiochon, *Anal. Chem.*, 63 (1991) 1154.
- 27 D. Demorest and R. Dubrow, *J. Chromatogr.*, 559 (1991) 43.
- 28 K.D. Altria, *Chromatographia*, 35 (1993), in press.

Determination of quaternary alkaloids from Phellodendri Cortex by capillary electrophoresis

Ying-Mei Liu and Shuenn-Jyi Sheu*

Department of Chemistry, National Taiwan Normal University, Taipei (Taiwan)

(First received November 5th, 1992; revised manuscript received December 9th, 1992)

ABSTRACT

A simple and rapid method for the simultaneous determination of six quaternary alkaloids (berberine, palmatine, jatrorrhizine, magnoflorine, phellodendrine and berberrubine) in the Chinese herbal drug Phellodendrine Cortex by capillary electrophoresis was developed. A buffer solution composed of 0.5 M sodium acetate solution (pH 4.6, adjusted with acetic acid)–acetonitrile (1:1) was found to be the most suitable electrolyte for this separation, whereby the contents of the quaternary alkaloids in crude and processed samples of Phellodendri Cortex could be easily determined. The differences in alkaloid contents of various Phellodendri Cortex growing in different locations (China, Taiwan, Japan) were also investigated.

INTRODUCTION

Phellodendri Cortex is a commonly used Chinese herbal drug having gastric, intestinal alternative, astringent and antiphlogistic effects and contains five quaternary ammonium salts (berberine, palmatine, jatrorrhizine, phellodendrine and magnoflorine) (Fig. 1) as its major bioactive components [1–4]. In addition, berberrubine, obtained from heat-treated Phellodendron bark, has been found to inhibit the growth of several tumour cell lines [5].

Several methods have been reported for the determination of some of these quaternary alkaloids, including spectrophotometry [6,7], thin-layer chromatography [7–10], electron microscopic analysis [11] and high-performance liquid chromatography (HPLC) [12–16]. However, none of these methods is entirely adequate because their resolution is limited to at the most four of the quaternary alkaloids [15]. So far,

there have been no reports dealing with the determination of phellodendrine and berberrubine.

We describe here the development of a simple, rapid and simultaneous method for determining these quaternary alkaloids in crude and processed samples of Phellodendri Cortex by capillary electrophoresis.

EXPERIMENTAL

Reagents and materials

Berberine chloride was purchased from Sigma (St. Louis, MO, USA), sodium acetate from Osaka (Osaka, Japan) and brucine, acetonitrile and acetic acid from Merck (Darmstadt, Germany). Palmatine and magnoflorine were isolated from *Phellodendron amurense* Pupr. [3]. Jatrorrhizine was isolated from *Coptis rhizome* [17]. Phellodendrine was provided by Brion Research Institute (Taiwan). Berberrubine was obtained by heating berberine chloride at 150°C for 30 min. *P. chinense* Schneid, *P. amurense* Pupr. var. *sachalinense* Fr. Schm. and *P. wilsonii*

* Corresponding author.

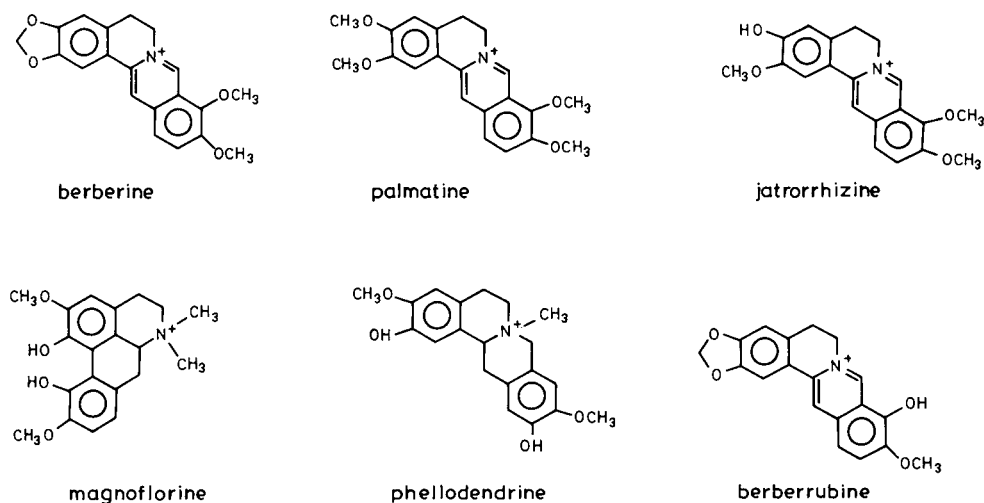


Fig. 1. Molecular structures of alkaloids in *Phellodendri* Cortex.

Hayata et Kanehira were purchased from Chinese herbal markets in China, Japan and Taiwan, respectively.

Preparation of *Phellodendri* Cortex extracts

A 0.5-g sample of pulverized *Phellodendri* Cortex was extracted with 70% methanol (7.5 ml) by stirring at room temperature for 30 min, then centrifuged at 1500 g for 10 min. Extraction was repeated three times. The extracts were combined and filtered through a No. 1 filter-paper. After the addition of 2.5 ml of internal standard solution (2 mg of brucine in 1 ml of 70% methanol), the *Phellodendri* Cortex extract was diluted to 25 ml with 70% methanol. This solution was passed through a 0.45- μ m filter and *ca.* 1.1 nl (15-s hydrostatic sampling) of the filtrate were injected directly into the capillary electrophoresis system.

Apparatus and conditions

The analysis was carried out on a Waters Quanta 4000 capillary electrophoresis system equipped with a UV detector set at 280 nm and a 50 cm \times 50 μ m I.D. uncoated capillary (Millipore, Bedford, MA, USA) with the detection window placed at 42.5 cm. The conditions were as follows: sampling time, 15 s, hydrostatic; run time, 9 min; applied voltage, 15 kV (constant voltage, positive to negative polarity); and tem-

perature, 24.5–25.0°C. The electrolyte was a buffer solution consisting of 0.5 M sodium acetate solution (pH 4.6, adjusted with acetic acid)–acetonitrile (1:1). The electrolyte was filtered through a 0.45- μ m filter before use.

RESULTS AND DISCUSSION

The quaternary alkaloids of *Phellodendri* Cortex are mostly the same as those of *Coptidis* Rhizoma. Therefore, we first tried to use the same capillary electrophoresis conditions as for *Coptidis* Rhizoma [18]. However, the magnoflorine peak of *Phellodendri* Cortex is much higher than that of *Coptidis* Rhizoma and there was interference with the solvent peak, hence different conditions were necessary.

Both magnoflorine and berberrubine are easily deprotonated in basic or neutral solution owing to their acidic phenolic hydroxy groups and will be partially overlapped by the solvent peak. As carboxylate is a good counter ion for the positively charged nitrogen of the alkaloids [18], we finally chose sodium acetate solution as the buffer solution and increased its acidity with acetic acid. The peaks of magnoflorine and berberrubine then appeared before the solvent peak, but other peaks were still partly overlapped and the electric current of the capillary was too high. Increasing the concentration of

sodium acetate improved the resolution and the use of a 50 μm instead of 100 μm I.D. capillary reduced the electric current.

After a series of experiments, it was found that 0.5 M sodium acetate solution (pH 4.6, adjusted with acetic acid) could separate all the alkaloids well. At higher pH (4.8), the peaks of berberrubine and phellodendrine could not be separated. At lower pH (4.5), jatrorrhizine and berberrubine were found to be partially overlapped. Addition of acetonitrile to the buffer solution could make the peaks sharper, produce a better separation effect and reduce the capillary electric current. An acetonitrile concentration of 50% gave the best result.

An electrolyte consisting of 0.5 M sodium acetate solution (pH 4.6, adjusted with acetic acid)–acetonitrile (1:1) was found to give the best resolution. Fig. 2 is an electropherogram showing the separation of the six authentic quaternary alkaloids with the following migration times: 5.5 min, berberine; 5.9 min, palmatine; 6.2 min, jatrorrhizine; 6.3 min, berber-

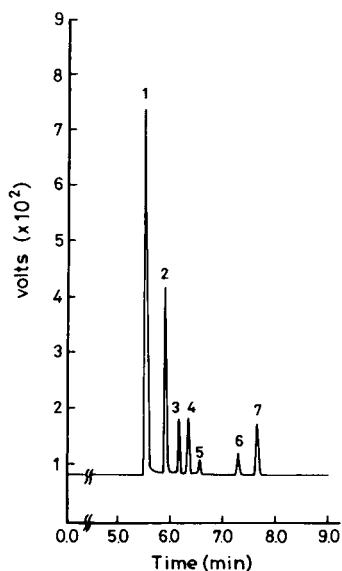


Fig. 2. Capillary electropherogram of a mixture of quaternary alkaloids usually present in crude and processed *Phellodendri Cortex*. Peaks: 1 = berberine, 0.600 mg/ml; 2 = palmatine, 0.200 mg/ml; 3 = jatrorrhizine, 0.040 mg/ml; 4 = berberrubine, 0.080 mg/ml; 5 = phellodendrine, 0.030 mg/ml; 6 = magnoflorine, 0.080 mg/ml; 7 = internal standard (brucine), 0.200 mg/ml.

rubine; 6.5 min, phellodendrine; 7.2 min, magnoflorine; and 7.6 min, internal standard (brucine). The measurement of all the constituents can be completed within 8 min. As the methanol–water extracts of *Phellodendri Cortex* were injected directly and analysed, the results were as good as those obtained with pure chemical samples without interference with each peak, as shown in Figs. 3–6.

Calibration graphs for quaternary alkaloids

Calibration graphs (peak-area ratio, y , vs. concentration, x , mg/ml) were constructed in the range 0.030–1.200 mg/ml for berberine, 0.010–0.300 mg/ml for palmatine, 0.002–0.060 mg/ml for jatrorrhizine, 0.003–0.090 mg/ml for berberrubine, 0.010–0.100 mg/ml for phellodendrine and 0.020–0.200 mg/ml for magnoflorine. The regression equations of these curves and their correlation coefficients were calculated as follows: berberine, $y = 12.35x + 0.07$ ($r = 0.9999$); palmatine, $y = 14.96x + 0.02$ ($r = 0.9999$); jatrorrhizine, $y = 21.64x + 0.01$ ($r = 0.9999$); berberrubine, $y = 15.84x + 0.00$ ($r = 0.9999$); phellodendrine, $y = 6.47x - 0.01$ ($r = 0.9997$); and magnoflorine, $y = 4.96x + 0.01$ ($r = 0.9997$).

Determination of quaternary alkaloids in *Phellodendri Cortex*

When the test solutions of *P. wilsonii* Hayata et Kanehira, *P. chinense* Schneid, *P. amurense* Pupr. var. *sachalinense* Fr. Schm. and heat-treated *P. amurense* Pupr. var. *sachalinense* Fr. Schm. were analysed by capillary electrophoresis under the selected conditions, the graphs shown in Figs. 3–6 were obtained. The peaks were identified by comparison with those obtained from authentic samples of the alkaloids. By substituting the area ratios of the individual peaks for y in the above equations, the content of each quaternary alkaloid in the *Phellodendri Cortex* samples was obtained as shown in Table I. It was found that there were great differences in the alkaloid contents of *Phellodendri Cortex* collected from different locations and also the heat-treated sample. Further studies on the relationship between the origins of plants and the contents of alkaloids and also the processing of *Phellodendri Cortex* are in progress.

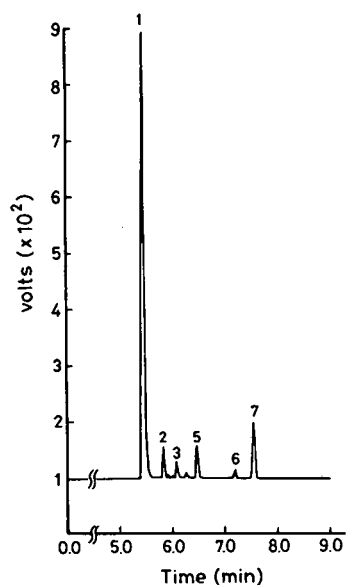


Fig. 3. Capillary electropherogram of the extract of a *P. wilsonii* Hayata et Kanehira sample (grown in Taiwan). Peak numbers as in Fig. 2.

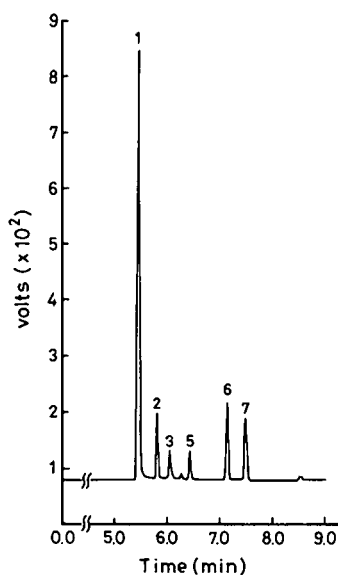


Fig. 5. Capillary electropherogram of the extract of a *P. amurense* Pupr. var. *sachalinense* Fr. Schm. sample (grown in Japan). Peak numbers as in Fig. 2.

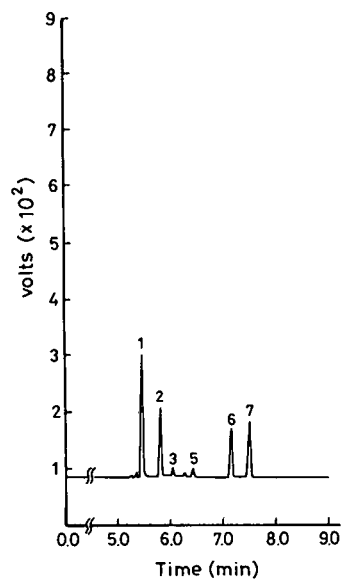


Fig. 4. Capillary electropherogram of the extract of a *P. chinense* Schneid sample (grown in China). Peak numbers as in Fig. 2.

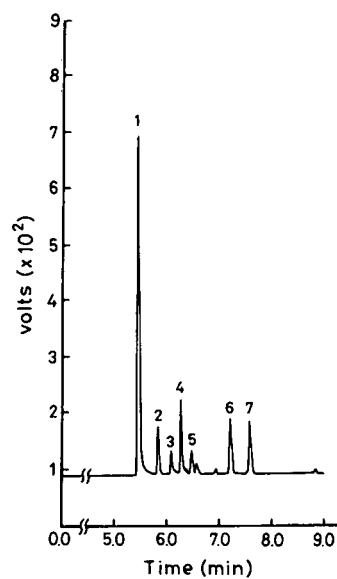


Fig. 6. Capillary electropherogram of the extract of a heat-treated *P. amurense* Pupr. var. *sachalinense* Fr. Schm. sample. Peak numbers as in Fig. 2.

Suitable amounts of the six quaternary alkaloids were added to a sample of *Phellodendri Cortex* of known alkaloid content and the mixture was extracted and analysed using the pro-

posed procedure. The recoveries of the alkaloids were 98.5–103.3% with relative standard deviations of 1.2–2.1%.

From the above results, it can be concluded

TABLE I
CONTENTS OF ALKALOIDS IN PHELLODENDRI CORTEX

Sample ^a	Concentration (%) ^b						
	Berberine	Palmitine	Jatrorrhizine	Phellodendrine	Magnoflorine	Berberrubine	Total
1	4.621 ± 0.038	0.141 ± 0.011	0.067 ± 0.003	0.364 ± 0.011	0.144 ± 0.002	–	5.360 ± 0.048
2	0.624 ± 0.007	0.317 ± 0.003	0.031 ± 0.003	0.117 ± 0.004	0.809 ± 0.007	–	1.923 ± 0.011
3	2.993 ± 0.019	0.253 ± 0.004	0.105 ± 0.004	0.281 ± 0.011	1.141 ± 0.028	–	4.747 ± 0.167
4	2.420 ± 0.027	0.216 ± 0.004	0.044 ± 0.002	0.260 ± 0.008	0.940 ± 0.012	0.342 ± 0.007	4.222 ± 0.063

^a 1 = *P. wilsonii* Hayata et Kanehira (grown in Taiwan); 2 = *P. chinense* Schneid (grown in China); 3 = *P. amurense* Pupr. var. *sachalinense* Fr. Schm. (grown in Japan); 4 = heat-treated *P. amurense* Pupr. var. *sachalinense* Fr. Schm.

^b Mean ± standard deviation ($n = 5$).

that the method for the simultaneous determination of the quaternary alkaloids in Phellodendri Cortex by capillary electrophoresis as established in this study has the advantages of the need for only small amounts of sample, a short analysis time and simple electrolyte preparation.

ACKNOWLEDGEMENT

Financial support (NSC 82-0208-M-003-012) from the National Science Council, Taiwan, is gratefully acknowledged.

REFERENCES

- 1 Y. Murayama and K. Shinozaki, *J. Pharm. Soc. Jpn.*, 46 (1926) 299.
- 2 M. Tomita and T. Nakano, *Pharm. Bull.*, 5 (1957) 10.
- 3 M. Tomita and J. Kunitomo, *Yakugaku Zasshi*, 78 (1958) 1444.
- 4 J. Kunitomo, *Yakugaku Zasshi*, 81 (1961) 1370.
- 5 Y. Kondo and H. Suzuki, *Shoyakugaku Zasshi*, 45 (1991) 35.
- 6 K. Yamaguchi, T. Tabata and H. Ito, *J. Pharm. Soc. Jpn.*, 73 (1953) 1189.
- 7 T. Yamagishi and M. Mori, *Hokkaidoritsu Eisei Kenkyusho Ho*, 26 (1976) 26; *C.A.*, 86 (1977) 47310s.
- 8 T. Mura and T. Tominaga, *Shoyakugaku Zasshi*, 27 (1974) 63.
- 9 X. Gan and K. Dai, *Tianran Chanwu Yanjiu Yu Kaifa*, 2 (1990) 9; *C.A.*, 115 (1991) 35800f.
- 10 M. Wang and M. Zhu, *Yaowu Fenxi Zazhi*, 4 (1984) 12; *C.A.*, 100 (1984) 126968y.
- 11 M. Mikage, T. Ushiyama and T. Namba, *Yakugaku Zasshi*, 107 (1987) 690.
- 12 O. Ishikawa, T. Hishimoto, T. Nakajima, O. Tanaka and H. Itokawa, *Yakugaku Zasshi*, 98 (1978) 976.
- 13 T. Misaki, K. Sagara, M. Ojima, S. Kakizawa, T. Oshima and H. Yoshizawa, *Chem. Pharm. Bull.*, 30 (1982) 354.
- 14 C. Zhang and Z. Zhang, *Zhongcaoyao*, 17 (1986) 16; *C.A.*, 104 (1986) 230552b.
- 15 S. Tosa, S. Ishihara, Y. Nose, T. Usikawa, S. Yoshida, H. Nakazawa and T. Tomimatsu, *Shoyakugaku Zasshi*, 43 (1989) 28.
- 16 G. Luo, Y. Wang, G. Zhou and Y. Yu, *J. Liq. Chromatogr.*, 13 (1990) 3825; *C.A.*, 114 (1991) 171391e.
- 17 A. Ikuta and H. Itakawa, *Shoyakugaku Zasshi*, 37 (1983) 195.
- 18 Y.M. Liu and S.J. Sheu, *J. Chromatogr.*, 623 (1992) 196.

Short Communication

Golay's paradox: linear *versus* non-linear chromatography

Friedrich G. Helfferich

Department of Chemical Engineering, The Pennsylvania State University, University Park, PA 16802 (USA)

(First received October 22nd, 1992; revised manuscript received January 11th, 1993)

ABSTRACT

Golay in 1964 posed the paradox that it should theoretically be possible to conduct an operation of single-component chromatography with linear isotherm and high column loading in such a way that the entropy of the system is decreased. The paradox is resolved by showing that the concentration dependence of the flow-rate, invoked by Golay, renders the system non-linear despite the linear isotherm. The result of the non-linearity is that one of the concentration variations spreads, instead of remaining sharp as it would in linear chromatography and as was assumed by Golay. This spreading negates the entropy decrease.

Golay [1] in 1964 posed a paradox, showing that gas chromatography under idealized conditions can defy thermodynamics by decreasing the entropy of a closed system. It puzzled all those attending the *Gas Chromatography* conference at which it was presented, and its resolution [2] still seems not to be generally known [3]. In abbreviated form and in our current language of wave theory (see, *e.g.*, ref. 4) the paradox can be formulated as follows:

A gas chromatographic column is loaded initially with two successive flat-top bands of the same solute; the bands are adjacent, and the solute concentration is higher in that on the upstream side (see Fig. 1). The concentrations are high enough for the volumetric flow-rate to be axially non-uniform. Specifically, the flow-rate is higher at higher solute concentrations [5]. This effect, sometimes called "sorption effect", arises because any solute present must be transported through the column cross-section in addition to the carrier gas, so that a higher molar and

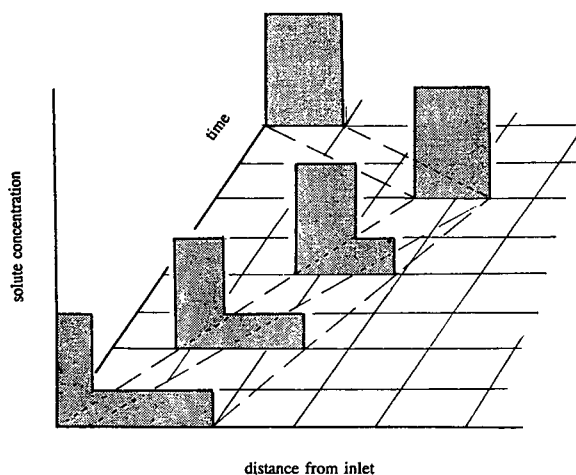


Fig. 1. Initial, intermediate, and final concentration profiles as postulated by Golay, shown in distance-time field; return of concentrated band to starting position upon flow reversal is included; thin dashed lines are wave trajectories in distance-time plane (schematic).

thus, in gases, volumetric flow-rate is required where the solute concentration is higher. The effect becomes significant at moderate to high mole fractions of solute. The isotherm is assumed to be linear. Since non-idealities—specifically: finite mass-transfer rates, non-plug flow, and axial diffusion—cause waves in linear chromatography to spread in proportion to the square root of traveled distance (see, e.g., ref. 6), the column and the bands need only be made sufficiently long for such spreading to remain an insignificant fraction of the band lengths upon passage through the column. Accordingly, for the purpose at hand, bands can be assumed to move like “box cars” between waves that remain practically sharp. Granted this point, the band of higher concentration, traveling faster because of the sorption effect, will “swallow up” that of lower concentration on its downstream side, so that eventually all of the solute will be in a single band at the higher concentration (see Fig. 1). The initially more dilute band has in effect been concentrated, and that amounts to a decrease in entropy! In Golay’s imaginary world of “frictionless chromatography”, this is achieved at no expenditure in energy or free energy. Golay does not say so but, granted his assumptions, flow could be reversed to move the single, high-concentration band back box-car style to where the two bands started, making it even more apparent that enrichment has been achieved at no cost (see Fig. 1).

The resolution of this paradox is simple and requires neither mathematics nor thermodynamics [2]. Golay makes mutually exclusive assumptions when he postulates that (1) waves spread in proportion to the square-root of traveled distance, and (2) the flow-rate is higher at higher concentrations. If condition 2 is met, the rear of the concentrated band cannot remain sharp: it contains high concentrations ahead of low ones, that is, faster concentrations ahead of slower ones, and therefore it spreads *in proportion to traveled distance* (see Fig. 2). This proportional spreading is in addition to the supposedly negligible square-root spreading caused by any non-idealities, and is an effect that *cannot* be suppressed by a scale-up to greater lengths of column and bands. As seen in Fig. 2, the real

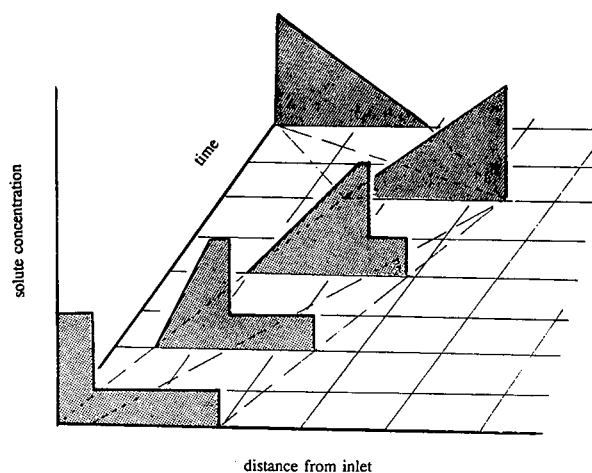


Fig. 2. Actual initial, intermediate, and final concentration profiles as resulting from sharpening and spreading behavior of non-linear waves; return of solute to starting position upon flow reversal is included (schematic; the slanting profiles are not necessarily linear; the high-concentration plateau may disappear earlier, or a portion of it may survive).

result of the operation is an asymmetrical peak or band with sharp front and diffuse rear, rather than Golay’s “box car” band of uniform high concentration. By a reversal of the flow direction, the peak or band could be moved back to where the two bands had started. The diffuse flank would then regain its sharpness because, in it, the faster, higher concentrations are now upstream of the slower, lower ones. However, in the other, still sharp flank the situations is the reverse, and this flank would now spread (see Fig. 2). Thus, the whole operation achieves no more than trading the initial step profile for a continuously slanting one, with no decrease in entropy.

It is true that condition 1 *can* be met, for instance, at concentrations low enough to make the sorption effect negligible. However, this would invalidate assumption 2, and the bands would move side by side without change in shape, that is, Golay’s effect would not materialize.

The spreading rear flank of the concentrated band is what is commonly called a nonsharpening wave (or rarefaction wave in gas dynamics). In ideal non-linear chromatography in the absence of the sorption effect, nonsharpening

waves are well known to arise as a result of an isotherm curvature that causes leading concentrations in the wave to move faster than trailing ones [4,7,8]. For instance, a solute band has a nonsharpening rear if the isotherm is of Type I (*i.e.*, with negative curvature), and a nonsharpening front if the isotherm is of Type II (with positive curvature). In Golay's case, the isotherm is assumed to be linear. However, *any* effect that makes leading concentrations in a wave travel faster than trailing ones (granted non-idealities are negligible) obviously produces proportional spreading. It is immaterial whether the cause is an isotherm curvature or the sorption effect. If the sorption effect is significant, it could be compensated by a slight Type II curvature of the isotherm [9] so as to meet Golay's postulate 1. Then, however, the result is the same as with a linear isotherm and negligible sorption effect: The bands move side by side without change in shape.

Golay admits the existence of non-idealities, being content with rendering their effect negligible by scale-up to very large column and band lengths. However, one could argue that, in a mathematical world of strictly ideal chromatography, the intermediate concentrations of the nonsharpening wave at the rear of the concentrated band (*i.e.*, those that form the spreading wave in Fig. 2) never come into existence, so that their velocities remain immaterial. The wave could then keep moving as a discontinuity, and the paradox would remain. Indeed, such behavior is described by a mathematically correct "weak solution" [10,11] to the differential mass balance and overall conservation of matter, analogous to the weak solutions that describe the shocks (*i.e.*, traveling concentration discontinuities) at the front of the low-concentration band and between the two bands. That the weak solution for the nonsharpening wave can have no physical reality can be shown by a rather involved argument that proves it would violate the second law of thermodynamics [12,13]. An alternative and much more simple argument is that mathematics of ideal chromatography is of practical interest only insofar as it provides a reasonable approximation to real behavior. This it does if it constitutes an asymptotic solution to

real chromatography with non-idealities made infinitesimally small. The weak solution for the nonsharpening wave does not meet that criterion because any non-ideality, even if only infinitesimal, lets the intermediate concentrations become physically realized and so causes the wave to spread in a proportional pattern rather than remaining ideally sharp [4].

Golay himself was on the right track when seeking an analogy with shocks in gas dynamics. He concluded correctly that the wave between the high- and low-concentration bands would have to be a shock—that is, a wave which sharpens or remains sharp despite the spreading effect of non-idealities—and so should produce entropy in the same way as shocks in compressible fluids are known to do. However, he was unable to resolve his paradox because he missed the key piece of the puzzle by not recognizing the rear of the high-concentration band as a nonsharpening wave (rarefaction wave in gas dynamics). Thus it can be said that, ultimately, the paradox arises from a failure to realize that, despite a linear isotherm, the sorption effect makes the system non-linear and thereby invalidates the familiar tenet of linear chromatography that all waves spread in proportion to the square root of traveled distance.

Much has been written about the complex thermodynamics of entropy production by traveling waves [12–14]. The only aspect of interest in the present context is the following. In Golay's "frictionless" world and granted the assumptions of ideal chromatography, the travel of a nonsharpening wave is entirely reversible and so produces no entropy; this is because a reversal of the direction of flow would make the wave self-sharpening and so let it regain its original sharpness while returning to its starting point. Likewise, the travel of an initially diffuse but self-sharpening wave remains reversible because flow reversal would cause the wave to spread to its original diffuseness. However, this is true only *as long as the wave has not yet sharpened into a shock* (*i.e.*, become a discontinuity). The travel of a shock is irreversible and so produces entropy even in the ideal world because a reversal of the flow direction would make the wave nonsharpening and cause it to spread. Entropy

production or the lack of it can also be linked to information theory, as Golay attempted but did not fully succeed: in the ideal world, any wave that is not a shock carries with itself complete information about its degree of sharpness at any previous point or time; in contrast, the shock “forgets” much of its history, not remembering for how long it has traveled as a shock. The longer it *may* have done so, the greater is the uncertainty about its original degree of sharpness.

It may seem paradoxical that a spreading (nonsharpening) wave does not produce entropy whereas a traveling shock, remaining sharp, does. As to the nonsharpening wave, we cannot equate spreading with mixing or diffusion effects. Any spreading caused by non-idealities is a dispersion in the usual sense, and so is irreversible and produces entropy. However, the spreading caused by the isotherm curvature is of a quite different nature: Being reversible, it does not increase the disorder of the system; we might say the system has “stored” the free energy needed to make the wave sharp again. As to the shock, it travels without change of its profile, not creating any apparent disorder, so how come it produces entropy? The answer is that the shock must not be viewed all by itself: It leaves the system in a different state from which no return

to the original state is possible without expenditure of free energy. For instance, if the shock has saturated a sorbent (*e.g.*, acted as the front of a peak), stripping (at the rear of the peak) would entail a nonsharpening wave, for a net result of solute dispersion, for which the shock is ultimately responsible.

REFERENCES

- 1 M.J.E. Golay, in A. Goldup (Editor), *Gas Chromatography 1964*, Institute of Petroleum, London, 1955, p. 143.
- 2 F.G. Helfferich, personal communication to M.J.E. Golay, 1965.
- 3 P. Valentin, *J. Chromatogr.*, 556 (1991) 25 (see page 27).
- 4 F.G. Helfferich and P.W. Carr, *J. Chromatogr.*, 629 (1993) 97.
- 5 M.J.E. Golay, *Nature*, 202 (1964) 489.
- 6 J.C. Giddings, *Dynamics of Chromatography*, Marcel Dekker, New York, 1965.
- 7 D. DeVault, *J. Am. Chem. Soc.*, 65 (1943) 532.
- 8 E. Glueckauf and J.I. Coates, *J. Chem. Soc.*, (1947) 1315.
- 9 D.L. Peterson and F. Helfferich, *J. Phys. Chem.*, 69 (1965) 1283.
- 10 R. Courant and K.O. Friedrichs, *Supersonic Flow and Shock Waves*, Wiley, New York, 1948.
- 11 P.D. Lax, *Comm. Pure Appl. Math.*, 10 (1957) 537.
- 12 H.-K. Rhee, R. Aris and N.R. Amundson, *Proc. Roy. Soc.*, A267 (1970) 419.
- 13 D.D. Frey, *J. Chromatogr.*, 409 (1987) 1.
- 14 D.D. Frey, *Chem. Eng. Sci.*, 45 (1990) 131.

Short Communication

Prediction of the retention of polynuclear aromatic hydrocarbons in programmed-temperature gas chromatography

T.C. Gerbino

Laboratorio Chimico, Castalia SpA, Via Borzoli 79, 16161 Genova (Italy)

G. Castello*

Istituto di Chimica Industriale, Università di Genova, Corso Europa 30, 16132 Genova (Italy)

U. Pettinati

West Srl, Via Borzoli Q, 16161 Genova (Italy)

(Received October 7th, 1992)

ABSTRACT

A procedure based on curve-fitting techniques for the calculation of the retention data in linear programmed-temperature gas chromatography was applied in order to calculate the elution temperature of fifteen polycyclic aromatic hydrocarbons on a DB-5 capillary column. The linear programmed-temperature retention data were calculated with a BASIC program starting from isothermal retention times and the calculated values were compared with experimental data. For five different linear temperature programmes the accuracy expressed as fractional difference was always better than 1% in spite of the simplifications introduced in the calculation methods.

INTRODUCTION

Programmed-temperature gas chromatography (PTGC) is widely used for the analysis of environmental samples containing compounds with a wide range of boiling points owing to the advantage of decreasing the analysis time and

improving the resolution for later eluting compounds. The prediction of the temperature-programmed retention time from isothermal retention data has been reported by several workers both using thermodynamic parameters or retention indices [1–19].

In a previous paper [20] it was shown that the method proposed by Said [21,22] can be applied without complex calculations for the prediction of retention data in different temperature-pro-

* Corresponding author.

grammed analyses. In this work, the retention times in linear PTGC of fifteen polynuclear aromatic hydrocarbons (PAHs) were calculated starting from data collected during different isothermal runs with the same column and were compared with experimental results.

The fundamental equation for temperature programming is

$$\frac{dt}{t_R} = \frac{dl}{L} \quad (1)$$

which when integrated gives

$$\int_0^{T_p} \frac{dt}{t_R} = \int_0^L \frac{dl}{L} \quad (2)$$

where L is the column length, dl is the distance travelled by the solute in time dt , t_R is the isothermal retention time of the same solute at absolute temperature T and T_p is the solute retention temperature.

The isothermal retention time, t_R , changes with temperature T according to

$$t_R = A + a \exp(b/T) \quad (3)$$

In eqn. 3 some simplifications are made [21]: a and b are constants and A is also a constant equal to the dead time. This means assuming that the mean gas velocity remains constant during the temperature programming. This assumption is not strictly valid [23] as the gas velocity should decrease with increasing temperature, but many instruments have a built-in system that automatically increases the inlet pressure in order to compensate for this effect and maintain a constant flow-rate. A is therefore approximately but not exactly equal to the dead time and can be defined as the mean dead time. With these simplifications, the three constants in eqn. 3 can be evaluated from three isothermal runs at different temperatures.

In linear PTGC, the column temperature is a linear function of the analysis time, t :

$$T = T_0 + rt \quad (4)$$

where T_0 is the absolute initial temperature and r is the programming rate in $^{\circ}\text{C min}^{-1}$.

By substituting eqns. 4 and 3 in eqn. 2, we obtain

$$1 = \frac{1}{r} \int_{\vartheta_0}^{\vartheta_i} \frac{d\vartheta}{A + a \exp[b/(273 + \vartheta)]} \quad (5)$$

or

$$1 = \frac{1}{r} \int_{\vartheta_0}^{\vartheta_i} y(\vartheta) d\vartheta \quad (6)$$

where $y(\vartheta)$ is the inverse retention time function:

$$y(\vartheta) = \frac{1}{A + a \exp[b/(273 + \vartheta)]} \quad (7)$$

and ϑ_0 and ϑ_i are inlet and outlet column temperatures in $^{\circ}\text{C}$.

The resulting integration has no analytical solution and eqn. 6 can be solved with approximate or iterative methods. In this work we applied the method proposed by Said [22], which uses curve-fitting techniques to replace the inverse retention time function $y(\vartheta)$ by a function that can be integrated. It can be shown that the normal distribution integral gives the best fit to eqn. 7 up to a value from 50 to 70 $^{\circ}\text{C}$ above the inflection point ϑ_i , which is the elution temperature range usually observed under experimental conditions. An exhaustive description of the theory can be found in Said's original work and our previous papers [20–22].

EXPERIMENTAL

The analyses were carried out using a Varian (Palo Alto, CA, USA) Model 3400 gas chromatograph, equipped with a standard flame ionization detector and a split-splitless injector. A narrow-bore DB-5 (5% phenyl–95% methylpolysiloxane bonded phase) silica column (J & W Scientific, Folsom, CA, USA) (30 m \times 0.25 mm I.D.) with a film thickness of 0.25 μm was used. Standard solution of PAHs in dichloromethane at concentrations ranging between 0.1 and 0.5 g l^{-1} were injected (1 μl) with a microsyringe in the splitless mode. Highly purified nitrogen was used as the carrier gas at an average flow-rate of 3 ml min^{-1} into the column. The make-up gas dispatched to the detector was set in order to maintain constant flow-rate of 30 ml min^{-1} at the flame tip. The detector and injector temperatures were 300 and 250 $^{\circ}\text{C}$, respectively.

Five replicate isothermal runs were performed for each compound at temperatures ranging from 373 to 598 K, in order to obtain three values of retention time with a reasonable temperature interval. The temperatures of the isothermal runs used for each compound were chosen in order to approximate its elution temperature (see Table I). Programmed-temperature runs were carried out at a variety of combinations of initial temperature and oven heating rate. The assumption was made that the operator-set value matches exactly the actual temperature of the column oven; for the Varian 3000 series instruments this is true to within $\pm 1.3^\circ\text{C}$. Calculations were performed with an IBM personal computer using a BASIC program [24].

RESULTS AND DISCUSSION

Five replicate isothermal runs were performed for each compound at three temperatures (Table I) in order to establish the reproducibility of retention data in isothermal analyses. The mean isothermal retention time, t_R , and overall standard deviation, σ , are also given in Table I.

By using the equations described in the Introduction, the programmed-temperature retention times, t_p , were calculated for various initial temperatures and heating rates. The calculated (t_{pc}) and experimental (t_{pe}) values are compared in Table II. The percentage difference between the experimental and calculated values, $\Delta (\%) = 100(t_{pe} - t_{pc})/t_{pc}$, is very small ($<1\%$), notwithstanding the simplifications introduced above, showing the adequacy of a normal distribution integral to fit the inverse retention time function $y(\vartheta)$, giving an almost perfect fit to $y(\vartheta)$ up to a ϑ value from 50 to 70°C above the inflection point ϑ_i . The fifteen solutes examined elute from the column more than 50°C above ϑ_i , as shown in Table III.

As pointed out in the Introduction, the velocity of the carrier gas is temperature dependent: an increase in temperature increases the viscosity and the velocity of the carrier gas decreases proportionally in a chromatographic system having a constant inlet pressure. This results in a linear dependence of dead time on temperature, but this variation is relatively small

when compared with the exponential variation of retention time with temperature. This effect is further reduced by the constant-flow regulator of the gas chromatograph used. Hence dead time can be replaced with the constant A in eqn. 3, where A is the mean dead time. Moreover, in eqn. 3 the thermodynamic terms $\beta \exp(\Delta S/R)$ and $-\Delta H/R$, where β is the column phase ratio, ΔS is the molar entropy of solution, ΔH is the molar enthalpy of solution and R is the gas constant, are replaced with the constants a and b , respectively, but some deviation from linearity of the $\ln t_R$ vs. T^{-1} relationship is possible, owing to the variation of these thermodynamic characteristics with temperature [12,14,25]. As pointed out elsewhere [14], these variations do not have a great effect on the calculated retention values because the decrease in the enthalpy produces an increase in the entropy term owing to the correlation of ΔH and ΔS through the molar free energy of solution. The early-eluting solutes with a retention time very close to the dead time are more influenced by errors in evaluating the hold-up time and therefore would have less reliable isothermal data. Moreover, in the time corresponding to the dead time the solutes expand in the gas phase and are transported along the column; the distance travelled can be non-negligible for solutes showing a small retention time, particularly if high initial temperatures are used. In order to ensure greater accuracy, the three temperatures for evaluating the constants in eqn. 3 should cover the whole temperature range during temperature programming because a greater contribution to the difference between calculated and predicted retention times can be expected if the retention time of a compound significantly exceeds the upper limit of isothermal runs.

It should be noted that the accuracy of the predicted retention values is fair over the whole range of the programmed-temperature runs, notwithstanding the fact that the isothermal retention times were not measured for all the compounds at the same temperature and in the same isothermal runs. This is important from both the theoretical and practical points of view. It is in fact almost impossible to achieve the elution of all the analyte compounds with a

TABLE I
EXPERIMENTAL MEAN VALUES ($n=5$) OF ISOTHERMAL RETENTION TIME, t_R (min), AND STANDARD DEVIATION, σ , ON A NARROW-BORE DB-5 COLUMN (30 m \times 0.25 mm I.D.) WITH NITROGEN AS CARRIER GAS

Compound	373 K		398 K		423 K		448 K		473 K		498 K		523 K		548 K		573 K		598 K			
	t_R	$\sigma \cdot 10^3$	t_R	$\sigma \cdot 10^3$	t_R	$\sigma \cdot 10^3$	t_R	$\sigma \cdot 10^3$	t_R	$\sigma \cdot 10^3$	t_R	$\sigma \cdot 10^3$										
Naphthalene	6.334	4.8	3.586	4.8	2.612	4.0																
Acenaphthylene			9.616	14.0	5.098	11.0	3.328	9.0														
Acenaphthene					5.620	0.0	3.548	4.0	2.730	0.0												
Fluorene					7.762	7.0	4.442	6.0	3.130	6.0												
Phenanthrene									4.510	0.0	3.254	4.8	2.702	4.0								
Anthracene									4.620	9.8	3.308	7.4	2.732	6.4								
Fluoranthene									8.644	19.0	5.140	8.0	3.636	13.0								
Pyrene									9.966	8.1	5.742	8.9	3.922	7.2								
Benzo[<i>a</i>]anthracene											11.140	8.9	6.482	17.0	4.380	8.9						
Chrysene													6.630	10.0	4.444	23.0	3.452	18.0				
Benzo[<i>b</i>]fluoranthene													1.632	8.2	6.846	26.0	4.656	23.0				
Benzo[<i>k</i>]fluoranthene													1.840	22.0	6.894	19.0	4.664	19.0				
Benzo[<i>a</i>]pyrene															7.894	34.0	5.266	4.1	3.902	24.0		
Dibenzo[<i>a,h</i>]anthracene															13.156	56.0	7.586	90.0	5.096	26.0		
Benzo[<i>ghi</i>]perylene															14.746	89.0	8.538	94.0	5.626	92.0		

TABLE II
COMPARISON OF EXPERIMENTAL, t_{pe} , AND CALCULATED, t_{pc} , MEAN VALUES OF RETENTION TIMES (min) FOR DIFFERENT TEMPERATURE PROGRAMMES

Compound	Initial temperature, θ_0 (°C), and programming rate, r (°C/min)				100 and 7.5				100 and 10				100 and 12.5			
	t_{pc}	t_{pe}	Δ (%)	t_{pc}	t_{pe}	Δ (%)	t_{pc}	t_{pe}	Δ (%)	t_{pc}	t_{pe}	Δ (%)	t_{pc}	t_{pe}	Δ (%)	
Naphthalene	6.860	6.882	-0.32	4.792	4.819	-0.60	4.306	4.298	0.18	3.980	3.994	-0.35	3.760	3.357	0.08	
Acenaphthylene	10.594	10.596	-0.01	7.634	7.653	-0.24	7.882	7.872	0.12	6.896	6.892	0.05	6.200	6.205	-0.08	
Acenaphthene	11.092	11.116	-0.21	8.014	8.048	-0.42	6.556	6.563	-0.10	7.318	7.336	-0.24	6.556	6.563	-0.10	
Fluorene	12.318	12.335	-0.13	9.008	9.028	-0.22	9.912	9.908	0.04	8.498	8.474	0.28	7.498	7.501	-0.04	
Phenanthrene	14.722	14.752	-0.20	10.928	10.971	-0.39	12.857	12.925	-0.52	10.762	10.794	-0.29	9.375	9.394	-0.20	
Anthracene	14.894	14.872	0.14	11.056	11.069	-0.11	13.124	13.075	0.37	10.918	10.912	0.05	9.458	9.492	-0.36	
Fluoranthene	17.720	17.715	0.02	13.376	13.378	-0.01	16.684	16.727	-0.26	13.690	13.721	-0.22	11.784	11.784	0.00	
Pyrene	18.214	18.267	-0.29	13.776	13.832	-0.40	17.402	17.448	-0.26	14.342	14.277	0.45	12.186	12.238	-0.42	
Benzo[<i>a</i>]anthracene	21.310	21.346	-0.17	16.302	16.325	-0.14	21.462	21.487	-0.11	17.302	17.347	-0.26	14.682	14.726	-0.29	
Chrysene	21.458	21.466	-0.04	16.406	16.421	-0.09	21.620	21.648	-0.13	17.450	17.467	-0.09	14.812	14.822	-0.07	
Benzo[<i>b</i>]fluoranthene	23.926	23.942	-0.07	18.442	18.440	0.01	24.860	24.850	0.04	19.942	19.940	0.01	16.846	16.840	0.03	
Benzo[<i>k</i>]fluoranthene	24.008	24.009	0.00	18.460	18.490	-0.16	24.992	24.964	0.11	20.124	20.010	0.56	16.902	16.891	0.06	
Benzo[<i>a</i>]pyrene	24.662	24.505	0.47	18.984	18.928	-0.29	25.758	25.525	0.90	20.602	20.506	0.46	17.390	17.330	0.34	
Dibenzo[<i>a,h</i>]anthracene	26.956	26.982	-0.09	20.964	20.890	0.35	28.802	28.882	-0.27	22.932	23.984	-0.22	19.378	19.298	0.41	
Benzo[<i>ghi</i>]perylene	27.454	27.531	-0.28	21.442	21.375	-0.31	29.562	29.534	0.09	23.624	23.531	0.39	19.864	19.775	0.44	

$$\Delta (\%) = 100(t_{pe} - t_{pc})/t_{pc}$$

TABLE III
CALCULATED INFLECTION POINT, ϑ_1 (°C), OF THE SOLUTES AND COMPARISON BETWEEN EXPERIMENTAL, ϑ_e , AND CALCULATED, ϑ_c , ELUTION TEMPERATURES FOR DIFFERENT TEMPERATURE PROGRAMMES

Compound	ϑ_1	Initial temperature, ϑ_0 (°C), and programming rate, r (°C/min)														
		60 and 10		80 and 12.5		100 and 7.5		100 and 10		100 and 12.5		Δ (%)	ϑ_c	Δ (%)		
		ϑ_e	ϑ_c	Δ (%)	ϑ_e	ϑ_c	Δ (%)	ϑ_e	ϑ_c	Δ (%)	ϑ_e				ϑ_c	
Naphthalene	115.13	128.60	128.82	-0.17	139.90	140.25	-0.25	132.29	132.24	0.03	139.80	139.94	-0.10	147.00	146.96	0.03
Acenaphthylene	154.38	165.94	165.97	-0.02	175.42	175.67	-0.14	159.04	159.11	-0.05	168.96	168.92	0.02	177.50	177.57	-0.04
Acenaphthene	158.92	170.92	171.16	-0.14	180.18	180.60	-0.28	162.99	163.41	-0.26	173.18	173.37	-0.11	181.95	182.04	-0.05
Fluorene	173.13	183.18	183.36	-0.10	192.60	192.85	-0.13	173.34	173.31	0.01	184.98	184.74	0.13	193.73	193.77	-0.02
Phenanthrene	195.19	207.22	207.53	-0.15	216.00	217.15	-0.25	196.43	196.34	0.04	207.62	207.95	-0.16	217.19	217.44	-0.12
Anthracene	196.41	208.94	208.71	0.11	218.20	218.37	-0.08	198.43	198.07	0.18	209.18	209.12	0.03	218.65	218.23	-0.19
Fluoranthene	226.74	237.20	237.10	0.05	247.20	247.23	-0.01	225.13	225.46	-0.15	236.90	237.22	-0.13	247.30	247.31	0.00
Pyrene	233.89	242.14	242.68	-0.22	252.20	252.91	-0.28	230.51	230.86	-0.15	243.52	242.77	0.27	252.32	252.98	-0.26
Benzo[a]anthracene	259.51	273.10	273.46	-0.13	284.07	283.77	0.10	261.00	261.15	-0.06	274.50	274.68	-0.06	283.53	284.08	-0.19
Chrysene	260.58	274.58	274.67	-0.03	285.08	285.27	-0.07	262.15	262.36	-0.08	273.02	273.48	-0.17	285.15	285.28	-0.05
Benzo[b]fluoranthene	290.63	299.26	299.40	-0.05	310.52	310.51	0.00	286.45	286.44	0.00	299.42	299.40	0.00	310.58	310.51	0.22
Benzo[k]fluoranthene	290.11	300.08	300.10	0.00	310.75	311.13	-0.12	287.44	287.23	0.07	301.24	300.10	0.56	311.28	311.13	0.05
Benzo[a]pyrene	307.97	306.22	305.05	0.38	317.30	316.62	0.21	293.18	291.44	0.59	306.02	305.06	0.31	317.37	316.63	0.23
Dibenzo[a,h]anthracene	315.50	329.56	329.85	-0.09	342.05	341.23	0.23	316.01	316.62	-0.19	329.32	329.85	-0.17	342.23	341.23	0.30
Benzo[ghi]perylene	320.10	334.54	335.31	0.23	348.02	347.19	0.24	312.72	321.51	0.06	336.24	335.31	0.28	348.30	347.19	0.32

$$\Delta (\%) = 100(\vartheta_e - \vartheta_c)/\vartheta_e.$$

single isothermal analysis; at low temperatures the retention time of high-boiling compounds is too long and the peak shapes (tailing or very wide) make correct measurement of retention times difficult unless large sample amounts are injected; at high temperatures, interference with the solvent peak tail and elution of many peaks within a very small interval impair the determination of early-eluting compounds.

The differences between the experimental and calculated values are also due to non-instantaneous cooling of the sample from the heated injector to the initial column temperature and to the temperature lag between the column and oven during programming. Probably this lag makes the greatest contribution because the difference between calculated and observed elution temperatures is always within $\pm 1.3^\circ\text{C}$ (see Table III), which represents the observed deviation between the set and actual temperatures of the column oven. The thermal mass of the capillary column and of its supporting cage is relatively small, but it may contribute further to the difference in the actual column temperature with respect to set oven values, mainly with high programming rates [26].

Notwithstanding these causes of error, the prediction of the retention times in the linear PTGC of complex mixtures of PAHs gives suitable results and can permit the identification of these compounds in environmental samples on the basis of retention data, without the need to perform a series of isothermal runs for each sample in order to identify compounds having a wide range of boiling points. By determining many standards, the flame ionization detection (FID) responses of PAHs were found to be very similar, as they are governed by their carbon content, which is fairly uniform for different compounds, and therefore they have very similar FID response factors (response/mass) [27]. Therefore, the identification on the basis of retention data and the similarity of response facilitate the determination of PAHs in environmental samples by reducing the number of standard mixtures required.

The method, which is easily applied with simple programming on personal computers, can also be used as an analogue of the Van Deemter

plot for optimization of carrier flow-rate, to establish whether the column used can give a satisfactory resolution of closely eluting peaks. If the application of the equation with many PTGC parameters does not give a sufficient difference in retention times, this means that further experiments in order to improve the resolution by changing the analysis conditions will be useless, and that other solutions must be tried, such as the choice of longer columns, the use of stationary phases with greater polarity and the combination of different length of polar and non-polar columns.

REFERENCES

- 1 J.C. Giddings, in N. Brenner, J.E. Callen and M.D. Willis (Editors), *Gas Chromatography*, Academic Press, New York, 1962, p. 57.
- 2 G. Guiochon, *Anal. Chem.*, 36 (1964) 661.
- 3 H.W. Habgood and W.E. Harris, *Anal. Chem.*, 36 (1964) 663.
- 4 R. Rowan, *Anal. Chem.*, 39 (1967) 1158.
- 5 D. Grant and H. Hollis, *J. Chromatogr.*, 158 (1978) 3.
- 6 R.V. Golovnya and V.P. Huraletz, *J. Chromatogr.*, 36 (1966) 276.
- 7 L. Erdey, J. Tuckacs and E. Szalancy, *J. Chromatogr.*, 46 (1970) 29.
- 8 L. Podmaniczky, L. Szepesy, K. Lakszner and G. Shomburg, *Chromatographia*, 21 (1986) 387.
- 9 B.J. Chen, X.J. Guo and S.Y. Peng, *Chromatographia*, 23 (1987) 888.
- 10 J. Krupcik, D. Repka, T. Hevesy and G. Garaj, *J. Chromatogr.*, 406 (1987) 117.
- 11 J. Curvers, J. Rijks, C. Cramers, K. Knauss and P. Larson, *J. High Resolut. Chromatogr. Chromatogr. Commun.*, 8 (1985) 607.
- 12 J. Curvers, J. Rijks, C. Cramers, K. Knauss and P. Larson, *J. High Resolut. Chromatogr. Chromatogr. Commun.*, 8 (1985) 611.
- 13 E.E. Akporhonor, S. Le Vent and D.R. Taylor, *J. Chromatogr.*, 405 (1987) 67.
- 14 E.E. Akporhonor, S. Le Vent and D.R. Taylor, *J. Chromatogr.*, 463 (1989) 271.
- 15 P. Lu, B. Liu, X. Chu, C. Luo, G. Lai and H. Li, *J. High Resolut. Chromatogr. Chromatogr. Commun.*, 9 (1986) 702.
- 16 J. Lee and D.R. Taylor, *Chromatographia*, 16 (1982) 286.
- 17 J.A. Garcia-Dominguez and J.M. Santiuste, *Chromatographia*, 32 (1991) 116.
- 18 L.H. Wright and J.F. Walling, *J. Chromatogr.*, 540 (1991) 311.
- 19 N.H. Snow, *J. Chromatogr. Sci.*, 30 (1992) 271.
- 20 T.C. Gerbino and G. Castello, in P. Sandra and M.L. Lee (Editors), *Proceedings of the 14th International*

- Symposium on Capillary Chromatography, Baltimore, MD, 1992*, Foundation for the International Symposium on Capillary Chromatography, Miami, FL, 1992, p. 70.
- 21 A.S. Said, in P. Sandra (Editor), *Proceedings of the 8th Symposium on Capillary Chromatography*, Hüthig, Heidelberg, 1987, p. 85.
- 22 A.S. Said, in P. Sandra and G. Redant (Editors), *Proceedings of the 10th Symposium on Capillary Chromatography*, Hüthig, Heidelberg, 1989, p. 163.
- 23 L.S. Ettre, *Chromatographia*, 18 (1984) 243.
- 24 T.C. Gerbino and G. Castello, *J. High Resolut. Chromatogr.*, in press.
- 25 H. Purnell, *Gas Chromatography*, Wiley, New York, 1962, p. 214.
- 26 P.Y. Shrotri, A. Mokashi and D. Mukesh, *J. Chromatogr.*, 387 (1987) 399.
- 27 H.Y. Tong and F.W. Karasek, *Anal. Chem.*, 56 (1984) 2124.

Short Communication

Chiral recognition of enantiomeric amides on a diamide chiral stationary phase by gas chromatography

Xianwen Lou, Xueliang Liu and Liangmo Zhou*

Dalian Institute of Chemical Physics, Chinese Academy of Sciences, 129 Street, Dalian 116012 (China)

(First received October 1st, 1992; revised manuscript received January 4th, 1993)

ABSTRACT

Several α -alkyl-, α -cycloalkyl- and α -aromatic-substituted ethylamine enantiomers were separated with a cross-linked polycyanoethyl vinyl siloxane-L-valine-*tert.*-butylamide fused-silica capillary column. Kováts retention indices of cyclohexane, benzene, anisole and the derivatized amines on the chiral stationary phase (CSP) were determined and compared with those on SE-30. By extrapolation of the retention behaviour, the chiral recognition mechanism of enantiomeric amides on diamide CSPs is discussed.

INTRODUCTION

Since the first successful direct resolution of enantiomers by gas chromatography (GC) in 1966 [1], a variety of enantiomeric pairs have been separated on various chiral stationary phases (CSPs) [2–5].

Amines are widely used as intermediates in the synthesis of a large number of organic compounds, including dyes, drugs, pesticides and plastics. The enantiomeric separation of chiral amines, generally derivatized as amides, has been reported by several workers [4–12]. Oi *et al.* [6] reported the direct separation of racemic amines on optically active copper(II) complexes, but the peak shapes were broad and tailing. Generally, amines are derivatized as N-perfluoroalkyl derivatives before chromatography on CSPs [13]. The enantiomeric separation of

derivatized chiral amines on cyclodextrin derivatives (CD-CSPs) [4,5] and chiral hydrogen-bonding GC phases such as peptide [10], diamide [8,11,12] and even monoamide [7] CSPs has also been reported.

In this work, α -alkyl-, α -cycloalkyl- and α -aromatic-substituted ethylamines were enantiomerically separated in a cross-linked polycyanoethyl vinyl siloxane-L-valine-*tert.*-butylamide fused-silica capillary column, prepared as described previously [14]. The reasons for difference in the α -values (separation factor) of the amides were investigated.

EXPERIMENTAL

Materials

Fused-silica capillary tubes (0.25 mm I.D.) were obtained from Yongnian Optical Fibre Manufacture. 2-Aminoheptane and 2-amino-octane were purchased from Tokyo Kasei Kogyo and α -phenylethylamine from Sigma. α -Cyclo-

* Corresponding author.

hexylethylamine was synthesized from cyclohexyl methyl ketone by the Leukart reaction [15]. Methoxy-substituted α -phenylethylamines were prepared in our laboratory [12].

Derivatization

The amines were derivatized into N-tri-fluoroacetyl (TFA), N-acetyl (Ac) or N-benzyl (Bz) derivatives [16,17].

Chromatographic conditions

Cross-linked polycyanoethyl vinyl siloxane-L-Val-*tert*-butylamide and cross-linked SE-30 fused silica capillary columns were prepared as reported previously [14,18]. The chromatographic separation was carried out with a GC R1A gas chromatograph equipped with a split injector and a flame ionization detector.

RESULTS AND DISCUSSION

The structures, separation factors (α), peak resolution (R_s) and capacity factors (k') of the N-TFA-amines tested are given in Table I. They have very similar structures and can all be considered as substituted N-TFA-ethylamines. The only difference among them is in the R groups of the ethylamine α -positions.

N-TFA-2-aminooctane, N-TFA- α -cyclohexylethylamine and N-TFA- α -phenylethylamine have the same carbon number. However, the difference in their α -values is considerable, and that of N-TFA- α -phenylethylamine is the highest, even at much higher temperatures.

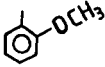
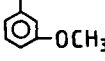
The difference in α -values between α -aromatic-substituted ethylamines and α -alkyl- or α -cycloalkyl-substituted ethylamines on monoamide CSPs has already been reported by Weinstein *et al.* [7]. In that case, the higher α -values of aromatic-substituted ethylamines were explained by an intercalation mechanism of the solutes into the parallel arrangements of aromatic rings of the monoamide CSPs. Unfortunately, this mechanism is not suitable to explain the difference in α -values in our experiments, because there is no aromatic ring in the diamide CSP used here.

For an optically active molecule, direct chiral recognition can only be effected by another chiral molecule (CSP). Although the amide

TABLE I

α , R_s AND $k'(S)$ VALUES OF N-TFA-AMINES

Amines: $\text{CH}_3\text{CH}(\text{R})\text{NH}_2$. $\alpha = [t_{R(2)} - t_0]/[t_{R(1)} - t_0]$; $R_s = [t_{R(2)} - t_{R(1)}]/[1/2(Wb_2 + Wb_1)]$; $k'(S) = [t_{R(2)} - t_0]/t_0$. Wb = width at base.

R	α	R_s	$k'(S)$	Temperature (°C)
$n\text{-C}_5\text{H}_{11}$	1.020	0.87	16.5	80
$n\text{-C}_6\text{H}_{13}$	1.022	1.08	32.0	80
	1.016	1.10	8.19	110
	1.026	1.76	5.78	130
	— ^a	0	8.87	130
	1.032	1.82	23.7	130
	1.033	1.95	25.4	130

^a No separation.

groups of the derivatized amines have two strong interaction sites (oxygen and hydrogen) connected directly to the asymmetric carbon, they can only be considered as “one point” according to the “three-point” rule suggested by Dalglish [19,20]. It has also been demonstrated that one strong attraction is sufficient for chiral recognition in many instances on a diamide CSP [21]. However, it is reasonable that the enantiomeric selective interactions of other groups connected to the asymmetric atom with the CSPs will certainly affect the chiral separation.

The only difference in the N-TFA-amines is in the R group. The higher α -values of α -aromatic-substituted ethylamines might be due to the stronger interaction of the phenyl group with the CSP than that of the alkyl or cycloalkyl groups.

Kováts retention indices (I), which are greatly influenced by both structures of the solutes and solvents, are the most widely used parameters for qualitative analysis in GC. The higher the I value, the stronger is the interaction between the solute and the solvent. The diamide CSP used is

an optically active polymeric siloxane stationary phase. The ΔI values, the difference in Kováts retention indices on the diamide CSP {for enantiomers $I = [I(S) + I(R)]/2$ } and on the dimethylsiloxane (SE-30) phase could be qualitatively assumed to be the contribution of the chiral side-chain to the I value [22].

The I and ΔI values of the derivatized amines and the R group in their α -positions, namely cyclohexane, benzene and anisole, on the cross-linked diamide CSP and SE-30 are given in Table II. Benzene, cyclohexane and hexane have the same carbon number, but both the I value on the CSP and the ΔI value of benzene are much greater than those of cyclohexane and hexane. From Table II, it can also be seen clearly that the ΔI values of all the N-TFA- α -aromatic-substituted ethylamines are much greater than those of N-TFA- α -alkyl or - α -cycloalkyl-substituted ethylamines. That is, in the derivatized amines, the interaction of a phenyl group with the CSP is much stronger than that of an alkyl or cycloalkyl group.

The introduction of a methoxy group in the *meta* and *para* positions on the benzene ring slightly improved the selectivity of enantiomers [12]. This is probably because the introduced group (methoxy) further enhanced the interaction of the benzene ring of the solutes with the CSP. The α -value of N-TFA-*o*-methoxy- α -phenylethylamine is much lower than that of the corresponding *meta* and *para* isomers owing to the intramolecular hydrogen bonding of the amide group [12]. The data in Table II show that the I values on the CSP and SE-30 and the ΔI value for N-TFA-*o*-methoxy- α -phenylethylamine are significantly lower than those for the corresponding *meta* and *para* isomers, also supporting the hypothesis of intramolecular hydrogen bonding.

The GC behaviour of N-Ac and N-Bz derivatives of α -alkyl-substituted ethylamine, 2-aminoheptane and 2-aminooctane was also studied (Tables II and III). On replacing N-TFA with N-Ac or N-Bz, the interaction of the strong interaction point, the amide group, with the CSP

TABLE II

KOVÁTS RETENTION INDICES (I) AND DIFFERENCE IN KOVÁTS RETENTION INDICES ON THE CSP AND SE-30 (ΔI)

Solute	I		ΔI^b	Temperature (°C)
	SE-30	CSP ^a		
Cyclohexane	664.34	692.00	27.66	60
Benzene	657.74	760.38	102.64	60
Anisole	899.91	1060.95	161.46	60
N-TFA-2-aminoheptane	1064.62	1464.46	399.84	150
N-TFA-2-aminooctane	1160.57	1561.73	401.16	150
N-TFA- α -cyclohexylethylamine	1226.82	1644.28	417.46	150
N-TFA- α -phenylethylamine	1215.24	1724.80	509.56	150
N-TFA- <i>o</i> -methoxy- α -phenylethylamine	1386.26	1817.26	421.00	150
N-TFA- <i>m</i> -methoxy- α -phenylethylamine	1430.77	2002.14	571.37	150
N-TFA- <i>p</i> -methoxy- α -phenylethylamine	1456.36	2020.04	563.68	150
N-Ac-2-aminoheptane	1269.04	1750.48	481.44	150
N-Ac-2-aminooctane	1362.70	1852.29	489.59	150
N-Bz-2-aminoheptane	1798.59	2329.92	531.33	180
N-Bz-2-aminooctane	1896.06	2429.28	533.22	180

^a For enantiomers on the CSP, $I = [I(S) + I(R)]/2$.

^b For enantiomers, $\Delta I = \{[I(S) + I(R)]/2\} - I(\text{SE-30})$; $I(S)$, $I(R)$ and $I(\text{SE-30})$ are the Kováts retention indices of the S or R configuration on the CSP and those on SE-30.

TABLE III

α , R_s AND $k'(S)$ VALUES OF N-Ac- AND N-Bz-AMINES AND N-TFA- α -PHENYLETHYLAMINE

Solute	α	R_s	$k'(S)$	Temperature (°C)
N-Ac-2-aminoheptane	1.017	1.21	14.55	110
N-Ac-2-aminooctane	1.021	1.50	24.25	110
N-Bz-2-aminoheptane	1.016	1.19	29.30	150
N-Bz-2-aminooctane	1.018	1.17	45.63	150
N-TFA- α -phenylethylamine	1.024	1.68	2.38	150

is enhanced and the I and ΔI values increase, but the comparatively weak interaction point, the alkyl group (R), remains the same. The α -values of the N-Ac and N-Bz chiral alkyl-substituted ethylamines are not substantially improved whereas the volatility is greatly reduced and a much higher column temperature is needed. Although the interaction of the carbonyl groups of N-Ac and N-Bz with the CSP is stronger than that of N-TFA, the α -values of N-Ac or N-Bz chiral alkyl-substituted ethylamines are still much smaller, at the same temperature or even at lower temperatures, than that of N-TFA-1-phenylethylamine (Table III). Hence increasing the interaction strength of the relatively weak

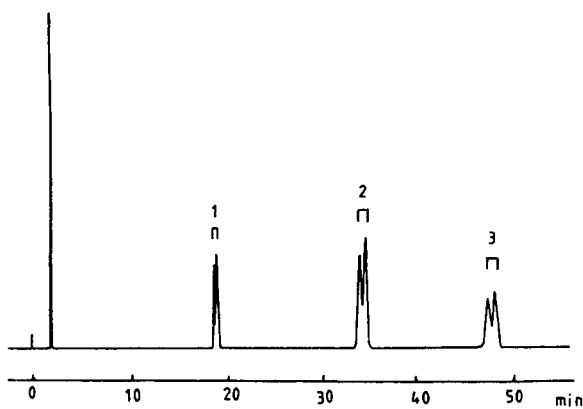


Fig. 1. Chromatogram of N-TFA-chiral α -alkyl- and α -cycloalkyl-substituted ethylamines. Column, cross-linked polycyanoethylvinylsiloxane-L-Val-*tert.*-butylamide fused-silica capillary (20 m \times 0.25 mm I.D.); column temperature, 90°C; carrier gas, nitrogen. 1 = N-TFA-2-Aminoheptane; 2 = N-TFA-2-aminooctane; 3 = N-TFA- α -cyclohexylethylamine (*R*-enantiomers eluted first).

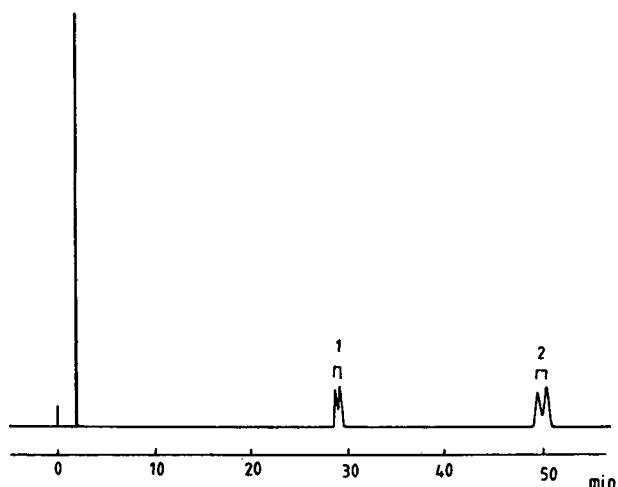


Fig. 2. Chromatogram of N-Ac chiral α -alkyl-substituted ethylamine. Column temperature, 110°C; other conditions as in Fig. 1. 1 = N-Ac-2-Aminoheptane; 2 = N-Ac-2-aminooctane (*R*-enantiomers eluted first).

interaction point (R group) with the CSP, *i.e.*, from an alkyl or cycloalkyl to a phenyl group, has a greater effect on chiral recognition than further increasing the strength of the strong interaction point (amide group) with the CSP.

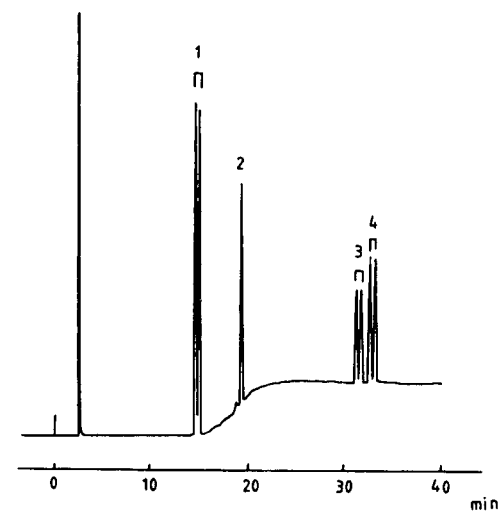


Fig. 3. Chromatogram of N-TFA chiral α -aromatic-substituted ethylamines. Column temperature, 150°C; other conditions same as in Fig. 1. 1 = N-TFA- α -Phenylethylamine; 2 = N-TFA-*o*-methoxy- α -phenylethylamine; 3 = N-TFA-*m*-methoxy- α -phenylethylamine; 4 = N-TFA-*p*-methoxy- α -phenylethylamine (*R*-enantiomers eluted first).

The chromatograms of some amides enantiomers are shown in Figs. 1–3.

CONCLUSIONS

The separation factors (α -values) of chiral α -aromatic substituted ethylamines are much greater than those of both chiral α -alkyl- and α -cycloalkyl-substituted ethylamines, derivatized as amides, on the diamide CSP used. The I values (Kováts retention indices) on the CSP and SE-30 and the ΔI values (difference in I values on the CSP and SE-30) of the chiral ethylamines and their substituents (R group) were tested. The higher α -values of the chiral α -aromatic-substituted ethylamines might be due to the stronger interaction of the benzene ring than the alkyl and cycloalkyl groups with the CSP.

ACKNOWLEDGEMENTS

The authors thank Professors Qinghai Wang, Daoqian Zhu and Yafeng Guan for valuable discussions and technical help. This work was supported by the National Science Foundation of China and the Youth Science Foundation of Dalian Institute of Chemical Physics.

REFERENCES

- 1 E. Gil-Av, B. Feibush and R. Charles-Sigler, *Tetrahedron Lett.*, 8 (1966) 1009.
- 2 H. Frank, G.L. Nicholson and E. Bayer, *J. Chromatogr. Sci.*, 15 (1977) 174.
- 3 E. Gil-Av, in F. Bruner (Editor), *The Science of Chromatography (Journal of Chromatography Library, Vol. 32)*, Elsevier, Amsterdam, 1985, p. 111.
- 4 D.W. Armstrong, W. Li, C. Chang and L. Pitha, *Anal. Chem.*, 62 (1990) 914.
- 5 V. Schurig and H. Nowotony, *Angew. Chem., Int. Ed. Engl.*, 29 (1990) 939.
- 6 N. Oi, K. Shiba, T. Tani, H. Kitahara and T. Doi, *J. Chromatogr.*, 211 (1981) 274.
- 7 S. Weinstein, B. Feibush and E. Gil-Av, *J. Chromatogr.*, 126 (1976) 97.
- 8 W.A. König, I. Benecke and S. Sievers, *J. Chromatogr.*, 217 (1981) 71.
- 9 N. Oi, Kitahara and D. Toi, *J. Chromatogr.*, 207 (1981) 252.
- 10 C.H. Lochmuller and J.V. Hinshaw, Jr., *J. Chromatogr.*, 202 (1980) 363.
- 11 B. Koppenhoefer and E. Bayer, in F. Bruner (Editor), *The Science of Chromatography (Journal of Chromatography Library, Vol. 32)*, Elsevier, Amsterdam, 1985, p. 1.
- 12 X. Lou, X. Liu, S. Zhang and L. Zhou, *J. Chromatogr.*, 586 (1991) 139.
- 13 M.L. Lee, F.J. Yang and K.D. Bartle, *Open Tubular Column Gas Chromatography*, Wiley, New York, 1984, p. 263.
- 14 X. Lou, X. Liu and L. Zhou, *J. Chromatogr.*, 552 (1991) 153.
- 15 A.W. Ingersoll, *Org. Synth., Coll. Vol.*, 2 (1943) 503.
- 16 B. Feibush and E. Gil-Av, *J. Gas Chromatogr.*, 5 (1967) 257.
- 17 X. Lou, X. Liu and L. Zhou, *J. Chromatogr.*, 605 (1992) 103.
- 18 L. Zhou, G. Wang, T. Zhang, E. Xia and D. Zhu, *Fenxi Huaxue*, 13 (1985) 406.
- 19 C. Dalglish, *J. Chem. Soc.*, (1952) 137.
- 20 R. Audebert, *J. Liq. Chromatogr.*, 2 (1979) 1063.
- 21 B. Koppenhoefer, H. Allmendinger and G. Nicholson, *Angew. Chem., Int. Ed. Engl.*, 25 (1985) 48.
- 22 B. Koppenhoefer and E. Bayer, *Chromatographia*, 19 (1984) 123.

Short Communication

Resolution of complex mixtures of flavonoid aglycones by analysis of gas chromatographic–mass spectrometric data

T.J. Schmidt and I. Merfort*

Institut für Pharmazeutische Biologie der Heinrich-Heine-Universität Düsseldorf, 4000 Düsseldorf (Germany)

U. Matthiesen

Spurenelementelabor der Medizinischen Einrichtungen der Heinrich-Heine-Universität Düsseldorf, 4000 Düsseldorf (Germany)

(First received October 26th, 1992; revised manuscript received December 24th, 1992)

ABSTRACT

Forty-nine flavones, flavonols, flavanones and chalcones were analysed without derivatization by GC and GC–MS using an OV-1 capillary column. Retention times are affected by the number, position and type of the substituents. The mass spectra show the same typical fragmentation pattern as obtained by the direct inlet method. The effectiveness of the proposed method is demonstrated by the GC and GC–MS analysis of a plant extract in which 21 different flavonoid aglycones could be identified.

INTRODUCTION

Flavonoid aglycones are valuable compounds because of their many biological and pharmacological effects [1,2]. Further, they are often used in chemotaxonomic studies [3]. Numerous chromatographic techniques have previously been applied to their separation and identification, *e.g.*, column chromatography, paper chromatography, thin-layer chromatography (TLC) and high-performance liquid chromatography (HPLC). However, these methods are time consuming or limited in separation power [4].

Few reports have been published on the gas chromatography (GC) of methyl or trimethylsilyl ethers of flavonoids, only one of the polymethoxylated flavones [4,5].

In this paper we report the analysis of 49 flavones, flavonols, flavanones and chalcones without derivatization by GC and GC–MS with an OV-1 capillary column. Further, we demonstrate the application of this rapid and sensitive method to a plant extract containing 21 flavonoid aglycones.

EXPERIMENTAL

Materials

Flavonoids were isolated from flowers of *Arnica* species and from *Heterotheca inuloides*

* Corresponding author.

Cass. [6–8], except for **22**, **26**, **27**, **30**, **42**, **43** and **46**, which were purchased from Roth (Karlsruhe, Germany). All products were identified by comparison of UV, mass and ^1H NMR-spectra with published data.

The plant extract examined was obtained from flowers of *Arnica alpina* ssp. *attenuata* by gel chromatography (Sephadex LH-20, methanol) of

the methanol-soluble part of the methylene chloride extract.

Gas chromatography

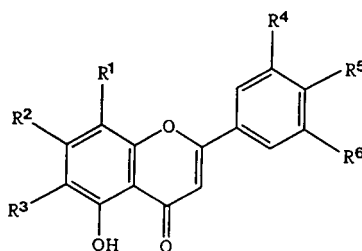
GC analysis was carried out on a Hewlett-Packard HP 5890 gas chromatograph equipped with a Permabond OV-1-capillary column (25 m \times 0.25 mm I.D.) (Macherey–Nagel) and a

TABLE I

STRUCTURES OF FLAVONOID AGLYCONES AND THEIR RELATIVE RETENTION TIMES

Values are expressed relative to hispidulin, corrected for the dead time.

Flavones:

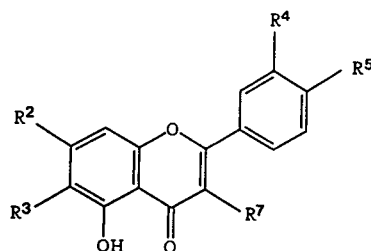


No.	Compound	Substituent						RRT
		R ¹	R ²	R ³	R ⁴	R ⁵	R ⁶	
1	Apigenin	H	OH	H	H	OH	H	1.02
2	Genkwanin	H	OCH ₃	H	H	OH	H	0.90
3	Acacetin	H	OH	H	H	OCH ₃	H	0.88
4	Apigenin 7,4'-di-Me	H	OCH ₃	H	H	OCH ₃	H	0.78
5	Chrysoeriol	H	OH	H	OCH ₃	OH	H	1.22
6	Diosmetin	H	OH	H	OH	OCH ₃	H	1.40
7	Velutin	H	OCH ₃	H	OCH ₃	OH	H	1.07
8	Piloin	H	OCH ₃	H	OH	OCH ₃	H	1.24
9	Luteolin 7,3',4'-tri-Me	H	OCH ₃	H	OCH ₃	OCH ₃	H	1.14
10	Hispidulin	H	OH	OCH ₃	H	OH	H	1.00
11	Pectolinarigenin	H	OH	OCH ₃	H	OCH ₃	H	0.87
12	Cirsimaritin	H	OCH ₃	OCH ₃	H	OH	H	1.32
13	Salvigenin	H	OCH ₃	OCH ₃	H	OCH ₃	H	1.15
14	Jaceosidin	H	OH	OCH ₃	OCH ₃	OH	H	1.19
15	Desmethoxycentaureidin	H	OH	OCH ₃	OH	OCH ₃	H	1.37
16	Eupatilin	H	OH	OCH ₃	OCH ₃	OCH ₃	H	1.27
17	Cirsilineol	H	OCH ₃	OCH ₃	OCH ₃	OH	H	1.55
18	Eupatorin	H	OCH ₃	OCH ₃	OH	OCH ₃	H	1.82
19	Tricin	H	OH	H	OCH ₃	OH	OCH ₃	1.06
20	Apigenin 6,3',5'-Tri-OMe	H	OH	OCH ₃	OCH ₃	OH	OCH ₃	1.95
21	Nevadensin	OCH ₃	OH	OCH ₃	H	OCH ₃	H	1.29

(Continued on p. 352)

TABLE I (continued)

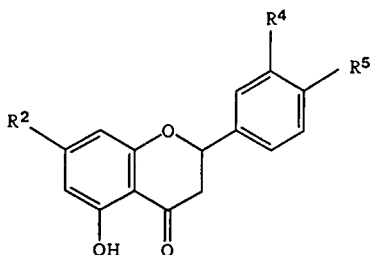
Flavonols:



No.	Compound	Substituent					RRT
		R ²	R ³	R ⁴	R ⁵	R ⁷	
22	Galangin	OH	H	H	H	OH	0.52
23	Kaempferol	OH	H	H	OH	OH	1.10
24	Kaempferid	OH	H	H	OCH ₃	OH	0.99
25	Kaempferol 3,7-di-Me	OCH ₃	H	H	OH	OCH ₃	0.83
26	Kaempferol 3,4'-di-Me	OH	H	H	OCH ₃	OCH ₃	0.95
27	Kaempferol 7,4'-di-Me	OCH ₃	H	H	OCH ₃	OH	0.84
28	Kaempferol 3,7,4'-tri-Me	OCH ₃	H	H	OCH ₃	OCH ₃	0.83
29	Isorhamnetin	OH	H	OCH ₃	OH	OH	1.33
30	Tamarixetin	OH	H	OH	OCH ₃	OH	1.57
31	Dillenetin	OH	H	OCH ₃	OCH ₃	OH	1.43
32	Quercetin 3,7,3'-tri-Me	OCH ₃	H	OCH ₃	OH	OCH ₃	1.10
33	Quercetin 3,7,4'-tri-Me	OCH ₃	H	OH	OCH ₃	OCH ₃	1.30
34	Quercetin 3,7,3',4'-tetra-Me	OCH ₃	H	OCH ₃	OCH ₃	OCH ₃	1.17
35	6-Methoxykaempferol	OH	OCH ₃	H	OH	OH	1.09
36	Betuletol	OH	OCH ₃	H	OCH ₃	OH	0.98
37	Penduletin	OCH ₃	OCH ₃	H	OH	OCH ₃	1.38
38	Spinacetin	OH	OCH ₃	OCH ₃	OH	OH	1.31
39	Quercetagenin 6,3',4'-tri-Me	OH	OCH ₃	OCH ₃	OCH ₃	OH	1.42
40	Veronicafolin	OCH ₃	OCH ₃	OCH ₃	OH	OH	1.69
41	Quercetagenin 3,6,7,4'-tetra-Me	OCH ₃	OCH ₃	OH	OCH ₃	OCH ₃	1.92

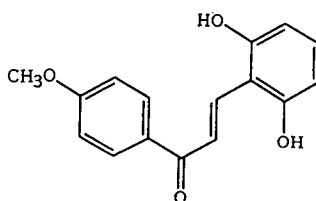
TABLE I (continued)

Flavanones:



No.	Compound	Substituent			RRT
		R ²	R ⁴	R ⁵	
42	Naringenin	OH	H	OH	0.60
43	Sakuranetin	OCH ₃	H	OH	0.53
44	Isosakuranetin	OH	H	OCH ₃	0.54
45	Naringenin 7,4'-di-Me	OCH ₃	H	OCH ₃	0.47
46	Hesperetin	OH	OH	OCH ₃	0.83
47	Eriodictyol 7,3'-di-Me	OCH ₃	OCH ₃	OH	0.62
48	Pescigenin	OCH ₃	OH	OCH ₃	0.71

Chalcone:



No.	Compound	RRT
49	2,6-Dihydroxy-4'-methoxychalcone	0.27

flame ionization detector. The carrier gas was nitrogen at a flow-rate of 1.3 ml/min, with a splitting ratio of 1:50. The injector and detector temperatures were 300°C and the column temperature was 270°C (isothermal).

Relative retention times (RRT) are expressed relative to hispidulin and were calculated after subtraction of the dead time (dead time = 0.94 min).

Gas chromatography–mass spectrometry

GC–MS analysis was carried out on a Varian-MAT CH7 A mass spectrometer in the elec-

tron impact mode (70 eV), coupled to a Varian 1700 gas chromatograph with an OV-1 capillary column. The carrier gas was helium and the injector and column temperatures were 270°C.

RESULTS AND DISCUSSION

The various flavonoid aglycones investigated, consisting of 21 flavones, 20 flavonols, 7 flavanones and 1 chalcone, with their relative retention times, expressed relative to hispidulin, are given in Table I.

Gas chromatography

Substitution at the various positions of the flavonoid nucleus affects the retention times characteristically. Conversion of a free hydroxyl group at C-4' or C-7 into the methyl ether decreases the retention time significantly (1–4, 42–45), but in the latter instance only if C-6 is unsubstituted. The retention times of 6,7-dimethoxylated flavones and flavonols are much higher than those of compounds unsubstituted at C-6 (compare, e.g., 12/2; 13/4; 17/7; 18/8), probably because of steric hindrance. Introduction of a methoxyl group causes different effects depending on the position. Methoxylation at C-6 has a negligible effect on retention times (compare, e.g., 1/10; 3/11; 5/14; 6/15), whereas methoxylation at C-3' causes significantly higher values (compare, e.g., 1/5; 10/14; 35/38; 42/46). The fact that hydroxylation at C-3 (compare, e.g., 1/23; 3/24; 10/35; 11/36) does not increase the retention times very much indicates that substituents at this position are somehow shielded.

The method is inapplicable to the examination of flavonoid aglycones with *o*-dihydroxy groups, such as luteolin, quercetin and patuletin, as they decompose under the chosen GC conditions. However, these compounds can easily be identified after TLC by their characteristic fluorescence after detection with diphenylboric acid, ethanolamine complex and polyethylene glycol.

Mass spectrometry

Compared with direct inlet mass spectra, those obtained by coupled GC–MS show the same typical fragmentation pattern but with slight differences in intensities. For 8-methoxyflavones and -flavonols it is typical with the direct inlet method, that the mass spectra show base peaks resulting from the fragment ion $[M - Me]^+$, whereas in the spectra of 6-methoxyflavones and -flavonols the molecular ion forms the base peak [9]. Under the chosen GC–MS conditions this differentiation based on mass intensities is not possible. The mass spectra of 6-methoxyflavonols exhibit base peaks formed by the fragment ion $[M - MeCO]^+$, whereas in those of 6-methoxyflavones the base peaks are either the molecular ion, the fragment ion $[M - MeCO]^+$ or m/z 69.

In the mass spectra of 6,7-dimethoxyflavones a loss of $[M - Me]^+$ leads to the most stable ion.

Applications

Fig. 1 shows the chromatogram obtained for a complex mixture of a plant extract containing 21 flavonoid aglycones belonging to different classes. Closely related compounds were separated and eluted as sharp peaks. In some instances, where the peaks consist of more than one compound, identities could be confirmed by comparison with retention times and mass spectra of the pure compounds. The combination of the separating power of this technique with mass spectrometry, which provides complementary structural information, represents an attractive

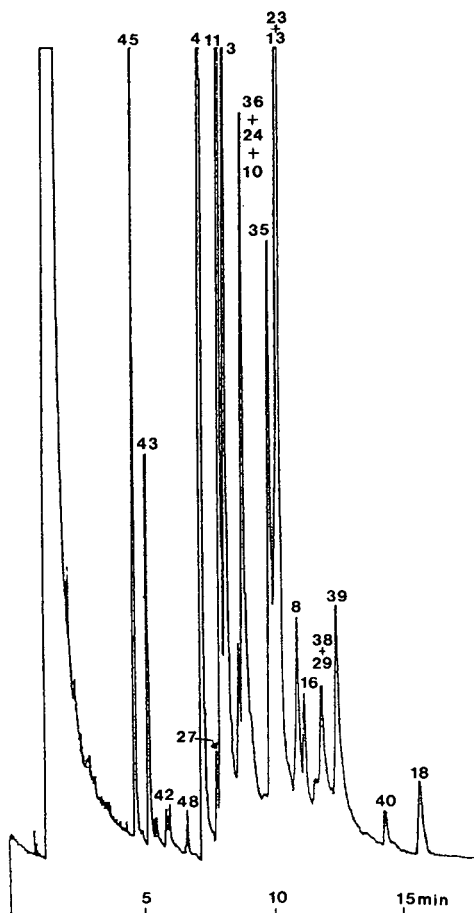


Fig. 1. Gas chromatogram of a crude fraction of flavonoid aglycones from a plant extract. See Table I for peak identification.

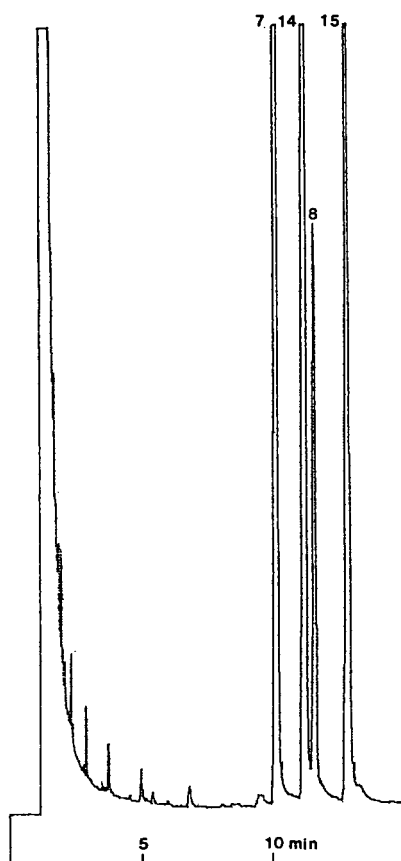


Fig. 2. Gas chromatogram of isomeric flavones. See Table I for peak identification.

and rapid method for the separation and identification of flavonoid aglycones in complex mixtures. Hence the method described here is able to play a valuable part in chemotaxonomic studies.

Another application of the above-described GC and GC–MS analyses is in the identification

of isomeric 3'-OH,4'-OCH₃- and 3'-OCH₃,4'-OH-flavones and -flavonols in mixtures. As these pairs yield identical mass spectra and cannot be distinguished by TLC, the only possibility of identifying them in a mixture has, up to now, been by ¹H NMR [7]. Fig. 2 shows the separation of two isomeric pairs of flavones, velutin (7)–pilloin (8) and jaceosidin (14)–desmethoxycentaureidin (15), by capillary GC. As compounds with a methoxyl group at C-4' have far longer retention times than their C-3' isomers, GC analysis represents a simple solution to the above-mentioned separation problem.

ACKNOWLEDGEMENT

We thank Mrs. E. Müller for experimental assistance.

REFERENCES

- 1 V. Cody, E. Middleton and J.B. Harborne (Editors), *Progress in Clinical and Biological Research*, Vol. 213, Alan R. Liss, New York, 1986.
- 2 V. Cody, E.M. Middleton, J.B. Harborne and A. Beretz (Editors), *Progress in Clinical and Biological Research*, Vol. 280, Alan R. Liss, New York, 1988.
- 3 J.B. Harborne, *Recent. Adv. Phytochem.*, 4 (1972) 107.
- 4 M.R. Koupai-Abyazani, C.S. Creaser and G.R. Stephenson, *Phytochem. Anal.*, 3 (1992) 80.
- 5 E.M. Gaydou, T. Berahia, J.-C. Wallet and J.P. Bianchini, *J. Chromatogr.*, 549 (1991) 440.
- 6 I. Merfort, *Planta Med.*, 50 (1984) 107.
- 7 I. Merfort, *Planta Med.*, 51 (1985) 136.
- 8 C. Jerga, I. Merfort and G. Willuhn, *Planta Med.*, 56 (1990) 122.
- 9 M. Goudard, J. Favre-Bonvin, P. Lebreton and J. Chopin, *Phytochemistry*, 17 (1978) 145.

Short Communication

Determination of some narcotic and toxic alkaloidal compounds by overpressured thin-layer chromatography with ethyl acetate as eluent

J. Pothier*, N. Galand and C. Viel

Laboratoire de Pharmacochimie des Produits Naturels et Analogues Structuraux, Faculté de Pharmacie, 2 bis Boulevard Tonnellé, 37042 Tours Cedex (France)

(First received September 15th, 1992; revised manuscript received December 24th, 1992)

ABSTRACT

A good separation of the components of various chemical classes of alkaloids is possible by overpressured thin-layer chromatography (OPTLC) on aluminium oxide plates with ethyl acetate alone as the mobile phase. The OPTLC method is efficient, rapid (15 min) and combines the advantages of classical TLC and HPLC, *i.e.*, large numbers of samples, high resolution and speed and the use of selective reagents. It is possible to separate the most commonly used narcotic and toxic agents with this method. For cannabinoids (narcotic phenolic compounds), the characterization requires the use of a binary eluent [hexane–ethyl acetate (70:30, v/v)].

INTRODUCTION

Toxicological laboratories are constantly engaged in studies of toxic and narcotic substances from different sources (powders, cigarettes, syringe residues, other pharmaceutical forms, etc.). Alkaloids are the most important group of narcotic and toxic agents and methods for the rapid detection of different classes of these compounds and their derivatives are required. Overpressured thin-layer chromatography (OPTLC) can be used for this purpose, as was demonstrated previously for the separation of alkaloids [1,2].

As a continuation of our investigations and the development of the process, we have applied OPTLC to the determination of the most fre-

quently used narcotic and toxic agents such as lysergide (LSD), heroin, cocaine, amphetamine, nicotine and opium alkaloids such as morphine and codeine.

EXPERIMENTAL

Apparatus

The samples were spotted with Minicaps (Hirschmann Laborgeräte, Eberstadt/Heilbronn, Germany). Chromatography was performed with 20 × 20 cm aluminium oxide 60 F₂₅₄ Type E 5713 precoated glass plates (Merck, Darmstadt, Germany). The plates were impregnated on three sides with Impress No. II polymer suspension (Laborate, Budapest, Hungary).

OPTLC was performed with a Chrompres 25 chromatograph (Laborate). During chromatog-

* Corresponding author.

raphy, the external pressure of the water cushion was 15 bar, the starting mobile phase (ethyl acetate) pressure was 7 bar and the flow-rate was 0.30 ml/min. The development of the plates (14 cm length) took 15 min.

Densitograms were recorded with a Camag Model 76510 TLC/HPTLC scanner at 540 nm after detection with Dragendorff's reagent.

Preparation of standard mixture and solutions

All solvents were of analytical-reagent grade from Merck. Before use, ethyl acetate was filtered through a 0.45- μm Millipore membrane after sonication.

A standard mixture was prepared by dissolving 10 mg of each of the following reference substance in 1 ml of methanol: LSD (Sandoz), heroin, cocaine, amphetamine, nicotine, morphine and codeine. The sample of opium was a tincture obtained by maceration for 24 h of 1 g of opium powder in 10 ml of 60% ethanol.

The volume of the spots applied on the chromatographic plates was 2 μl , corresponding to 20 μg for each sample. After elution the plates were sprayed with Dragendorff's reagent as modified by Munier and Macheboeuf [3] or potassium iodoplatinate reagent [4], which gave characteristic shades for the different spots (Table I), then read with the densitometer.

A 0.1- μg amount of cannabis resin was extracted by shaking at room temperature for 20 min with 10 ml of hexane, the filtrate was evaporated to dryness and the residue dissolved in 1 ml of toluene. A 20- μl volume of the toluene solution was spotted on the plate.

Standard solutions of Δ^9 -tetrahydrocannabinol (Δ^9 -THC) and cannabiol were obtained by dissolving 1 mg of each in 5 ml of toluene. Volumes of 20 μl of the cannabis resin extract, corresponding to 2 μg , and 2 μl of the Δ^9 -THC and cannabiol solutions, corresponding to 0.4 μg , were spotted on the chromatographic plates.

For cannabinoids, Fast Blue B Salt reagent was used as the spray reagent [5].

RESULTS AND DISCUSSION

The most interesting result of this work is the separation of alkaloidal drugs with use of only

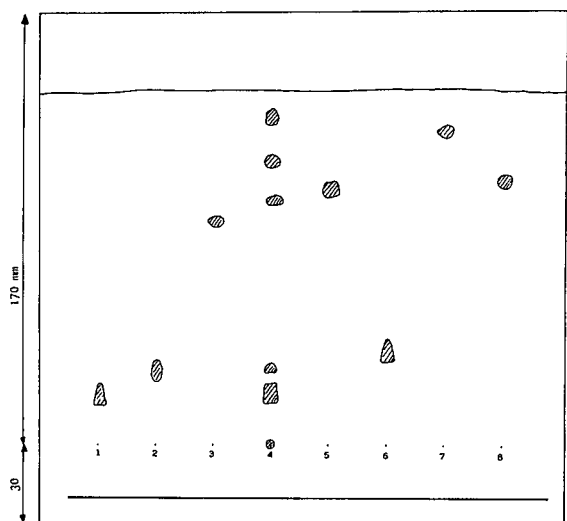


Fig. 1. Chromatogram of some narcotic and toxic alkaloids. 1 = Morphine; 2 = codeine; 3 = heroin; 4 = opium alkaloids; 5 = nicotine; 6 = amphetamine; 7 = cocaine; 8 = LSD. a = Start of elution.

ethyl acetate as the mobile phase. This is a significant improvement because usually in TLC and OPTLC systems three or more components in the mobile phase are required [6–11]. Such mixtures of eluents are not easy to use with basic components such as ammonia and diethylamine, which can both affect detection by visualization and determination by densitometry. The use of a single solvent also ensures good reproducibility of the method.

The procedure is also interesting because the

TABLE I

hR_F VALUES OF THE DIFFERENT ALKALOIDS AND THE COLOURS OBTAINED WITH IODOPLATINATE AND DRAGENDORFF'S REAGENTS

Alkaloid	hR_F	Dragendorff's reagent	Iodoplatinate reagent
Amphetamine	20	Yellow-orange	Light pink
Codeine	26	Orange	Pink-violet
Cocaine	92	Orange	Violet
Heroin	61	Orange	Yellow
LSD	67	Brown	Pink-brown
Morphine	13	Orange	Deep blue
Nicotine	77	Red-orange	Black-blue
Noscapine	95	Orange	Pink-brown
Papaverine	82	Orange	Light pink
Thebaine	72	Orange	Brown-violet

different compounds studied are cleanly separated. The chromatogram of opium alkaloids (Fig. 1) shows an efficient separation which permits the identification of all major alkaloids, which is not always the case in the TLC separation of alkaloids.

For other narcotic and toxic agents we obtained good separations. A list of the standards studied and their hR_F values are given in Table I.

The densitogram obtained from a standard mixture containing LSD, heroin, cocaine, amphetamine nicotine and the principal opium alkaloids morphine and codeine (Fig. 2) shows a clean separation of the different compounds after detection by dipping in or spraying with Dragendorff's reagent. Detection with iodoplatinate reagent gives different characteristic shades, which permits rapid identification (Table I).

It was observed that it is often possible for there to be a slight difference in migration if standards are spotted alone or in mixtures. These differences were observed particularly for codeine and LSD (Fig. 1). However it is easy to determine the nature of the compounds by the specific coloration developed with the different reagents used for spraying the plates (Table I).

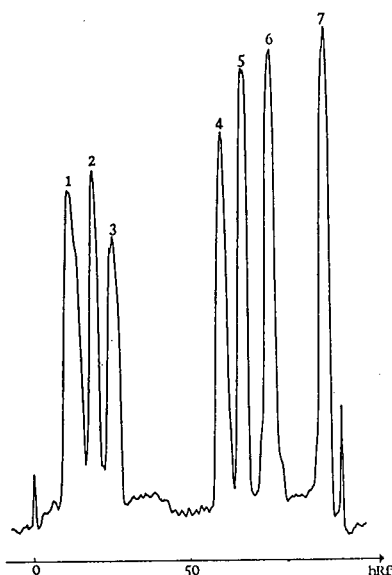


Fig. 2. Densitogram of standard mixture. 1 = Morphine; 2 = amphetamine; 3 = codeine; 4 = heroin; 5 = LSD; 6 = nicotine; 7 = cocaine.

With ethyl acetate as the mobile phase, Δ^9 -THC and other cannabinoids (narcotic phenolic compounds) from *Cannabis sativa* var. *indica* migrate up to the solvent front, but it is possible to separate them by reducing the mobile phase polarity by addition of hexane [hexane–ethyl acetate (70:30, v/v)]. The characterization of these compounds is as usual with Fast Blue B salt reagent. In this instance a good separation of cannabinoids is obtained, particularly of cannabiniol, which is found in all cannabis species, and Δ^9 -THC, which is the major active euphoric principle. The hR_F values are 82 for cannabiniol and 77 for Δ^9 -THC.

CONCLUSIONS

The method reported is efficient, reproducible and rapid (15–20 min per analysis). In comparison with the TLC of alkaloidal compounds under the same experimental conditions, OPTLC with ethyl acetate as the mobile phase gives a better resolution with longer development distances and the sensitivity is better because there is less diffusion of the compounds than in TLC. The same applies to the separation of cannabinoids with hexane–ethyl acetate as the mobile phase.

REFERENCES

- 1 J. Pothier, N. Galand and C. Viel, *J. Planar Chromatogr.*, 4 (1991) 392–396.
- 2 J. Pothier, N. Galand and C. Viel, *Phytotherapy*, No. 34/35 (1990) 3–7.
- 3 A. Baerheim Svendsen and R. Verpoorte, *Chromatography of Alkaloids, Part A: Thin-Layer Chromatography*, Elsevier, Amsterdam, 1983, p. 505.
- 4 A. Baerheim Svendsen and R. Verpoorte, *Chromatography of Alkaloids. Part A: Thin-Layer Chromatography*, Elsevier, Amsterdam, 1983, p. 506.
- 5 A. Baerheim Svendsen and R. Verpoorte, *Chromatography of Alkaloids. Part A: Thin-Layer Chromatography*, Elsevier, Amsterdam, 1983, p. 503.
- 6 E. Stahl, *Analyse Chromatographique et Microscopique des Drogues*, Entreprise Moderne d'Édition, Technique et Documentation, Paris, 1974.
- 7 H. Wagner, S. Bladt and E.M. Zgainski, *Plant Drug Analysis*, Springer, Berlin, 1984, pp. 260–261.
- 8 H. Gulyas, G. Kemeny, I. Hollosi and J. Pucsok, *J. Chromatogr.*, 291 (1984) 471–475.
- 9 P. Oroszlan, G. Verzar-Petri, M. Elek, E. Mincsovcics and

- A. Vastag, oral communication cited in Z. Witkiewicz and J. Bladec, *J. Chromatogr.*, 373 (1986) 111–140.
- 10 D. Pradeau, J.J. Prat, P. Delvordre and P. Prognon, *Ann. Falsif. Expert. Chim.*, 81 (1988) 229–241.
- 11 E. Tyihak and E. Mincsovics, *J. Planar Chromatogr.*, 1 (1988) 6–19.

Author Index

- Adersen, A., see Jäger, A.K. 634(1993)135
- Altria, K.D.
Determination of salbutamol-related impurities by capillary electrophoresis 634(1993)323
- Amparo Blázquez, M., see Tomás-Barberán, F.A. 634(1993)41
- Asplund, L., see Haglund, P. 634(1993)79
- Athanasiadou, M., see Haglund, P. 634(1993)79
- Baillet, A., Corbeau, L., Rafidison, P. and Ferrier, D.
Separation of isomeric compounds by reversed-phase high-performance liquid chromatography using Ag⁺ complexation. Application to *cis-trans* fatty acid methyl esters and retinoic acid photoisomers 634(1993)251
- Bayer, E., see Lohmiller, K. 634(1993)65
- Beeson, M.D. and Vigh, Gy.
Examination of the retention behavior of underivatized profen enantiomers on cyclodextrin silica stationary phases 634(1993)197
- Bergman, Å., see Haglund, P. 634(1993)79
- Blaschke, G., see Hampe, Th.R.E. 634(1993)205
- Boon, J.J., see Van der Hage, E.R.E. 634(1993)263
- Brandt, K.H., see Hampe, Th.R.E. 634(1993)205
- Brinkman, U.A.Th., see Van de Merbel, N.C. 634(1993)1
- Brinkman, U.A.Th., see Van der Hage, E.R.E. 634(1993)263
- Bromberg, L. and Levin, G.
Extraction chromatography with modified poly(vinyl chloride) and di(2-ethylhexyl)di thiophosphoric acid 634(1993)183
- Bruins, A.P., see Kostianen, R. 634(1993)113
- Cacia, J., Quan, C.P., Vasser, M., Sliwowski, M.B. and Frenz, J.
Protein sorting by high-performance liquid chromatography. I. Biomimetic interaction chromatography of recombinant human deoxyribonuclease I on polyionic stationary phases 634(1993)229
- Careri, M., Mori, G., Predieri, G., Souza de Rezende, N. and Sappa, E.
High-performance liquid chromatography of trinuclear ruthenium acetylido-carbonyl compounds 634(1993)143
- Castello, G., see Gerbino, T.C. 634(1993)338
- Ching, C.B., Lim, B.G., Lee, E.J.D. and Ng, S.C.
Preparative resolution of praziquantel enantiomers by simulated counter-current chromatography 634(1993)215
- Corbeau, L., see Baillet, A. 634(1993)251
- Crimmins, D.L. and Thoma, R.S.
Semi-automated chromatographic procedure for the isolation of acetylated N-terminal fragments from protein digests 634(1993)241
- Denizli, A., see Tuncel, A. 634(1993)161
- Dentraygues, P., see Pyell, U. 634(1993)169
- Estienne, J., see Mouly, P. 634(1993)129
- Félix, G., see Pyell, U. 634(1993)169
- Ferreres, F., see Tomás-Barberán, F.A. 634(1993)41
- Ferrier, D., see Baillet, A. 634(1993)251
- Frenz, J., see Cacia, J. 634(1993)229
- Fu, C., Xu, H. and Wang, Z.
Sensitive assay system for nitrosamines utilizing high-performance liquid chromatography with peroxyoxalate chemiluminescence detection 634(1993)221
- Galand, N., see Pothier, J. 634(1993)356
- García-Viguera, C., see Tomás-Barberán, F.A. 634(1993)41
- Garrigues, P., see Pyell, U. 634(1993)169
- Gaspard, S., see Margaron, P. 634(1993)57
- Gaydou, E.M., see Mouly, P. 634(1993)129
- Gerbino, T.C., Castello, G. and Pettinati, U.
Prediction of the retention of polynuclear aromatic hydrocarbons in programmed-temperature gas chromatography 634(1993)338
- Gielen, H., see Houben, R.J.H. 634(1993)317
- Göhlin, K. and Larsson, M.
Vinyl modification of fused-silica surfaces in polysiloxane-coated 10–50 μm I.D. capillaries for open-tubular liquid chromatography 634(1993)31
- Gudiksen, L., see Jäger, A.K. 634(1993)135
- Hageman, J.J., see Van de Merbel, N.C. 634(1993)1
- Haglund, P., Jakobsson, E., Asplund, L., Athanasiadou, M. and Bergman, Å.
Determination of polychlorinated naphthalenes in polychlorinated biphenyl products via capillary gas chromatography–mass spectrometry after separation by gel permeation chromatography 634(1993)79
- Häkkinen, V.M.A., see Kostianen, R. 634(1993)113
- Hampe, Th.R.E., Schlüter, J., Brandt, K.H., Nagel, J., Lamparter, E. and Blaschke, G.
Rapid and complete chiral chromatographic separation of racemic quaternary tropane alkaloids. Complementary use of a cellulose-based chiral stationary-phase in reversed-phase and normal-phase modes—a mechanistic study 634(1993)205
- Hartonen, K., see Hawthorne, S.B. 634(1993)297
- Hawthorne, S.B., Riekkola, M.-L., Serenius, K., Holm, Y., Hiltunen, R. and Hartonen, K.
Comparison of hydrodistillation and supercritical fluid extraction for the determination of essential oils in aromatic plants 634(1993)297
- Helferich, F.G.
Golay's paradox: linear versus non-linear chromatography 634(1993)334
- Hendrix, C., Zhu, Y., Wijzen, C., Roets, E. and Hoogmartens, J.
Comparative study of liquid chromatographic methods for the determination of cefadroxil 634(1993)257
- Henkel, B., see Kunath, A. 634(1993)119
- Hiltunen, R., see Hawthorne, S.B. 634(1993)297
- Hirokawa, T., Ohmori, A. and Kiso, Y.
Analysis of a dilute sample by capillary zone electrophoresis with isotachophoretic preconcentration 634(1993)101
- Holm, Y., see Hawthorne, S.B. 634(1993)297
- Hoogmartens, J., see Hendrix, C. 634(1993)257

- Houben, R.J.H., Gielen, H. and Van der Wal, S.J.
Automated preseparation derivatization on a capillary electrophoresis instrument 634(1993)317
- Huie, C.W., see Wu, N. 634(1993)309
- Jäger, A.K., Gudiksen, L., Adersen, A. and Smitt, U.W.
High-performance liquid chromatography of thapsigargin 634(1993)135
- Jakobsson, E., see Haglund, P. 634(1993)79
- Karg, F.P.M.
Determination of phenylurea pesticides in water by derivatization with heptafluorobutyric anhydride and gas chromatography-mass spectrometry 634(1993)87
- Kimball, B.A. and Mishalanie, E.A.
Gas chromatographic determination of sodium monofluoroacetate as the free acid in an aqueous solvent 634(1993)289
- Kiso, Y., see Hirokawa, T. 634(1993)101
- Koppenhoefer, B., see Lohmiller, K. 634(1993)65
- Korpela, T., see Paavilainen, S. 634(1993)273
- Kostiainen, R., Bruins, A.P. and Häkkinen, V.M.A.
Identification of degradation products of some chemical warfare agents by capillary electrophoresis-ion spray mass spectrometry 634(1993)113
- Kraak, J.C., see Stegeman, G. 634(1993)149
- Kunath, A., Henkel, B. and Wagner, J.
Direct optical resolution of 3,5-substituted δ -valerolactones and related 3,5-dihydroxyvaleric methyl esters on modified amylose and cellulose chiral stationary phases 634(1993)119
- Lamparter, E., see Hampe, Th.R.E. 634(1993)205
- Larsson, M., see Göhlin, K. 634(1993)31
- Lavagnini, I., see Pastore, P. 634(1993)47
- Lee, E.J.D., see Ching, C.B. 634(1993)215
- Levin, G., see Bromberg, L. 634(1993)183
- Lim, B.G., see Ching, C.B. 634(1993)215
- Lingeman, H., see Van der Hage, E.R.E. 634(1993)263
- Liu, X., see Lou, X. 634(1993)281
- Liu, X., see Lou, X. 634(1993)345
- Liu, Y.-M. and Sheu, S.-J.
Determination of quaternary alkaloids from *Phellodendri Cortex* by capillary electrophoresis 634(1993)329
- Lohmiller, K., Bayer, E. and Koppenhoefer, B.
Recognition of enantiomers by Chirasil-Val and oligopeptide analogues as studied by gas-phase calorimetry and ^1H NMR spectroscopy in solution 634(1993)65
- Lou, X., Liu, X. and Zhou, L.
Series-coupled capillary columns for the separation of N,(O)-trifluoroacetyl isopropyl derivatives of D,L-aspartic acid and L-hydroxyproline by gas chromatography 634(1993)281
- Lou, X., Liu, X. and Zhou, L.
Chiral recognition of enantiomeric amides on a diamide chiral stationary phase by gas chromatography 634(1993)345
- Lowe, C.R., see Tuncel, A. 634(1993)161
- Margaron, P., Gaspard, S. and Van Lier, J.E.
Chromatographic analysis of asymmetric sulphophthalocyanines using a diode-array detector 634(1993)57
- Matthiesen, U., see Schmidt, T.J. 634(1993)350
- McGhie, T.K.
Analysis of sugarcane flavonoids by capillary zone electrophoresis 634(1993)107
- Merfort, I., see Schmidt, T.J. 634(1993)350
- Mishalanie, E.A., see Kimball, B.A. 634(1993)289
- Mori, G., see Careri, M. 634(1993)143
- Mouly, P., Gaydou, E.M. and Estienne, J.
Column liquid chromatographic determination of flavanone glycosides in *Citrus*. Application to grapefruit and sour orange juice adulterations 634(1993)129
- Nagel, J., see Hampe, Th.R.E. 634(1993)205
- Ng, S.C., see Ching, C.B. 634(1993)215
- Ohmori, A., see Hirokawa, T. 634(1993)101
- Paavilainen, S. and Korpela, T.
Comparison of high-performance liquid and gas chromatography in the determination of organic acids in culture media of alkaliphilic bacteria 634(1993)273
- Pastore, P., Lavagnini, I. and Versini, G.
Ion chromatographic determination of monosaccharides from trace amounts of glycosides isolated from grape musts 634(1993)47
- Pettinati, U., see Gerbino, T.C. 634(1993)338
- Pişkin, E., see Tuncel, A. 634(1993)161
- Poppe, H., see Stegeman, G. 634(1993)149
- Pothier, J., Galand, N. and Viel, C.
Determination of some narcotic and toxic alkaloidal compounds by overpressured thin-layer chromatography with ethyl acetate as eluent 634(1993)356
- Predieri, G., see Careri, M. 634(1993)143
- Purvis, D., see Tuncel, A. 634(1993)161
- Pyell, U., Garrigues, P., Félix, G., Rayez, M.T., Thienpont, A. and Dentraygues, P.
Separation of tetrachloro-*p*-dioxin isomers by high-performance liquid chromatography with electron-acceptor and electron-donor stationary phases 634(1993)169
- Quan, C.P., see Cacia, J. 634(1993)229
- Rafidison, P., see Baillet, A. 634(1993)251
- Rayez, M.T., see Pyell, U. 634(1993)169
- Riekkola, M.-L., see Hawthorne, S.B. 634(1993)297
- Roets, E., see Hendrix, C. 634(1993)257
- Saitoh, K., see Tsukahara, S. 634(1993)138
- Sappa, E., see Careri, M. 634(1993)143
- Schlüter, J., see Hampe, Th.R.E. 634(1993)205
- Schmidt, T.J., Merfort, I. and Matthiesen, U.
Resolution of complex mixtures of flavonoid aglycones by analysis of gas chromatographic-mass spectrometric data 634(1993)350
- Serenius, K., see Hawthorne, S.B. 634(1993)297
- Sheu, S.-J., see Liu, Y.-M. 634(1993)329
- Simonzadeh, N.
Ion chromatographic method for the simultaneous determination of trifluoromethanesulfonic acid and trifluoroacetic acid 634(1993)125
- Sliwowski, M.B., see Cacia, J. 634(1993)229
- Smitt, U.W., see Jäger, A.K. 634(1993)135
- Souza de Rezende, N., see Careri, M. 634(1993)143
- Stegeman, G., Kraak, J.C. and Poppe, H.
Dispersion in packed-column hydrodynamic chromatography 634(1993)149

- Suzuki, N., see Tsukahara, S. 634(1993)138
- Thienpont, A., see Pyell, U. 634(1993)169
- Thoma, R.S., see Crimmins, D.L. 634(1993)241
- Tomás-Barberán, F.A., Ferreres, F., Amparo Blázquez, M., García-Viguera, C. and Tomás-Lorente, F.
High-performance liquid chromatography of honey flavonoids 634(1993)41
- Tomás-Lorente, F., see Tomás-Barberán, F.A.
634(1993)41
- Tsukahara, S., Saitoh, K. and Suzuki, N.
Modification of reversed-phase liquid chromatographic retention characteristics for metal-tetraphenylporphyrin complexes using octane as a mobile phase additive 634(1993)138
- Tuncel, A., Denizli, A., Purvis, D., Lowe, C.R. and Pişkin, E.
Cibacron Blue F3G-A-attached monosize poly(vinyl alcohol)-coated polystyrene microspheres for specific albumin adsorption 634(1993)161
- Van de Merbel, N.C., Hageman, J.J. and Brinkman, U.A.Th.
Membrane-based sample preparation for chromatography (Review) 634(1993)1
- Van der Hage, E.R.E., Van Loon, W.M.G.M., Boon, J.J., Lingeman, H. and Brinkman, U.A.Th.
Combined high-performance aqueous size-exclusion chromatographic and pyrolysis-gas chromatographic-mass spectrometric study of lignosulphonates in pulp mill effluents 634(1993)263
- Van der Wal, S.J., see Houben, R.J.H. 634(1993)317
- Van Lier, J.E., see Margaron, P. 634(1993)57
- Van Loon, W.M.G.M., see Van der Hage, E.R.E.
634(1993)263
- Vasser, M., see Cacia, J. 634(1993)229
- Versini, G., see Pastore, P. 634(1993)47
- Viel, C., see Pothier, J. 634(1993)356
- Vigh, Gy., see Beeson, M.D. 634(1993)197
- Wagner, J., see Kunath, A. 634(1993)119
- Wang, Z., see Fu, C. 634(1993)221
- Wijsen, C., see Hendrix, C. 634(1993)257
- Wu, N. and Huie, C.W.
Peroxyoxalate chemiluminescence detection in capillary electrophoresis 634(1993)309
- Xu, H., see Fu, C. 634(1993)221
- Zhou, L., see Lou, X. 634(1993)281
- Zhou, L., see Lou, X. 634(1993)345
- Zhu, Y., see Hendrix, C. 634(1993)257

Errata

corrected 3 May 93/AP

J. Chromatogr., 609 (1992) 141–146.

Page 141, Introduction. The second paragraph contains three sentences that do not belong to this paper. Below is the whole Introduction as it should have read.

INTRODUCTION

Glutathione transferases (GSTs) are a widespread family of isoenzymes implicated in the detoxification of electrophilic xenobiotics as well as in several endogenous functions. One isoform is membrane-bound [1] and another is nuclear [2]. Cytosolic GST isoenzymes are dimers of a number of subunits with molecular masses of about 25 000 and have been grouped into four classes with respect to physiological, structural and genetic similarities: α , μ , π and θ [3,4]. 1-Chloro-2,4-dinitrobenzene (CDNB) is used as a universal substrate for GST isoenzymes.

A wide variety of structurally unrelated compounds have been shown to increase hepatic GST activity in a number of organisms, mostly in laboratory animals (mice and rats). Differential induction of GST isoenzymes has been reported [5,6]. Induction of a particular isoform by a given compound can be masked if only the overall GST activity of a crude extract is ana-

lysed, hence the whole isoenzyme pattern needs to be determined. To this end, several methods have been devised which include an initial affinity chromatography step on GSH–Sepharose or S-hexylglutathione–Sepharose [7,8] followed by either chromatofocusing [9], isoelectric focusing [10], hydroxyapatite chromatography [11] or reversed-phase high-performance liquid chromatography (HPLC) [12]. The latter method is based on protein subunit determination and is not dependent on the preservation of activity, whereas the others are based on the quantification of enzymatic activity. All rely on a similar initial step that uses an affinity matrix to which some of the isoenzymes do not bind or bind loosely, lowering recovery yields [6,9,12].

This paper reports a single-step analytical method based on ion-exchange HPLC with automatic on-line detection of activity for the rapid determination of GST isoenzymes in crude biological samples, using CDNB as a non-specific substrate.

J. Chromatogr., 624 (1992) 103–152.

Page 125, Table 10, third column, second row from bottom: “Cyclohexane–H₄folic acid” should read “Cyclohexane–THF”.

Page 143, Table 21, third column, second row from bottom: “1.8% H₄folic acid” should read “1.8% THF”.

PUBLICATION SCHEDULE FOR THE 1993 SUBSCRIPTION

Journal of Chromatography and Journal of Chromatography, Biomedical Applications

MONTH	O 1992	N 1992	D 1992	J	F	M	A	
Journal of Chromatography	623/1 623/2 624/1 + 2	625/1 625/2	626/1 626/2 627/1 + 2	628/1 628/2 629/1 629/2	630/1 + 2 631/1 + 2 632/1 + 2 633/1 + 2	634/1 634/2	635/1 635/2 636/1 636/2	The publication schedule for further issues will be published later.
Cumulative Indexes, Vols. 601–650								
Bibliography Section						649/1		
Biomedical Applications				612/1	612/2	613/1	613/2 614/1	

INFORMATION FOR AUTHORS

(Detailed *Instructions to Authors* were published in Vol. 609, pp. 437–443. A free reprint can be obtained by application to the publisher, Elsevier Science Publishers B.V., P.O. Box 330, 1000 AH Amsterdam, Netherlands.)

Types of Contributions. The following types of papers are published in the *Journal of Chromatography* and the section on *Biomedical Applications*: Regular research papers (Full-length papers), Review articles, Short Communications and Discussions. Short Communications are usually descriptions of short investigations, or they can report minor technical improvements of previously published procedures; they reflect the same quality of research as Full-length papers, but should preferably not exceed five printed pages. Discussions (one or two pages) should explain, amplify, correct or otherwise comment substantively upon an article recently published in the journal. For Review articles, see inside front cover under Submission of Papers.

Submission. Every paper must be accompanied by a letter from the senior author, stating that he/she is submitting the paper for publication in the *Journal of Chromatography*.

Manuscripts. Manuscripts should be typed in **double spacing** on consecutively numbered pages of uniform size. The manuscript should be preceded by a sheet of manuscript paper carrying the title of the paper and the name and full postal address of the person to whom the proofs are to be sent. As a rule, papers should be divided into sections, headed by a caption (e.g., Abstract, Introduction, Experimental, Results, Discussion, etc.) All illustrations, photographs, tables, etc., should be on separate sheets.

Abstract. All articles should have an abstract of 50–100 words which clearly and briefly indicates what is new, different and significant. No references should be given.

Introduction. Every paper must have a concise introduction mentioning what has been done before on the topic described, and stating clearly what is new in the paper now submitted.

Illustrations. The figures should be submitted in a form suitable for reproduction, drawn in Indian ink on drawing or tracing paper. Each illustration should have a legend, all the *legends* being typed (with double spacing) together on a *separate sheet*. If structures are given in the text, the original drawings should be supplied. Coloured illustrations are reproduced at the author's expense, the cost being determined by the number of pages and by the number of colours needed. The written permission of the author and publisher must be obtained for the use of any figure already published. Its source must be indicated in the legend.

References. References should be numbered in the order in which they are cited in the text, and listed in numerical sequence on a separate sheet at the end of the article. Please check a recent issue for the layout of the reference list. Abbreviations for the titles of journals should follow the system used by *Chemical Abstracts*. Articles not yet published should be given as "in press" (journal should be specified), "submitted for publication" (journal should be specified), "in preparation" or "personal communication".

Dispatch. Before sending the manuscript to the Editor please check that the envelope contains four copies of the paper complete with references, legends and figures. One of the sets of figures must be the originals suitable for direct reproduction. Please also ensure that permission to publish has been obtained from your institute.

Proofs. One set of proofs will be sent to the author to be carefully checked for printer's errors. Corrections must be restricted to instances in which the proof is at variance with the manuscript. "Extra corrections" will be inserted at the author's expense.

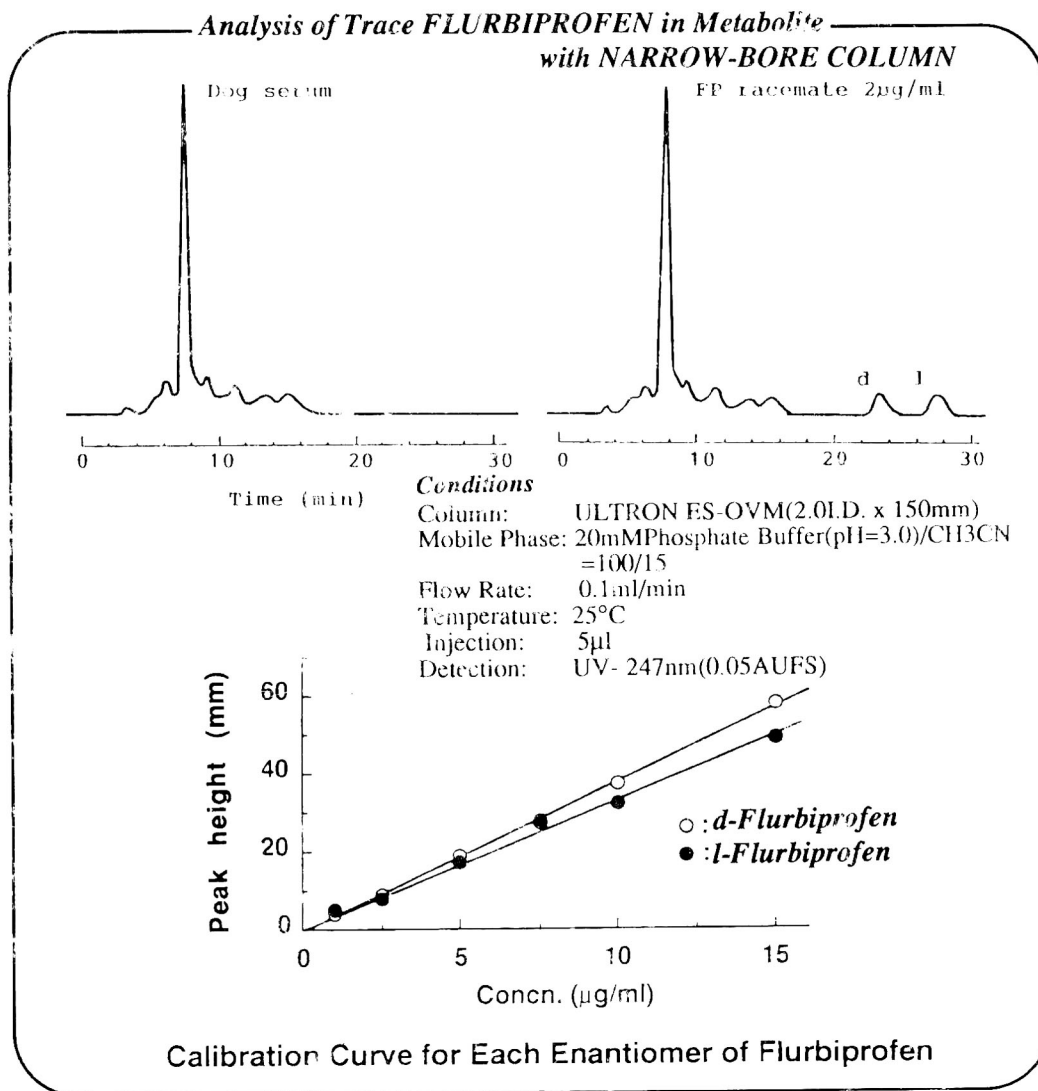
Reprints. Fifty reprints will be supplied free of charge. Additional reprints can be ordered by the authors. An order form containing price quotations will be sent to the authors together with the proofs of their article.

Advertisements. The Editors of the journal accept no responsibility for the contents of the advertisements. Advertisement rates are available on request. Advertising orders and enquiries can be sent to the Advertising Manager, Elsevier Science Publishers B.V., Advertising Department, P.O. Box 211, 1000 AE Amsterdam, Netherlands; courier shipments to: Van de Sande Bakhuyzenstraat 4, 1061 AG Amsterdam, Netherlands; Tel. (+31-20) 515 3220/515 3222, Telefax (+31-20) 6833 041, Telex 16479 els vi nl. *UK*: T.G. Scott & Son Ltd., Tim Blake, Portland House, 21 Narborough Road, Cosby, Leics. LE9 5TA, UK; Tel. (+44-533) 753 333, Telefax (+44-533) 750 522. *USA and Canada*: Weston Media Associates, Daniel S. Lipner, P.O. Box 1110, Greens Farms, CT 06436-1110, USA; Tel. (+1-203) 261 2500, Telefax (+1-203) 261 0101.

Ovomucoid Bonded Column for Direct Chiral Separation

ULTRON ES-OVM

Narrow-Bore Column (2.0 I.D. x 150 mm) for Trace Analyses
Analytical Column (4.6 I.D. , 6.0 I.D. x 150 mm) for Regular Analyses
Semi-Preparative Column (20.0 I.D. x 250 mm) for Preparative Separation



SHINWA CHEMICAL INDUSTRIES, LTD.

50 Kagekatsu-cho, Fushimi-ku, Kyoto 612, JAPAN
Phone:+81-75-621-2360 Fax:+81-75-602-2660

In the United States and Europe, please contact:

Rockland Technologies, Inc.

538 First State Boulevard, Newport, DE 19804, U.S.A.

Phone: 302-633-5880 Fax: 302-633-5893

This product is licenced by Eisai Co., Ltd.